2. Type of Mathematical Model

☐ Process Model   ☒ Abstraction Model   ☐ System Model

Describe Intended Use of Model

The purpose of the saturated zone (SZ) flow and transport model abstraction is to provide radionuclide transport simulation results for use in the Total System Performance Assessment (TSPA) calculations.

Technical Contact/Department:

B. W. Arnold, Saturated Zone

3. Title

Saturated Zone Flow and Transport Model Abstraction

4. DI (including Rev. No. and Change No., if applicable):

MDL-NBS-HS-000021, REV 01

5. Total Attachments	6. Attachment Numbers - No. of Pages in Each
1	I - 28

	Printed Name	Signature	Date
7. Originator	B.W. Arnold and S.P. Kuzio		12/22/2003
8. CSO	M. Zhu		12/22/03
9. Checker	T. Lowry		12/22/2003
10. QER	J. Graff		12/22/2003
11. Responsible Manager/Lead	S.P. Kuzio		12/22/2003
12. Responsible Manager	P.R. Dixon		12/22/03

13. Remarks:

This report contains an analysis of the background gross alpha concentration in groundwater.

This report also documents analyses with the SZ Transport Abstraction Model using updated uncertainty distributions for some sorption coefficients.

This report also documents analyses with the SZ Transport Abstraction Model for a new radionuclide class defined as the fast fraction of radionuclides irreversibly attached to colloids.

2. Model Title:
Saturated Zone Flow and Transport Model Abstraction

3. DI (including Rev. No. and Change No., if applicable):
MDL-NBS-HS-000021, REV01

4. Revision/Change No.	5. Description of Revision/Change
REV00	Initial Issue
REV01	This report contains an analysis of the background gross alpha concentration in groundwater. This report also documents analyses with the SZ Transport Abstraction Model using updated uncertainty distributions for some sorption coefficients. This report also documents analyses with the SZ Transport Abstraction Model for a new radionuclide class defined as the fast fraction of radionuclides irreversibly attached to colloids.

CONTENTS

CONTENTS (Continued)

FIGURES

TABLES

Page

ACRONYMS AND ABBREVIATIONS

1-D   One-Dimensional

ACM   Alternative Conceptual Model
AMR   Analysis/Model Report
ATC   Alluvial Tracer Complex

BSC   Bechtel SAIC Company

C   Centigrade
CDF   Cumulative Distribution Function
cm   centimeter

DOE   U. S. Department of Energy
DIRS   Document Input Reference System
DTN   Data Tracking Number

ESF   Exploratory Studies Facility

FEPs   Features, Events, and Processes

g   gram

HFM   Hydrogeologic Framework Model

K   Kelvin
kg   kilogram
km   kilometer

l   liter
LA   License Application
LANL   Los Alamos National Laboratory

m   meter
ml   milliliter

N/A   Not Applicable
NE   Northeast
NRC   Nuclear Regulatory Commission
NTS   Nevada Test Site
NW   Northwest

PDF   Probability Density Function

QA   Quality Assurance

ACRONYMS AND ABBREVIATIONS (Continued)

RH   Relative Humidity
RMEI   Reasonably Maximally Exposed Individual

s   second
SE   Southeast
SNL   Sandia National Laboratories
STN   Software Tracking Number
SR   Site Recommendation
SW   Southwest
SZ   Saturated Zone

TDS   Total Dissolved Solids
TSPA   Total System Performance Assessment
TWP   Technical Work Plan

UTM   Universal Transverse Mercator
USGS   United States Geological Survey
UZ   Unsaturated Zone

YMP   Yucca Mountain Project
YMRP   Yucca Mountain Review Plan

1. PURPOSE

The purpose of the saturated zone (SZ) flow and transport model abstraction task is to provide radionuclide transport simulation results for use in the Total System Performance Assessment (TSPA) calculations. This task also includes assessment of uncertainty in parameters related to both groundwater flow and radionuclide transport in the models used for this purpose. This model report documents the following:

The SZ Transport Abstraction Model, which consists of a set of radionuclide breakthrough curves at the accessible environment for use in the TSPA simulations of radionuclide releases to the biosphere. These radionuclide breakthrough curves contain information on the radionuclide transport times through the SZ.

The SZ One-Dimensional (1-D) Transport Model, which is incorporated in the TSPA model to simulate the transport, decay, and ingrowth of radionuclide decay chains in the SZ.

The analysis of uncertainty in groundwater flow and radionuclide transport input parameters for the SZ Transport Abstraction Model and the SZ 1-D Transport Model.

The analysis of background concentration of alpha-emitting species in the groundwater of the SZ.

Revision 01 of this AMR includes several changes relative to Revision 00 (BSC 2003 [164870]. Simulations with the SZ Transport Abstraction Model have been updated to incorporate changes in the input regarding uncertainty distributions for sorption coefficients. An analysis of the background concentration of alpha-emitters in groundwater of the SZ has been added.

This model report includes the technical basis for Features Events and Processes (FEPs) and contributes to the characterization of the SZ as a natural barrier, which provides evidence related to the capability of the SZ to delay movement of radionuclides through the SZ to the accessible environment. The scope of this report also contributes to the technical basis for the SZ transport system description used in the License Application (LA), and provides evidence for the acceptance criteria as specified in the Yucca Mountain Review Plan (YMRP) (NRC 2003 [163274]). The scope of the model report is limited to adaptation of an existing model, the SZ Site-Scale Transport Model, for the uncertainty analysis as reflected in the SZ radionuclide breakthrough curves developed in this model report.

Use of the SZ Transport Abstraction Model and the SZ 1-D Transport Model is subject to the limitations imposed by the assumptions listed in Section 5 of this model report. Limitations in knowledge of specific parameter values are addressed in the analysis of parameter uncertainties in this report. The radionuclide breakthrough curves generated for the SZ Transport Abstraction model are limited to 100,000 years, for present climatic conditions. This limits the time period that can be simulated with the TSPA model using these breakthrough curves for the SZ. Because the SZ breakthrough curves are scaled for higher groundwater flow rates under future climatic conditions, the time period that can be simulated with the TSPA model would be significantly less than 100,000 years. If the glacial-transition climate state is applied for most of simulation

period in the TSPA model, the SZ breakthrough curves would be scaled by a factor of approximately 4, limiting the TSPA model simulation time to about 25,000 years.

Information on the correlation between distribution coefficients (K_d's) used in the sampling of uncertain parameters for the SZ Transport Abstraction Model and the SZ 1-D Transport Model is given in Table 4-3 and Table 6-8. The technical bases for correlations between distribution coefficients (or the lack thereof) are documented in BSC 2003 [162419], Section I.10.

Evaluation of uncertainty in horizontal anisotropy of permeability is summarized in Section 6.5.2.10. Complete documentation of the technical basis for this evaluation of uncertainty is given in BSC 2003 [162415], Section 6.2.6. Implementation of uncertainty in horizontal anisotropy in the SZ Transport Abstraction Model and the SZ 1-D Transport Model is discussed in Section 6.5.3.1 and Section 6.5.1.2, respectively.

The impacts of spatial variability of parameters affecting radionuclide transport in the alluvium are incorporated in the evaluation of uncertainties in model parameters in Section 6.5.2.3, Section 6.5.2.7, Section 6.5.2.8, Section 6.5.2.9, and Section 6.5.2.11. The technical bases for uncertainty in distribution coefficients are documented in BSC 2003 [162419], Section I.

Information on the geological uncertainty in the location of the contact between tuff and alluvium and the consequent uncertainty in the flow path lengths in the alluvium is presented in Section 6.5.2.2. This evaluation of uncertainty includes currently available information from the Nye County drilling program.

The sensitivity analysis of matrix diffusion in the SZ Transport Abstraction Model is presented in the assessment of alternative conceptual models in Section 6.4.

This model report is governed by the Office of Civilian Radioactive Waste Management (OCRWM) *Technical Work Plan For: Saturated Zone Flow and Transport Modeling and Testing*, TWP-NBS-MD-000002 (BSC 2003 [166034]), Work Package ASZM04. This model report deviates from the *Technical Work Plan For: Saturated Zone Flow and Transport Modeling and Testing*, TWP-NBS-MD-000002 (BSC 2003 [166034]) because it does not contain documentation of the Irrigation Recycling Transport Model. The Irrigation Recycling Transport Model is not needed because the FEPs screening decision has been changed to exclude this process. Documentation of the screening argument related to the recycling of radionuclides beneath irrigated fields is being developed in the upcoming revision (REV02) of *Features, Events, and Processes in SZ Flow and Transport* (BSC 2003 [163128]) The work documented in this model report was conducted in accordance with the quality assurance procedure AP-SIII.10Q, *Models* [165553].

In this report, a unique six-digit numerical identifier (the Document Input Reference System [166034] number) is placed in the text following the reference callout (e.g., BSC 2001 [155950]). The purpose of the DIRS numbers is to assist the reader in locating a specific reference in the DIRS database.

2. QUALITY ASSURANCE

Development of this model report and the supporting modeling activities is subject to the Yucca Mountain Project (YMP) quality assurance (QA) program (BSC 2003 [166034], Section 8, Work Package ASZM04). Approved QA procedures identified in the technical work plan (BSC 2003 [166034], Section 4) have been used to conduct and document the activities described in this model report. The technical work plan also identifies the methods used to control the electronic management of data (BSC 2003 [166034], Section 8).

This model report provides values for hydrologic properties of a natural barrier that is important to the demonstration of compliance with the post-closure performance objectives prescribed in 10 CFR 63.113. Therefore, it is classified on the Q-List (BSC 2003 [165179]) as "SC" (Safety Category), reflecting its importance to waste isolation, as defined in AP-2.22Q, Rev 1, ICN 0, *Classification Analyses and Maintenance of the Q-List* [164786]. The report contributes to the analysis and modeling data used to support postclosure performance assessment; the conclusions do not directly impact preclosure engineered features important to safety, as defined in AP-2.22Q.

3. USE OF SOFTWARE

3.1 SOFTWARE TRACKED BY CONFIGURATION MANAGEMENT

The computer software codes used directly in this model report are listed in Table 3-1. The qualification status of the software is indicated in the Software Configuration Management (SCM) database. All software was obtained from SCM and is appropriate for the application. Qualified codes were used only within the range of validation as required by AP-SI.1Q, Rev. 5, ICN 0, *Software* Management [163085].

Table 3-1. Computer Software Used in this Model Report

Software Name and Version (V)	Software Tracking Number (STN)	Description	Computer Type, Platform, and Location	Date Baselined
FEHM V 2.20 (LANL 2003 [161725])	10086-2.20-00	This code is a finite-element heat- and mass-transport code that simulates nonisothermal, multiphase, multicomponent flow and solute transport in porous media.	Sun UltraSPARC - SunOS 5.7 Sandia National Laboratories	01/28/2003
GoldSim V 7.50.100 (BSC 2003 [161572])	10344-7.50.100-00	This code is the modeling software used in the TSPA. Probabilistic simulations are represented graphically in GoldSim.	Dell OptiPlex GX260 - Windows 2000 Professional 5.0.2195 Sandia National Laboratories	01/07/2003
SZ_Pre V 2.0 (SNL 2003 [163281])	10914-2.0-00	This software is an automated method for preparing the FEHM input files for the SZ site-scale flow and transport model for use in TSPA analyses.	Sun UltraSPARC - SunOS 5.7 Sandia National Laboratories	04/28/2003
SZ_Post V 3.0 (SNL 2003 [163571])	10915-3.0-00	This software is used to translate the output files from the SZ site-scale model into the format used by the SZ_Convolute software code. SZ_Post reads the output files from the FEHM software code and writes the breakthrough curve data for radionuclide transport in the SZ.	Sun UltraSPARC - SunOS 5.7, Solaris 2.7 Sandia National Laboratories	05/22/2003
CORPSCON V 5.11.08 (LANL 2001 [155082])	10547-5.11.08-00	This software is used to convert coordinate data to the Universal Transverse Mercator (UTM) coordinate system.	IBM Thinkpad 770Z - Windows NT 4.0 Sandia National Laboratories	08/27/2001
SZ_Convolute V.2.2 (SNL 2003 [163344])	10207-2.2-00	This software is used to calculate saturated-zone response curves based on unsaturated-zone radionuclide source terms, generic saturated-zone responses, and climate scenarios for the YMP.	Dell OptiPlex GX260 - Windows 2000 Professional 5.0.2195 Sandia National Laboratories	01/13/2003

NOTE: The SZ_Convolute v. 2.2 software code (STN: 10207-2.2-00, SNL 2003 [163344]) was used in the modeling and analyses in this report. SZ_Convolute v. 3.0 (STN: 10207-3.0-00, SNL 2003 [164180]) will be used for implementation of the SZ Transport Abstraction Model in TSPA-LA. The summary description of the changes in the SZ_Convolute software code in the software baseline report between versions 2.2 and 3.0 gives no indication that the changes in functionality would have any impact on the model validation performed in this AMR.

3.2 EXEMPT SOFTWARE

The commercially available software cited below is appropriate for use in this application. The results were spot-checked by hand to ensure the results were correct. The computer used was a Dell OptiPlex GX1 with Pentium II processor, running Microsoft Windows 2000 5.0.2195. The range of validation for Excel, Surfer, and Grapher is the set of real numbers.

Commercially available software:

- **Excel 2000**: Used for simple spreadsheet calculations in support of plotting and visualization. The formulas, listing of inputs, listing of outputs, and other required information can be found in the following spreadsheets: Eff_MtrxDif_11.xls, bulkd_matr_eff_La.xls, and geonames.xls. These spreadsheets can be found in DTN:SN0306T0502103.006.

- **Surfer 8.0**: Used for plotting and visualization.

- **Grapher 4.0**: Used for plotting graphs.

- **Igor 4.07**: Used for plotting graphs.

4. INPUTS

4.1 DATA, PARAMETERS, AND OTHER MODEL INPUTS

All data, parameters, and other model inputs documented in Section 4.1 are used as direct inputs to the analyses of parameter uncertainty and/or the SZ Transport Abstraction Model and SZ 1-D Transport Model.

4.1.1 Data and Other Model Inputs

The data providing input for the development of parameters used in the models documented in this report are identified in Table 4-1.

These input data are considered appropriate for the development of uncertain parameters for the SZ Transport Abstraction Model and the SZ 1-D Transport Model. The data that are used as direct input to the models developed in this report are the best relevant qualified data because they are taken from the Yucca Mountain site and region. Where available and appropriate, non-qualified data are used to corroborate those data that are used as direct input (see Section 6.5.2).

Uncertainty associated with the model, including development of parameter values and their implementation in the SZ Transport Abstraction Model and the SZ 1-D Transport Model, is discussed in Section 6.5.1 and 6.5.2. Parameter uncertainties are addressed by providing ranges, probability distributions and bounding assumptions as appropriate for each parameter.

Table 4-1. Direct Inputs

Data Name	Originating Report	DTN
Matrix Porosity in the Volcanic Units (HFM Units 15-8)	MDL-NBS-GS-000004 (HFM Units 15-13, 10-8) (BSC 2002 [159530])	SN0004T0501399.003 [155045] (HFM Units 15-13, 10-8)
	OFR 94-469 (Buesch et al. 1996 [100106]); Flint 1998 [100033]; OFR 94-460 (Moyer and Geslin 1995 [101269]); (HFM Units 12 and 11)	MO0109HYMXPROP.001 [155989] (HFM Units 12 and 11)
	TDR-NBS-GS-000020, BSC 2001 [163479] (HFM Units 12 and 11)	MO0010CPORGLOG.002 [155229] (HFM Units 12 and 11)
Effective Porosity Alluvium	Bedinger, et al. 1989 [129676] (HFM Units 19 and 7)	MO0105HCONEPOR.000 [155044] (HFM Units 19 and 7)
	EDCON 2000 [154704] (HFM Units 19 and 7)	MO0105GPLOG19D.000 [163480] (HFM Units 19 and 7)
	Burbey and Wheatcraft [129679] 1986 (HFM Units 19 and 7)	Burbey and Wheatcraft is considered Technical Information, no DTN. (HFM Units 19 and 7)
	DOE 1997 [103021], Table 8-2, p. 8-6, Table 8-1 p. 8-5 (HFM Units 19 and 7)	DOE 1997 is considered Technical Information, no DTN. (HFM Units 19 and 7)

Table 4-1.   Direct Inputs (Continued)

Data Name	Originating Report	DTN
Effective Porosity in the Other Units	Bedinger, et al. 1989 [129676] (HFM Units, 18, 17, 16, 6-2, 1)	MO0105HCONEPOR.000 [155044] (HFM Units, 18, 17, 16, 6-2, 1)
Bulk Density in the Volcanic Units	MDL-NBS-GS-000004 (HFM Units 15-13, 10-8) (BSC 2002 [159530]) OFR 94-469 (Buesch et al. 1996 [100106]); Flint 1998 [100033]; OFR 94-460 (Moyer and Geslin 1995 [101269]), (HFM Units 12 ,11 and 9) TDR-NBS-GS-000020, BSC 2001 [163479] (HFM Units 17, 12, 11, 6-2)	SN0004T0501399.002 [155046] (HFM Units 15-13, 10, 8) SN0004T0501399.003 [155045] (HFM Units 15-13, 10-8) MO0109HYMXPROP.001 [155989] (HFM Units 12 11, and 9) MO0010CPORGLOG.002 [155229] (HFM Units 17, 12 and 11, 6-2)
Effective Diffusion Coefficient	BSC 2001 [163566] (HFM Units 8-15)	MO0109HYMXPROP.001 [155989] (HFM Units 8-15)
Bulk Density - Alluvium	EDCON 2000 [154704] (HFM Units 19 and 7)	MO0105GPLOG19D.000 [163480] (HFM Units 19 and 7)
Flowing Interval Porosity in the Volcanic Units	BSC 2003 [161773], p. 41 and 64 (HFM Units 8-15) BSC 2003 [162415] DOE 1997 [103021], p. 5-14 (HFM Units 8-15)	Product Output, information not in DTN (HFM Units 8-15) LA0303PR831231.005 [166259] GS031008312315.002 [166261] Technical Information no DTN (HFM Units 8-15)
Lithostratigraphy in Wells EWDP-10SA and EWDP-22SA	N/A	GS030108314211.001 [163483]
Coordinates of Well Locations and Depth to Water Table	USGS 2001 [157611]	GS010908312332.002 [163555]
Uncertainty in Groundwater Specific Discharge	CRWMS M&O 1998 [100353]	MO0003SZFWTEEP.000 [148744]
Uncertainty in Groundwater Specific Discharge at the Alluvial Tracer Complex	BSC 2003 [162415]	LA0303PR831231.002 [163561]
UZ Site-Scale Model Flow Fields – Infiltration for Climate States	BSC 2003 [163045]	LB03023DSSCP9I.001 [163044]
Gross Alpha Concentrations in Groundwater	CRWMS M&O 1999 [150420], Section 3.2.1, Table 3	MO9904RWSJJS98.000 [165866]

NOTE: The column containing the originating report is provided for reference only. The direct source of the data used in this AMR is listed in the DTN column. The HFM Unit numbers given refer to the unit definitions in Table 6-9.

Other model input information is listed in Table 4-2.

Table 4-2. Other Model/Analysis Inputs

Input Name	Input Description	DTN / IED
Site-Scale Saturated Zone Transport Model	The SZ site-scale model that forms the basis of the SZ Transport Abstraction Model.	LA0306SK831231.001 [164362]
Matrix Diffusion Type Curves	The analytical solution type curves for matrix diffusion in fractured media. These type curves are used in the particle tracking algorithm of the FEHM software to simulate radionuclide transport in fractured porous media.	LA0302RP831228.001 [163557]
Repository Design	The coordinates of the outline of the repository design are used in defining the SZ source regions at the water table below the repository.	800-IED-EBS0-00401-000-00C, BSC 2003 [162289] 800-IED-EBS0-00402-000-00B, BSC 2003 [161727]
Boundary of Accessible Environment	Latitude of the accessible environment, as defined by regulation	10 CFR 63.302 [156605], regulatory input, technical information, no DTN

4.1.2 Parameters and Parameter Uncertainty

The parameters and parameter uncertainty from external sources used directly in the modeling documented in this report are shown in Table 4-3. Parameters are those variables that are used as direct inputs to the models documented in this report.

The input parameters are considered appropriate as direct input to the SZ Transport Abstraction Model and the SZ 1-D Transport Model. The data used in this report are appropriate for this study because they represent various parameter properties of the SZ at Yucca Mountain.

Table 4-3. Input Parameters

Parameter Name	Parameter Source	DTN	Value(s)		Units	Parameter Type
KDNPVO (neptunium sorption coefficient in volcanic units)	BSC 2003 [162419]	LA0310AM831341.002 [165891]	CDF:		ml/g	Distribution
			Probability	Value		
			0.0	0.0		
			0.05	0.99		
			0.90	1.83		
			1.0	6.0		
KDNPAL (neptunium sorption coefficient in alluvium)	BSC 2003 [162419]	LA0310AM831341.002 [165891]	CDF:		ml/g	Distribution
			Probability	Value		
			0.0	1.8		
			0.05	4.0		
			0.95	8.7		
			1.0	13.0		
KDSRVO (strontium sorption coefficient in volcanic units)	BSC 2003 [162419]	LA0310AM831341.002 [165891]	Uniform: Minimum 20. Maximum 400.		ml/g	Distribution
KDSRAL (strontium sorption coefficient in alluvium)	BSC 2003 [162419]	LA0310AM831341.002 [165891]	Uniform: Minimum 20. Maximum 400.		ml/g	Distribution
KDUVO (uranium sorption coefficient in volcanic units)	BSC 2003 [162419]	LA0310AM831341.002 [165891]	CDF:		ml/g	Distribution
			Probability	Value		
			0.0	0.0		
			0.05	5.39		
			0.95	8.16		
			1.0	20.0		
KDUAL (uranium sorption coefficient in alluvium)	BSC 2003 [162419]	LA0310AM831341.002 [165891]	CDF:		ml/g	Distribution
			Probability	Value		
			0.0	1.7		
			0.05	2.9		
			0.95	6.3		
			1.0	8.9		
KDRAVO (radium sorption coefficient in volcanic units)	BSC 2003 [162419]	LA0310AM831341.002 [165891]	Uniform: Minimum 100. Maximum 1000.		ml/g	Distribution

Table 4-3. Input Parameters (Continued)

Parameter Name	Parameter Source	DTN	Value(s)	Units	Parameter Type
KDRAAL (radium sorption coefficient in alluvium)	BSC 2003 [162419]	LA0310AM831341.002 [165891]	Uniform: Minimum 100. Maximum 1000.	ml/g	Distribution
KD_Pu_Vo (plutonium sorption coefficient in volcanic units)	BSC 2003 [162419]	LA0310AM831341.002 [165891]	CDF: Probability Value 0.0 10. 0.25 89.9 0.95 129.87 1.0 300.	ml/g	Distribution
KD_Pu_Al (plutonium sorption coefficient in alluvium)	BSC 2003 [162419]	LA0310AM831341.002 [165891]	Beta: Mean 100. Standard Deviation 15. Minimum 50. Maximum 300.	ml/g	Distribution
KD_Am_Vo (americium sorption coefficient in volcanic units)	BSC 2003 [162419]	LA0310AM831341.002 [165891]	Truncated Normal: Mean 5500. Standard Deviation 1500. Minimum 1000. Maximum 10000.	ml/g	Distribution
KD_Am_Al (americium sorption coefficient in alluvium)	BSC 2003 [162419]	LA0310AM831341.002 [165891]	Truncated Normal: Mean 5500. Standard Deviation 1500. Minimum 1000. Maximum 10000.	ml/g	Distribution
KD_Cs_Vo (cesium sorption coefficient in volcanic units)	BSC 2003 [162419]	LA0310AM831341.002 [165891]	CDF: Probability Value 0.0 100. 0.05 3000.59 1.0 6782.92	ml/g	Distribution
KD_Cs_Al (cesium sorption coefficient in alluvium)	BSC 2003 [162419]	LA0310AM831341.002 [165891]	Truncated Normal: Mean 728. Standard Deviation 464. Minimum 100. Maximum 1000.	ml/g	Distribution

Table 4-3. Input Parameters (Continued)

Parameter Name	Parameter Source	DTN	Value(s)	Units	Parameter Type
FISVO (flowing interval spacing in the volcanic units)	BSC 2001 [156965]	SN9907T0571599.001 [122261]	CDF: (Log$_{10}$-transformed) Probability Value 0.0 0.087 0.05 0.588 0.25 1.00 0.50 1.29 0.75 1.58 0.95 1.90 1.0 2.62	m	Distribution
CORAL (colloid retardation factor in the alluvium)	BSC 2003 [162729]	LA0303HV831352.004 [163559]	CDF : (Log$_{10}$-transformed) Probability Value 0.0 0.903 0.331 0.904 0.50 1.531 1.0 3.715	NA	Distribution
CORVO (colloid retardation factor in the volcanic units)	BSC 2003 [162729]	LA0303HV831352.002 [163558]	CDF : (Log$_{10}$-transformed) Probability Value 0.0 0.778 0.15 0.779 0.25 1.010 0.50 1.415 0.80 1.778 1.0 2.903	NA	Distribution
HAVO (ratio of horizontal anisotropy in permeability)	BSC 2003 [162415]	SN0302T0502203.001 [163563]	CDF : Probability Value 0.0 0.05 0.10 1.0 0.60 5. 1.0 20.	NA	Distribution
LDISP (longitudinal dispersivity)	CRWMS M&O 1998 [100353]	MO0003SZFWTEEP.000 * [148744]	Truncated Normal: (Log$_{10}$-transformed) Mean 2.0 Standard Deviation 0.75	m	Distribution
Kd_Pu_Col (plutonium sorption coefficient onto colloids)	BSC 2003 [161620]	SN0306T0504103.006 [164131]	CDF: Probability Value 0.0 1.e3 0.04 5.e3 0.12 1.e4 0.37 5.e4 0.57 1.e5 0.92 5.e5 1.0 1.e6	ml/g	Distribution

Table 4-3. Input Parameters (Continued)

Parameter Name	Parameter Source	DTN	Value(s)		Units	Parameter Type
Kd_Am_Col (americium sorption coefficient onto colloids)	BSC 2003 [161620]	SN0306T0504103.006 [164131]	CDF: Probability Value 0.0 1.e4 0.07 5.e4 0.17 1.e5 0.40 5.e5 0.60 1.e6 0.92 5.e6 1.0 1.e7		ml/g	Distribution
Kd_Cs_Col (cesium sorption coefficient onto colloids)	BSC 2003 [161620]	SN0306T0504103.006 [164131]	CDF: Probability Value 0.0 1.e2 0.2 5.e2 0.45 1.e3 0.95 5.e3 1.0 1.e4		ml/g	Distribution
Conc_Col (groundwater concentration of colloids)	BSC 2003 [161620]	SN0306T0504103.005 [164132]	CDF: (Log_{10}-transformed) Probability Value 0.0 -9.0 0.50 -7.0 0.75 -6.0 0.90 -5.0 0.98 -4.3 1.0 -3.6		g/ml	Distribution
Correlation coefficient for U K_d in volcanic units and alluvium	BSC 2003 [162419]	LA0310AM831341.002 [165891]	0.75		ml/g	Single Value
Correlation coefficient for Np K_d in volcanic units and alluvium	BSC 2003 [162419]	LA0310AM831341.002 [165891]	0.75		ml/g	Single Value
Correlation coefficient for Pu K_d in volcanic units and alluvium	BSC 2003 [162419]	LA0310AM831341.002 [165891]	0.50		ml/g	Single Value
Correlation coefficient for U K_d and Np K_d	BSC 2003 [162419]	LA0310AM831341.002 [165891]	0.50		ml/g	Single Value

NOTE: MO0003SZFWTEEP.000 [148744] contains qualified data from an Expert Elicitation that was determined to comply with Expert Elicitation Procedure AP-AC.1Q [138711], which is consistent with the Branch Technical Position on Expert Elicitation NUREG-1563 (Kotra et al. 1996 [100909]).

4.2 CRITERIA

The general requirements to be satisfied by the TSPA are stated in 10 CFR 63.114 (10 CFR 63 [156605]).   Technical requirements to be satisfied by the TSPA are identified in the *Yucca Mountain Project Requirements Document* (Canori and Leitner 2003 [161770], Table B-9). The acceptance criteria that will be used by the Nuclear Regulatory Commission (NRC) to determine whether the technical requirements have been met are identified in the *Yucca Mountain Review Plan, Final Report* (YMRP; NRC 2003 [163274]).   The pertinent requirements and criteria for this report are summarized in Table 4-4.

Table 4-4. Project Requirements for This Model Report

Requirement Number[a]	Requirement Title[a]	10 CFR 63 Link [156605]	YMRP Acceptance Criteria[b]
PRD-002/T-014	Performance Objectives for the Geologic Repository After Permanent Closure	10 CFR 63.113	2.2.1.1.3, criteria 1 to 3
PRD -002/T-015	Requirements for Performance Assessment	10 CFR 63.114	2.2.1.3.8.3, criteria 1 to 4; 2.2.1.3.9.3, criteria 1 to 5
PRD -002/T-016	Requirements for Multiple Barriers	10 CFR 63.115	2.2.1.1.3, criteria 1 to 3

NOTES: [a] from Canori and Leitner 2003 [161770].

       [b] from NRC 2003 [163274]

The acceptance criteria identified in Sections 2.2.1.1.3, 2.2.1.3.8.3, and 2.2.1.3.9.3 of the YMRP (NRC 2003 [163274]) are given below, followed by a short description of their applicability to this model report. Criteria item numbers not shown are considered to not apply to this model.

Section 2.2.1.1.3 *Acceptance Criteria* [for 2.2.1.1 *System Description and Demonstration of Multiple Barriers*], which are based on meeting the requirements at 10 CFR 63.113(a) and 63.115(a)–(c):

- Acceptance Criterion 1, Identification of Barriers is Adequate

   Barriers relied on to achieve compliance with 10 CFR 63.113(b), as demonstrated in the total system performance assessment, are adequately identified, and are clearly linked to their capability. The barriers identified include at least one from the engineered system and one from the natural system.

   This model report describes the SZ radionuclide transport simulation results for use in the TSPA calculation.   This includes the 1-D model description, which is incorporated in the TSPA calculations to simulate transport, decay, and ingrowth of radionuclide decay chains in the SZ. Also discussed in Section 6.5.2 is the analysis of uncertainty in input parameters for the SZ Transport Abstraction Model and for the SZ 1-D Transport Model.

- Acceptance Criterion 2, Description of Barrier Capability to Isolate Waste is Acceptable

  The capability of the identified barriers to prevent or substantially reduce the rate of movement of water or radionuclides from the Yucca Mountain Repository is adequately identified and described:

  1. The information on the time period over which the SZ barrier performs its intended function, including any changes during the compliance period, is provided in Section 6.7.

  2. The uncertainty associated with barrier capabilities is adequately described in Section 6.7.

- Acceptance Criterion 3, Technical Basis for Barrier Capability is Adequately Presented

  The technical bases are consistent with the technical basis for the performance assessment, although not explicitly addressed in this report it is addressed in the TSPA. The technical basis for assertions of barrier capability is commensurate with the importance of each barrier's capability and the associated uncertainties.

Section 2.2.1.3.8.3 *Acceptance Criteria* (for 2.2.1.3.8 *Flow Paths in the Saturated Zone*), which are based on meeting the requirements of 10 CFR 63.114(a)–(c) and (e)–(g), relating to flow paths in the saturated zone model abstraction:

- Acceptance Criterion 1, System Description and Model Integration are Adequate:

  2. The description of the aspects of hydrology, geology, geochemistry, design features, physical phenomena, and couplings that may affect flow paths in the saturated zone is adequate. Conditions and assumptions in the abstraction of flow paths in the saturated zone are readily identified and consistent with the body of data presented in the description (see Section 6.3).

  3. The abstraction of flow paths in the saturated zone uses assumptions, technical bases, data, and models that are appropriate and consistent with other related DOE abstractions. For example, the assumptions used for flow paths in the saturated zone are consistent with the total system performance assessment abstraction of representative volume (Section 2.2.1.3.12 of NRC 2003 [163274]). The descriptions and technical bases provide transparent and traceable support for the abstraction of flow paths in the saturated zone (see Section 6.3).

  5. Sufficient data and technical bases to assess the degree to which features, events, and processes have been included in this abstraction are provided (see Section 6.2).

  7. Long-term climate change, based on known patterns of climatic cycles during the Quaternary period, particularly the last 500,000 years, and other paleoclimate data, are adequately evaluated (see the introductory text in Section 6.5).

  10. Guidance in NUREG-1297 (Altman et al. 1988 [103597]) and NUREG-1298 (Altman et al. 1988 [103750]) or other acceptable approaches for peer review and data qualification is followed (see Section 6.5.2.1).

- Acceptance Criterion 2, Data are Sufficient for Model Justification:

    1. Geological, hydrological, and geochemical values used in the safety case to evaluate flow paths in the saturated zone are adequately justified. Adequate descriptions of how the data were used, interpreted, and appropriately synthesized into the parameters are provided, as described in Section 6.5.2.

    3. Data on the geology, hydrology, and geochemistry of the saturated zone used in the total system performance assessment abstraction are based on appropriate techniques. These techniques may include laboratory experiments, site-specific field measurements, natural analog research, and process-level modeling studies (see Section 6.5.2).

- Acceptance Criterion 3, Data Uncertainty is Characterized and Propagated Through the Model Abstraction:

    1. Models use parameter values, assumed ranges, probability distributions, and/or bounding assumptions that are technically defensible, and reasonably account for uncertainties and variabilities (see Section 6.5.2).

    2. Uncertainty is appropriately incorporated in model abstractions of hydrologic effects of climate change, based on a reasonably complete search of paleoclimate data (see the introduction to Section 6.5).

    3. Uncertainty is adequately represented in parameter development for conceptual models, process-level models, and alternative conceptual models considered in developing the abstraction of flow paths in the saturated zone (see Section 6.5.2).

    4. Where sufficient data do not exist, the definition of parameter values and conceptual models is based on appropriate use of expert elicitation, conducted in accordance with NUREG-1563 (Kotra et al. 1996 [100909]) (see Section 6.5.2.1).

- Acceptance Criterion 4, Model Uncertainty is Characterized and Propagated Through the Model Abstraction:

    1. Alternative modeling approaches of features, events, and processes are considered and are consistent with available data and current scientific understanding, and the results and limitations are appropriately considered in the abstraction (see Section 6.2).

    2. Conceptual model uncertainties are adequately defined and documented, and effects on conclusions regarding performance are properly assessed (see Section 6.4).

    4. Appropriate alternative modeling approaches are consistent with available data and current scientific knowledge and appropriately consider their results and limitations, using tests and analyses that are sensitive to the processes modeled, as described in Section 6.4.

- Acceptance Criterion 5, Model Abstraction Output Is Supported by Objective Comparisons:

    1. The models implemented in this total system performance assessment abstraction provide results consistent with output from detailed process-level models and/or empirical observations (laboratory and field testing and/or natural analogs) (see Section 7).

    2. Outputs of flow paths in the saturated zone abstractions reasonably produce or bound the results of corresponding process-level models, empirical observations, or both (see Sections 6.6 and 7).

    3. Well-documented procedures that have been accepted by the scientific community to construct and test the mathematical and numerical models are used to simulate flow paths in the saturated zone (Section 7).

Section 2.2.1.3.9.3 *Acceptance Criteria* [for 2.2.1.3.9 *Radionuclide Transport in the Saturated Zone*], which are based on meeting the requirements of 10 CFR 63.114(a)–(c) and (e)–(g), relating to the radionuclide transport in the saturated zone model abstraction:

- Acceptance Criterion 1, System Description and Model Integration are Adequate:

    2. The description of the aspects of hydrology, geology, geochemistry, design features, physical phenomena, and couplings that may affect radionuclide transport in the saturated zone is adequate, as described in Section 6.3

    3. The abstraction of radionuclide transport in the saturated zone uses assumptions, technical bases, data, and models that are appropriate and consistent with other related DOE abstractions (see Section 6.5).

    4. Boundary and initial conditions used in the abstraction of radionuclide transport in the saturated zone are propagated throughout its abstraction approaches (see Section 6.3).

    5. Sufficient data and technical bases for the inclusion of features, events, and processes related to radionuclide transport in the saturated zone in the total system performance assessment abstraction are provided, as described in Section 6.2.

    6. Guidance in NUREG-1297 (Altman et al. 1988 [103597]) and NUREG-1298 (Altman et al. 1988 [103750]) or other acceptable approaches for peer review and data qualification is followed (see Section 6.5.2.9).

- Acceptance Criterion 2, Data are Sufficient for Model Justification:

    1. Geological, hydrological, and geochemical values used in the safety case are adequately justified (e.g., flow path lengths, sorption coefficients, retardation factors, colloid concentrations, etc.). Adequate descriptions of how the data were used, interpreted, and appropriately synthesized into the parameters are provided (see Section 6.5.2).

- Acceptance Criterion 3, Data Uncertainty is Characterized and Propagated Through the Model Abstraction:

  1. Models use parameter values, assumed ranges, probability distributions, and/or bounding assumptions that are technically defensible, and reasonably account for uncertainties and variabilities (see Section 6.5.2).

  4. Parameter values for processes, such as matrix diffusion, dispersion, and groundwater mixing, are based on reasonable assumptions about climate, aquifer properties, and groundwater volumetric fluxes (Section 2.2.1.3.8 of NRC 2003 [163274]) (see Section 6.5.2).

  5. Uncertainty is adequately represented in parameter development for conceptual models, process-level models, and alternative conceptual models considered in developing the abstraction of radionuclide transport in the saturated zone (see Sections 6.3 and 6.5.2).

  6. Where sufficient data do not exist, the definition of parameter values and conceptual models is based on appropriate use of expert elicitation, conducted in accordance with NUREG-1563 (Kotra et al. 1996 [100909]) (see Section 6.5.2.9).

- Acceptance Criterion 4, Model Uncertainty is Characterized and Propagated Through the Model Abstraction:

  1. Alternative modeling approaches of features, events, and processes are considered and are consistent with available data and current scientific understanding, and the results and limitations are appropriately considered in the abstraction (see Section 6.2).

  2. Conceptual model uncertainties are adequately defined and documented, and effects on conclusions regarding performance are properly assessed (see Section 6.4).

  4. Appropriate alternative modeling approaches are consistent with available data and current scientific knowledge and appropriately consider their results and limitations, using tests and analyses that are sensitive to the processes modeled (see Section 6.4).

- Acceptance Criterion 5, Model Abstraction Output is Supported by Objective Comparisons:

  2. Outputs of radionuclide transport in the saturated zone abstractions reasonably produce or bound the results of corresponding process-level models, empirical observations, or both (see Section 7).

  3. Well-documented procedures that have been accepted by the scientific community to construct and test the mathematical and numerical models are used to simulate radionuclide transport through the saturated zone (see Sections 6.5 and 7).

  4. Sensitivity analyses or bounding analyses are provided, to support the total system performance assessment abstraction of radionuclide transport in the saturated zone, that cover ranges consistent with site data, field or laboratory experiments and tests, and natural analog research (see Section 7).

4.3 CODES AND STANDARDS

No specific formally established codes or standards have been identified as applying to this modeling activity. This activity does not directly support License Application (LA) design.

5. ASSUMPTIONS

There are several types of assumptions related to model development. The assumptions listed in this section of the AMR are restricted to those that meet the definition given in the quality assurance procedure AP-SIII.10Q, *Models* [165553], Section 3.2. This definition states that an assumption is "a statement or proposition that is taken to be true or representative in the absence of direct confirming data or evidence." There are additional technical modeling bases (assumptions) related to the modeling framework that are documented in Section 6 of this AMR (primarily in Section 6.3).

1. For the transport of radionuclides irreversibly attached to colloids in the SZ, it is assumed that radionuclides will not desorb from colloids. This assumption is carried forward from the *Saturated Zone Colloid Transport* scientific analysis report (BSC 2003 [162729], Section 6.3) and is consistent with the mineralogic characteristics of colloids from the degradation of the glass waste form. This assumption is also conservative with regard to repository performance due to the comparatively high mobility of colloids in the SZ relative to the sorptive characteristics of the radionuclides (Pu and Am) that are subject to colloid-facilitated transport. This assumption is used in Sections 6.3.1, 6.3.2, 6.5.1, and 6.5.2.11. This assumption needs no further confirmation, given that it is a bounding assumption that maximizes the rate of radionuclide migration in the SZ.

2. Colloids with irreversibly attached radionuclides are assumed to be subject to attachment and detachment to mineral grains in the aquifer, but not to be subject to permanent filtration from the groundwater of the SZ. This assumption is carried forward from the *Saturated Zone Colloid Transport* scientific analysis report (BSC 2003 [162729], Section 6.3). The kinetically controlled attachment and detachment of colloids in the aquifer is consistent with tracer testing in the SZ using microspheres. The permanent filtration of colloids in the SZ has not been demonstrated by field testing, although this process may occur. The alternative to this assumption, in which permanent filtration were simulated to occur, would lead to significant attenuation of the migration of radionuclides irreversibly attached to colloids. This assumption is used in Sections 6.3.1, 6.3.2, 6.5.1, and 6.5.2.11. This assumption needs no further confirmation, given that it is a bounding assumption that maximizes the migration of radionuclides in the SZ.

3. The assumption is made that the average concentration of radionuclides in the groundwater supply of the hypothetical community in which the reasonably maximally exposed individual (RMEI) resides is an appropriate estimate of radionuclide concentration for the calculation of radiological dose. Realistically, the concentrations of radionuclides encountered by wells in the hypothetical community in which the RMEI resides would vary from location to location within the contaminant plume in the SZ. However, radionuclide transfer processes within the biosphere (e.g., redistribution of agricultural products, communal water supplies, etc.) would tend to average the overall dose received by the population of the community in which the RMEI resides. This assumption is used in Section 6.3.3. This assumption needs no further confirmation, given that there is a regulatory basis for this approach to calculating average concentrations of radionuclides and radiological dose at 10 CFR 63.332 (10 CFR 63 [156605]).

4. The assumption is made that the horizontal anisotropy in permeability applies to the fractured and faulted volcanic units of the SZ system along the groundwater flow path from the repository to the south and east of Yucca Mountain. This assumption is carried forward from the *Saturated Zone In-Situ Testing* scientific analysis report (BSC 2003 [162415], Section 6.2.6). The inferred flowpath from beneath the repository extends to the south and east. This is the area in which pumping tests were conducted at the C-holes well complex (BSC 2003 [162415]), from which horizontal anisotropy was inferred. Given the conceptual basis for the anisotropy model, it is appropriate to apply anisotropy only to those hydrogeologic units that are dominated by groundwater flow in fractures. This assumption is used in Section 6.5.2.10. This assumption needs no further confirmation, given the wide range of uncertainty in horizontal anisotropy used in the SZ Transport Abstraction Model.

5. It is assumed that the change in groundwater flow in the SZ from one climatic state to another occurs rapidly and is approximated by an instantaneous shift from one steady-state flow condition to another steady-state flow condition. In reality, even an extremely rapid shift in climatic conditions would result in a transient response of the SZ flow system because of changes in groundwater storage associated with water table rise or fall and because of the response time in the UZ flow system. The assumption of instantaneous shifts to new steady-state conditions would tend to overestimate the rate of radionuclide transport in the TSPA calculations. The progression of climate states in the 10,000 years following repository closure is anticipated to be from drier to wetter climatic conditions and thus from slower to more rapid groundwater flow in the SZ. By assuming an instantaneous shift to higher groundwater flux in the SZ the simulations tend to overestimate the radionuclide transport velocities during the period of transition from drier conditions to wetter conditions. This assumption is used in Section 6.5. This assumption needs no further confirmation, given that this simplified approach tends to underestimate the transport times for radionuclides in the SZ and is thus pessimistic with regard to repository performance.

6. Groundwater flow pathways in the SZ from beneath the repository to the accessible environment are assumed not to be significantly altered for wetter climatic states. Scaling of present-day groundwater flux and radionuclide mass breakthrough curves by a proportionality factor implies that only the groundwater velocities are changed in the SZ system in response to climate change. This assumption is supported by the observation that the shape of the simulated potentiometric surface downgradient from Yucca Mountain remains basically the same under glacial-transition climatic conditions in simulations using the SZ regional-scale flow model (D'Agnese et al. 1999 [120425], p. 30). Water table rise directly beneath the repository under wetter climatic conditions would tend to place volcanic units higher in the stratigraphic sequence at or just below the water table. These higher volcanic units (Prow Pass Tuff and Calico Hills Formation) have lower values of permeability than the underlying Bullfrog Tuff. This approximation of climate change with unaltered SZ flow paths is shown to underestimate radionuclide transport times in sensitivity studies documented in BSC 2003 [162419], Attachment V. This assumption is used in Section 6.5. This assumption needs no further confirmation, given that this simplified approach tends to underestimate the transport times for radionuclides in the SZ.

6. MODELS DISCUSSION

6.1 MODELING OBJECTIVES

The primary objective of the SZ Transport Abstraction Model and the SZ 1-D Transport Model is to provide a method of simulating radionuclide transport in the SZ for use in the TSPA Model of repository performance. Analyses of parameter uncertainty and multiple realizations of the SZ system using the SZ Transport Abstraction Model constitute an assessment of uncertainty in the SZ system for direct implementation in the TSPA model. The general approach to modeling radionuclide migration and the assessment of uncertainty in the SZ is also described by Arnold et al. 2003 [163857]. The objective of the SZ 1-D Transport Model is to provide a simplified, yet accurate representation of SZ transport for the simulation of four radionuclide decay chains for implementation with the TSPA model.

In the TSPA analyses the convolution integral method is used by the SZ Transport Abstraction Model to determine the radionuclide mass flux at the SZ/biosphere interface, 18 km downgradient of the repository at 36°40'13.6661" North latitude (10 CFR 63.302 (10 CFR 63 [156605])) as a function of the transient radionuclide mass flux at the water table beneath the repository. This computationally efficient method combines information about the unit response of the system, as simulated by the SZ Transport Abstraction Model, with the radionuclide source history from the UZ to calculate transient system behavior. The fundamental concepts of the convolution integral method, as applied to solute transport in groundwater, are presented by Jury et al. 1986 [164314], in which the method is called the transfer function model. The most important assumptions of the convolution method are linear system behavior and steady-state flow conditions in the saturated zone.

The SZ 1-D Transport Model is used in the TSPA analyses for the purpose of simulating radioactive decay and ingrowth for four decay chains. This simplified model is required because the radionuclide transport methodology used in the SZ Transport Abstraction Model is not capable of simulating ingrowth by radioactive decay. Although it is not anticipated that the decay products generated from these radioactive decay chains during transport in the SZ are significant contributors to the total radiological dose, regulations concerning groundwater protection contained in 10 CFR 63.331 (10 CFR 63 [156605]) require explicit analysis of the total concentrations of Ra-226 plus Ra-228, gross alpha emitters, and beta plus photon emitters in the water supply of the RMEI. Consequently, only the results for decay product-radionuclides from the SZ 1-D Transport Model are input to the TSPA simulations. Although transport of the parent radionuclides is also included in the SZ 1-D Transport Model, the results for parent-radionuclides input to the TSPA simulations are those derived from the SZ Transport Abstraction Model. The SZ 1-D Transport Model for TSPA differs from the SZ Transport Abstraction Model in that it is implemented directly with the GoldSim v. 7.50.100 software code (STN: 10344-7.50.100-00, BSC 2003 [161572]) in the TSPA model.

6.2 FEATURES, EVENTS, AND PROCESSES FOR THIS MODEL REPORT

The development of a comprehensive list of FEPs potentially relevant to post-closure performance of the potential Yucca Mountain repository is an ongoing, iterative process based on site-specific information, design, and regulations. The approach for developing an initial list of FEPs in support of the TSPA-SR (CRWMS M&O 2000 [153246]) was documented by Freeze et al. 2001 [154365]. The initial FEPs list contained 328 FEPs, of which 176 were included in TSPA-SR models (CRWMS M&O 2000 [153246], Tables B-9 through B-17). To support the TSPA-LA, the FEPs list was re-evaluated in accordance with *The Enhanced Plan for Features, Events, and Processes (FEPs) at Yucca Mountain* (BSC 2002 [158966], Section 3.2). The included FEPs abstractions incorporated in the TSPA-LA model, which are implemented through specific process models or input parameters, are specifically addressed in saturated zone model reports (Table 6-1). The rationale for excluding a FEP from the TSPA-LA model will be given in the upcoming revision (REV02) of *Features, Events, and Processes in SZ Flow and Transport* (CRWMS M&O 2001 [153931]). The assignments of included FEPs to SZ reports for documentation are found in the *Technical Work Plan For: Saturated Zone Flow and Transport Modeling and Testing*, TWP-NBS-MD-000002 (BSC 2003 [166034], Section 2.5).

Table 6-1.   Included FEPs for the Saturated Zone TSPA-LA

FEP Number	FEP Name	Responsible SZ Report
1.2.02.01.0A	Fractures	this report
1.2.02.02.0A	Faults	this report
1.4.07.01.0A	Water Management Activities	this report
1.4.07.02.0A	Wells	this report
2.2.03.01.0A	Stratigraphy	*Site-Scale Saturated Zone Flow Model*, (BSC 2003 [162649])
2.2.03.02.0A	Rock Properties of Host Rock and Other Units	this report
2.2.07.12.0A	Saturated Groundwater Flow in the Geosphere	*Site-Scale Saturated Zone Flow Model*, (BSC 2003 [162649])
2.2.07.13.0A	Water-Conducting Features in the SZ	this report
2.2.07.15.0A	Advection and Dispersion in the SZ	*Site-Scale Saturated Zone Transport*, (BSC 2003 [162419])
2.2.07.16.0A	Dilution of Radionuclides in Groundwater	this report
2.2.07.17.0A	Diffusion in the SZ	*Site-Scale Saturated Zone Transport*, (BSC 2003 [162419])
2.2.08.01.0A	Chemical Characteristics of Groundwater in the SZ	*Site-Scale Saturated Zone Transport*, (BSC 2003 [162419])
2.2.08.06.0A	Complexation in the SZ	*Site-Scale Saturated Zone Transport*, (BSC 2003 [162419])
2.2.08.08.0A	Matrix Diffusion in the SZ	*Site-Scale Saturated Zone Transport*, (BSC 2003 [162419])
2.2.08.09.0A	Sorption in the SZ	*Site-Scale Saturated Zone Transport*, (BSC 2003 [162419])

Table 6-1. Included FEPs for the Saturated Zone TSPA-LA (Continued)

FEP Number	FEP Name	Responsible SZ Report
2.2.08.10.0A	Colloid Transport in the SZ	this report
2.2.08.11.0A	Groundwater Discharge to Surface Within the Reference Biosphere	this report
2.2.10.03.0A	Natural Geothermal Effects on Flow in the SZ	*Site-Scale Saturated Zone Flow Model*, (BSC 2003 [162649])
2.2.12.00.0B	Undetected Features in the SZ	this report
3.1.01.01.0A	Radioactive Decay and Ingrowth	this report

Table 6-2 lists the FEPs included in the TSPA-LA for which this model report provides the technical basis and provides a summary of their disposition in TSPA-LA. Table 6-3 lists the FEPs that are partially addressed by results of this model report. These results are used elsewhere (as shown in Table 6-1) to determine the include/exclude status of the FEP and/or its implementation in TSPA-LA. Details of the implementation of these FEPs are summarized in Sections 5, 6.3, 6.5, and 6.7.

Table 6-2. Saturated Zone Included FEPs for Which This Model Report Provides the Technical Basis

FEP Number and Name	FEP Description	Section in Report Where FEP Discussed	Disposition in TSPA-LA
1.2.02.01.0A Fractures	Groundwater flow in the Yucca Mountain region and transport of any released radionuclides may take place along fractures. The rate of flow and the extent of transport in fractures are influenced by characteristics such as orientation, aperture, asperity, fracture length, connectivity, and the nature of any linings or infills.	6.5.2.1, 6.5.2.4, 6.5.2.5, 6.5.2.9, 6.5.2.10, 6.5.2.12 6.5.2.15	The SZ Transport Abstraction Model includes fractures and uncertainty in the hydraulic and transport properties of the fracture system in volcanic units along the flow path from beneath the repository. The characteristics of the fracture properties such as fracture orientation, connectivity, aperture size, degree of infilling, and tortuosity are modeled in the SZ Transport Abstraction Model and the SZ 1-D Transport Model through the following probabilistically modeled parameters: flowing interval porosity (FPVO), flowing interval spacing (FISVO), groundwater specific discharge (GWSPD), longitudinal dispersivity (LDISP), horizontal anisotropy (HAVO), and colloid retardation (CORVO).
1.2.02.02.0A Faults	Numerous faults of various sizes have been noted in the Yucca Mountain Region and in the repository area in specific. Faults may represent an alteration of the rock permeability and continuity of the rock mass, alteration or short-circuiting of the flow paths and flow distributions close to the repository, and represent unexpected pathways through the repository.	6.5.2.1 6.5.2.10	Geologic features and hydrostratigraphic units are explicitly included in the SZ Transport Abstraction Model in a configuration that accounts for the effects of existing faults, based on the hydrogeologic framework model. Model configuration of these discrete features is developed in the SZ Site-Scale Flow Model (BSC 2003 [162649], Section 6.3.2). The offsets of hydrostratigraphic units across major faults are incorporated into the model, and some key faults (e.g., Solitario Canyon fault, Highway 95 fault, and Fortymile Wash structure) are explicitly included as high- or low-permeability features. Model parameters, including horizontal anisotropy (HAVO) and groundwater specific discharge (GWSPD), implicitly include the potential impacts of faults on groundwater flow and are modeled probabilistically to account for the uncertainty in hydraulic properties associated with faults and fractures in the volcanic units.
1.4.07.01.0A Water Management Activities	Water management is accomplished through a combination of dams, reservoirs, canals, pipelines, and collection and storage facilities. Water management activities could have a major influence on the behavior and transport of contaminants in the biosphere.	6.3.4, 6.5.1.3, 6.5.3.3, 6.7	The effects of existing water management activities on the saturated flow system, while not directly quantifiable, are implicitly incorporated in the calibrated heads of the SZ flow model. Future water management activities, other than future well withdrawal rates specifically covered in 10 CFR Section 63.332, are presumed to be those currently in practice as stated by regulation Section 63.305 [156605]

Table 6-2. Saturated Zone Included FEPs for Which This Model Report Provides the Technical Basis (Continued)

FEP Number and Name	FEP Description	Section in Report Where FEP Discussed	Disposition in TSPA-LA
1.4.07.02.0A Wells	One or more wells drilled for human use (e.g., drinking water, bathing) or agricultural use (e.g., irrigation, animal watering) may intersect the contaminant plume. The plume may include radionuclides that have leached out of the soil and back into the groundwater.	5. 6.3.3	The effects of wells on the dose to the RMEI are included through the volume of contaminated groundwater used by the population of the hypothetical community in which the RMEI resides. The groundwater system in the vicinity of the well system of the hypothetical community in which the RMEI resides is modeled assuming that all the contaminants discharged at the 18-km boundary are intercepted by the community's wells. The total volume extracted from all wells to be used by the community in which the RMEI resides is 3,000 acre-feet per year (per guidance given in 10 CFR Part 63 Subpart 63.332, (3) [156605]).
2.2.03.02.0A Rock Properties of Host Rock and Other Units	Physical properties such as porosity and permeability of the relevant rock units, soils, and alluvium are necessary for the performance assessment. Possible heterogeneities in these properties should be considered. Questions concerning events and processes that may cause these physical properties to change over time are considered in other FEPs.	6.5.2.1, 6.5.2.2, 6.5.2.3, 6.5.2.4, 6.5.2.5, 6.5.2.7, 6.5.2.8, 6.5.2.9 6.5.2.10	Geologic features and heterogeneous hydrostratigraphic units are explicitly included in the SZ Transport Abstraction Model as cells with specific hydrologic parameter values in a configuration based on the hydrogeologic framework used in the SZ Site-Scale Flow Model (BSC 2003 [162649], Section 6.3.2). Spatial variability in rock properties is encompassed within uncertainty distributions for key parameters, such as groundwater specific discharge (GWSPD), horizontal anisotropy (HAVO), flowing interval spacing (FISVO), and sorption coefficients. Uncertainty in the location of the contact between alluvium and volcanic units at the southern end of the site-scale model is modeled probabilistically using the parameters related to the northern and western boundaries of the alluvial uncertainty zone, respectively (FPLAN and FPLAW).

Table 6-2. Saturated Zone Included FEPs for Which This Model Report Provides the Technical Basis (Continued)

FEP Number and Name	FEP Description	Section in Report Where FEP Discussed	Disposition in TSPA-LA
2.2.07.13.0A Water-Conducting Features in the SZ	Geologic features in the saturated zone may affect groundwater flow by providing preferred pathways for flow.	6.5.2.1, 6.5.2.4, 6.5.2.5, 6.5.2.9, 6.5.2.10	Groundwater flow in fractures of the volcanic units is an explicit feature of the SZ Transport Abstraction Model and the SZ 1-D Transport Model. These models simulate saturated flow and advective transport through flowing intervals, a subset of water-conducting features within the fracture system. The uncertainty in the system is represented in the model using probabilistic simulations of flowing interval porosity (FPVO), flowing interval spacing (FISVO), groundwater specific discharge (GWSPD), longitudinal dispersivity (LDISP), and horizontal anisotropy (HAVO). The ranges of uncertainty in these parameters encompass the possibility of channelized flow along preferred pathways.
2.2.07.16.0A Dilution of Radionuclides in Groundwater	Dilution due to mixing of contaminated and uncontaminated water may affect radionuclide concentrations in groundwater during transport in the saturated zone and during pumping at a withdrawal well.	5., 6.5.2.9, 6.7.2	The process of transverse hydrodynamic dispersion is explicitly incorporated in the SZ Transport Abstraction Model, leading to dilution of simulated contaminant concentrations. Dilution as a result of pumping is implicitly included in the TSPA exposure model. The SZ Transport Abstraction Model is used to estimate the flux of contaminants into the volume of water consumed in the regulatory-mandated exposure scenario. The volume of water (per guidance given in 10 CFR Part 63 Subpart 63.332, (3) [156605]) pumped from the hypothetical community in which the RMEI resides is 3000 acre-feet (about 3.7×10^9 liters) which is larger than the simulated volumetric flow of contaminated groundwater crossing the 18 km boundary. Therefore, the degree of dilution is the ratio of the flux of contaminated groundwater to volume of water pumped by the hypothetical community in which the RMEI resides.

Table 6-2. Saturated Zone Included FEPs for Which This Model Report Provides the Technical Basis (Continued)

FEP Number and Name	FEP Description	Section in Report Where FEP Discussed	Disposition in TSPA-LA
2.2.08.10.0A Colloidal Transport in the SZ	Radionuclides may be transported in groundwater in the SZ as colloidal species. Types of colloids include true colloids, pseudo colloids, and microbial colloids.	6.3.1, 6.5.1, 6.5.2.11, 6.5.2.12	The colloid-facilitated transport of radionuclides is explicitly included in the SZ Transport Abstraction Model and the SZ 1-D Transport Model. Colloids are subject to advection in the fractures of tuff units and are excluded from diffusion into the rock matrix. Radionuclide transport in association with colloids is simulated to occur by two modes: 1) as reversibly sorbed onto colloids, and 2) as irreversibly attached to colloids. Reversible sorption of radionuclides may occur onto any colloidal material present in the groundwater, and measurements of natural colloids in groundwater of the SZ include mineral and microbial colloids. Colloids with irreversibly attached radionuclides originate from the degradation of the glass waste form in the repository. The parameters related to reversible sorption onto colloids are Kd_Am_Col, Kd_Pu_Col, Kd_Cs_Col, and Conc_Col. The parameters related to the retardation of colloids with irreversibly attached radionuclides are CORVO and CORAL.
2.2.08.11.0A Groundwater Discharge to Surface Within the Reference Biosphere	Radionuclides transported in groundwater as solutes or solid materials (colloids) from the far field to the biosphere will discharge at specific "entry" points that are within the reference biosphere. Natural surface discharge points, including those resulting from water table or capillary rise, may be surface water bodies (rivers, lakes), springs, wetlands, holding ponds, or unsaturated soils.	5, 6.3.3	The groundwater system in the vicinity of the well system of the hypothetical community in which the RMEI resides is modeled such that all the contaminants discharged at the 18-km boundary are intercepted by the community's wells. Direct discharge of groundwater to the surface via springs, unsaturated soils, etc. is not included, given the simplifying assumption of complete capture of the contaminant plume in the wells.
2.2.12.00.0B Undetected Features in the SZ	This FEP is related to undetected features in the SZ portion of the geosphere that can affect long-term performance of the disposal system. Undetected but important features may be present and may have significant impacts. These features include unknown active fracture zones, inhomogeneities, faults and features connecting different zones of rock, and different geometries for fracture zones.	6.5.2.1, 6.5.2.2, 6.5.2.3, 6.5.2.4, 6.5.2.5, 6.5.2.7, 6.5.2.8, 6.5.2.9, 6.5.2.10	Undetected features in the SZ, such as fracture zones, inhomogeneities, and faults and their potential impacts on groundwater flow are implicitly incorporated in the SZ Transport Abstraction Model and the SZ 1-D Transport Model. Such features could impact groundwater flow with regard to the specific discharge in the SZ system, the direction of groundwater flow from horizontal anisotropy, and/or the degree of groundwater flow focusing in flowing intervals. The impacts of such potential features are encompassed within uncertainty distributions for key parameters, such as groundwater specific discharge (GWSPD), horizontal anisotropy (HAVO), flowing interval spacing (FISVO).

Table 6-2. Saturated Zone Included FEPs for Which This Model Report Provides the Technical Basis (Continued)

FEP Number and Name	FEP Description	Section in Report Where FEP Discussed	Disposition in TSPA-LA
3.1.01.01.0A Radioactive Decay and Ingrowth	Radioactivity is the spontaneous disintegration of an unstable atomic nucleus that results in the emission of subatomic particles. Radioactive isotopes are known as radionuclides. Radioactive decay of the fuel in the repository changes the radionuclide content in the fuel with time and generates heat. Radionuclide quantities in the system at any time are the result of the radioactive decay and the growth of daughter products as a consequence of that decay (i.e., ingrowth). Over a 10,000-year performance period, these processes will produce daughter products that need to be considered in order to adequately evaluate the release and transport of radionuclides to the accessible environment.	6.3.1, 6.5, 6.5.1	Radioactive decay during transport in the SZ is explicitly included in the convolution integral method used to couple the SZ Transport Abstraction Model with the TSPA model and in the SZ 1-D Transport Model. Ingrowth is accounted for in two different ways in the TSPA models. First, the initial inventory in the waste is adjusted to account for the radionuclide parents that obviously impact the simulated dose, resulting in a "boosting" of the initial inventory of some decay products in the SZ Transport Abstraction Model. Second, a separate set of SZ transport simulations is run to calculate explicitly the decay and ingrowth for the four main radionuclide chains, using the SZ 1-D Transport Model.

Table 6-3. Saturated Zone Included FEPs Supported by the Results in This Model Report

FEP Number and Name	FEP Description	Section in Report Where FEP is Discussed
2.2.03.01.0A Stratigraphy	Stratigraphic information is necessary information for the performance assessment. This information should include identification of the relevant rock units, soils and alluvium, and their thickness, lateral extents, and relationships to each other. Major discontinuities should be identified.	6.5.2.1 6.5.2.2
2.2.07.15.0A Advection and Dispersion in the SZ	Advection and dispersion processes affect contaminant transport in the SZ.	6.5.2.1 6.5.2.9 6.5.2.10
2.2.07.17.0A Diffusion in the SZ	Molecular diffusion processes may affect radionuclide transport in the SZ.	6.5.2.1 6.5.2.4 6.5.2.5 6.5.2.6
2.2.08.01.0A Chemical Characteristics of Groundwater in the SZ	Chemistry and other characteristics of groundwater in the saturated zone may affect groundwater flow and radionuclide transport of dissolved and colloidal species. Groundwater chemistry and other characteristics, including temperature, pH, Eh, ionic strength, and major ionic concentrations, may vary spatially throughout the system as a result of different rock mineralogy.	6.5.2.8 6.5.2.11 6.5.2.12
2.2.08.06.0A Complexation in the SZ	Complexing agents such as humic and fulvic acids present in natural groundwaters could affect radionuclide transport in the SZ.	6.5.2.8 6.5.2.11 6.5.2.12
2.2.08.08.0A Matrix Diffusion in the SZ	Matrix diffusion is the process by which radionuclides and other species transported in the SZ by advective flow in fractures or other pathways move into the matrix of the porous rock by diffusion. Matrix diffusion can be a very efficient retarding mechanism, especially for strongly sorbed radionuclides, due to the increase in rock surface accessible to sorption.	6.5.2.4 6.5.2.5 6.5.2.6
2.2.08.09.0A Sorption in the SZ	Sorption of dissolved and colloidal radionuclides in the SZ can occur on the surfaces of both fractures and matrix in rock or soil along the transport path. Sorption may be reversible or irreversible, and it may occur as a linear or nonlinear process. Sorption kinetics and the availability of sites for sorption should be considered. Sorption is a function of the radioelement type, mineral type, and groundwater composition.	6.5.2.8 6.5.2.11 6.5.2.12

6.3 BASE-CASE CONCEPTUAL MODEL

The base-case conceptual model for radionuclide transport, as implemented in the SZ Transport Abstraction Model, implicitly includes the conceptual models of groundwater flow and transport incorporated in the SZ Site-Scale Flow Model and the SZ Site-Scale Transport Model (BSC 2003 [162649], Section 6.3; BSC 2003 [162419], Sections 5 and 6.3). The SZ Site-Scale Flow Model and alternative conceptualizations of groundwater flow are also described by Zyvoloski et al. 2003 [163341]. The base-case conceptual model for the SZ 1-D Transport Model also implicitly includes the conceptual models in these underlying models, with the conceptual simplifications in flow associated with representation by one-dimensional groundwater flow. The SZ Transport Abstraction Model and the SZ 1-D Transport Model also include the concept of uncertainty in key model parameters. The probabilistic analysis of uncertainty is implemented through Monte Carlo realizations of the SZ flow and transport system, in a manner consistent with the TSPA simulations.

6.3.1 SZ Transport Abstraction Model

The conceptual model of groundwater flow in the SZ includes steady-state flow conditions in a three-dimensional flow system (BSC 2003 [162649], Section 6.3.3). Groundwater flow occurs in a continuum fracture network in the fractured volcanic rocks beneath the repository site, at the scale of individual grid blocks in the SZ Transport Abstraction Model. The effective continuum conceptual model is appropriate, given the relatively large horizontal scale (500 m by 500 m) of the grid in the model. Grid resolution studies with the SZ Site-Scale Flow Model indicate that the 500 m grid resolution and the effective continuum conceptual model are adequate to capture the flow behavior of the SZ system and to calibrate the model (Bower et al. 2000 [149161]). Groundwater flow is conceptualized to occur in a continuum porous medium in the alluvium and valley-fill units of the SZ Transport Abstraction Model. Contrasting values of average permeability among hydrogeologic units influence the patterns of groundwater flow in the SZ (BSC 2003 [162649], Sections 6.3 and 6.6).

Some of the major faults and other discrete geological features are conceptualized to impact the groundwater flow due to contrasts in permeability with surrounding hydrogeologic units. In addition, the prevailing structural fabric in the volcanic hydrogeologic units near Yucca Mountain may impart horizontal anisotropy in the permeability between the major faults in this area of the SZ system. Significant variations in the hydraulic gradient near Yucca Mountain occur to the north of Yucca Mountain at the Large Hydraulic Gradient and to the west of Yucca Mountain at the Moderate Hydraulic Gradient, corresponding to the Solitario Canyon fault (Luckey et al. 1996 [100465], p. 21-26). Analysis of the different conceptualizations of the Large Hydraulic Gradient showed that the specific discharge was only mildly sensitive to choice of conceptual model if the hydraulic head measurements along the flow path were reasonably well matched by the numerical model (BSC 2003 [162649], Section 6.4.1).

Groundwater flow enters the SZ site-scale flow system primarily as underflow at the lateral boundaries of the model domain (BSC 2003 [162649], Section 6.3.2). The conceptual model of recharge to the SZ includes distributed recharge, primarily in the northern part of the model domain, and focused recharge along the Fortymile Wash channel (BSC 2003 [162649],

Section 6.3.2). Recharge within the area of the SZ Transport Abstraction Model domain constitutes a small fraction of the entire groundwater budget of the site-scale flow system. Groundwater flow paths from beneath Yucca Mountain to the south are conceptualized to occur near the water table, due to the generally small amount of recharge in this area.

The conceptual model of the SZ flow system for future climatic conditions includes significant changes in the groundwater flow rates for potential wetter, cooler climate states. Increases in recharge at both the local and regional scales for monsoonal and glacial-transition climatic conditions would increase the specific discharge of groundwater in the SZ. Given the likelihood of such climatic variations within the 10,000 year time period of regulatory concern, the conceptual model of SZ flow includes higher groundwater fluxes for the future.

The conceptual model of radionuclide transport in the SZ includes the processes of advection, dispersion, matrix diffusion in fractured volcanic units, sorption, and colloid-facilitated transport (BSC 2003 [162419], Section 6.3). In addition, radionuclides are subject to radioactive decay and ingrowth during migration in the SZ in the TSPA analyses. These processes are illustrated in Figure 6-1 and Figure 6-2.
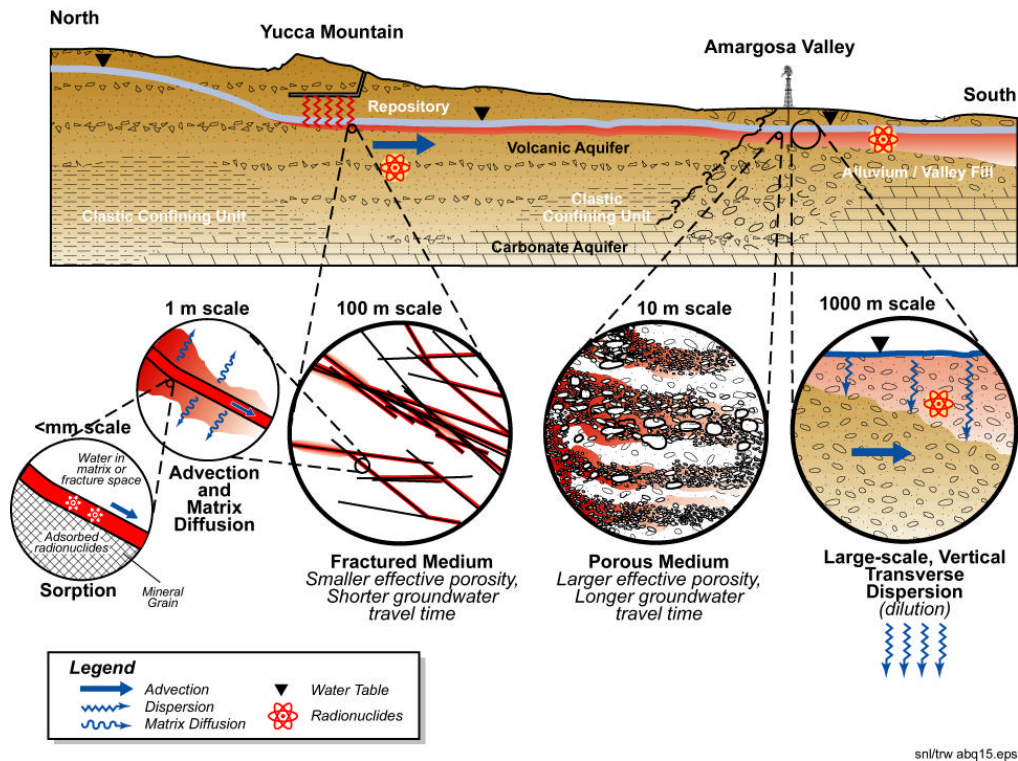
Figure 6-1. Illustration of the Conceptual Model of Radionuclide Transport Processes in the Saturated Zone

Groundwater advection is the primary mechanism to drive the migration of contaminants from the SZ beneath the repository to the accessible environment. Advective transport of radionuclides is conceptualized to occur primarily within the fracture network of the volcanic hydrogeologic units (BSC 2003 [162419], Section 6.3) due to the very high contrast in permeability between the fractures and the rock matrix. The conceptual model of advection within the porous medium of the alluvium units envisions the flow of groundwater to be much more widely distributed, but excludes groundwater flow from zones or sedimentary facies of lower permeability material within the alluvium.

Dispersion of contaminant mass during transport in the SZ is conceptualized to occur because of hydrodynamic dispersion and molecular diffusion. Hydrodynamic dispersion is the result of variations in groundwater flow rates induced by heterogeneities within the aquifer, both in fractured and porous media. The conceptual model of hydrodynamic dispersion distinguishes between longitudinal dispersion, which occurs in the direction of groundwater flow, and transverse dispersion, which occurs perpendicular to the direction of groundwater flow. Longitudinal dispersion is typically much greater than transverse dispersion (see Section 6.5.2.9). Molecular diffusion also contributes to dispersion in radionuclide transport in the advective domain, but to a much lesser degree than hydrodynamic dispersion.

The dual-porosity conceptual model of matrix diffusion in fractured media describes the transfer of radionuclide mass from the flowing groundwater within the fractures to the relatively stagnant groundwater contained in the pores of the rock matrix. This mass transfer, either into or out of the rock matrix, occurs by molecular diffusion, which is driven by differences in the concentration of the contaminant in the fractures and matrix. The simplified conceptual model of the spatial distribution of groundwater-conducting fractures and matrix is a set of parallel, uniformly-spaced fractures, separated by blocks of porous matrix (BSC 2003 [162419], Section 6.5.2.4). This conceptual model considers that groundwater flow occurs only in the fractures and that the groundwater in the rock matrix has no advective groundwater movement. Although this aspect of the dual-porosity conceptual model is difficult to confirm, the contrast in permeability between the rock matrix and the fracture network in fractured tuff tends to support this approach. Groundwater flow is conceptualized to not necessarily occur in all fractures of the system, but is limited to those fractures that are interconnected in the through-going fracture network. The matrix diffusion process is controlled primarily by the effective diffusion coefficient in the rock matrix, the spacing between fractures carrying flowing groundwater, and the aperture of the fractures.

The conceptual model of matrix diffusion also recognizes the possibility of groundwater flow in fracture zones, in which numerous, closely spaced fractures may transmit groundwater. Such fracture zones could exist along faults, which have experienced multiple episodes of displacement and potentially contain zones of rubblized bedrock. Diffusion of contaminants into the relatively small blocks of matrix within a fracture zone would be rapid in comparison to the matrix diffusion that would occur into the large blocks that exist between such zones. The contaminant storage capacity of the small blocks within such a fracture zone would be the total matrix porosity (and sorption capacity of mineral grains) of the blocks, corresponding to essentially complete matrix diffusion within the small matrix blocks.

The conceptual model of radionuclide sorption in the SZ is local equilibrium distribution of radionuclide mass between the aqueous phase and the mineral grains of the aquifer. This equilibrium distribution of contaminant mass is defined by the linear sorption coefficient relationship. In fractured media, sorption is conceptualized to occur in the rock matrix; no sorption is conceptualized to occur on the fracture surfaces or coatings. In the porous media of the alluvium, sorption is conceptualized to occur in that portion of the aquifer corresponding to the effective porosity of the alluvium. In other words, sorption can occur in that part of the alluvium through which significant groundwater flow occurs; zones or layers of low permeability are effectively excluded from the sorption process.

In the conceptual model of colloid-facilitated transport radionuclide migration associated with colloids can occur by two modes (BSC 2003 [162729], Section 6.3), as illustrated in Figure 6-2. In the first mode, radionuclides that are reversibly attached to colloids are in equilibrium with the aqueous phase and the aquifer material. In this mode of transport, the effective retardation of these radionuclides during transport in the SZ is dependent on the sorption coefficient of the radionuclide onto colloids, the concentration of colloids in the groundwater, and the sorption coefficient of the radionuclide onto the aquifer material. In the second mode, radionuclides that are irreversibly attached to colloids are transported at the same rate as the colloids. The colloids with the irreversibly attached radionuclides are themselves retarded by interaction (attachment and detachment) with the aquifer material. Specifically, the colloids undergo reversible filtration, which is represented by a retardation factor in the model. This conceptual model also recognizes that a small fraction of colloids with irreversibly attached radionuclides could be transported through the SZ with no retardation, due to kinetic effects of colloid attachment and detachment. This fast fraction of the colloids with irreversibly attached radionuclides is transported with no retardation in the SZ (similar to non-sorbing solutes), but without diffusion into the matrix of the volcanic units.

The conceptual model of radioactive decay in the SZ Transport Abstraction Model is that radionuclides experience a decrease in mass during transport time using the first-order kinetic decay constant for that radionuclide. Because the ingrowth of radionuclides is not explicitly included in the SZ Transport Abstraction Model, a simplified approach is used to account for this process for those radionuclides that have parent radionuclides. In this simplified approach, the mass of the decay product-radionuclide is boosted by the maximum mass of the parent radionuclide that would decay over the remaining TSPA simulation time. The boosting of the decay product-radionuclide mass occurs for the input to the SZ Transport Abstraction Model (i.e., at the UZ – SZ interface). The decay product-radionuclides that are boosted in this manner are Pu-239 (from Am-243), Np-237 (from Am-241), U-236 (from Pu-240), U-238 (from Pu-242), and U-234 (from U-238 and Pu-238).
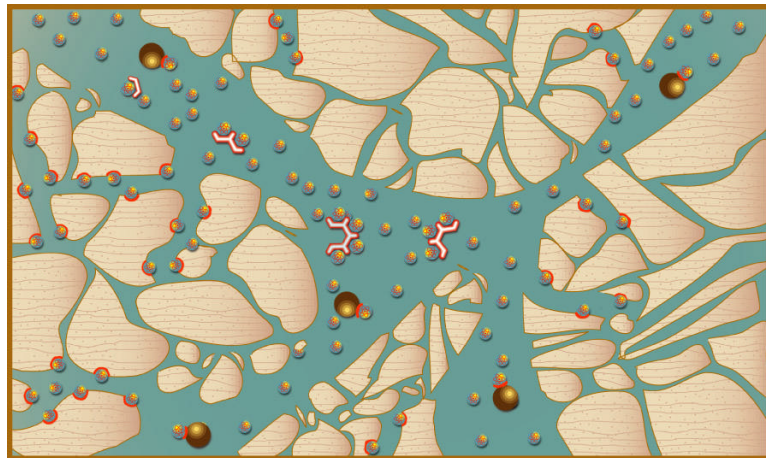
abq0063G031.ai

- Radionuclide
- Sorbed Radionuclide
- Reversible Sorption Type Colloid shown with radionuclide temporarily attached
- Reversible Sorption Type Colloid shown without radionuclide attached
- Irreversible Sorption Type Colloid shown with radionuclide permanently attached

Figure 6-2.   Illustration of the Conceptual Model of Colloid-Facilitated Radionuclide Transport in Fractured Tuff in the Saturated Zone

Homogeneous material properties are assigned to individual hydrogeologic units. The assumption of intra-unit homogeneity is justified primarily on the basis of scale in the SZ Transport Abstraction Model. The horizontal grid resolution of 500 m implies averaging of spatially variable properties over a very large volume. In addition, variations among realizations for stochastic parameters in the analysis encompass probable spatial variations in material properties within the model domain.

It is also assumed that the groundwater flow conditions in the SZ system are in steady state. This approach is carried forward from the *Site-Scale Saturated Zone Flow Model* report (BSC 2003 [162649], Section 5). The Site-Scale Saturated Zone Flow Model is a steady-state model of the flow conditions, reflecting the conclusion that a steady-state representation of the SZ system is accurate. This conclusion is supported by the lack of consistent, large-magnitude variations in water levels observed in wells near Yucca Mountain (Luckey et al. 1996 [100465], p. 29-32). The convolution integral method has been extended to incorporate multiple steady-state flow conditions for alternative climate states in the TSPA analyses.

The conceptual model of matrix diffusion in the fractured volcanic units of the SZ assumes groundwater flow in evenly spaced, parallel-walled fractures separated by impermeable matrix. Although this dual-porosity conceptual model of radionuclide transport represents a significant simplification of the complex fracture network observed in fractured volcanic rocks at the site, it is an acceptable approximation at the scale of individual grid blocks in the SZ Transport Abstraction Model. Individual grid blocks in the transport model have horizontal dimensions of 500 m by 500 m, in comparison to a geometric mean flowing interval spacing of approximately 21 m. This comparison indicates that the grid blocks in the numerical model are more than an order of magnitude larger than the expected spacing between fracture zones that contain flowing groundwater. In addition, the relatively broad range of uncertainty in the flowing interval spacing used in this analysis encompasses the variability in spacing of the actual fracture network. Thus, the variability in flowing interval spacing among stochastic realizations in the TSPA simulations tends to capture the impact of variable spacing between fractures in an ensemble fashion.

For transport of radionuclides reversibly attached to colloids in the SZ, it is assumed that equilibrium conditions exist among radionuclides sorbed onto colloids, the aqueous phase concentration, and those sorbed onto the aquifer material. This approach is carried forward from the *Site-Scale Saturated Zone Transport* model report (BSC 2003 [162419], Section 6.3) and is related to the general assumption regarding linear, equilibrium sorption presented in Section 5. This approach is consistent with laboratory observations of sorption onto colloids, particularly given the time scales of transport in the SZ. This modeling approach is appropriate, given the broad ranges of uncertainty applied to parameters underlying the simulated transport of radionuclides reversibly attached to colloids in the SZ.

Pumping of groundwater by the hypothetical community in which the RMEI resides is assumed not to alter significantly the groundwater pathways or radionuclide travel times in the SZ. Calibration of the SZ site-scale flow model is based on the present-day potentiometric surface observed in the model domain. Whereas the SZ site-scale model does not explicitly include the withdrawal of groundwater by pumping at the location of the hypothetical community in which the RMEI resides, the model does implicitly account for the drawdown of water levels associated

with pumping at the southern boundary of the model domain. The values of specified head along the western part of the southern boundary reflect the lower water levels resulting from pumping in the Amargosa Farms region. Consequently, the model does implicitly include the influence of pumping in terms of increased hydraulic head gradients.

6.3.2   SZ 1-D Transport Model

Many components of the conceptual model for the SZ Transport Abstraction Model also apply to the SZ 1-D Transport Model. Representation of the groundwater flow processes in the three-dimensional SZ Transport Abstraction Model is simplified to one-dimensional streamtubes in the SZ 1-D Transport Model. However, characteristics of the conceptual model of groundwater flow in the SZ Transport Abstraction Model are implicitly included in the SZ 1-D Transport Model because the average values of groundwater flow rate used in the SZ 1-D Transport Model are extracted from the three-dimensional flow model. The conceptual model of aquifer properties has also been simplified in the SZ 1-D Transport Model, relative to the SZ Transport Abstraction Model. Material properties in the SZ 1-D Transport Model streamtubes are for average fractured tuff or for alluvium; no distinctions among volcanic hydrogeologic units are made.

The conceptual model of radionuclide transport in the SZ 1-D Transport Model includes the same processes of advection, dispersion, matrix diffusion in fractured volcanic units, sorption, and colloid-facilitated transport described in the previous section. The conceptualization of dispersion in the SZ 1-D Transport Model is simplified to the extent that transverse dispersion is precluded in the streamtube representation of the SZ system. The conceptual model of radionuclide decay in the SZ 1-D Transport Model includes both decay and ingrowth of radionuclides in decay chains.

The final radionuclide decay product in three of the radionuclide decay chains simulated in the one-dimensional radionuclide transport model is calculated to be in secular equilibrium with its parent radionuclide (see Section 6.5.1.2). This is a reasonable approach because it simplifies the analysis and the final decay product-radionuclides have relatively short half lives (less than 25 years). This approach overestimates the concentration of decay products because it implies an instantaneous increase in the mass of the final decay product to be in equilibrium with the mass of parent radionuclide present.

The groundwater flux within each one-dimensional "pipe" segment used in the model is assumed to be constant along the length of the pipe. Each pipe segment used in the model consists of homogenous material properties, for which the radionuclide transport process is simulated. This constitutes a reasonable approach because the average groundwater flux along that portion of the radionuclide flowpath is derived from the corresponding region of the three-dimensional SZ Transport Abstraction Model.

6.3.3 Interfaces with the UZ and the Biosphere

The source of radionuclides in the SZ Transport Abstraction Model is conceptualized to be a point source from the UZ transport model. The location of this source is treated as uncertain and constant for a given realization of the system. This conceptual model is consistent with a contaminant source to the SZ resulting from a single leaking waste package, focused groundwater flow in the UZ, or the human intrusion scenario in which a borehole intersects a waste package and extends to the water table (CRWMS M&O 2000 [153246], Section 4.4).

The conceptual model of radionuclide releases from the SZ to the biosphere includes pumping of groundwater from wells by the hypothetical community in which the RMEI resides. The extent of the controlled area is specified in the regulations for the Yucca Mountain site (10 CFR 63.302 (10 CFR 63 [156605])) and the location of the hypothetical community in which the RMEI resides is taken to be adjacent to the controlled area. In addition, the quantity of groundwater used by the hypothetical community in which the RMEI resides is specified by the regulations to be 3,000 acre-ft/year (10 CFR 63.332 (10 CFR 63 [156605])). The conceptualization of the pumping system is that the entire plume of radionuclides in the SZ would be captured by the pumping wells of the hypothetical community in which the RMEI resides and that these contaminants would be homogeneously distributed in the specified volume of groundwater. Although variations in radionuclide concentration would probably exist among the pumping wells, the radiological dose among the population of this community in which the RMEI resides would tend to be homogenized by exchange of radionuclides through various pathways within the biosphere.

The interface between radionuclide transport in the UZ and the SZ is assumed to be a point source near the water table. This approach is physically consistent with a single leaking waste package and highly focused transport of radionuclides in the UZ flow system, as may occur early in the history of the repository. This approach is also consistent with the human intrusion scenario, in which a borehole penetrates a waste package and provides a direct pathway for radionuclide migration to the SZ. The approach of a point source for radionuclides in the SZ transport simulations, while not physically realistic for the situation in which multiple, dispersed leaking waste packages exist, provides a generally conservative approximation of the source term to the SZ. This approximation results in less dispersion of the radionuclide transport times through the SZ and thus to less attenuation of peaks in radionuclide discharge. Although *in situ* concentrations of radionuclides are not utilized in the analysis of SZ transport, a point source tends to maximize the simulated concentrations of radionuclides at the outlet to the accessible environment.

The location of the point source of radionuclides for transport in the SZ site-scale flow and transport model is assumed to be randomly located within the four source regions defined at the water table (see Figure 6-27). This approach implies that there are no consistent spatial patterns of waste package failure or delivery of radionuclides at the water table within each of the four source regions. Many of the processes that may lead to waste package failure are spatially random (e.g., manufacturing defects, seepage onto waste packages, etc.). The spatial pattern of preferential groundwater flow pathways in the UZ flow model is represented in a general sense by the locations of the four source regions (e.g., the southeastern source region corresponds to focused vertical groundwater flow along the Ghost Dance fault).

An assumption inherent to the convolution integral method is that the system being simulated exhibits a linear response to the input function. In the case of solute transport in the SZ system this approach implies, for example, that a doubling of the input mass flux results in a doubling of the output mass flux. This approach is valid for the SZ Transport Abstraction Model because the underlying transport processes (e.g., advection and sorption) are all linear with respect to solute mass (BSC 2003 [162419], Section 6.5.2). The processes of colloid filtration and sorption are both represented as equilibrium retardation processes. Simple retardation affects the timing of the release of radionuclides from the SZ, but still constitutes a linear relationship between mass input and mass output to the SZ .

It is assumed that all radionuclide mass crossing the regulatory boundary (at approximately 18 km distance from the repository at the boundary of the controlled area (10 CFR 63.302 (10 CFR 63 [156605]) in the SZ is captured by pumping wells of the hypothetical community in which the RMEI resides, based on 10 CFR 63.332 (10 CFR 63 [156605]). This approach implies that the total volumetric groundwater usage by the hypothetical community in which the RMEI resides is large relative to the volumetric flow in the plume of contaminated groundwater in the SZ. This approach is justified on the basis of conservatism with respect to the analysis of repository performance. The total mass of radionuclides released to the biosphere for a given time period cannot be larger than the amount of radionuclide mass delivered by groundwater flow (for the nominal case).

6.4 CONSIDERATION OF ALTERNATIVE CONCEPTUAL MODELS

Two significant alternative conceptual models (ACMs) regarding groundwater flow and radionuclide transport in the SZ have been considered in this report. Both of these ACMs are encompassed in the range of uncertainty evaluated in the SZ Transport Abstraction Model and the SZ 1-D Transport model and are thus implicitly carried forward to the TSPA-LA modeling analyses. Consequently, these ACMs need not be separately evaluated from the base case. Information on ACMs is summarized in Table 6-4. The ACMs are consistent with available data and current scientific knowledge and appropriately consider their results and limitations.

Table 6-4.   Alternative Conceptual Models Considered

Alternative Conceptual Model	Key Assumptions	Screening Assessment and Basis
Minimal Matrix Diffusion	Diffusion of radionuclides into the pore space of the rock matrix in the fractured volcanic units is extremely limited due to highly channelized groundwater flow, fracture coatings, or other factors.	This ACM is implicitly included in the SZ Transport Abstraction Model and in the SZ 1-D Transport Model through the range of uncertainty in key input parameters. The uncertain input parameters influencing matrix diffusion include effective diffusion coefficient (DCVO), flowing interval spacing (FISVO), and flowing interval porosity (FPVO).
Horizontal Anisotropy in Permeability	Alternative interpretations of pump test results in the fractured volcanic units indicate preferential permeability along structural features oriented in the NNE-SSW direction or in the WNW-ESE direction.	This ACM is implicitly included in the SZ Transport Abstraction Model and in the SZ 1-D Transport Model through the range of uncertainty in an input parameter. The uncertain input parameter influencing horizontal anisotropy in permeability in the volcanic units near Yucca Mountain is the ratio of N-S to E-W permeability (HAVO, see Section 6.5.2.10). This continuously distributed parameter varies from less than one to greater than one with most of the realizations greater than one.

A sensitivity analysis using the SZ Transport Abstraction Model was conducted to show that the minimal matrix diffusion ACM is included within the range of parameter uncertainties considered. Figure 6-3 shows the solute mass breakthrough curves for a non-sorbing tracer, using the expected values of flow and transport parameters. The short-dashed line shows the simulated breakthrough curve for transport with no diffusion into the matrix of the fractured volcanic units, and the long-dashed line shows the breakthrough curve for maximum matrix diffusion. The solid line shows the simulated breakthrough curve using the 95th percentile value for flowing interval spacing (79.4 m) from the uncertainty distribution in this parameter. These results indicate that the breakthrough curve using the 95th percentile value of flowing interval spacing is very near the bounding case of no matrix diffusion. Similarly, low values of effective diffusion coefficient and low values of flowing interval porosity would produce breakthrough curves tending toward the no-matrix-diffusion case. This sensitivity analysis demonstrates that the minimal matrix diffusion ACM is captured within the range of uncertainty used in the model.
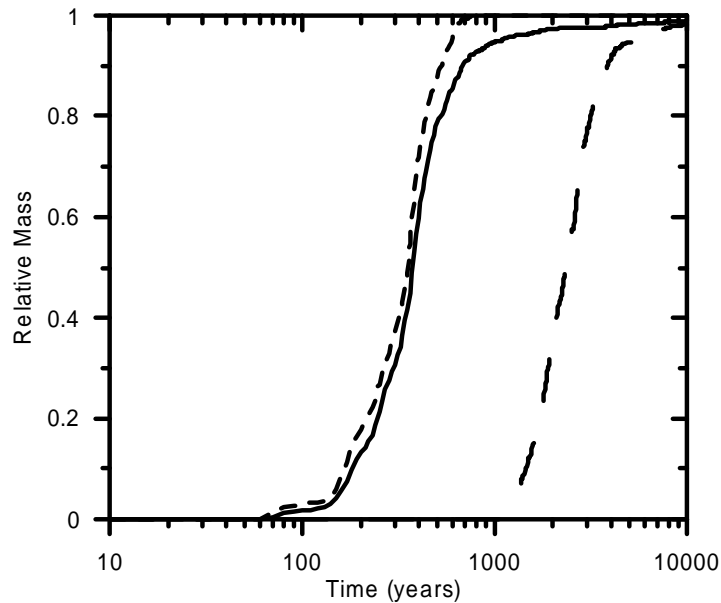
NOTE: The case of no matrix diffusion is shown with the short-dashed line. The case of maximum matrix diffusion is shown with the long-dashed line. The case for which flowing interval spacing is set to its 95th percentile value (79.4 m) is shown with the solid line. Mass breakthrough curves are for present climate and do not include radionuclide decay.

Figure 6-3.   Mass Breakthrough Curves at 18-km Distance Showing Sensitivity to Matrix Diffusion

The incorporation of the horizontal anisotropy ACM into the SZ Transport Abstraction Model is inherent in the range of parameter values used for the parameter HAVO in the analyses. A complete discussion of uncertainty in horizontal anisotropy of permeability and the basis for the uncertainty distribution are provided in the *Saturated Zone In Situ Testing* scientific analysis report (BSC 2003 [162415], Section 6.2.6). The uncertainty distribution for HAVO indicates that there is a 10% probability that the direction of maximum horizontal permeability is east-west with a ratio between 1 and 20. The uncertainty distribution also indicates that there is a 90% probability that the direction of maximum horizontal permeability is north-south with a ratio between 1 and 20. The isotropic case, corresponding to a horizontal permeability ratio of 1, is included in this continuous uncertainty distribution for the parameter HAVO.

6.5   MODEL FORMULATION FOR BASE-CASE MODELS

SZ Transport Abstraction Model

The SZ Site-Scale Flow Model (BSC 2003 [162649]) and the SZ Site-Scale Transport Model (BSC 2003 [162419]) form the bases for the SZ Transport Abstraction Model. The progression in the development of models is from the SZ Site-Scale Flow Model to the SZ Site-Scale Transport Model to the SZ Transport Abstraction Model. The SZ Site-Scale Flow Model includes the implementation of the hydrogeologic framework, the numerical grid, and the boundary conditions for steady-state groundwater flow. The SZ Site-Scale Flow Model is calibrated to water-level measurements in wells and estimates of groundwater flow rates at the lateral boundaries. The SZ Site-Scale Transport Model begins with the SZ Site-Scale Flow Model and adds the model input files required for the simulation of radionuclide transport using the particle-tracking method. A set of representative parameter values for radionuclide transport is included in the SZ Site-Scale Transport Model and the range of behavior associated with parameter uncertainty is examined. Finally, the SZ Transport Abstraction Model begins with the SZ Site-Scale Transport Model and adds the capability to perform probabilistic uncertainty analyses using multiple Monte Carlo realizations of the SZ flow and transport system. The resulting radionuclide breakthrough curves are then used in the convolution integral method to couple the SZ Transport Abstraction Model with the TSPA model.

The SZ Site-Scale Flow Model, the SZ Site-Scale Transport Model, and the SZ Transport Abstraction Model share a common model domain, hydrogeologic framework, numerical grid, and boundary conditions. The model domain is shown in Figure 6-4 with the blue dashed line overlain on a shaded relief map of the surface topography. The nodes that constitute the model grid form an orthogonal mesh with 500-m spacing in the north-south and east-west directions. The repository outline is shown with the bold blue line and the nodes that occur along the regulatory boundary of the accessible environment are shown as overlapping red crosses.

The groundwater flow boundary conditions for the SZ Site-Scale Flow Model, the SZ Site-Scale Transport Model, and the SZ Transport Abstraction Model are specified head at the lateral boundaries and specified groundwater flux for recharge at the upper boundary. These boundary conditions are described in detail in BSC 2003 [162649], Section 6.3.2 and are the same for all three models with the following exception. For the SZ Transport Abstraction Model, the specified flux for recharge is scaled in proportion to the uncertainty in groundwater specific discharge (see Section 6.5.2.1). Scaling the recharge flux and the values of permeability in proportion to the groundwater specific discharge uncertainty factor maintains the calibration of the flow model with regard to water-level measurements.
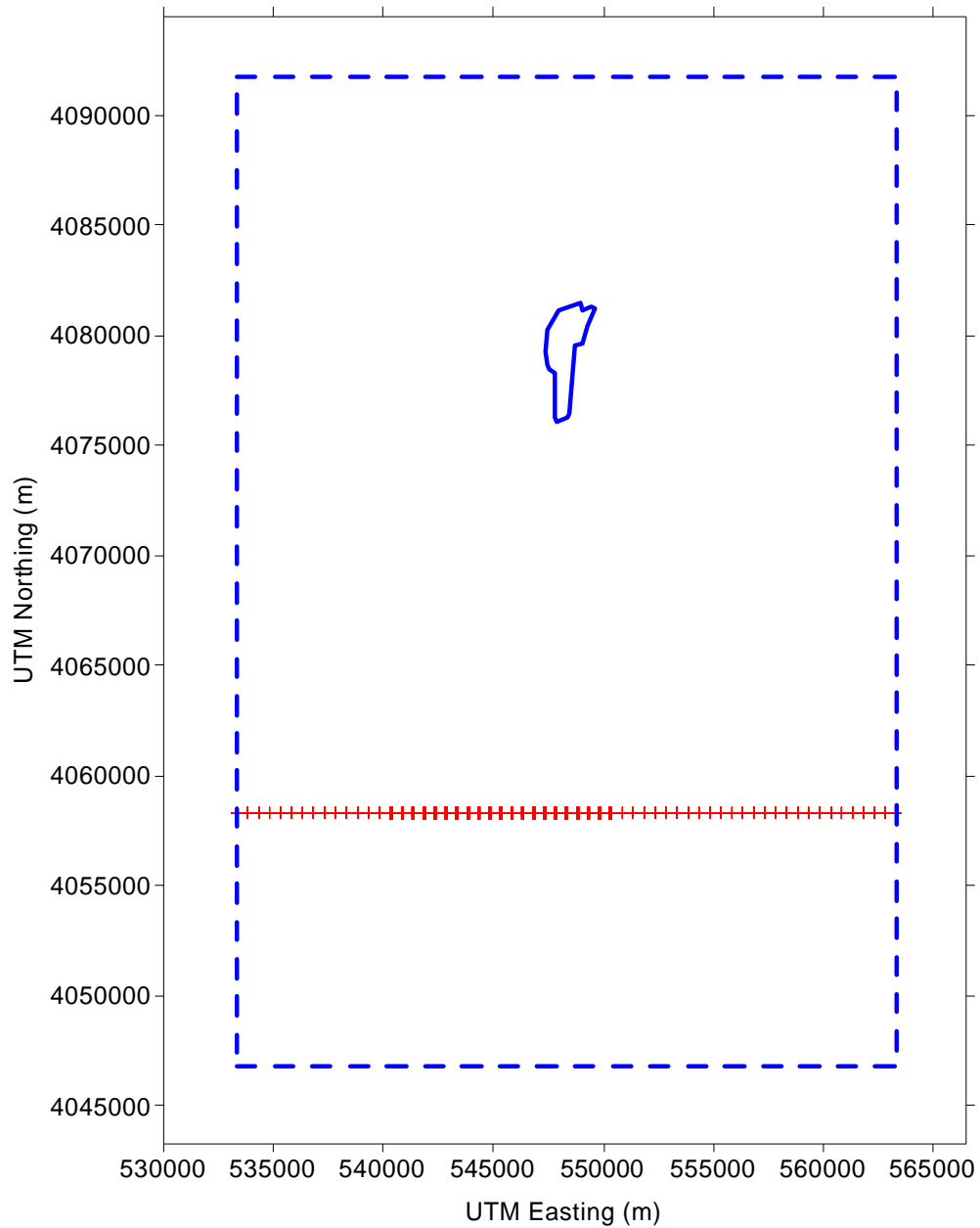
Source for repository outline: 800-IED-EBS0-00401-000-00C, BSC 2003 [162289]

NOTE: The dashed blue line indicates the boundaries of the SZ Transport Abstraction Model, the solid blue line shows the outline of the repository, and the red crosses indicate the boundary to the accessible environment for radionuclide transport in the SZ.

Figure 6-4. Model Domain of the SZ Site-Scale Flow Model, SZ Site-Scale Transport Model, and the SZ Transport Abstraction Model.

Radionuclide transport is simulated in the SZ Transport Abstraction Model using a particle tracking method. This method, as implemented by the FEHM v. 2.20 software code (STN: 10086-2.20-00, LANL 2003 [161725]), simulates advection along groundwater streamlines, random-walk dispersion, retardation due to sorption, and matrix diffusion. Each simulation uses 500 particles, which results in a continuous, generally smooth cumulative mass breakthrough curve at the boundary of the accessible environment. The time-step size that determines output intervals varies from 10 years to 100 years, depending on the radionuclide. Internally, the simulation uses local flow conditions to determine time steps for dispersion and matrix diffusion calculations. This internal time step is controlled such that the particles take approximately 20 internal time steps to traverse each cell in the model.

In the TSPA analyses the convolution integral method used in the SZ Transport Abstraction Model provides an approximation of the transient radionuclide mass flux at a specific point downgradient in the SZ in response to the transient radionuclide mass flux from transport in the UZ. This coupling method makes full use of detailed SZ flow and transport simulations for a given realization of the system, without requiring complete numerical simulation of the SZ for the duration of each TSPA realization. The two input functions to the convolution integral method are: 1) a unit radionuclide mass breakthrough curve in response to a step-function mass flux source as simulated by the SZ Transport Abstraction Model; and, 2) the radionuclide mass flux history as simulated for transport in the UZ. The output function is the radionuclide mass flux history downgradient in the SZ.

There are several important assumptions in the use of the convolution integral method. Groundwater flow in the SZ is assumed to be steady state. The transport processes in the SZ must be linear with respect to the solute source term (i.e., a doubling of the solute mass source results in a doubling of mass flux). In addition, the flow and transport processes in the UZ and the SZ must be independent of one another.

Radioactive decay is also applied to radionuclide mass flux calculated with the convolution integral computer code SZ_Convolute v. 3.0 software code (STN: 10207-3.0-00, SNL 2003 [164180]) in the TSPA analyses. The convolution integral method consists of numerical integration that accounts for the contributions to the outlet radionuclide mass flux from a series of time intervals. Because the travel time for each contribution to radionuclide mass flux is known, the loss of radionuclide mass (and consequent decrease in mass flux) during transport is calculated by first-order decay for that time interval.

The effects of climate change on radionuclide transport in the saturated zone are incorporated into the convolution integral analysis in the TSPA by assuming instantaneous change from one steady-state flow condition to another steady-state condition in the saturated zone. Changes in climate state are assumed to affect the magnitude of groundwater flux through the saturated zone system but have a negligible impact on flowpaths. The effect of changes in groundwater flux is incorporated into the convolution method by scaling the timing of radionuclide mass breakthrough curves proportionally to the change in saturated zone specific discharge.

Three climate states are defined for the period from repository closure to 10,000 years in the future in the TSPA-SR calculations (CRWMS M&O 2000 [153246], p. 3-25). For the base-case TSPA analyses, present-day climatic conditions are modeled to occur from the time of repository

closure to 600 years in the future, monsoonal conditions are imposed from 600 years to 2000 years in the future, and glacial-transition climatic conditions occur from 2000 years to 10,000 years. The monsoonal climatic state is wetter than present-day conditions and the glacial-transition state is conceptualized to be wetter and cooler than present-day conditions. Note that the glacial-transition climate state is approximately equivalent to the long-term average climate state, as referenced in CRWMS M&O 1998 [100365], Table 8-16, p. T8-20.

Estimates of the scaling factors for groundwater flux in the SZ under alternative climatic conditions are based on simulations using the SZ regional-scale flow model (D'Agnese et al., 1999 [120425]; CRWMS M&O 1998 [100365]) and on the infiltration for the UZ site-scale flow model (BSC 2003 [163045], Section 6.1.4). Simulations using the SZ regional-scale flow model were conducted for the past-climate state that likely existed about 21,000 years ago (D'Agnese et al., 1999 [120425]). This climatic state approximately corresponds to the glacial-transition state, as defined for TSPA-SR calculations. A comparison of the groundwater flux in the SZ near Yucca Mountain under past-climate conditions (i.e., 21,000 years ago) using the SZ regional-scale model indicates that the simulated flux under the past-climate conditions was approximately 3.9 times the flux of present-day simulations, as shown in Table 6-5.

Simulations of SZ flow under monsoonal climatic conditions have not been performed using the SZ regional-scale flow model. Information on the increased infiltration through the UZ site-scale flow model is used as the basis for estimating flux increases in the SZ for monsoonal conditions (DTN: LB03023DSSCP9I.001 [163044]) (see also BSC 2003 [163045], Table 6.1-2). Values of average infiltration in the area of the UZ site-scale flow model (second column of (Table 6-5) are taken from the "GENER" card of the TOUGH2 input files "*preq_mA.dat*", "*glaq_mA.dat*", and "*monq_mA.dat*". Similarly, the total infiltration through the UZ site-scale flow model for present and glacial-transition climatic conditions is calculated (DTN: LB03023DSSCP9I.001 [163044]). Note in Table 6-5 that the ratio of glacial-transition infiltration in the UZ model to the present-day infiltration (a factor of 3.8) is approximately the same value as the estimate of increased SZ groundwater flux from the SZ regional-scale flow model (i.e., 3.9). This correspondence suggests that the UZ infiltration ratio provides a reasonable estimate of the flux ratio for the SZ. Thus, the values of the SZ groundwater flux ratio for TSPA simulations of future climatic states are derived from the estimates of increased UZ infiltration at Yucca Mountain. For monsoonal climatic conditions, the ratio of UZ infiltration to the infiltration for present-day conditions is 2.7 (see Table 6-5) and this value is applied to the SZ flux as well. The values of flux ratio used as scaling factors of SZ flow and transport for alternative climate states are given in the last column of Table 6-5.

Table 6-5. Groundwater Flow Scaling Factors for Climate Change

Climate State	Average Infiltration, UZ Model (Mean Case) (mm/yr)	Ratio to Present Climate, UZ Model	SZ Groundwater Flux Ratio from SZ Regional-Scale Model	SZ Groundwater Flux Ratio for TSPA Simulations
Present-Day	4.4279 [a]	1.0	1.0	1.0
Glacial-Transition	17.0196 [a]	3.8	3.9 [b]	3.9
Monsoonal	11.8290 [a]	2.7	N/A	2.7

NOTES: [a] DTN: LB03023DSSCP9I.001 [163044]
        [b] CRWMS M&O 1998 [100365], Table 8-16, p. T8-20.

SZ 1-D Transport Model

The SZ 1-D Transport Model is implemented with the GoldSim v. 7.50.100 software code (STN: 10344-7.50.100-00, BSC 2003 [161572]) in the TSPA simulator as a series of "pipes." The same radionuclide transport processes that are simulated in the three-dimensional SZ Transport Abstraction Model (e.g., sorption, matrix diffusion in fractured units, and colloid-facilitated transport) are analyzed in the "pipe" segments, with the exception of transverse dispersion. Transverse dispersion is not very important to the modeling results, given the assumption that all radionuclide mass is captured by the wells of the receptor group. Although strict consistency between the SZ 1-D Transport Model and the three-dimensional SZ Transport Abstraction Model is not possible, average groundwater flow and transport characteristics of the SZ Transport Abstraction Model are used to define flow and transport properties within the "pipe" segments of the one-dimensional model. Average specific discharge along different segments of the flowpath is estimated using the 3-D SZ Transport Abstraction Model. The resulting values of average specific discharge are applied to the individual "pipe" segments in the one-dimensional transport model.

6.5.1 Mathematical Description of Base-Case Conceptual Model

6.5.1.1 SZ Transport Abstraction Model

The mathematical descriptions of the processes of groundwater flow and radionuclide transport in the SZ Site-Scale Flow Model (BSC 2003 [162649], Section 6.5) and the SZ Site-Scale Transport Model (BSC 2003 [162419], Section 6.5.2) are presented in the corresponding reports for these models. The SZ Site-Scale Flow Model forms the direct basis for the SZ Site-Scale Transport Model and the SZ Site-Scale Transport Model forms the direct basis for the SZ Transport Abstraction Model. Therefore, the mathematical bases for those models, as implemented by the FEHM v. 2.20 software code (STN: 10086-2.20-00, LANL 2003 [161725]), apply to the SZ Transport Abstraction Model and are not reproduced here.

The particle tracking method is used to simulate radionuclide transport in the SZ Transport Abstraction Model (see BSC 2003 [162419], Section 6.5.2 for description of the particle tracking method). This method exhibits very limited numerical dispersion relative to standard finite-difference and finite-element methods of solute transport simulation. Consequently, particle tracking is appropriate for use in the SZ Transport Abstraction Model, in which the spatial discretization (500 m) exceeds the values of dispersivity being simulated for many of the model realizations.

Convolution Integral

The convolution integral method is used to couple the radionuclide transport in the UZ with the simulations of mass transport in the SZ in the TSPA analyses. The convolution integral method takes the radionuclide mass breakthrough curve for a continuous, unitary mass source from the SZ and the time-varying radionuclide mass from the UZ as inputs. The output is the time-varying radionuclide mass exiting the SZ.

The mathematical expression for the convolution integral method is written as:

$$M_{sz}(t) = \int_0^t \dot{m}_{uz}(t - t') \frac{\overline{M}_{sz}(t')}{m_p} dt' \qquad \text{(Eq. 6-1)}$$

where $M_{sz}(t)$ is the radionuclide mass flux downstream in the SZ [M], t is time [T], $\dot{m}_{uz}(t)$ is the time dependent radionuclide mass flux entering the SZ from the UZ [M], t' is a time lag [T], and $\overline{M}(t')$ is the derivative of the downstream radionuclide mass flux-time response curve [M] to a step input of mass m_p [M]. This expression is taken from the convolution integral for concentration (CRWMS M&O 1998 [100365], p. 8-39) and rewritten in terms of radionuclide mass.

Correction of Retardation

The retardation factor for linear sorption of radionuclides during transport in porous media is defined as (Freeze and Cherry 1979 [101173], p. 404):

$$R_f = 1 + \frac{\rho_b}{\phi} K_d \qquad \text{(Eq. 6-2)}$$

where R_f is the retardation factor in the porous media [-], ρ_b is the bulk density [M/L^3], ϕ is the porosity of the porous media [-], and K_d is the distribution coefficient [L^3/M]. The FEHM v. 2.20 software code (STN: 10086-2.20-00, LANL 2003 [161725]) to be used in the SZ Transport Abstraction Model automatically calculates R_f based on input values of ρ_b, ϕ, and K_d.

Effective porosity (ϕ_e) [-] is a macroscopic parameter that helps account for discrete flow paths and channelized flow (see Section 6.5.2.3). The effective porosity parameter in the alluvium is used to correctly calculate the pore velocity of groundwater. Effective porosity is not intended to be used to estimate surface areas in Equation 6-2. Therefore, it is necessary to adjust another parameter in the equation to compensate for the lower effective porosity that is entered. If this

were not done, then the calculated values of R_f would be overestimated, given that values of K_d used in Equation 6-2 are based on laboratory-scale measurements. For the SZ Transport Abstraction Model and the SZ 1-D Transport Model, the K_d values for the alluvium are adjusted according to the following relationship (CRWMS M&O 1998 [100365], Equation 8-4, p. 8-55):

$$K_d^{new} = K_d \cdot \frac{\phi_e}{\phi_T} \qquad \text{(Eq. 6-3)}$$

where K_d^{new} is the adjusted distribution coefficient [L^3/M] and ϕ_T is the total porosity [-]. The total porosity is 0.30, which is the upper bound of the effective porosity uncertainty distribution and also documented in Section 6.5.2.14.

Colloid-Facilitated Transport

For colloid-facilitated radionuclide transport in which radionuclides are reversibly attached to colloids, a partition coefficient is defined to represent the potential for enhanced migration of radionuclides in association with colloids. This unitless constant, K_c, is defined as:

$$K_c = K_d^{coll} C_{coll} \qquad \text{(Eq. 6-4)}$$

where K_d^{coll} is the sorption coefficient for the radionuclide onto colloids [L^3/M] and C_{coll} is the concentration of colloids in the groundwater [M/L^3]. The conceptual model of colloid-facilitated transport of reversibly sorbed radionuclides is described in Section 6.3 and the underlying theoretical derivation of the model is presented in CRWMS M&O 1997 [124052], pp. 8-32 to 8-36.

For equilibrium conditions in a porous medium, the effective sorptive capacity of the aquifer is reduced when the groundwater colloids carry a significant fraction of radionuclide mass in the system. The values of the sorption coefficient in the alluvium and undifferentiated valley fill hydrogeologic units for the colloid-facilitated transport of radionuclides with the K_c model are modified by the value of K_c, according to the relationship:

$$K_d^{adjusted} = \frac{K_d}{(1 + K_c)} \qquad \text{(Eq. 6-5)}$$

as derived from Equation 6-2 and CRWMS M&O 1998 [100365], Equation 8-8, p. 8-54 and 8-56, and assigning the retardation factor for colloids with reversibly attached radionuclides a value of 1. $K_d^{adjusted}$ is the adjusted distribution coefficient [L^3/M] to account for reversible sorption onto colloids.

For transport in fractured media, the effective diffusion coefficient into the rock matrix is reduced due to the affinity of radionuclides for sorption onto colloids in the fractures. To evaluate this effect with constant velocity and dispersion, consider the one-dimensional advection-dispersion equation for a solute in the fractures (BSC 2003 [162419], Section 6.5.2) with a term for retardation and a final term added for diffusion into the matrix:

$$R_{f,f} \frac{\partial C}{\partial t} = D\frac{\partial^2 C}{\partial x^2} - v\frac{\partial C}{\partial x} - \frac{q}{b} \qquad \text{(Eq. 6-6)}$$

where $R_{f,f}$ is the retardation factor in the fractures [-], D is the dispersion coefficient in the fracture [L^2/T], C is aqueous concentration of the solute [M/L^3], t is time [T], x is distance [L], v is groundwater velocity in the fractures [L/T], q is the diffusive flux into the rock matrix [M/L^2T], and b is the half-aperture of the fracture [L]. For that part of the solute mass that is sorbed onto colloids the advection-dispersion equation is:

$$R_{coll} \frac{\partial C^{coll}}{\partial t} = D\frac{\partial^2 C^{coll}}{\partial x^2} - v\frac{\partial C^{coll}}{\partial x} \qquad \text{(Eq. 6-7)}$$

where R_{coll} is the retardation factor of the colloids in the fractures [-] and C^{coll} is the concentration of the solute in the groundwater [M/L^3]. Adding the two advection dispersion equations and using the relationship that $K_c = C^{coll}/C$, the combined advection-dispersion equation for colloid-facilitated transport of radionuclides reversibly sorbed onto colloids can be written as:

$$\left(\frac{R_{f,f} + K_c R_{coll}}{1 + K_c} \right)\frac{\partial C}{\partial t} = D\frac{\partial^2 C}{\partial x^2} - v\frac{\partial C}{\partial x} - \frac{q}{b(1 + K_c)} \qquad \text{(Eq. 6-8)}$$

As seen by comparing this equation with Equation 6-6, the term for diffusive mass flux into the rock matrix is modified by dividing by the factor $(1+K_c)$ to account for the equilibrium colloid-facilitated transport. One approach would be to adjust the value of fracture half-aperture by multiplying by the factor $(1+K_c)$. An alternative approach is possible based on examination of the ω term in the analytical solution for transport in fractures with matrix diffusion by Sudicky and Frind 1982 [105043], Equation 34, p. 1638. In the ω term, adjusting the value of b by multiplying it by the factor $(1+K_c)$ is equivalent to dividing the effective diffusion coefficient in the matrix by the factor $(1+K_c)^2$. In the SZ Transport Abstraction Model and the SZ 1-D Transport Model the values of effective diffusion coefficient for radionuclides subject to the K_c model of colloid-facilitated transport are adjusted according to the relationship:

$$D_e^{adjusted} = \frac{D_e}{(1 + K_c)^2} \qquad \text{(Eq. 6-9)}$$

where $D_e^{adjusted}$ is the adjusted effective diffusion coefficient in the rock matrix [L^2/T] and D_e is the effective diffusion coefficient in the rock matrix [L^2/T].

For colloid-facilitated radionuclide transport in which radionuclides are irreversibly attached to colloids, most of the colloids (and attached radionuclides) are delayed during transport in the SZ by a retardation factor. A small fraction of colloids with irreversibly attached radionuclides are subject to rapid transport without retardation, as described in BSC 2003 [162729], Section 6.6. In fractured volcanic units, the retardation factor for the majority of colloids is applied directly in the SZ Transport Abstraction Model input files as an input parameter. In porous medium, it is not possible to directly specify a retardation factor in the SZ Transport Abstraction Model; therefore, an effective sorption coefficient is specified that results in the sampled value of the retardation factor. In the porous medium of the alluvium, the colloid retardation factor in the alluvium units is converted to a value of effective sorption coefficient according to the relationship:

$$K_d^{eff} = \frac{(R_f - 1)\phi_e}{\rho_b} \qquad \text{(Eq. 6-10)}$$

where K_d^{eff} is the effective K_d in the porous media [L^3/M].

<u>Retardation in Fracture Zones</u>

As described in the conceptual model of transport in fractured media of the SZ (Section 6.3.1), relatively small blocks of rock matrix or rubblized material in fracture zones may participate in radionuclide transport via diffusion on a short time scale. The impact of rapid diffusion into small matrix blocks on the calculation of average linear velocity of groundwater is captured with a correspondingly larger value of flowing interval porosity for the volcanic units. In this conceptualization, the flowing interval porosity includes the fracture porosity with flowing groundwater plus it may include the matrix porosity of the small matrix blocks within the fracture zones. The possibility of small matrix blocks within fracture zones is encompassed within a range of uncertainty in transport behavior in fractured tuff. If this process of rapid diffusion occurs, the sorptive capacity of the small matrix blocks would also be important to the transport of sorbing radionuclides. This is handled in the following way. If the flowing interval porosity (ϕ_f) [-] is less than the average fracture porosity (ϕ_f^{avg}) [-], then groundwater flow is conceptualized to occur only in fractures and no retardation due to sorption within small matrix blocks occurs. If the flowing interval porosity is greater than the average fracture porosity, then the retardation factor within the fracture domain due to sorption within small matrix blocks (R_f') is calculated as:

$$R_f' = 1 + \frac{(fraction * \rho_b K_{dm})}{\phi_m} \qquad \text{(Eq. 6-11)}$$

where K_{dm} is the sorption coefficient in the rock matrix [L^3/M], ϕ_m is the rock matrix porosity [-] and *fraction* is calculated as:

$$fraction = \frac{(\phi_f - \phi_f^{avg})}{(\phi_m - \phi_f^{avg})}$$ (Eq. 6-12)

The term *fraction* [-] describes the fraction of the entire rock matrix that is accessible to rapid matrix diffusion within the small matrix blocks of the fracture zone. Typically, the value of *fraction* would be small for the range of uncertainty in flowing interval porosity. For example, if the flowing interval porosity is 0.01 (80th percentile from Figure 6-13), the rock matrix porosity is 0.20, and the average fracture porosity is 0.001, then the value of *fraction* is 0.045. This means that 4.5% of the total rock matrix is available for direct interaction with radionuclide advection and

6.5.1.2 SZ 1-D Transport Model

The SZ 1-D Transport Model provides simulation results for several radionuclide chains that are not simulated in the SZ Transport Abstraction Model. The simplified decay chains considered (CRWMS M&O 2000 [153246], Figure 3.5-5, p. F3-67) consist of the following.

1) Actinium series:

$$^{243}Am \rightarrow {}^{239}Pu \rightarrow {}^{235}U \rightarrow {}^{231}Pa$$

2) Neptunium Series:

$$^{241}Am \rightarrow {}^{237}Np \rightarrow {}^{233}U \rightarrow {}^{229}Th$$

3) Thorium Series:

$$^{240}Pu \rightarrow {}^{236}U \rightarrow {}^{232}Th$$

4) Uranium Series:

$$\left.\begin{array}{c} ^{242}Pu \rightarrow {}^{238}U \\ {}^{238}Pu \end{array}\right\} \rightarrow {}^{234}U \rightarrow {}^{230}Th \rightarrow {}^{226}Ra$$
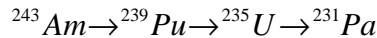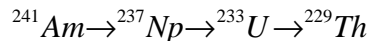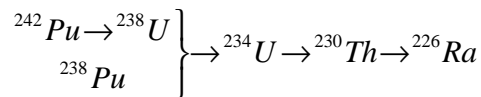
The radionuclide decay chain analysis is simplified in a manner that overestimates the concentration of decay product-radionuclides by calculating secular equilibrium between the final decay products and their parents in three of these chains. ^{227}Ac is in secular equilibrium with ^{231}Pa in the actinium chain at the downstream end of the SZ analysis. ^{228}Ra is in secular equilibrium with ^{232}Th in the thorium series. ^{210}Pb is in secular equilibrium with ^{226}Ra in the uranium series. In the model setup, radionuclides ^{241}Am, ^{243}Am, ^{239}Pu, ^{240}Pu, and ^{242}Pu are

subject to transport as irreversibly attached to colloids; and ^{243a}Am, ^{238}Pu, ^{239a}Pu, ^{240a}Pu, ^{242a}Pu, ^{231}Pa, ^{229}Th, ^{230}Th, and ^{232}Th are subject to the equilibrium colloid-facilitated transport mode. The one-dimensional model is set up using the Pathway Component of the Contaminant Transport Module in the GoldSim Graphical Simulation Environment. The pipe component is able to simulate advection, longitudinal dispersion, retardation, decay and ingrowth, and matrix diffusion (Figure 6-5) (Miller and Kossik 1998 [100449]).
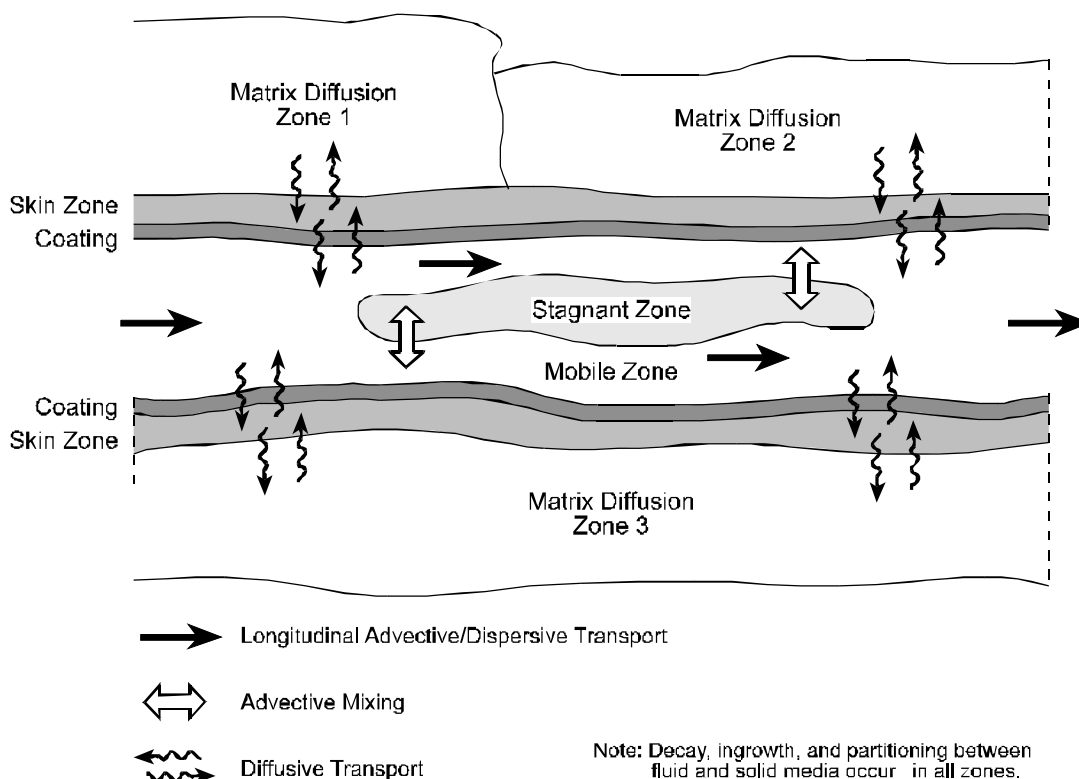
Figure 6-5. Transport Processes Simulated in One-Dimensional Pipe Pathways in the GoldSim v. 7.50.100 Software Code (STN: 10344-7.50.100-00), BSC 2003 [161572]

Each pipe in the GoldSim v. 7.50.100 software code (STN: 10344-7.50.100-00, BSC 2003 [161572]) represents a one-dimensional mass transport model with uniform properties. The ratio of the volumetric outflow rate to the cross-sectional area of each pipe pathway represents the specific discharge in the pipe. A mass flux loading at the beginning of the first pipe is the source of the radionuclides that are transported along the connected pipes. The GoldSim v. 7.50.100 software code (STN: 10344-7.50.100-00, BSC 2003 [161572]) also provides a graphical container that isolates all of the model components in one compartment to better organize the model components graphically on screen.

Transport from the four source regions in the SZ are represented by four sets of connected pipes in the SZ 1-D Transport Model. Each set of pipes consists of three pipe segments. The first segment extends from the center of the corresponding source region beneath the repository to a distance of 5 km. The second pipe segment extends from 5 km to the contact between the volcanic aquifer and the alluvium. The third pipe segment extends from the contact between the volcanic aquifer and the alluvium to the regulatory boundary with the accessible environment.

The mathematical representation of radionuclide transport in the SZ 1-D Transport Model is the same as that in the SZ Transport Abstraction Model, as presented in Equation 6-2 to Equation 6-5 and Equation 6-9. There are some differences in the mathematical implementation between the models with regard to retardation in fractures, as described below.

In the SZ 1-D Transport Model the retardation factor in fractures cannot be directly specified. The retardation in fractures for colloids with irreversibly attached radionuclides is calculated according to the retardation factor (CORVO) of the colloids using the fracture coating option in the GoldSim v. 7.50.100 software code (STN: 10344-7.50.100-00, BSC 2003 [161572]). The equation for calculating the retardation factor in the fracture with the coating on fracture surface is:

$$R_{m,s} = 1 + \frac{PT}{A_m \phi_p} (\rho_c K_{c,s} + \phi_c)$$ (Eq. 6-13)

where $R_{m,s}$ is the retardation factor due to the coating [-], P is the perimeter of the fracture pathway [L], T is the thickness of the coating [L], A_m is the cross-sectional area of the mobile zone [L^2], ϕ_p is the porosity in the pipe (equal to 1.0 for fractures), ρ_c is the dry bulk density of the coating material [M/L^3], $K_{c,s}$ is the sorption coefficient of the coating [L^3/M], and ϕ_c is the porosity of the coating material [-]. For a given value of $R_{m,s}$, the sorption coefficient is specified by rearranging Equation 6-13:

$$K_{c,s} = \frac{1}{\rho_c} \left[\frac{A_m \phi_p}{PT} (R_{m,s} - 1) - \phi_c \right]$$ (Eq. 6-14)

It should be noted that representation of retardation in the fractures using the coating option in GoldSim v. 7.50.100 software code (STN: 10344-7.50.100-00, BSC 2003 [161572]) is for mathematical convenience only. The retardation factor for colloids with irreversibly attached radionuclides is specified as an input parameter in the SZ 1-D Transport Model and a corresponding value of the sorption coefficient of the fracture coating is calculated using Equation 6-14 within the parameter definitions used in the model. This does not constitute an inconsistency in the conceptual model between the SZ 1-D Transport Model and the SZ Transport Abstraction Model. The values of the parameters T and ϕ_c are chosen to be realistic, but are essentially irrelevant because they are only used to back-calculate the value of $K_{c,s}$. The value of the fracture perimeter is 2 m because the cross section of the pipes in the SZ 1-D Transport Model is specified as 1 m by 1m and a single fracture within the pipe would have a corresponding perimeter of 2 m.

There is no matrix diffusion in fractured media for colloids with irreversibly attached radionuclides. Consequently, there is no sorption in the matrix for radionuclides irreversibly attached to colloids. This is simulated by specifying an arbitrarily small value of matrix porosity ($\sim 10^{-10}$) and zero sorption coefficients for these species in the volcanic matrix. The matrix diffusion coefficient for those radionuclides that do experience matrix diffusion is implemented by calculating an effective tortuosity, based on the sampled value of effective diffusion coefficient and the free water diffusion coefficient. The free water diffusion coefficient is adjusted by a factor approximately equivalent to the volcanic matrix porosity, using the parameter "Adjusted_Diffusion_Free" to match results from the three-dimensional SZ Site-Scale Transport Model

Values of specific discharge for segments represented by pipe pathways in the SZ 1-D Transport Model vary along the flowpath from the repository. A plot of the particle paths in the SZ Transport Abstraction Model indicates that the flowpath length through the alluvium varies, depending on uncertainty in the SZ flow field (see Figure 6-6). This uncertainty is represented by variation in the geometry of the alluvial uncertainty zone in the SZ Transport Abstraction Model. Specifically, the lengths of the flow paths in the volcanic units and the alluvium are functions of the western boundary of the alluvial uncertainty zone (as controlled by the FPLAW stochastic parameter). Secondarily, this variability is the result of different flowpaths (i.e., width of the plume). The lengths of the flow paths are also functions of the anisotropy ratio in horizontal permeability of the volcanic units (as controlled by the HAVO stochastic parameter) (see Figure 6-6). In the one-dimensional radionuclide transport model, the length of the alluvium (out to 18-km distance) is varied from 2 km to 10 km as functions of the FPLAW and HAVO parameter values and the source region beneath the repository (see Table 6-7 and supporting text).
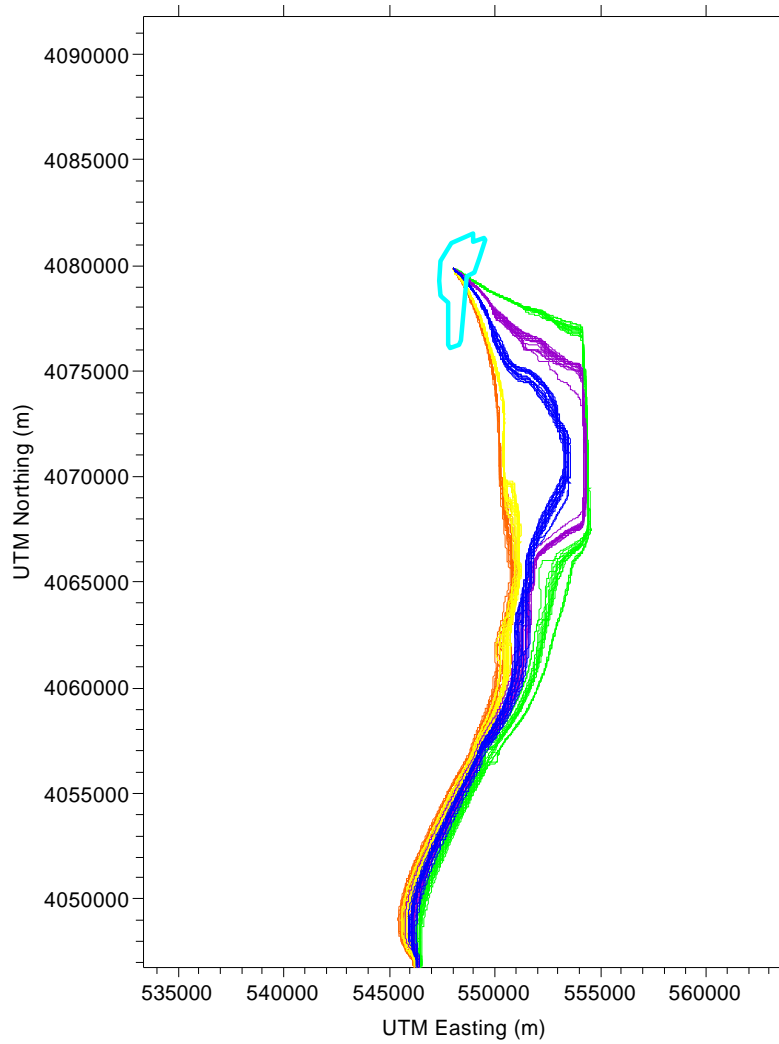
Source for repository outline: 800-IED-EBS0-00401-000-00C, BSC 2003 [162289]

NOTE: Green lines, purple lines, blue lines, yellow lines, and red lines show simulated particle paths for horizontal anisotropy values of 0.05, 0.20, 1.0, 5.0, and 20.0, respectively.

Figure 6-6. Simulated Particle Paths for Different Values of Horizontal Anisotropy in Permeability

The SZ 1-D Transport Model represents a significant simplification of the three-dimensional groundwater flow system, relative to the SZ Transport Abstraction Model. To accurately capture the three-dimensional characteristics of the SZ flow and transport system in this one-dimensional model, the SZ 1-D Transport Model is divided into three sets of "pipe" segments. The lengths and groundwater flow rates of these "pipe" segments are estimated from the SZ Transport Abstraction Model.

Average specific discharge along different segments of the flow path is estimated using the SZ Transport Abstraction Model in the following way. 1000 particles are released beneath the repository in the simulation, matrix diffusion is not used, and all porosities are assigned a value of 1.0 for the assessment of average specific discharge. The "average specific discharge" is calculated by dividing the flow path length by the 50th percentile of travel times among the particles, for that flow path segment. The average specific discharge also varies as a function of the horizontal anisotropy (parameter HAVO). The resulting values of average specific discharge, as used in the SZ 1-D Transport Model, are shown in Table 6-6. The values in Table 6-6 are input as a GoldSim v. 7.50.100 software code (STN: 10344-7.50.100-00, BSC 2003 [161572]) look-up table in the SZ 1-D Transport Model. Also note that the values of specific discharge scale linearly with the groundwater specific discharge scaling factor (parameter GWSPD) for the consideration of uncertainty in specific discharge. The values of specific discharge within the three pipe segments are calculated within the model by interpolating between the values of HAVO and scaling by the value of GWSPD. The volumetric flow rate is the same for all segments in the SZ 1-D Transport Model and the variations in specific discharge along the flow path are incorporated by varying the cross-sectional areas of the pipe segments.

Table 6-6. Average Specific Discharge in Flow Path Segments

HAVO	Average Specific Discharge (m/year)		
	0-5 km	5-13 km	13-18 km
0.05	0.312	7.50	1.936
1.00	0.536	1.824	2.357
5.00	0.722	2.694	2.793
20.00	0.870	4.465	3.183

The flow path length of each pipe segment in the SZ 1-D Transport Model varies as a function of FPLAW, HAVO, and the source region from which the radionuclide source originates beneath the repository. The first pipe segment is 5 km in length for all cases. The second pipe segment represents that portion of the flow path from 5 km distance to the contact between the volcanic units and the alluvium in the SZ. The third pipe segment represents the portion of the flow path from the contact between the volcanic units and the alluvium out to the regulatory boundary to the accessible environment. The lengths of the second and third pipe segments were estimated from the particle tracking results of the 3-D SZ Transport Abstraction Model, as shown in Figure 6-6 and as summarized in Table 6-7. The estimated pipe segment lengths are shown in Table 6-7 for differing values of HAVO and for the four source regions. Each entry in the table contains a

range of values in length, where the minimum value shown for the 5-13 km pipe segment (second pipe segment) corresponds to FPLAW equal to 1.0 and the maximum value corresponds to FPLAW equal to 0.0. By contrast, the minimum value of length for the 13-18 km pipe segment (third pipe segment) corresponds to FPLAW equal to 0.0 and the maximum value corresponds to FPLAW equal to 1.0. In other words, the maximum length of the flow path in the alluvium corresponds to the maximum westerly extent of the alluvium uncertainty zone and the minimum length of the flow path in the alluvium corresponds to the minimum westerly extent of the alluvium uncertainty zone. The values in Table 6-7 are input as a GoldSim v. 7.50.100 software code (STN: 10344-7.50.100-00, BSC 2003 [161572]) look-up table in the SZ 1-D Transport Model.

Table 6-7. Flow Path Lengths of Pipe Segments

| HAO | Minimum and Maximum Flow Path Lengths of Pipe Segments (km) | | | | | | | |
| | Source Region 1 | | Source Region 2 | | Source Region 3 | | Source Region 4 | |
	5-13 km	13-18 km	5-13 km	13-18 km	5-13 km	13-18 km	5-13 km	13-18 km
0.05	12.0 - 14.5	7.5 – 10.0	12.0 – 14.0	7.0 – 9.0	13.0 – 16.0	3.0 – 6.0	12.5 – 15.0	3.5 – 6.0
1.00	12.0 – 14.0	5.5 – 7.5	12.0 – 14.5	4.5 – 7.0	10.0 – 13.5	2.0 – 5.5	10.0 – 12.0	3.0 – 5.0
5.00	12.5 – 14.5	3.0 – 5.0	11.5 – 14.0	3.0 – 5.5	10.5 – 14.0	1.0 – 4.5	10.5 – 12.5	2.0 – 4.0
20.00	12.5 – 14.5	2.5 – 4.5	11.5 – 14.0	3.0 – 5.5	10.5 – 14.0	1.0 – 4.5	10.5 – 12.5	2.0 – 4.0

6.5.2   Base-Case Model Inputs

The SZ Transport Abstraction Model and the SZ 1-D Transport Model include uncertainty through stochastic simulations of uncertain parameters. Parameter uncertainties are quantified through uncertainty distributions, which numerically represent our state of knowledge about a particular parameter on a scale of the model domain. The uncertainty distribution (either cumulative distribution function (CDF) or probability density function (PDF)) of a parameter, represents what we know and what we do not know about the parameter and reflects the current knowledge of the range and likelihood of the appropriate parameter values when used in these models (BSC 2002 [158794], p. 45). The uncertainty distributions incorporate uncertainties associated with field or laboratory data, knowledge of how the parameter will be used in the model, and theoretical considerations. Geologic uncertainty is incorporated with regard to the location of the contact between the tuff and alluvium at the water table (see Section 6.5.2.2) In some cases, parameters are assigned constant values because radionuclide transport is relatively insensitive to the parameter or the uncertainty is relatively small. Constant parameters are defined to vary from one hydrogeologic unit to another, but for a given hydrogeologic unit, the parameter remains constant for all realizations. The development and justification for the parameter uncertainty distributions are discussed below. See Table 6-8 for a comprehensive list

of the models/analyses inputs used in the SZ Transport Abstraction Model and the SZ 1-D Transport Model. The unit numbers given in Table 6-8 are defined by hydrogeologic unit in Table 6-9. Please note that parameter values are developed for the 19 hydrogeologic units in Table 6-9 for completeness; however, 18 units are included in the SZ Site-Scale Flow Model, the SZ Site-Scale Transport Model, and the SZ Transport Abstraction Model. The valley-fill confining unit has a very small volume relative to other units in the model domain and occurrences of this unit do not occur along the flow path from the repository. Consequently, it is not included in the models as a separate unit.

Table 6-8. Model/Analyses Inputs Used in the SZ Transport Abstraction Model and the SZ 1-D Transport Model

Input Name	Input Description	Input Source (DTN, if applicable)	Value or Distribution		Units	Type of Uncertainty
KDNPVO	Neptunium sorption coefficient in volcanic units	LA0310AM831341.002 [165891]	CDF: Probability 0.0 0.05 0.90 1.0	Value 0.0 0.99 1.83 6.0	ml/g	Epistemic
KDNPAL	Neptunium sorption coefficient in alluvium	LA0310AM831341.002 [165891]	CDF: Probability 0.0 0.05 0.95 1.0	Value 1.8 4.0 8.7 13.0	ml/g	Epistemic
KDSRVO	Strontium sorption coefficient in volcanic units	LA0310AM831341.002 [165891]	Uniform: Minimum 20. Maximum 400.		ml/g	Epistemic
KDSRAL	Strontium sorption coefficient in alluvium	LA0310AM831341.002 [165891]	Uniform: Minimum 20. Maximum 400.		ml/g	Epistemic
KDUVO	Uranium sorption coefficient in volcanic units	LA0310AM831341.002 [165891]	CDF: Probability 0.0 0.05 0.95 1.0	Value 0.0 5.39 8.16 20.0	ml/g	Epistemic
KDUAL	Uranium sorption coefficient in alluvium	LA0310AM831341.002 [165891]	CDF: Probability 0.0 0.05 0.95 1.0	Value 1.7 2.9 6.3 8.9	ml/g	Epistemic

Table 6-8. Model/Analyses Inputs Used in the SZ Transport Abstraction Model and the SZ 1-D Transport Model (Continued)

Input Name	Input Description	Input Source (DTN, if applicable)	Value or Distribution	Units	Type of Uncertainty
KDRAVO	Radium sorption coefficient in volcanic units	LA0310AM831341.002 [165891]	Uniform: Minimum 100. Maximum 1000.	ml/g	Epistemic
KDRAAL	Radium sorption coefficient in alluvium	LA0310AM831341.002 [165891]	Uniform: Minimum 100. Maximum 1000.	ml/g	Epistemic
KD_Pu_Vo	Plutonium sorption coefficient in volcanic units	LA0310AM831341.002 [165891]	CDF: Probability Value 0.0 10. 0.25 89.9 0.95 129.87 1.0 300.	ml/g	Epistemic
KD_Pu_Al	Plutonium sorption coefficient in alluvium	LA0310AM831341.002 [165891]	Beta: Mean 100. Standard Deviation 15. Minimum 50. Maximum 300.	ml/g	Epistemic
KD_Am_Vo	Americium sorption coefficient in volcanic units	LA0310AM831341.002 [165891]	Truncated Normal: Mean 5500. Standard Deviation 1500. Minimum 1000. Maximum 10000.	ml/g	Epistemic
KD_Am_Al	Americium sorption coefficient in alluvium	LA0310AM831341.002 [165891]	Truncated Normal: Mean 5500. Standard Deviation 1500. Minimum 1000. Maximum 10000.	ml/g	Epistemic
KD_Cs_Vo	Cesium sorption coefficient in volcanic units	LA0310AM831341.002 [165891]	CDF: Probability Value 0.0 100. 0.05 3000.59 1.0 6782.92	ml/g	Epistemic
KD_Cs_Al	Cesium sorption coefficient in alluvium	LA0310AM831341.002 [165891]	Truncated Normal: Mean 728. Standard Deviation 464. Minimum 100. Maximum 1000.	ml/g	Epistemic

Table 6-8. Model/Analyses Inputs Used in the SZ Transport Abstraction Model and the SZ 1-D
Transport Model (Continued)

Input Name	Input Description	Input Source (DTN, if applicable)	Value or Distribution	Units	Type of Uncertainty
FISVO	Flowing interval spacing in volcanic units	SN9907T0571599.001 [122261]	CDF : (Log$_{10}$-transformed) Probability Value 0.0 0.087 0.05 0.588 0.25 1.00 0.50 1.29 0.75 1.58 0.95 1.90 1.0 2.62	m	Epistemic
CORAL	Colloid retardation factor in alluvium	LA0303HV831352.004 [163559]	CDF : (Log$_{10}$-transformed) Probability Value 0.0 0.903 0.331 0.904 0.50 1.531 1.0 3.715	NA	Epistemic
CORVO	Colloid retardation factor in volcanic units	LA0303HV831352.002 [163558]	CDF : (Log$_{10}$-transformed) Probability Value 0.0 0.778 0.15 0.779 0.25 1.010 0.50 1.415 0.80 1.778 1.0 2.903	NA	Epistemic
HAVO	Ratio of horizontal anisotropy in permeability	SN0302T0502203.001 [163563]	CDF: Probability Value 0.0 0.05 0.0042 0.2 0.0168 0.4 0.0379 0.6 0.0674 0.8 0.10 1.0 0.60 5. 0.744 8. 0.856 11. 0.936 14. 0.984 17. 1.0 20.	NA	Epistemic
LDISP	Longitudinal dispersivity	MO0003SZFWTEEP.000 [148744]	Truncated Normal: (Log$_{10}$-transformed) Mean 2.0 Standard Deviation 0.75	m	Epistemic

Table 6-8. Model/Analyses Inputs Used in the SZ Transport Abstraction Model and the SZ 1-D Transport Model (Continued)

Input Name	Input Description	Input Source (DTN, if applicable)	Value or Distribution	Units	Type of Uncertainty
Kd_Pu_Col	Plutonium sorption coefficient onto colloids	SN0306T0504103.006 [164131]	CDF: Probability Value 0.0 1.e3 0.04 5.e3 0.12 1.e4 0.37 5.e4 0.57 1.e5 0.92 5.e5 1.0 1.e6	ml/g	Epistemic
Kd_Am_Col	Americium sorption coefficient onto colloids	SN0306T0504103.006 [164131]	CDF: Probability Value 0.0 1.e4 0.07 5.e4 0.17 1.e5 0.40 5.e5 0.60 1.e6 0.92 5.e6 1.0 1.e7	ml/g	Epistemic
Kd_Cs_Col	Cesium sorption coefficient onto colloids	SN0306T0504103.006 [164131]	CDF: Probability Value 0.0 1.e2 0.2 5.e2 0.45 1.e3 0.95 5.e3 1.0 1.e4	ml/g	Epistemic
Conc_Col	Groundwater concentration of colloids	SN0306T0504103.005 [164132]	CDF : (Log_{10}-transformed) Probability Value 0.0 -9.0 0.50 -7.0 0.75 -6.0 0.90 -5.0 0.98 -4.3 1.0 -3.6	g/ml	Epistemic
R_U_Kd	Correlation coefficient for U K_d in volcanic units and alluvium	LA0310AM831341.002 [165891]	0.75	ml/g	N/A
R_Np_Kd	Correlation coefficient for Np K_d in volcanic units and alluvium	LA0310AM831341.002 [165891]	0.75	ml/g	N/A

Table 6-8. Model/Analyses Inputs Used in the SZ Transport Abstraction Model and the SZ 1-D Transport Model (Continued)

Input Name	Input Description	Input Source (DTN, if applicable)	Value or Distribution	Units	Type of Uncertainty
R_Pu_Kd	Correlation coefficient for Pu K_d in volcanic units and alluvium	LA0310AM831341.002 [165891]	0.50	ml/g	N/A
R_U_Np	Correlation coefficient for U K_d and Np K_d	LA0310AM831341.002 [165891]	0.50	ml/g	N/A
FPLAW	Western boundary of alluvial uncertainty zone	Internal to this report	Uniform: Minimum 0.0 Maximum 1.0	N/A	Epistemic
FPLAN	Northern boundary of alluvial uncertainty zone	Internal to this report	Uniform: Minimum 0.0 Maximum 1.0	N/A	Epistemic
NVF19	Effective porosity in shallow alluvium	Internal to this report	Truncated Normal: Mean 0.18 Standard Deviation 0.051 Minimum 0.00 Maximum 0.30	N/A	Epistemic
NVF7	Effective porosity in undifferentiated valley fill	Internal to this report	Truncated Normal: Mean 0.18 Standard Deviation 0.051 Minimum 0.00 Maximum 0.30	N/A	Epistemic
FPVO	Fracture porosity in volcanic units	Internal to this report	CDF: (Log_{10}-transformed) Probability Value 0.0 -5.0 0.05 -4.0 0.50 -3.0 0.80 -2.0 1.0 -1.0	N/A	Epistemic
DCVO	Effective diffusion coefficient in volcanic units	Internal to this report	CDF: (Log_{10}-transformed) Probability Value 0.0 -11.3 0.08 -10.7 0.50 -10.3 0.83 -9.9 1.0 -9.3	m^2/s	Epistemic

Table 6-8.   Model/Analyses Inputs Used in the SZ Transport Abstraction Model and the SZ 1-D
Transport Model (Continued)

Input Name	Input Description	Input Source (DTN, if applicable)	Value or Distribution	Units	Type of Uncertainty
GWSPD	Groundwater specific discharge multiplier	Internal to this report	CDF: (Log$_{10}$-transformed) Probability Value 0.0 -1.477 0.10 -0.477 0.50 0.0 0.90 0.477 1.0 1.0	N/A	Epistemic
bulkdensity	Bulk density of alluvium	Internal to this report	Normal: Mean 1910 Standard Deviation 78	kg/m^3	Epistemic
SRC1X SRC1Y SRC2X SRC2Y SRC3X SRC3Y SRC4X SRC4Y	Source regions beneath the repository	Internal to this report	Uniform: Minimum 0.0 Maximum 1.0	N/A	Epistemic and Aleatory
Alluv_xmin1	UTM minimum easting, SW corner alluvial uncertainty zone	Internal to this report	548285.	m	N/A
Alluv_xmax1	UTM maximum easting, SW corner alluvial uncertainty zone	Internal to this report	546669.	m	N/A
Alluv_ymin1	UTM minimum northing, SW corner alluvial uncertainty zone	Internal to this report	4057240.	m	N/A
Alluv_ymax1	UTM maximum northing, SW corner alluvial uncertainty zone	Internal to this report	4057620.	m	N/A
Alluv_xmin2	UTM minimum easting, SE corner alluvial uncertainty zone	Internal to this report	555550.	m	N/A
Alluv_xmax2	UTM maximum easting, SE corner alluvial uncertainty zone	Internal to this report	555550.	m	N/A

Table 6-8. Model/Analyses Inputs Used in the SZ Transport Abstraction Model and the SZ 1-D
Transport Model (Continued)

Input Name	Input Description	Input Source (DTN, if applicable)	Value or Distribution	Units	Type of Uncertainty
Alluv_ymin2	UTM minimum northing, SE corner alluvial uncertainty zone	Internal to this report	4055400.	m	N/A
Alluv_ymax2	UTM maximum northing, SE corner alluvial uncertainty zone	Internal to this report	4055400.	m	N/A
Alluv_xmin3	UTM minimum easting, NE corner alluvial uncertainty zone	Internal to this report	557424.	m	N/A
Alluv_xmax3	UTM maximum easting, NE corner alluvial uncertainty zone	Internal to this report	557758.	m	N/A
Alluv_ymin3	UTM minimum northing, NE corner alluvial uncertainty zone	Internal to this report	4065430.	m	N/A
Alluv_ymax3	UTM maximum northing, NE corner alluvial uncertainty zone	Internal to this report	4067430.	m	N/A
Alluv_xmin4	UTM minimum easting, NW corner alluvial uncertainty zone	Internal to this report	554192.	m	N/A
Alluv_xmax4	UTM maximum easting, NW corner alluvial uncertainty zone	Internal to this report	553579.	m	N/A
Alluv_ymin4	UTM minimum northing, NW corner alluvial uncertainty zone	Internal to this report	4065430.	m	N/A
Alluv_ymax4	UTM maximum northing, NW corner alluvial uncertainty zone	Internal to this report	4067430.	m	N/A
A1_1_x	UTM easting, SW corner source zone 1	Internal to this report	547570.	m	N/A
A1_1_y	UTM northing, SW corner source zone 1	Internal to this report	4078630.	m	N/A

Table 6-8. Model/Analyses Inputs Used in the SZ Transport Abstraction Model and the SZ 1-D Transport Model (Continued)

Input Name	Input Description	Input Source (DTN, if applicable)	Value or Distribution	Units	Type of Uncertainty
A1_2_x	UTM easting, SE corner source zone 1	Internal to this report	548500.	m	N/A
A1_2_y	UTM northing, SE corner source zone 1	Internal to this report	4078630.	m	N/A
A1_3_x	UTM easting, NE corner source zone 1	Internal to this report	548500.	m	N/A
A1_3_y	UTM northing, NE corner source zone 1	Internal to this report	4081090.	m	N/A
A1_4_x	UTM easting, NW corner source zone 1	Internal to this report	547570.	m	N/A
A1_4_y	UTM northing, NW corner source zone 1	Internal to this report	4081090.	m	N/A
A2_1_x	UTM easting, SW corner source zone 2	Internal to this report	548500.	m	N/A
A2_1_y	UTM northing, SW corner source zone 2	Internal to this report	4078630.	m	N/A
A2_2_x	UTM easting, SE corner source zone 2	Internal to this report	549320.	m	N/A
A2_2_y	UTM northing, SE corner source zone 2	Internal to this report	4078630.	m	N/A
A2_3_x	UTM easting, NE corner source zone 2	Internal to this report	549320.	m	N/A
A2_3_y	UTM northing, NE corner source zone 2	Internal to this report	4081210	m	N/A
A2_4_x	UTM easting, NW corner source zone 2	Internal to this report	548500.	m	N/A
A2_4_y	UTM northing, NW corner source zone 2	Internal to this report	4081210.	m	N/A
A3_1_x	UTM easting, SW corner source zone 3	Internal to this report	547720.	m	N/A

Table 6-8. Model/Analyses Inputs Used in the SZ Transport Abstraction Model and the SZ 1-D Transport Model (Continued)

Input Name	Input Description	Input Source (DTN, if applicable)	Value or Distribution	Units	Type of Uncertainty
A3_1_y	UTM northing, SW corner source zone 3	Internal to this report	4076170.	m	N/A
A3_2_x	UTM easting, SE corner source zone 3	Internal to this report	548500.	m	N/A
A3_2_y	UTM northing, SE corner source zone 3	Internal to this report	4076170.	m	N/A
A3_3_x	UTM easting, NE corner source zone 3	Internal to this report	548500.	m	N/A
A3_3_y	UTM northing, NE corner source zone 3	Internal to this report	4078630.	m	N/A
A3_4_x	UTM easting, NW corner source zone 3	Internal to this report	547720.	m	N/A
A3_4_y	UTM northing, NW corner source zone 3	Internal to this report	4078630.	m	N/A
A4_1_x	UTM easting, SW corner source zone 4	Internal to this report	548500.	m	N/A
A4_1_y	UTM northing, SW corner source zone 4	Internal to this report	4076170.	m	N/A
A4_2_x	UTM easting, SE corner source zone 4	Internal to this report	548890.	m	N/A
A4_2_y	UTM northing, SE corner source zone 4	Internal to this report	4076170.	m	N/A
A4_3_x	UTM easting, NE corner source zone 4	Internal to this report	548890.	m	N/A
A4_3_y	UTM northing, NE corner source zone 4	Internal to this report	4078630.	m	N/A
A4_4_x	UTM easting, NW corner source zone 4	Internal to this report	548500.	m	N/A
A4_4_y	UTM northing, NW corner source zone 4	Internal to this report	4078630.	m	N/A

Table 6-8. Model/Analyses Inputs Used in the SZ Transport Abstraction Model and the SZ 1-D
Transport Model (Continued)

Input Name	Input Description	Input Source (DTN, if applicable)	Value or Distribution	Units	Type of Uncertainty
Max_al_por	Total alluvium porosity	Internal to this report	0.30	N/A	N/A
Fpor	Average fracture porosity in volcanic units	Internal to this report	0.001	N/A	N/A
Mpor	Average matrix porosity in volcanic units	Internal to this report	0.22	N/A	N/A
Bdens	Average bulk density in volcanic units	Internal to this report	1.88	g/ml	N/A
Matrix porosity	Expected values for matrix porosity per volcanic unit	SN0004T0501399.003 [155045] Units 15-13, 10 and 8 Units 12, 11, and 9 are Internal to this report	Unit 15: 0.15 Unit 14, 10 and 8: 0.25 Unit 13: 0.23 Unit 12: 0.18 Unit 11: 0.21 Unit 9: 0.21	N/A	N/A
Bulk Density	Expected bulk density values per volcanic unit	Units 15-13, 10, 8; SN0004T0501399.002 [155046] and SN0004T0501399.003 [155045] Units 17, 12, 11, 9 and 6-2 are internal to this report	Unit 18: 2.50 Unit 17, 6, 5, and 3: 2.77 Unit 16: 2.44 Unit 15: 2.08 Unit 14, 10 and 8: 1.77 Unit 13: 1.84 Unit 12: 2.19 Unit 11: 2.11 Unit 9: 2.05 Unit 4 and 2: 2.55 Unit 1: 2.65	g/cm^3	N/A
Effective Porosity	Expected effective porosity values for other units (see Section 6.5.2.20)	Units 18-16 and 1: MO0105HCONEPOR.000 [155044] Units 6-2 Internal to this report	Unit 18: 0.32 Unit 17: 0.01 Unit 16: 0.08 Unit 6,5 and 3: 0.01 Unit 4: 0.18 Unit 2: 0.18 Unit 1: 0.0001	N/A	N/A

Table 6-9. Hydrogeologic Unit Definition

Hydrogeologic Unit	Hydrogeologic Unit Identification Number
Valley Fill	19
Valley Fill Confining Unit	18
Cenozoic Limestones	17
Lava Flows	16
Upper Volcanic Aquifer	15
Upper Volcanic Confining Unit	14
Lower Volcanic Aquifer Prow Pass	13
Lower Volcanic Aquifer Bullfrog	12
Lower Volcanic Aquifer Tram	11
Lower Volcanic Confining Unit	10
Older Volcanic Aquifer	9
Older Volcanic Confining Unit	8
Undifferentiated Valley Fill	7
Upper Carbonate Aquifer	6
Lower Carbonate Aquifer Thrust	5
Upper Clastic Confining Unit	4
Lower Carbonate Aquifer	3
Lower Clastic Confining Unit	2
Granites	1

NOTE: Hydrogeologic Units adapted from USGS 2001 [158608], Table 6-2

6.5.2.1 Groundwater Specific Discharge

Uncertainty exists in the groundwater specific discharge in the SZ along the flow path from beneath the repository to the hypothetical point of release to the biosphere. This uncertainty was quantified as a distribution of specific discharge in the volcanic aquifer near Yucca Mountain by the SZ expert elicitation project (CRWMS M&O 1998 [100353], p. 3-43). Conclusions regarding the uncertainty in specific discharge by the expert elicitation panel primarily were based on single- and multi-well hydraulic testing of wells in the volcanic units near Yucca Mountain. The aggregate uncertainty distribution of specific discharge in the SZ from the expert elicitation had a median value of about 0.6 m/year, with a range of values from less than 0.01 m/year to about 10 m/year (CRWMS M&O 1998 [100353], p. 3-43).

More recently, estimates of groundwater specific discharge in the SZ have been obtained at another location in the SZ system from field testing at the alluvial tracer complex (ATC) (BSC 2003 [162415], Section 6.5.4.3). The ATC is approximately located at the boundary of the accessible environment, as specified in regulations for the Yucca Mountain project,

10 CFR 63.302 (10 CFR 63 [156605]). The location of the ATC is approximately 18 km from Yucca Mountain and testing was performed in the alluvium aquifer. Estimates of groundwater specific discharge at the ATC range from 1.2 m/year to 9.4 m/year (DTN: LA0303PR831231.002, [163561]), using alternative means of analyzing the single-well tracer testing results. The simulated average specific discharge in this region of the SZ system using the SZ Transport Abstraction Model ranges from 1.9 m/year to 3.2 m/year for differing values of horizontal anisotropy in permeability, as shown in Table 6-6. Correspondingly, the simulated average specific discharge in the volcanic aquifer near Yucca Mountain using the SZ Transport Abstraction Model ranges from 0.31 m/year to 0.87 m/year for differing values of horizontal anisotropy in permeability. These results show that the average groundwater specific discharge tends to increase along the flow path from beneath Yucca Mountain to the south. This increase in the specific discharge is due to convergent groundwater flow in this region of the SZ system. These results also indicate that there is general consistency between the simulated specific discharge and the median values of uncertainty ranges estimated for the volcanic aquifer and the alluvial aquifer along the flow path.

The additional data from the ATC constitutes new information on the specific discharge in the SZ and significantly reduces uncertainty in the specific discharge relative to the assessment by the expert elicitation panel. The range of estimated specific discharge at the ATC spans about a factor of 7.8 (i.e., 1.2 m/year to 9.4 m/year). This indicates range of uncertainty in specific discharge that is somewhat less than one order of magnitude, which is considerably less than the degree of uncertainty from the SZ expert elicitation project (CRWMS M&O 1998 [100353]). Consequently, the uncertainty distribution for the groundwater specific discharge factor (GWSPD) is reevaluated to reflect the reduced uncertainty. From this information, a discrete CDF of uncertainty in specific discharge is constructed, in which 80% of the probability is between 1/3 and 3 times the best estimate of specific discharge. The lower tail of the uncertainty distribution extends to 1/30 of the expected value and 10% of the probability is assigned to this lower tail. The upper tail of the uncertainty distribution extends to 10 times the expected value and 10% of the probability is assigned to this upper tail. The lower and upper tails of the uncertainty distribution approximately correspond to the greater uncertainty reflected in the SZ expert elicitation results.

Uncertainty in the groundwater specific discharge is incorporated into the SZ Transport Abstraction Model using the continuously distributed GWSPD parameter. This parameter is a multiplication factor that is applied to all values of permeability and values of specified boundary fluxes in the SZ Transport Abstraction Model to effectively scale the simulated specific discharge in the model. Note that a separate steady-state groundwater flow field is simulated for each realization of the system, using the value of GWSPD (and the value of HAVO, for horizontal anisotropy). The sampling of GWSPD is performed on the log-transformed values of the specific discharge multiplication factor, as indicated in Table 6-8. The CDF of uncertainty in the groundwater specific discharge multiplier is shown in Figure 6-7.
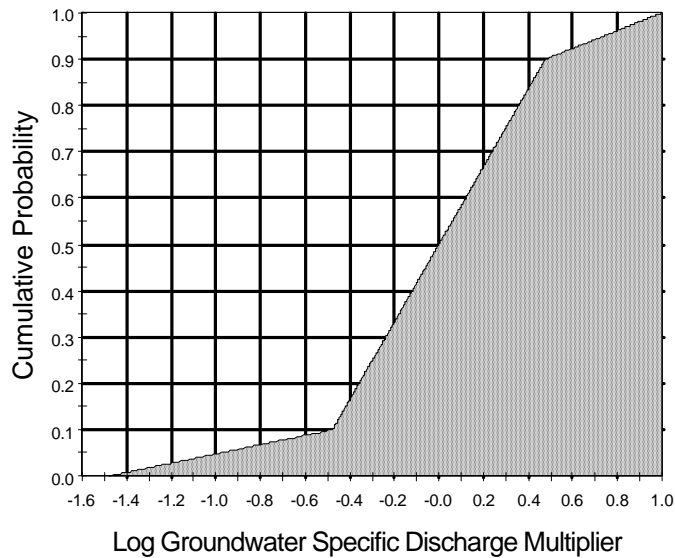
Figure 6-7. CDF of Uncertainty in Groundwater Specific Discharge Multiplier

6.5.2.2 Alluvium Uncertainty Zone

Uncertainty in the geology below the water table exists along the inferred flowpath from the potential repository at distances of approximately 10 km to 20 km down gradient of the repository. The location at which groundwater flow moves from fractured volcanic rocks to alluvium is of particular significance from the perspective of repository performance assessment. This is because of contrasts between the fractured volcanic units and the alluvium in terms of groundwater flow (fracture dominated flow vs. porous medium flow) and in terms of sorptive properties of the media for some radionuclides.

The uncertainty in the northerly extent of the alluvium in the SZ of the site-scale flow and transport simulations is abstracted as a polygonal region that is assigned radionuclide transport properties representative of the valley-fill aquifer hydrogeologic unit (Table 6-9). The dimensions of the polygonal region are randomly varied in the SZ Transport Abstraction Model for the multiple realizations. The northern boundary of the uncertainty zone is varied between the dashed lines at the northern end of the polygonal area shown in Figure 6-8. The western boundary of the uncertainty zone is varied between the dashed lines along the western side of the polygonal area shown in the figure.

The uncertainty in the contact between volcanic rocks and alluvium at the water table along the northern part of the uncertainty zone is approximately bounded by the location of well UE-25 JF#3, in which the water table is below the contact between the volcanic rocks and the overlying alluvium, and by the location of well EWDP-10S, in which the water table is above the contact between the volcanic rocks and the alluvium. The uncertainty in the contact along the western part of the uncertainty zone is defined by the locations of wells EWDP-10S, EWDP-22S, and EWDP-19D1, in which the water table is above the contact between volcanic rocks and the overlying alluvium, and outcrops of volcanic bedrock to the west.

The lower boundary of the alluvium uncertainty zone varies from an elevation of 670 m in the northwestern corner of the uncertainty zone to 400 m along the southern edge of the uncertainty zone. This corresponds to saturated alluvium thickness of approximately 50 m in the northwestern corner varying to about 300 m along the southern boundary of the uncertainty zone.

The boundaries of the alluvium uncertainty zone are determined for a particular realization by the parameters FPLAW and FPLAN. These parameters have uniform distributions from 0.0 to 1.0, where a value of 0.0 corresponds to the minimum extent of the uncertainty zone and 1.0 corresponds to the maximum extent of the uncertainty zone in a westerly direction and northerly direction, respectively. A uniform distribution is appropriate for these uncertainty distributions because only the bounding values are known. A uniform distribution is the best statistically unbiased choice in this situation. These parameters are used to independently and uniformly vary the northern and western contacts of the volcanic rocks and alluvium at the water table. The maximum and minimum coordinates of the alluvium uncertainty zone, corresponding to the plot shown in Figure 6-8, are given in Table 6-8 (Alluv_xmin1 to Alluv_ymax4).
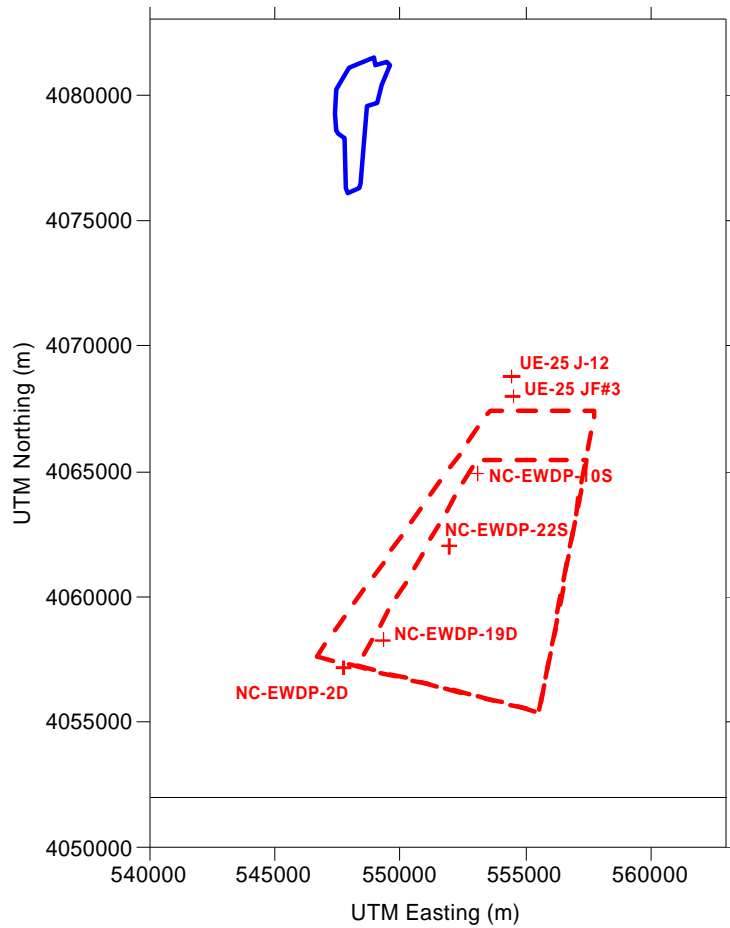
Source for repository outline: 800-IED-EBS0-00401-000-00C, BSC 2003 [162289]
Source for well locations: DTN: GS010908312332.002 [163555]
DTN: GS030108314211.001 [163483]

NOTE: Repository outline is shown by the solid line and the minimum and maximum boundaries of the alluvium uncertainty zone are shown by the dashed lines. Key well locations and well numbers are shown with the cross symbols.

Figure 6-8. Minimum and Maximum Extent of the Alluvium Uncertainty Zone

6.5.2.3 Effective Porosity of Alluvium

For the TSPA-SR calculations, effective porosity in the alluvium was a truncated normal distribution with a mean of 0.18, a standard deviation of 0.051, a lower bound of 0, and an upper bound of 0.35 (CRWMS M&O 2000 [147972], Section 6.3). The basis for this parameter is from Bedinger et al. 1989 [129676], p. A18, Table 1. There were no site-specific data for effective porosity in the alluvium at the time of the TSPA-SR. Bedinger et al. 1989 [129676]) include a study of hydraulic characteristics of alluvium within the Southwest Basin and Range Province. This study is relevant to the local basin fill conditions and provides values for effective porosity as a stochastic parameter. Since TSPA-SR a site-specific value was determined for effective porosity from well EWDP-19D1 at the ATC based on a single-well pumping test (BSC 2003 [162415], Sections 6.4 and 6.5). There are also total porosity values from the same well based on borehole gravimeter surveys, which are used in developing the upper bound of the effective porosity in the alluvium uncertainty distribution.

Effective porosity is important in determining the average linear ground water velocities used in the simulation of radionuclide transport. They are customarily calculated by dividing the specific discharge of groundwater through a model grid cell by the porosity, ϕ_e. Groundwater velocities are rendered more accurate when dead end pores are eliminated from consideration because they do not transmit water. The effective porosity results from that elimination. As a result ϕ_e will always be less than or equal to total porosity, ϕ_T. The retardation coefficient, R_f, is also a function of porosity. Reducing total porosity to ϕ_e can erroneously raise the magnitude of this value within the model. The correction for this is detailed in the discussion in Section 6.5.1, Equation 6-3.

Effective porosity is treated as an uncertain parameter for the two alluvium units (19 and 7) of the nineteen SZ model hydrogeologic units. Uncertain, in this sense, means that ϕ_e will be constant spatially for each unit for any particular model realization, but that value will vary from one realization to the next. In comparison, constant parameters are constant spatially and also do not change from realization to realization.

The parameter input sources used in this analysis are described in Table 4-1 and corroborative data are discussed in this section. The uncertainty distribution used for the analysis is the distribution used for TSPA-SR with a change to the upper bound. The effective porosity uncertainty distribution used for TSPA-SR is shown in Figure 6-9. Figure 6-9 compares the distribution of Bedinger et al. 1989 [129676] (DTN: MO0105HCONEPOR.000 [155044]) to distributions, ranges, and values from the other sources that were considered to develop the uncertainty distribution. The site-specific effective porosity data point from well EWDP-19D1 of 0.1 (BSC 2003 [162415], Section 6.4) is shown on Figure 6-9. This is considered a corroborative data point and falls within the uncertainty distribution for TSPA-SR.
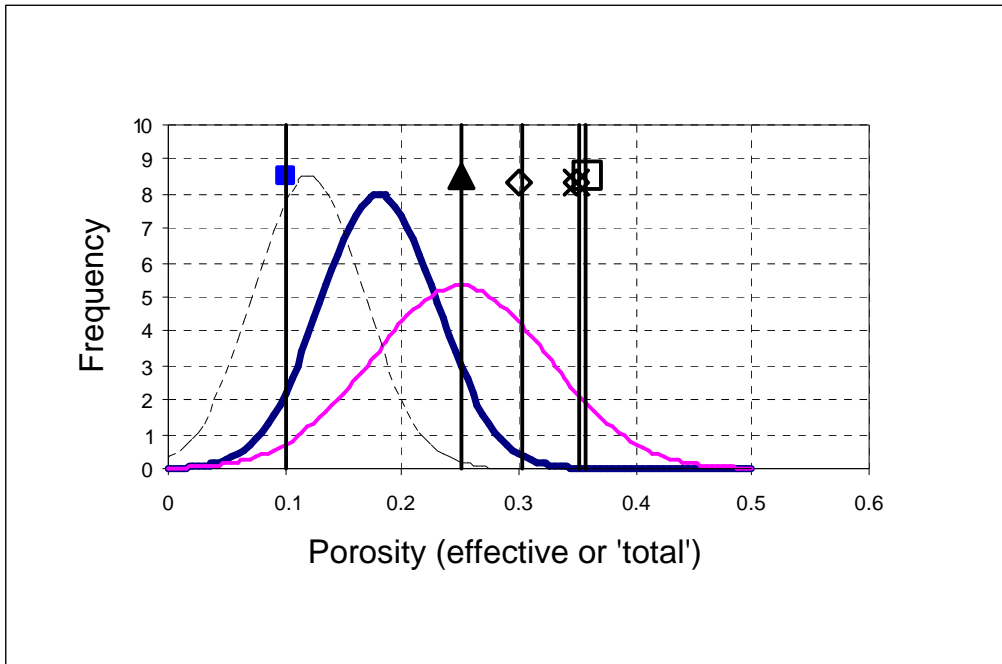
DTN: MO0003SZFWTEEP.000 [148744]
BSC 2003 [162415], Section 6.5
Burbey and Wheatcraft 1986 [129679], pp. 23-24
DOE 1997 [103021], Table 8-1, p. 8-5 and Table 8-2, p. 8-6

NOTE: The dashed black line is Neuman (MO0003SZFWTEEP.000 [148744]); the solid heavy blue line is MO0105HCONEPOR.000 [155044]; the solid pink line is Gelhar (MO0003SZFWTEEP.000 [148744]); the solid blue block is the effective porosity value calculated from EWDP-19D1 (BSC 2003 [162415], Section 6.5). The single value data points do not have a y scale value, but do correspond to the x-axis. These points are shown for comparison purposes only. The solid black triangle is DOE 1997 [103021], Table 8-1, mean matrix porosity; the diamond outlined shapes are Burbey and Wheatcraft 1986 [129679] total porosity; the X is DOE 1997 [103021], Table 8-2, total porosity and the square outlined shape is DOE 1997 [103021], Table 8-1 mean bulk porosity.

Figure 6-9. Effective Porosity Distributions and Values Compared

The upper bound of the uncertainty distribution for effective porosity is re-evaluated because of new site-specific data obtained since TSPA-SR. The new upper bound is based on the total porosity values from well EWDP-19D1 and the average of the total porosity values from the Cambric study (Burbey and Wheatcraft 1986 [129679], p. 23 and 24) within the Nevada Test Site (NTS) but several kilometers to the east, in Frenchman Flat; and total porosity shown in Tables 8-1 and 8-2 of the DOE 1997 [103021] report, pp. 8-5 and 8-6, see Table 6-10. The computed total porosity values from 19-D1 are shown in Table 6-11, which have an average value of 0.24.

Table 6-10. Total Porosity Summary(ϕ_T)

Reference	Total Porosity	Comments
DOE 1997 [103021], Table 8-1, p. 8-5	0.36	Mean bulk porosity
DOE 1997 [103021], Table 8-2, p. 8-6	0.35	Total porosity
Burbey and Wheatcraft 1986 [129679], pp. 23-24	0.34	Average of porosity values from Table 3 of that study
average of above	0.35	N/A

The average of the total porosity values in Table 6-10 and the average of the site-specific data from well EWDP-19D1 were used to develop the upper bound of the effective porosity uncertainty distribution. The average total porosity value of 0.35 and the average value from EWDP-19D1 of 0.24 result in a mean of 0.30. Figure 6-10 shows the truncated normal distribution developed in this analysis for effective porosity in the alluvium (parameter NVF19 and NVF7) with a mean of 0.18, standard deviation of 0.051, a lower bound of 0, and an upper bound of 0.30. Note that parameter NVF7 has the same distribution as NVF19 and is sampled independently.
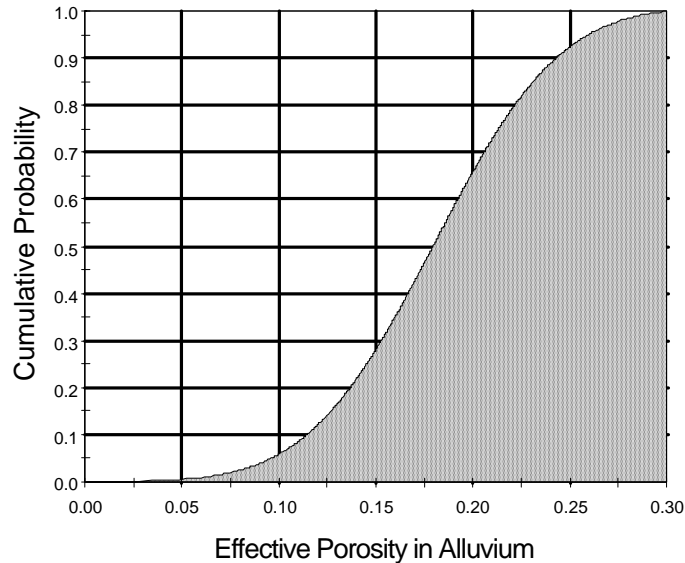
DTN: SN0310T0502103.009

Figure 6-10. CDF of Uncertainty in Effective Porosity in the Alluvium

6.5.2.4 Flowing Interval Spacing

The flowing interval spacing is a key parameter in the dual porosity model that is included in the SZ Transport Abstraction Model. A flowing interval is defined as a fractured zone that transmits fluid in the SZ, as identified through borehole flow meter surveys (see Figure 6-11). This figure shows a borehole that is intersected by multiple, irregularly spaced fractures. The figure also shows several black bands, labeled as flowing intervals, in which a flow meter survey has detected groundwater flow into (or out of) the borehole. The analysis uses the term "flowing interval spacing" as opposed to fracture spacing, which is typically used in the literature. Fracture spacing was not used because field data identified zones (or flowing intervals) that contain fluid-conducting fractures but do not distinguish how many or which fractures comprise the flowing interval. These data also indicate that numerous fractures between flowing intervals do not transmit significant amounts of groundwater. The flowing interval spacing is the distance between the midpoints of each flowing interval.
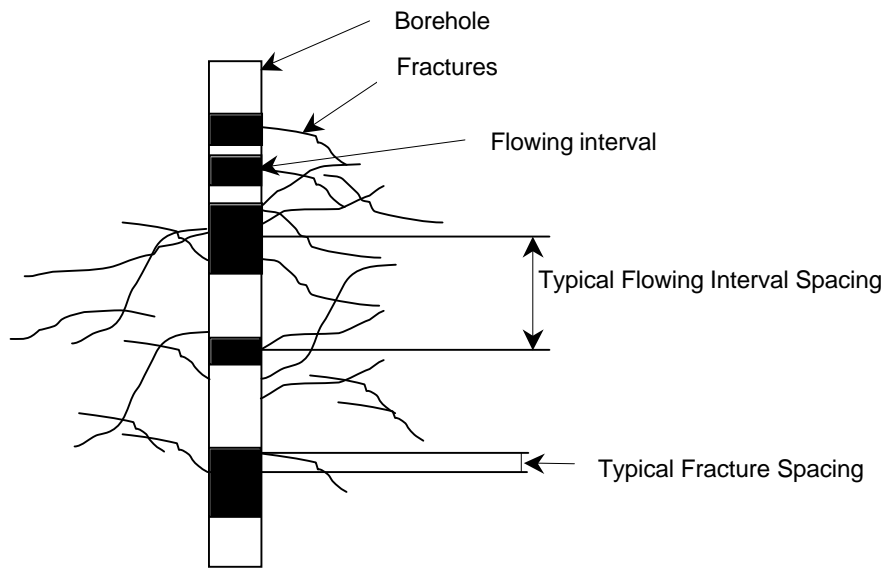
Figure 6-11. Example of Flowing Interval Spacing (BSC 2001 [156965]) for a Typical Borehole

There is considerable uncertainty regarding the flowing interval spacing parameter due to the limited number of data points available. The data set used for the analysis consisted of borehole flow meter survey data. This analysis is described in detail in BSC 2001 [156965], *Probability Distributions for Flowing Interval Spacing*.

There are no new data available to reevaluate the uncertainty distribution for this parameter, therefore a CDF based on the log-normal distribution (BSC 2001 [156965], Section 7) that was used in TSPA-SR is used as input to the TSPA-LA model and is shown in Figure 6-12. The flowing interval spacing parameter is specified for a particular realization by the parameter FISVO. See Table 6-8 for the associated probabilities for the flowing interval spacing CDF.
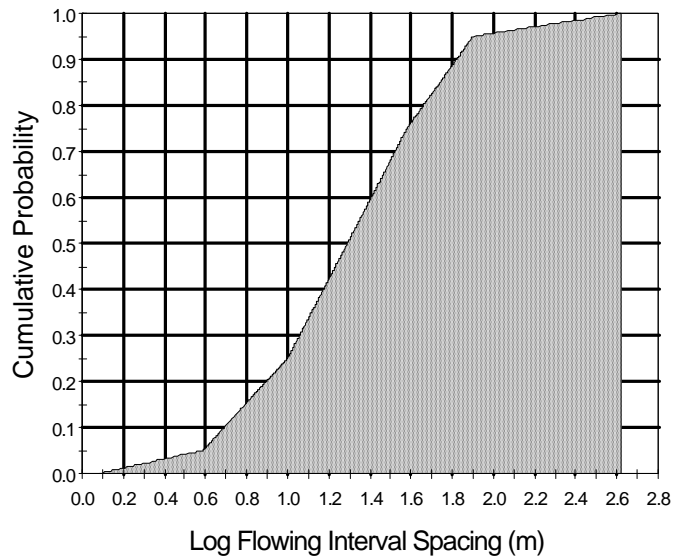
Figure 6-12. CDF of Uncertainty in Flowing Interval Spacing

DTN: SN0310T0502103.009

6.5.2.5 Flowing Interval Porosity

The flowing interval porosity is defined as the volume of the pore space through which significant groundwater flow occurs, relative to the total volume. At Yucca Mountain, rather than attempt to define the porosity within all fractures, a flowing interval is defined as the region in which significant groundwater flow occurs at a well. The fracture porosity then characterizes these flowing intervals rather than all fractures. The advantage to this definition of fracture porosity is that *in situ* well data may be used to characterize the parameter. The flowing interval porosity may also include the matrix porosity of small matrix blocks within fracture zones that potentially experience rapid matrix diffusion.

For the TSPA-SR calculations, the flowing interval (fracture) porosity probability distribution was a uniform distribution with an upper bound of $\log_{10}$ (flowing interval porosity) of • 1.0 and a lower bound of $\log_{10}$ (flowing interval porosity) of -5.0 (CRWMS M&O 2000 [147972], Section 6.7). The basis for this uncertainty distribution includes estimates of fracture porosity in intact cores of volcanic rock and the results of pumping tests and tracer tests in the Bullfrog Tuff at the C-wells Complex (CRWMS M&O 2000 [147972], Section 6.7).

The TSPA-SR probability distribution for the flowing interval porosity has been modified based on new sources of information about flowing interval porosity. New information has been derived from tests in unsaturated tuff in the Exploratory Studies Facility (ESF). Fracture porosity has been estimated in unsaturated volcanic tuff in the ESF for the middle nonlithophysal welded tuff (UZ model layer tsw34) using gas tracer testing. The assumptions used in obtaining the fracture porosity from gas tracer tests are that the diffusion of gas into the rock matrix is negligible compared to the flow through the fractures, that the fracture network is well connected, and that the gas flow is approximately radial toward the pumped borehole. This calculation of fracture porosity is documented in the *Analysis of Hydrologic Properties Data AMR* (BSC 2003 [161773], p. 41). The estimated average value of fracture porosity is 0.01.

Fracture porosity has also been estimated using the residence time of conservative tracers during cross-hole tracer tests at the C-wells Complex (CRWMS M&O 1997 [100328], p. 2-4 and BSC 2003 [162415]). This method assumes that the mean tracer arrival time is equal to the time required to drain a homogenous, fractured cylinder of rock with a radius equal to the distance between the pumping well and the tracer-injection well. A large range in estimated fracture porosity for the saturated Bullfrog Tuff resulted from this method because the tracers were interpreted to have traveled along two paths with different travel times. The path with the longer travel time resulted in a larger estimate of fracture porosity. The resulting lower and upper bounds of fracture porosity were 0.003 and 0.10, respectively (DTNs: LA0303PR831231.005 [166259] and GS031008312315.002 [166261]).

The Nevada Environmental Restoration Project (DOE 1997 [103021]) evaluated the fracture spacing and apertures in seven cores from wells at Pahute Mesa. The volcanic rocks in these cores include the Timber Mountain Tuff, Tuff Cones, Belted Range Aquifer and undistinguished welded tuff deposits. The estimated open fracture porosities based on the assumption of parallel plates, range from 6.1×10^{-6} to 4.7×10^{-4} in the welded tuffs and 2.6×10^{-6} to 4.7×10^{-4} in the tuff cores (DOE 1997 [103021], p. 5-14). Information compiled for TSPA-1993 (Wilson et al. 1994 [100191], Volume 1, Chapter 7, Table 7-19, p. 7-30) indicates average fracture porosities of 8.0×10^{-5} to 2.8×10^{-3}, in core from USW G-1, USW GU-3, USW G-4 and UE25a#1e, when parallel plate fracture geometry is assumed. This information generally corroborates the estimates of fracture porosity from DOE 1997 [103021]. There is large uncertainty in the flowing interval porosity parameter.

Given the estimates of this parameter from values based on theoretical models, pumping tests, and tracer data, the parameter uncertainty ranges over 4 orders of magnitude. To estimate the lower bound of flowing interval porosity the estimates of fracture porosity of intact cores of volcanic rock were used. The upper bound of uncertainty in the flowing interval porosity is based on interpretations of pumping test and tracer data. The new data from the ESF provide an estimate of flowing interval porosity that falls in the upper half of the distribution used for this parameter (CRWMS M&O 2000 [147972], Section 6.7) in the TSPA-SR.

For the TSPA-LA calculations, a cumulative distribution with a lower bound of $\log_{10}$ (flowing interval porosity) of • 5.0, an upper bound of $\log_{10}$ (flowing interval porosity) • 1.0 is selected for this parameter as shown in Figure 6-13. This distribution places more weight in the middle of the distribution range compared to the TSPA-SR uniform distribution (CRWMS M&O 2000 [147972], Section 6.7) that results in equal probabilities for the given range. The 0.5 probability

value of −3.0 is representative of the smallest values of fracture porosity estimated from the new data from the ESF and previous field tests. See Table 6-8 for the associated probabilities for the flowing interval porosity CDF. The flowing interval porosity parameter is specified for a particular realization by the parameter FPVO.
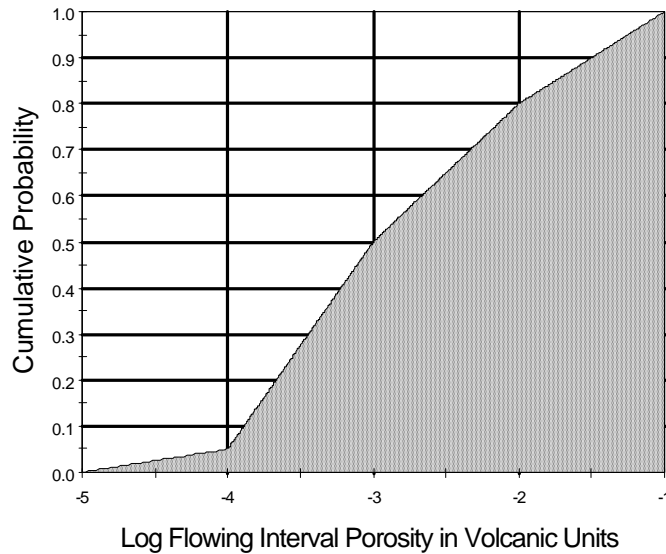
DTN: SN0310T0502103.009

Figure 6-13. CDF of Uncertainty in Flowing Interval Porosity

6.5.2.6 Effective Diffusion Coefficient

Matrix diffusion is a process in which diffusing particles move, via Brownian motion, through both mobile and immobile fluids. Diffusion is a Fickian process, that is, diffusing species move from high to low concentrations. It is dependent on the free water molecular diffusion coefficient for individual constituents and the characteristics of the flow path in which the diffusing species passes. Because diffusion through porous media is less than free water molecular diffusion, it is quantitatively defined as the effective diffusion coefficient, D_e.

Matrix diffusion has been demonstrated to occur in the volcanic rocks within the vicinity of Yucca Mountain (Reimus et al. 2002 [162956]; Reimus et al. 2002 [163008]). Thus, it is modeled in the volcanic units of the SZ Transport Abstraction Model and the SZ 1-D Transport Model for TSPA-LA. It is the transport mechanism that occurs in the rock matrix portion of the volcanic units. Consequently, it can be an important process that physically retards net radionuclide transport in fractured media.

The variability in D_e in saturated media is caused by the variability in: 1) the individual constituents' size (atom, ion, or molecule) and charge; 2) fluid temperature; and, 3) the unique properties of a porous media's lithology at a microscopic scale. The contribution of these uncertainties and variabilities in deriving a value of D_e is evaluated in the following subsections.

Variability between Lithologic Units

There are several derived 'lumped' parameters, used as adjustments to the free water molecular diffusion, to account for the impact of lithology on molecular diffusion. Tortuosity, formation, and constrictivity factors are common adjustment parameters. These lumped parameters are based on various linear regression models, fit to field and laboratory experimental results and measured properties of the host rock, such as porosity, permeability, and formation electrical resistivity (from geophysical logs).

Diffusion cell experiments have demonstrated that D_e is more affected by the structural properties of the porous medium, such as porosity, pore size distribution, and pore geometry, than by the mineralogy or geochemistry (Skagius and Neretnieks 1986 [156862], p. 389-398). Specific to Yucca Mountain, diffusion cell experiments documented by Coen 1987 [162960] on dilute sodium halite salt solutions diffusing through NTS tuff samples demonstrated D_e was directly proportional to the variability in matrix porosity and pore size distributions. Buchholtz ten Brink et al. 1991 [162954]) found D_e for [238]U on various Yucca Mountain tuff samples to be dependent on the pore size distribution of the hydrostratigraphic units

Many mathematical models have been formulated to derive a value of D_e. Most, if not all, rely on porosity, with some adding other "lumped" parameters. As an example, Bear 1972 [156269], Sections 4.8.2 and 4.8.3 relate effective matrix diffusion to porosity, formation factor (derived from geophysical logs), and the free water molecular diffusion coefficient as follows:

$$D_m = \frac{D_0}{\phi \, F}$$
(Eq. 6-15)

where D_m is the effective diffusion coefficient in a porous medium [L^2/T], D_0 is the diffusion coefficient in water [L^2/T] and F is the formation factor [-]. The formation factor is defined by the electrical resistivity of the porous medium saturated with electrolyte divided by the resistivity of the electrolyte. This method has limitations in that it relies on formation factor measurements.

Domenico and Schwartz 1990 [100569], p. 368 document the relationship between porosity and effective diffusion with the following:

$$D_m = (\phi / \tau) D_0 \qquad \text{(Eq. 6-16)}$$

where τ ($= L_e/L$) is the tortuosity [-], L_e is the length of the channel for the fluid particle [L], L is the length of the porous media channel [L]. This method has limitations in that it relies on multiple diffusion cell measurements on a wide variety of rock samples to derive a global value for τ.

Domenico and Schwartz, 1990 [100569], p. 368 define a range for D_m with the following empirical equation:

$$D_m = \frac{\phi D_0}{2} \quad \text{to} \quad D_0 \left(\frac{\phi}{2 - \phi} \right)^2 \qquad \text{(Eq. 6-17)}$$

$$\text{Bound 1} \qquad\qquad \text{Bound 2}$$

This relationship captures the uncertainty and range of D_m in a heterogeneous system. It is only dependent on porosity and, because there are many matrix porosity measurements on Yucca Mountain tuffs, site specific data can be used as input.

Using Equation 6-17 and site specific porosity data a range in effective diffusion coefficient in the volcanic rock matrix (D_e) can be calculated. Mean porosity values were calculated using the relative humidity (RH) porosities found in DTN MO0109HYMXPROP.001 [155989] for the SZ hydrostratigraphic units defined in *Characterization of Hydrogeologic Units Using Matrix Properties, Yucca Mountain, Nevada* (Flint 1998 [100033]) as input. RH porosity is measured by drying the sample in an oven for 48 hours at $60^{\circ}C$ and 65% relative humidity. (Note, Flint's hydrostratigraphic units are subunits of the SZ HFM Units adopted in TSPA-LA.) Using Flint's hydrostratigraphic units to represent a "mean" porosity is appropriate for this exercise because Flint's basis for categorizing her units are heavily based on matrix rather than fracture properties, and it is the matrix properties that are important to diffusion in the SZ.

Using RH porosity values in MO0109HYMXPROP.001 [155989], the minimum "average" porosity is 0.042, located in the Calico Hills-vitric unit (a subunit of the SZ's Upper Volcanic Confining, Unit 14), the maximum "average" is 0.321, located in unit TC (Tiva Canyon Tuff, a subunit of the SZ Upper Volcanic Aquifer, Unit 15). For this exercise D_0 is that of ^{3}HHO (tritiated water), 2.44×10^{-5} cm^2/s. The resulting range in D_e is between 3.92×10^{-6} and 1.12×10^{-8} cm^2/s when the largest porosity in used as input in bound 1, and the smallest porosity is used as input to bound 2. The variability in D_e is a factor of:

$$\frac{3.92 \times 10^{-6} \, cm^2/s}{1.12 \times 10^{-8} \, cm^2/s} = 350 \qquad \text{(Eq. 6-18)}$$

Reimus et al. 2002 [163008] have developed an empirical relationship between D_e and porosity and permeability measurements based on diffusion cell experiments on rock samples from the Yucca Mountain area. Diffusing species used in the experiments are ^{99}Tc (as TcO$_4^-$), ^{14}C (as HCO$_3^-$) and ^{3}HHO. Rock samples used were taken from within the vicinity of Yucca Mountain, under Pahute Mesa and Area 25 of the Nevada Test Site. Based on these experiments Reimus et al. 2002 [163008] described three different approaches in deriving D_e. Two are dependent on linear regression relationships fitting the experimental results to diffusion cell measurements for: 1) both matrix porosity and permeability, and 2) only matrix porosity measurements. The third approach is simply compiling a cumulative distribution function based on their numerous diffusion cell results. Reimus et al. 2002 [163008], Section 4 found that differences in rock type account for the largest variability in the effective diffusion coefficients, rather than variability between diffusing species, size, and charge. The highest predictability in determining a value of D_e occurs when both matrix porosity and log permeability are known, with log permeability as the most important predictive variable.

The following equation defines their linear regression relationship based on porosity and permeability values and diffusion cell results (Reimus et al. 2002 [163008], p. 2.25):

$$\log_{10}(D_e) = -3.49 + 1.38\phi_m + 0.165(\log_{10} k_m) \qquad \text{(Eq. 6-19)}$$

where D_e is in units of cm^2/s and k_m is matrix permeability [L^2] in units of m^2.

Again, using matrix properties base on Flint's hydrostratigraphic subdivisions (denoted as hydrogeologic units in this report), the variability in D_e can be calculated using Equation 6-19 and the following inputs:

- Find the maximum and minimum "geometric mean" permeability in DTN: MO0109HYMXPROP.001 [155989] within the Flint defined set of hydrostratigraphic units (listed as hydraulic conductivities in DTN: MO0109HYMXPROP.001 [155989], then converted to permeability).

- Determine the maximum and minimum average porosity within the Flint defined set of hydrostratigraphic units (listed as RH porosities in DTN: MO0109HYMXPROP.001 [155989]).

The highest mean log permeability is • 13.25 in Calico Hill-vitric unit (a subunit of the SZ HFM Unit 14), the lowest mean log permeability is • 19.39 in unit TLL (a subunit of SZ HFM Unit 15). The largest porosity, 0.321, is in Calico Hill-vitric unit; the smallest porosity, 0.042, is in unit TC (Tiva Canyon Tuff).

The variation in D_e using Equation 6-19 and "average" maximum and minimum permeabilities and porosities values, expressed as a ratio of maximum to minimum estimated D_e, is as:

$$\frac{5.84 \times 10^{-6} \, cm^2/s}{2.34 \times 10^{-7} \, cm^2/s} = 25 \qquad \text{(Eq. 6-20)}$$

Variability from Ionic Radius and Charge

Empirical correlations exist in the literature to adjust free diffusion coefficients dependent on species size and charge. For this analysis, general guidance provided by Newman 1973 [148719], Table 75-1, p. 230, which lists diffusion coefficients for ions and cations of varying charges and size, is adopted in the scaling of radionuclide diffusion coefficients.

Diffusion coefficients listed for the simple monovalent ions Br^- and I^- are the largest values listed by Newman. Consequently, diffusion coefficient scaling factors for all other ions and cations are relative to those listed for Br^- and I^-. The rationale for specific scaling factors is given below.

1. Simple monovalent cations tend to be more hydrated than anions, resulting in larger effective radii than anions, and concomitantly, diffusion coefficients are about 0.90 and 0.95 times that of simple monovalent anions such as Br^- and I^-. PuO_2^+ and NpO_2^+ would fall into this category, since they both have relatively low charge to mass ratios and should not be highly hydrated.

2. Cations, such as Na^+ and Li^+, with high charge to mass ratios have a diffusion coefficient between 0.65 and 0.5 times that of Br^- and I^-.

3. Multivalent anions (which are generally multi-atom species) tend to have diffusion coefficients of 0.4 to 0.6 times that of Br^- and I^-.

4. Multivalent cations have diffusion coefficients between 0.3 to 0.4 times that of Br^- and I^-.

5. Diffusion coefficients of organic molecules can be considered reasonable lower bounds for diffusion coefficients of large anionic radionuclide complexes. An example is the large monovalent anions, such as pentafluorobenzoate, which have diffusion coefficients about 0.33 times that of Br^- and I^- (Callahan et al. 2000 [156648], Tables 5 and 6, p. 3553).

6. Cations with charges of +3 typically hydrolyze or form complexes in solution, resulting in a lower charge and higher mass species (e.g., hydroxyl or carbonate complexes). Consequently, the multivalent and complexed species could diffuse between 0.3 and 0.25 times that of Br^- and I^-.

Concluding from the above, the variation between the diffusion coefficients for simple, and relatively small monovalent ions and the larger multivalent complexed cations can be as much as

$$\frac{1}{0.25} = 4.0 \qquad \text{(Eq. 6-21)}$$

The variability in D_e due to ionic charge and species size can be as much as a factor of 4.0.

Variability from Temperature

The uncertainty and variability in diffusion due solely to temperature variations (over space and time) will affect all contaminants equally. Hence the uncertainty in temperature will not affect the decision to use a single diffusion coefficient. The Stokes-Einstein relationship can be used to approximate the molecular diffusion of ions in water with concentrations of ions as high as seawater and with temperatures ranging from 0 to 100°C (Li and Gregory 1974 [129827], p.704; Simpson and Carr 1958 [139449], p. 1201). Using the Stokes-Einstein relationship, the molecular diffusion coefficient for a given temperature, can be estimated as a function of the diffusion coefficient at a reference absolute temperature (T_0) and the relative change in temperature and water viscosity, (η) [M/(LT)] (Li and Gregory 1974 [129827], p. 704):

$$D_0(T_1) = \frac{T_1}{T_0}\frac{\eta_0}{\eta_1}D_0(T_0) \qquad \text{(Eq. 6-22)}$$

Given the maximum potential range in temperature for the Yucca Mountain groundwater along the transport pathway of 20 to 50 $^{\circ}$C, based on the ambient geothermal gradient and range in depth to the shallow SZ (293.15 to 323.15 K and the viscosity of water at those temperatures (Viswanath and Natarajan 1989 [129867], p. 714), Equation 6-22 can be rewritten and solved as follows:

$$\frac{D_0(T_1)}{D_0(T_0)} = \frac{T_1}{T_0}\frac{\eta_0}{\eta_1} = \frac{323.15K}{293.15K}\frac{1.007Ns/m^2}{0.516Ns/m^2} = 2.15 \qquad \text{(Eq. 6-23)}$$

Thus D_0 can vary by a factor of about 2.2 due to changes in water temperature.

Effective Diffusion Coefficients for Yucca Mountain Volcanic Units

Given the above arguments, it is demonstrated that the largest variability in D_e is due to differences in lithology. The variability in D_e using Equation 6-19 is not as high as that derived using Equation 6-17. However, Equation 6-19 will be adopted in deriving the uncertainty distribution of D_e for the following reasons:

1. Because Equation 6-19 is derived based on site-specific data it is more appropriate in determining the range of D_e due to lithology specific to Yucca Mountain.

2. There are a large number of permeability and porosity measurements taken from the saturated zone hydrogeologic units where flow is expected to take place. Averages of these measurements can be used as input to Equation 6-19.

3. Using maximum and minimum averages from matrix porosity and permeability as input yields a range in D_e that approaches that of the few laboratory derived D_e measurements specific to Yucca Mountain tuffs for TcO_4^- (1.0×10^{-7} to 2.0×10^{-6}) and HTO^- (1.2×10^{-7} to 3.5×10^{-6}) (see Triay et al. 1993 [145123]; Rundberg et al. 1987 [106481]) as indicated on the "Flint_Reim_TrRnd" spreadsheet in the EXCEL workbook "Eff_MtrxDif_11.xls" file (DTN: SN0306T0502103.006).

The CDF for uncertainty in the effective diffusion coefficient used in this analysis is derived as follows:

1. Mean porosity and permeability values (calculated from values found in DTN: MO0109HYMXPROP.001 [155989]) were calculated for the volcanic hydrostratigraphic units TC, TR, TUL, TMN, TLL, TM2, TM1, CHV, CHZ, PP4, PP3, PP2, PP1, BF3 and BF2 , defined by Flint, 1998 [100033]. These are subunits of the more broadly defined SZ HFM Units 11, 12, 13, 14 and 15, and are units where flow and transport are expected to take place. Mean porosity and permeability values are given on the spreadsheets "LVA (12 &11)", "LVA (13)", "UVC (14)", and "UVA (15)" in the EXCEL file "Eff_MtrxDf_11.xls" (DTN: SN0306T0502103.006).

2. A CDF for D_e was calculated with Equation 6-19 using the mean permeability and porosity values for the above hydrostratigraphic units as input. These values are given on the spreadsheet "drns_all_straight", (Column AG, Rows 34 through 49) in the EXCEL file "Eff_MtrxDf_11.xls" (DTN: SN0306T0502103.006).

3. The derived CDF was then scaled down to account for the variability in D_e to account for ionic charge and size. The scaling factors used are: 1) 0.9, to represent diffusion of simple monovalent cations, 2) 0.65 and 0.50, to represent cations with a high charge to mass ratios, 3) 0.3 to represent large monovalent anions, and 4) 0.25, to represent multivalent and complexed cations (Figure 6-14). Note, the rationale for the above scaling factors were discussed in the subsection "Variability from Ionic Radius and Charge". These values are given on the spreadsheet "drns_all_straight" in the EXCEL file "Eff_MtrxDf_11.xls" (Column AG, Rows 50 through 109) (DTN: The resulting CDF yields a distribution given in Figure 6-14 with a range in log space of –5.3 to –7.12 cm^2/s.

The range captures laboratory ^{3}HHO and TcO$_4^-$ measured values of D_e on Yucca Mountain tuffs reported by Triay et al. 1993 [145123] and Rundberg et al. 1987 [106481] and ^{3}HHO, TcO$_4$, and ^{14}C D_e reported by Reimus et al. 2002 [163008] and 2003 [162950]). Additionally, this range incorporates the interpreted diffusion coefficients (6.0×10^{-6} cm^2/s and 1.3×10^{-7} cm^2/s) derived from field tests using Br$^-$, PFBA (a fluorinated organic acid) as the diffusing species (Reimus et al. 2003 [162950]).

The distribution for the derived values of effective diffusion coefficient using Equation 6-19 is about half an order of magnitude lower than the distribution of values from laboratory and field results. This is because the derived distribution scales effective diffusion coefficient to take into account species not measured in laboratory or field experiments, as described in step 3 above. The lowest values of effective diffusion coefficient are those for hydrolyzed or complexed ions having a low charge and high mass, which would have diffusion coefficients about 0.25 times the values for Br$^-$ and I$^-$ ions.

To account for uncertainties in D_e at the lower end the uncertainty range is expanded to span a full 2 orders of magnitude (log –5.3 to –7.3 cm^2/s), with the 50 percentile set at –6.3. cm^2/s. Converted to m^2/s results in a log D_e range of –9.3 to –11.3 m^2/s, with the 50 percentile set at –10.3. m^2/s (See Figure 6-15). The effective matrix diffusion coefficient is determined for a particular realization by the parameter DCVO. See Table 6-8 for the associated probabilities for the effective matrix diffusion coefficient CDF.
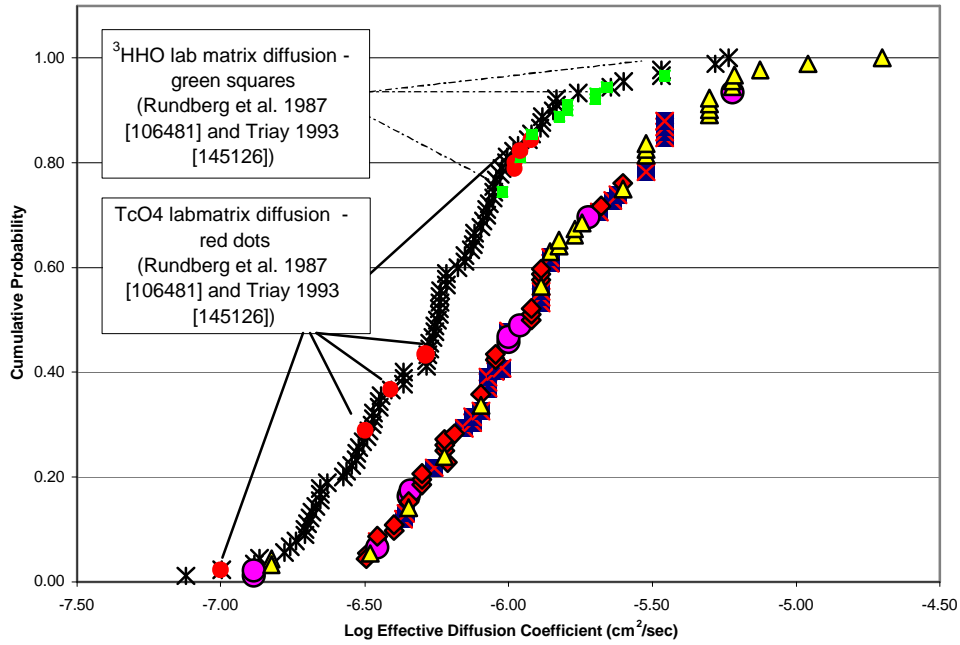
DTN: SN0306T0502103.006

NOTE: The CDF to the left represents values of effective diffusion coefficient derived using Equation 6-19. Included in the plot are laboratory measurements of effective diffusion coefficient from Triay 1993 [145126] and Rundberg et al. 1987 [106481] to demonstrate the reasonableness of the derived values of effective diffusion coefficient. The CDF to the right represents laboratory and field-derived estimates. Triangles - ^{14}C laboratory values; Squares - ^{3}HHO laboratory values; Diamonds – TcO_4 laboratory values; Circles – Br^- and PFBA field values (Reimus et al., 2002 [163008] and Reimus et al., 2003 [162950]).

Figure 6-14. CDFs of Data Used in the Assessment of Uncertainty in Effective Diffusion Coefficient
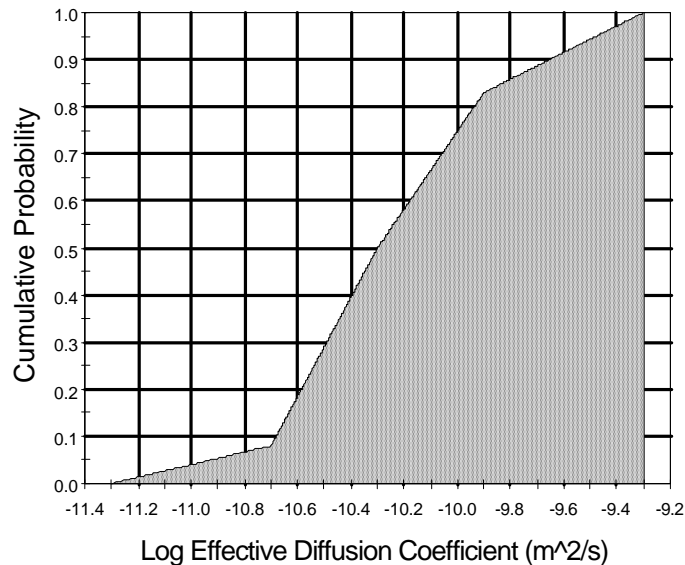
Figure 6-15. CDF of Uncertainty in Effective Diffusion Coefficient

DTN: SN0310T0502103.009

6.5.2.7 Bulk Density of Alluvium

For the TSPA-SR, the dry bulk density was considered to be a constant and set to 1.27 g/cm^3 (CRWMS M&O 2000 [147972], Section 6.9). The basis for this parameter value is a set of tests performed on four five-foot alluvial intervals from each of the EWDP boreholes 2D, 9S, and 3S at depths of 395 to 415 feet, 145 to 165 feet, and 60 to 80 feet, respectively (DTN: LA0002JC831341.001 [147081]). These samples were drill cuttings and thus highly disturbed from their condition in the aquifer. The range of the dry bulk density values in laboratory columns packed with alluvium from these wells was 1.2 to 1.3 g/cm^3. The data are presented in *Unsaturated Zone and Saturated Zone Transport Properties (U0100)* (CRWMS M&O 2000 [152773], p. 86) with a note stating that densities were measured in the laboratory and do not represent *in situ* conditions.

The values used in the TSPA-SR were low compared to dry bulk densities measured in alluvium at Frenchman Flat and the NTS near Yucca Mountain (Howard 1985 [153266], Table 3, p. 31, and Table A-1, p. 38). Similarly, a comparison to the range of dry bulk densities of alluvial material in general (Manger 1963 [154474], pp. E41 to E42) led to the conclusion that the values used in the TSPA-SR were likely an underestimate of the true bulk density. Consequently, bulk density in the alluvium and its uncertainty has been reevaluated using data from the Yucca Mountain area that have been measured at a larger, more representative scale.

The dry bulk density of the alluvium is used in the computation of the retardation of sorbing radionuclides. The dry bulk density is related to the matrix retardation coefficient as indicated in Equation 6-2.

Borehole gravimeter surveys were conducted by EDCON 2000 [154704], pp. 1 to 23 at well EWDP-19D1 directly south of Yucca Mountain near U.S. Highway 95. A total of 36 values of saturated bulk density were estimated based on the geophysical measurements taken from this well (EDCON 2000 [154704], p. 3). Seventeen measurements were taken from a depth corresponding to the inferred depth of the flow path through the alluvium near Yucca Mountain (401.5 to 776 feet). The wet bulk density computed from gravimeter measurements is presented in Table 6-11 as well as the porosity and dry bulk density computed from Freeze and Cherry 1979 [101173], p. 337:

$$\phi_T = \frac{\rho_{sat} - \rho_{grain}}{\rho_w - \rho_{grain}} \qquad\qquad \text{(Eq. 6-24)}$$

$$\rho_b = \rho_{grain}\left(1 - \phi_T\right) \qquad\qquad \text{(Eq. 6-25)}$$

where ρ_{sat} is the saturated bulk density [M/L^3], ρ_{grain} is the average grain density for these samples [M/L^3] (2.52 g/cm^3), and ρ_w is the density of water (1.0 g/cm^3).

The average grain density was computed to be 2.52 g/cm^3 (2520 kg/m^3) from alluvial samples from other boreholes in the vicinity of Yucca Mountain (USGS n.d. [154495], pp. 3 to 4). The grain density varied little (2.49 to 2.55 g/cm^3), and so the average was used in the computation of the porosity and dry bulk density.

The mean dry bulk density for this set of measurements was 1.91 g/cm^3 (1910 kg/m^3). This value is close to dry bulk density values previously measured at Frenchman Flat and the NTS in similar material at similar depth (Howard 1985 [153266], Table 3, p. 31, and Table A-1, p. 38), and it is the value used as the mean in the uncertainty distribution. The computed standard deviation for these measurements is 0.078 g/cm^3. A normal distribution was selected to characterize the uncertainty in the dry bulk density based on the frequency plot shown in Figure 6-16. The relatively large volume of the medium interrogated by the borehole gravimeter method suggests that the variability observed is appropriate for the uncertainty in this parameter at the scale of individual grid cells in the SZ Transport Abstraction Model. The CDF of uncertainty in bulk density of the alluvium is shown in Figure 6-17. The bulk density in the alluvium is specified for a particular realization by the parameter bulk density.

Table 6-11. Measured Saturated Density, Computed Porosity, and Computed Dry Bulk Density for Depths from 402 to 776 Feet Below the Surface at the Nye County Well EWDP-19D1

Sample Depth (ft)	Drift-Corrected Saturated Bulk Density, ρ_{sat} (g/cm^3)	Computed Total Porosity, ϕ_T	Computed Dry Bulk Density, ρ_b (g/cm^3)
402	2.231	0.190	2.04
422	2.156	0.239	1.92
442	2.180	0.224	1.96
485	2.163	0.235	1.93
505	2.174	0.228	1.95
525	2.214	0.201	2.01
569.95	2.148	0.245	1.90
589.9	2.142	0.249	1.89
610	2.105	0.273	1.83
630	2.079	0.290	1.79
649.95	2.077	0.291	1.79
669.95	2.133	0.255	1.88
690	2.121	0.262	1.86
715.95	2.158	0.238	1.92
736	2.143	0.248	1.90
756	2.105	0.273	1.83
776	2.239	0.185	2.05

Source DTN: MO0105GPLOG19D.000 [163480]
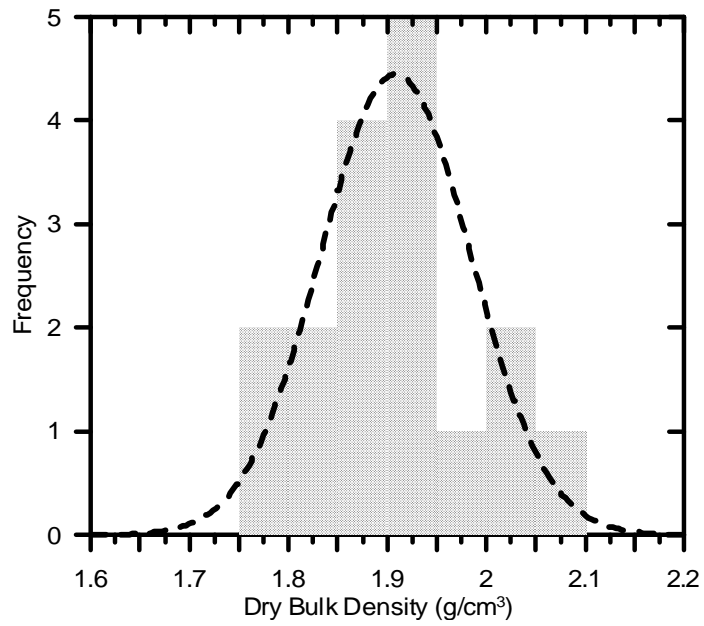
NOTE: Normal distribution fit to the data shown with the dashed line.

Figure 6-16. Histogram of Dry Bulk Density from Borehole Gravimeter Data
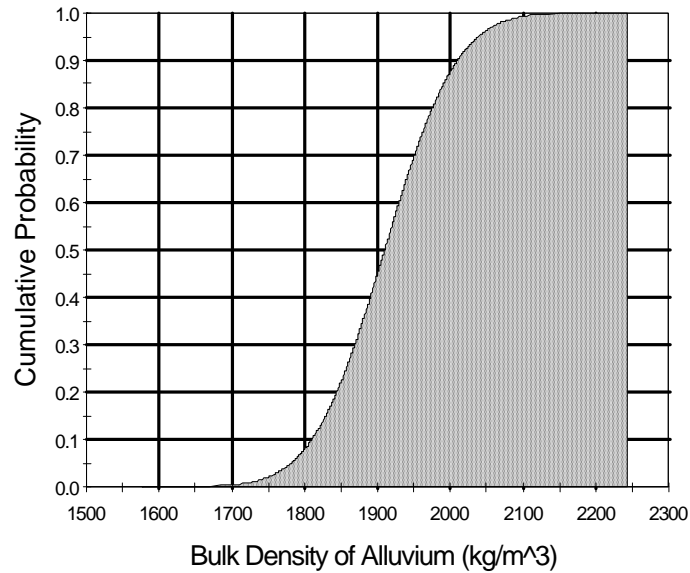
Figure 6-17. CDF of Uncertainty in Bulk Density of Alluvium

6.5.2.8 Sorption Coefficients

Sorption or adsorption is the process by which dissolved radionuclides temporarily adhere or bond to rock and alluvial substrate along a transport path. Sorption occurs because of the electrochemical affinity between the dissolved species and the substrate. The significance of sorption to the SZ Transport Abstraction Model and the SZ 1-D Transport Model is that sorption results in a retardation of the radionuclide because part of the radionuclide transport time is spent on an immobile surface.

A linear, equilibrium, sorption coefficient, K_d, is considered appropriate for the radionuclides that exhibit sorption during transport. The K_d model also depends on chemical equilibrium between the aqueous phase and sorbed phase of a given species.

The K_d relationship is defined as follows (Domenico and Schwartz 1990 [100569], p. 441):

$$S = K_d C \qquad \text{(Eq. 6-26)}$$

where S [moles/M] is the mass sorbed on the surface of the substrate, and C [moles/L^3] is the concentration of the dissolved mass. The K_d model determines transport retardation as described earlier per Equation 6-2.

A detailed discussion of the uncertainty distributions for sorption coefficients used in the SZ Transport Abstraction Model and the SZ 1-D Transport Model is given by BSC 2003 [162419], Attachment I. The documentation provided by BSC 2003 [162419], Attachment I includes the technical bases for the values of sorption coefficient for the relevant radionuclides in volcanic units and alluvium at Yucca Mountain.

6.5.2.9 Dispersivity

Longitudinal dispersion is the mixing of a solute in groundwater that occurs along the direction of flow. This mixing is a function of many factors including the relative concentrations of the solute, the velocity pattern within the flow field, and the host rock properties. An important component of this dispersion is the dispersivity, a coarse measure of solute (mechanical) spreading properties of the rock. The dispersion process causes spreading of the solute in directions transverse to the flow path as well as in the longitudinal flow direction (Freeze and Cherry 1979 [101173], p. 394). Longitudinal dispersivity will be important only at the leading edge of the advancing plume, while transverse dispersivity (horizontal transverse and vertical transverse) is the strongest control on plume spreading and possible dilution for the Yucca Mountain repository (CRWMS M&O 1998 [100353], p. LG-12).

Temporal changes in the groundwater flow field may significantly increase the apparent dispersivity displayed by a contaminant plume, particularly with regard to transverse dispersion. However, observations of water levels in wells at Yucca Mountain have not indicated large or consistent variations (Luckey et al. 1996 [100465], p. 29-32), suggesting that transience in the SZ flow system would not lead to much greater dispersion. The thick UZ in the area of Yucca Mountain likely dampens the response of the SZ flow system to seasonal variations or transience in infiltration on time scales of less than centuries.

These dispersivities (longitudinal, vertical transverse, and horizontal transverse) are used in the advection-dispersion equation governing solute transport and are implemented into the SZ Transport Abstraction Model as stochastic parameters. Recommendations from the expert elicitation were used as the basis for determining the distribution for longitudinal and transverse dispersivity. As part of the expert elicitation, Dr. Lynn Gelhar provided statistical distributions for longitudinal dispersivity at 5 km and 30 km (CRWMS M&O 1998 [100353], p. 3-21). These distributions for longitudinal dispersivity are consistent with his previous work (Gelhar 1986 [101131], pp. 135s-145s). CRWMS M&O 2000 [152259], p. 53 provided estimates of the transverse and longitudinal dispersion that may occur at the sub gridblock scale within the SZ site-scale model. The estimation of dispersivity using sub-gridblock scale modeling is also described in McKenna et al. 2003 [163578]. The results from the sub-gridblock scale modeling (CRWMS M&O 2000 [152259], p. 55) are in general agreement with the estimates by the expert elicitation panel (CRWMS M&O 1998 [100353], p. 3-21). However, it should be noted that there is a significant difference in the spatial scale at which the analyses in CRWMS M&O 2000 [152259] (500 m) were conducted and the scales at which the expert elicitation (CRWMS M&O 1998 [100353]) estimates were made (5 km and 30 km). Nonetheless, both sources of information on dispersivity are mutually supportive.

In the SZ Transport Abstraction Model, the longitudinal dispersivity parameter is sampled as a log-transformed parameter and the transverse dispersivities are then calculated as indicated by CRWMS M&O 1998 [100353], p. 3-21 according to the following relationships:

$$\alpha_h = \frac{\alpha_L}{200} \qquad \text{(Eq. 6-27)}$$

$$\alpha_v = \frac{\alpha_L}{20000} \qquad \text{(Eq. 6-28)}$$

where α_L is the longitudinal dispersivity [L], α_h is the transverse horizontal dispersivity [L] and α_v is transverse vertical dispersivity [L].

The longitudinal dispersivity is specified for a particular realization by the parameter LDISP. The statistical distribution is a log-normal distribution: $E[\log_{10}(\alpha_L)]$: 2.0 and $S.D.[\log_{10}(\alpha_L)]$: 0.75. The CDF of uncertainty in longitudinal dispersivity is shown in Figure 6-18.
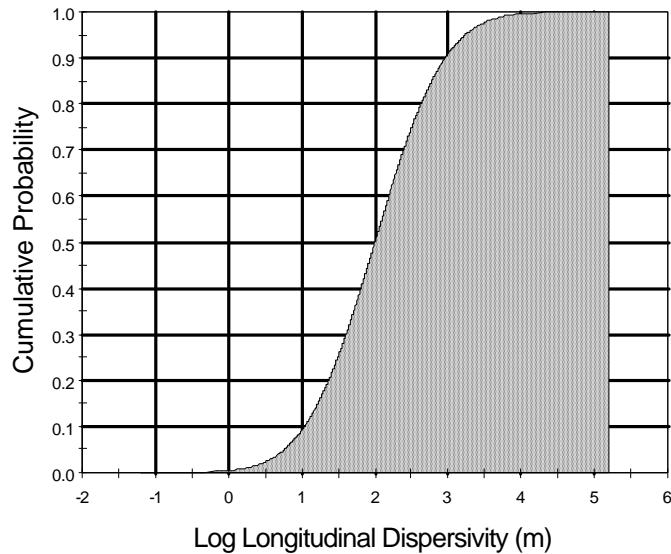
Figure 6-18. CDF of Uncertainty in Longitudinal Dispersivity

Effective Longitudinal Dispersivity in the SZ Transport Abstraction Model

Longitudinal dispersivity for radionuclide transport simulations in the SZ Transport Abstraction Model is specified as a transport parameter. The dispersion process is simulated by the random-walk displacement algorithm on the local scale for each time step in the transport simulation. In addition, the spatial distribution of hydrogeologic units of contrasting permeability within the model imparts additional dispersion to the simulated transport of particles as the flow paths diverge during transport. The effective longitudinal dispersivity simulated by the SZ Transport Abstraction Model may be significantly larger than the specified value due to the additive effects of these two processes.

The effective longitudinal dispersivity in the SZ Transport Abstraction Model is analyzed for a range of values of specified longitudinal dispersivity to evaluate this effect. A point source beneath the repository is used for the analysis. Neither sorption nor matrix diffusion is included in the simulations. Effective longitudinal dispersivity is estimated using the relationship from Kreft and Zuber 1978 [107306]:

$$\alpha_L = \frac{L_f}{2}\left(\frac{\sigma_t}{m_t}\right)^2 \qquad \text{(Eq. 6-29)}$$

where L_f is the flow path length [L], σ_t is the standard deviation in travel time [T], and m_t is the mean travel time [T]. The standard deviation is estimated from the particle mass breakthrough curve at 18 km distance by taking the difference in time between the arrival of 0.159 fraction of the mass (the mean minus one standard deviation for a Gaussian distribution) and the arrival of 0.841 fraction of the mass (the mean plus one standard deviation for a Gaussian distribution) and dividing by 2. The mean travel time is estimated using the arrival time of 0.500 fraction of the mass.

The results of this analysis are shown in Figure 6-19 with the plotted open circles. The effective simulated longitudinal dispersivity is consistently about one order of magnitude higher (bold dashed line) than the specified longitudinal dispersivity (for values of specified longitudinal dispersivity of less than 1000 m). These results indicate that the heterogeneous distribution of permeability in the SZ Transport Abstraction Model in the region along the flow path is contributing approximately one order of magnitude of dispersivity relative to the specified value.
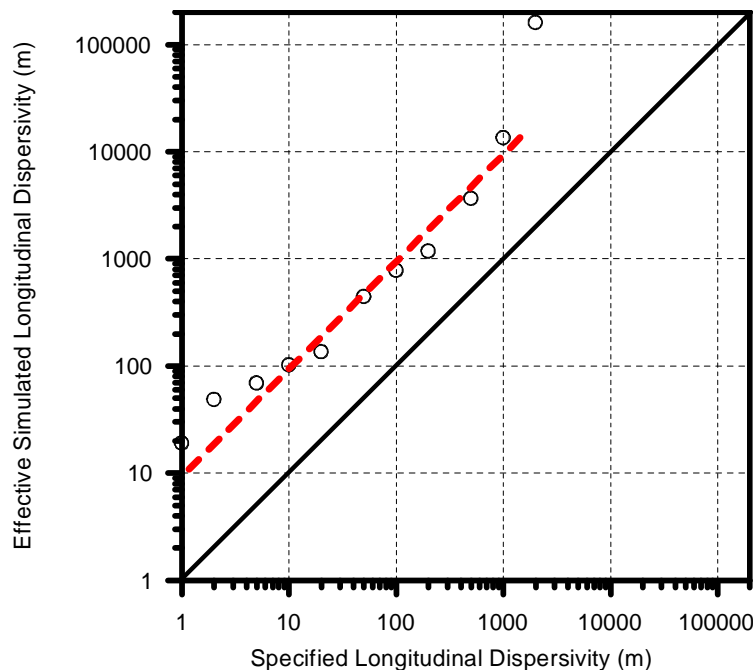
Figure 6-19. Effective Simulated Longitudinal Dispersivity Versus the Specified Longitudinal Dispersivity in the SZ Transport Abstraction Model

These results indicate that the effective longitudinal dispersivity in the SZ Transport Abstraction Model is significantly higher than the value input to the model. In order to avoid the excessive effective dispersion in the SZ Transport Abstraction Model, the input value of longitudinal dispersivity can be reduced. Based on these results, the value of specified longitudinal

dispersivity used in the SZ Transport Abstraction Model for the TSPA abstraction simulations is adjusted to yield the correct value of effective simulated longitudinal dispersivity. This is accomplished by scaling the input value of longitudinal dispersivity down by one order of magnitude (i.e., dividing the longitudinal dispersivity by 10) in the input files for each realization.

6.5.2.10 Horizontal Anisotropy in Permeability

Although a detailed description of the analysis and derivation of the distribution of anisotropy ratio in the saturated zone near the C-Wells complex is presented in the *Saturated Zone In Situ Testing* report (BSC 2003 [162415], Section 6.2.6), some background information and a short summary are presented here. Interpretation of well test data with analytical solutions consists of inferring the hydraulic properties of the system from its measured responses based on an assumed flow geometry (i.e., radial). The problem becomes more complicated, however, when the system geometry cannot be specified with reasonable certainty. In a layered sedimentary system lacking extreme heterogeneity, flow might reasonably be expected to be radial during a hydraulic test. When hydraulic tests are conducted at some arbitrary point within a three-dimensional (3-D) fractured rock mass, however, the flow geometry is complex. Radial flow would occur only if the test were performed in a single uniform fracture of effectively infinite extent or within a network of fractures confined to a planar body in which the fractures were so densely interconnected that the network behaves like an equivalent porous medium. More likely, flow in fractured tuff is nonradial and variable, as fracture terminations and additional fracture intersections were reached. Therefore, it must be emphasized that assumptions required in the analytical treatment of anisotropy may not be strictly consistent with site geology.

Through the fractured tuff and alluvium near Yucca Mountain, there is significant heterogeneity in hydraulic properties, which not only vary spatially, but also differ depending upon the direction in which they are measured (both horizontally and vertically). In this analysis, transmissivity and storativity are the hydrologic parameters required to calculate and define large-scale anisotropy, and their measured values reflect the heterogeneity of the media. The concept of anisotropy is typically associated with a homogeneous medium—a criterion not met here. Nevertheless, there are clearly spatial and directional variations in transmissivity, and the notion remains that, over a large enough representative elementary volume, there exists a preferential flow direction that can be termed anisotropy.

Data from the long-term pumping test conducted from May 8, 1996, to November 12, 1997, were used to evaluate the anisotropy in the vicinity of the C-wells complex in BSC 2003 [162415], Section 6.2.6. After filtering the drawdown data in response to pumping at UE-25 c#3, transmissivity and storativity were calculated at four distant wells (USW H-4, UE-25 ONC1, UE-25 wt#3, and UE-25 wt#14).

A distribution of anisotropies must be specified so that an anisotropy ratio can be selected for each of the 200 stochastic model realizations used as input to the SZ Transport Abstraction Model. Because the current version of the FEHM v. 2.20 software code (STN: 10086-2.20-00, LANL 2003 [161725]) can only implement anisotropy oriented in alignment with the grid direction, principal directions discussed above are not directly applicable in the model. The net result of being unable to specify a principal direction is that uncertainty in the anisotropy ratio increases. For example, the analytical result for anisotropy using the Cooper-Jacob 1946 [150245] method is a ratio of 3.3 in a direction 15° east of north. A projection that orients the principal direction north-south (0°) results in a new anisotropy ratio of 2.5. In fact, this line of reasoning suggests that it is possible for the projected north-south anisotropy ratio to be significantly less than one.

Based on consultations with USGS staff, the YMP Parameters Team, scientific judgment, and results from the analytical anisotropy analyses, Figure 6-20a represents the best estimate of the PDF for the anisotropy ratio (north-south / east-west) in the saturated zone near the C-wells complex. Figure 6-20b is the corresponding CDF.
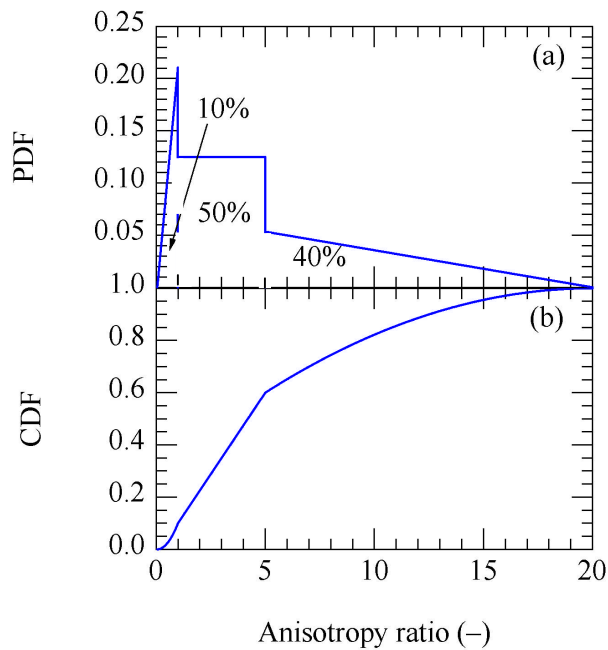
DTN: SN0302T0502203.001 [163563]

Figure 6-20. Probability Density Function (a) and Corresponding Cumulative Distribution Function (b) for the Uncertainty in North-South/East-West Anisotropy Ratio

There are several noteworthy points based on three distinct regions of the anisotropy ratio distribution (DTN: SN0302T0502203.001 [163563]).

- *Anisotropy ratio between 5 and 20*. The maximum anisotropy ratio of 20:1 is based upon the highest calculated anisotropy ratio of 17:1 reported by Ferrill et al. 1999 [118941], p. 7. The maximum reported value of 17:1 was rounded to 20:1 and set as the upper limit for horizontal anisotropy. Furthermore, although features such as high transmissivity zones and fractures may yield very large anisotropy ratios locally, globally, their effects are attenuated, and 20 is a reasonable maximum. The 5.5 anisotropy ratio calculated by the second approach of the modified Papadopulos-PEST method (see BSC 2003 [162415], Section 6.2.6) lies in this range near its highest probability point. Therefore, between 5 and 20, a triangular distribution of anisotropy ratio is constructed that decreases to zero probability at 20. A 40% probability is assigned to this portion of the probability density function.

- *Anisotropy ratio between 0.05 and 1*. Discussions among Sandia National Laboratories (SNL) and USGS staff established that, although it is likely the SZ is anisotropic with principal direction approximately northeast, it is possible the media could be isotropic, as well as a small probability that the principal direction could be significantly different from north-northeast. Correspondingly, an anisotropy ratio of less than one is possible, and the minimum anisotropy ratio is set equal to the inverse of the maximum, 1:20, with a triangular distribution of 10% probability decreasing to zero at a ratio of 0.05. An additional Papadopulos solution yielding an anisotropy ratio of 3.5 at 79° west of north (BSC 2003 [162415], Section 6.2.6) falls in this range.

- *Anisotropy ratio between 1 and 5*. A uniformly distributed 50% probability is assigned to the range of anisotropy ratio between 1 and 5. This interval comprises the more likely values of anisotropy ratios with no specific value more likely than another. It should be noted that in a previous model of the saturated zone near Yucca Mountain (CRWMS M&O 2000 [147972], Section 6.12), anisotropy was binomially distributed with a 50% probability of isotropy (1:1) and a 50% probability of a 5:1 ratio.

It is assumed that the potential anisotropy of permeability in the horizontal direction is adequately represented by a permeability tensor that is oriented in the north-south and east-west directions. This approach is carried forward from the *Saturated Zone In-Situ Testing* scientific analysis report (BSC 2003 [162415], Section 6.2.6). The numerical grid in the SZ site-scale flow and transport model is aligned in the north-south and east-west directions and values of permeability may only be specified in directions parallel to the grid. Analysis of the probable direction of horizontal anisotropy shows that the direction of maximum transmissivity may be about N 15°E, indicating that the anisotropy applied on the SZ Transport Abstraction Model grid is within approximately 15° of the inferred anisotropy.

Figure 6-20(a) and Figure 6-20(b) are the best estimates for the PDF and the CDF, respectively, of north-south anisotropy ratios in the saturated zone to be modeled with the FEHM v. 2.20 software code (STN: 10086-2.20-00, LANL 2003 [161725]) in the SZ Transport Abstraction Model. Horizontal anisotropy in permeability is determined for a particular realization by the parameter HAVO.

6.5.2.11 Retardation of Colloids with Irreversibly Sorbed Radionuclides

For TSPA-LA, colloid-facilitated transport of radionuclides in the SZ is simulated to occur by two basic modes. In the first mode, radionuclides that are irreversibly attached to colloids are transported at the same rate as the colloids, which are themselves retarded by interaction with the aquifer material. In the second mode, radionuclides that are reversibly attached to colloids are in equilibrium with the aqueous phase and the aquifer material. In this mode of transport, the effective retardation of these radionuclides during transport in the SZ is dependent on the sorption coefficient of the radionuclide onto colloids, the concentration of colloids, and the sorption coefficient of the radionuclide onto the aquifer material. This section deals with the first mode of colloid-facilitated transport and Section 6.5.2.12 addresses the second mode.

The SZ transport simulations of radionuclides that are irreversibly attached to colloids are conducted for radioisotopes of Pu and Am. The retardation of colloids with irreversibly attached radionuclides is a kinetically controlled process, which approaches equilibrium behavior for long transport times. For transport of colloids through the SZ, equilibrium behavior is nearly achieved. However, non-equilibrium behavior results in unimpeded migration of some of the colloids. Consequently, a small fraction of these colloids are transported through the SZ with no retardation; whereas the larger fraction is delayed by a retardation factor. For the SZ transport simulations, a small (uncertain) fraction of the radionuclide mass irreversibly attached to colloids is transported without retardation and the remaining fraction of the radionuclide mass is retarded. A discussion of the fraction of colloids transported with no retardation is in BSC 2003 [162729], Section 6.6. The fraction of irreversibly sorbed to reversibly sorbed radionuclides is determined in the waste-form component of TSPA-LA and is used as input to the SZ Transport Abstraction Model and the SZ 1-D Transport Model.

The processes important to the transport of irreversible colloids in the volcanic units of the SZ are as follows: advection and dispersion of colloids in the fracture water, exclusion of the colloids from the matrix waters, and chemical filtration or adsorption of the colloids onto the fracture surfaces.

Modeling of the advective/dispersive processes is handled as if the colloids were solute in the SZ Transport Abstraction Model and the SZ 1-D Transport Model. Matrix exclusion in the volcanic units is considered to be appropriate because of the large size and small diffusivities of the colloids compared to the solute, plus the possibility of similar electrostatic charge of the colloids and the tuff matrix. Matrix exclusion is implemented by reducing the values of the effective diffusion coefficients for radionuclides (see Section 6.5.2.6 for a discussion of the solute diffusion coefficient) by ten orders of magnitude, thus preventing essentially all matrix diffusion. Chemical (i.e., reversible) filtration of irreversible colloids is modeled by applying a retardation factor to the transport in the fractures. The implementation of the retardation factor in the SZ Transport Abstraction model is described in Section 6.5.1.

BSC 2003 [162729], Section 6.4 describes the development of colloid retardation factors for fractured tuff from field and experimental data. Figure 6-21 shows the CDF used for retardation factors in the volcanic units for the SZ Transport Abstraction model and Table 6-8 provides the associated probabilities. This CDF is based on the uncertainty distribution developed by BSC 2003 [162729], Table 7. A log cumulative probability distribution is used because the

retardation factors span slightly more than 2 orders of magnitude. Retardation of colloids with irreversibly sorbed radionuclides in the volcanic units is specified for a particular realization by the parameter CORVO.
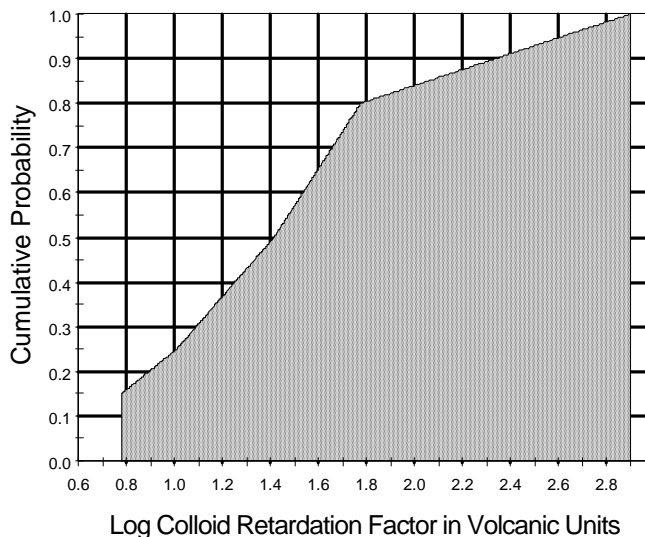
Figure 6-21. CDF of Uncertainty in Colloid Retardation Factor in Volcanic Units

The processes modeled for irreversible colloids in the alluvium are the same as those modeled for irreversible colloids in the volcanic units, with the exception of matrix exclusion, because the alluvium is modeled as a single porous medium. BSC 2003 [162729], Section 6.5 describes the development of colloid retardation parameters for the alluvium using experimental data specific to colloid transport in alluvial material from Yucca Mountain as well as bacteriophage field studies in alluvial material, which are thought to be good analogs for colloid transport. As with irreversible colloids in the volcanic units, filtration in the alluvium is modeled by applying a retardation factor to transport in the porous medium. Figure 6-22 shows the CDF used for retardation factors in the alluvium for the SZ Transport Abstraction model and Table 6-8 provides the associated probabilities. This CDF is based on the uncertainty distribution developed by BSC 2003 [162729], Table 8. A log cumulative probability distribution is used because the retardation factors span slightly more than 3 orders of magnitude. The implementation of the retardation factor in the SZ Transport Abstraction model is described in Section 6.5.1. Retardation of colloids with irreversibly sorbed radionuclides in the alluvium is specified for a particular realization by the parameter CORAL.
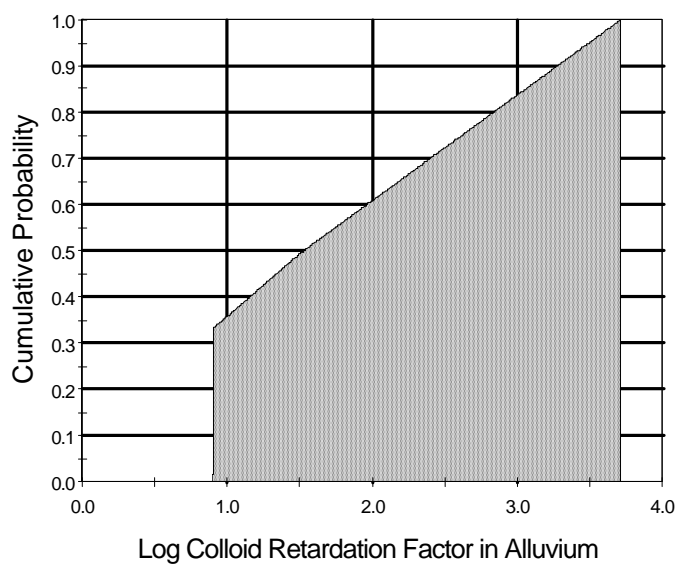
Figure 6-22. CDF of Uncertainty in Colloid Retardation Factor in Alluvium

6.5.2.12 Transport of Radionuclides Reversibly Sorbed on Colloids

Radionuclides that are reversibly sorbed onto colloids are modeled to be temporarily attached to the surface of colloids. Thus, these radionuclides are available for dissolution in the aqueous phase and their transport characteristics are a combination of the transport characteristics of solute and colloids. The SZ transport simulations of radionuclides that are reversibly attached to colloids are conducted for radioisotopes of Pu, Am, Th, Pa, and Cs, which is consistent with the radionuclides selected for reversible sorption (BSC 2003 [161620], Section 6.3.3.1). For these transport simulations, radioisotopes of Pu are transported as one group, radioisotopes of Am, Th, and Pa are transported as a second group, and Cs is transported as a third species. Americium and plutonium can also be transported as irreversibly sorbed onto colloids, see Section 6.5.2.11.

The K_c parameter is a distribution coefficient that represents the equilibrium partitioning of radionuclides between the aqueous phase and the colloidal phase, as given in Equation 6-4. The K_c is a function of only radionuclide sorption properties, colloid substrate properties, and colloid mass concentration, and not any properties of the immobile media through which transport occurs; thus the same K_c applies to transport of a radionuclide in both the volcanic units and the alluvium.

For TSPA-LA, the K_d^{coll} uncertainty distributions for Pu, Am, Th, Pa, and Cs were developed by BSC 2003 [161620], Table 10. Figure 6-23 to Figure 6-25 show the uncertainty distributions input to the SZ Transport Abstraction Model for sorption coefficients onto colloids. The C_{col} uncertainty distribution was also developed by BSC 2003 [161620], Table 5 (see Figure 6-26).

Retardation of colloids with reversibly sorbed radionuclides is determined for a particular realization by the following uncertain parameters: Conc_Col for groundwater colloid concentrations; Kd_Cs_Col for cesium sorption coefficient onto colloids; Kd_Am_Col for americium, thorium and protactinium sorption coefficients onto colloids; Kd_Pu_Col plutonium sorption coefficient onto colloids. Implementation of the K_c model in the SZ Transport Abstraction Model is discussed in Section 6.5.1 Note that the values given for the parameter vectors of Kd_Pu_Col, Kd_Am_Col, and Kd_Cs_Col in Attachment I are the $\log_{10}$-transformed values.
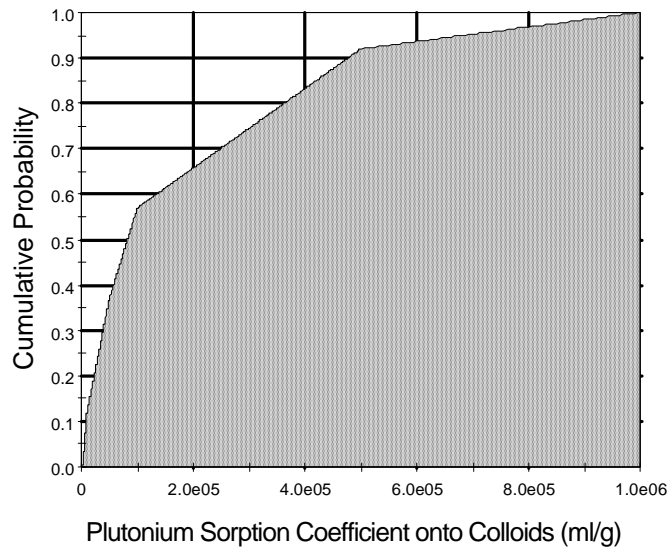
DTN: SN0306T0504103.006 [164131], Table 1

Figure 6-23. CDF of Uncertainty in Plutonium Sorption Coefficient onto Colloids

Figure 6-24. CDF of Uncertainty in Americium Sorption Coefficient onto Colloids

Figure 6-25. CDF of Uncertainty in Cesium Sorption Coefficient onto Colloids
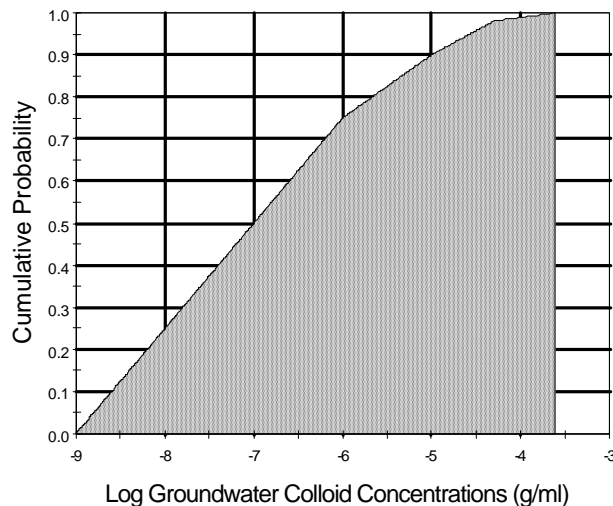
Figure 6-26. CDF of Uncertainty in Groundwater Colloid Concentrations

Accompanying the K_c model is the partitioning of radionuclides between the aqueous phase and the sorbed phase onto the tuff matrix and the alluvium, as described by K_d for the radionuclide onto the aquifer material. The K_d uncertainty distributions for americium, plutonium, and cesium are described in Table 6-8 (DTN: LA0310AM831341.002, [165891]).

6.5.2.13   Source Regions

Variations in radionuclide transport pathways and travel times in the SZ from various locations beneath the repository are considered by defining four radionuclide source regions at the water table. For any particular TSPA realization a point source of radionuclides is defined within each of the four regions for simulation of radionuclide transport in the SZ Transport Abstraction Model. A point source of radionuclides in the saturated zone is appropriate for a single leaking waste package or for highly focused groundwater flow along a fault or single fracture in the unsaturated zone. Whereas a more diffuse source of radionuclides at the water table may be more physically realistic for later times when numerous leaking waste packages occur, use of a point source in the SZ is an approach that tends to overestimate the concentration of radionuclides near the source.

The SZ source region locations are based on the extent of the repository design and on the general pattern of groundwater flow in the unsaturated zone as simulated by the UZ site-scale flow and transport model. Variations in the pattern of groundwater flow from the repository to the water table exist among infiltration models, alternative conceptual models, and climate states for the UZ site-scale model (BSC 2003 [163045], Section 6.6). The UZ flow and transport simulations indicate varying degrees of lateral diversion of groundwater to the east of the

repository and downward redirection by interception of flow at major faults. The SZ source region locations are defined to accommodate the general range in UZ transport pathways simulated by the suite of UZ site-scale flow model simulations.

The four SZ radionuclide source regions are shown in Figure 6-27. Note that the CORPSCON software code (v. 5.11.08, STN: 10547-5.11.08-00, LANL 2001 [155082]) was used to convert the coordinates of the repository design (given in state plane coordinates in meters) to UTM coordinates. The coordinates of the corners of the source regions are given in Table 6-8. Source regions 1, 3, and part of 2 are located directly below the repository to capture radionuclide transport that occurs vertically downward in the UZ site-scale flow and transport model. In addition, regions 1, 2, and 3 are appropriate source locations for radionuclides arriving at the water table in the human intrusion scenario (see CRWMS M&O 2000 [153246], Section 4.4) , in which a hypothetical borehole penetrates the repository and extends to the saturated zone. Source regions 2 and 4 are located to the east of the repository to capture radionuclide transport that is subject to lateral diversion of groundwater to the east along dipping volcanic strata in the unsaturated zone. Also note that the northern part of source region 2 underlies a northeasterly extension of the repository.

The random locations of the radionuclide source term for each realization are defined by eight stochastic parameters. The parameters SRC1X, SRC1Y, SRC2X, SRC2Y, SRC3X, SRC3Y, SRC4X, SRC4Y determine the x coordinate and y coordinate for the source location within regions 1 to 4, respectively. These parameter values are drawn from independent, uniform distributions from 0.0 to 1.0. The result is a randomly located point source within each of the four source regions for each realization of the SZ Transport Abstraction Model.
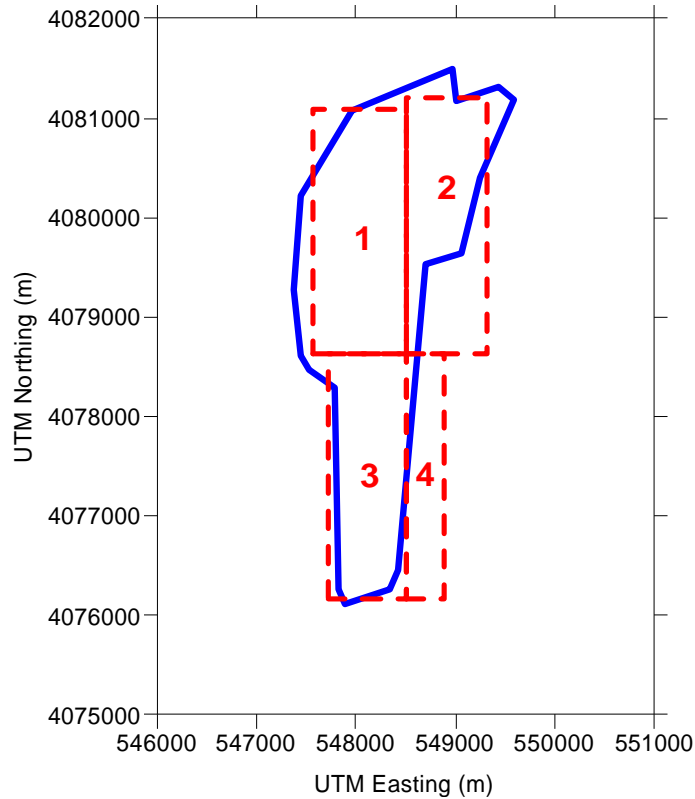
Sources for repository outline: 800-IED-EBS0-00401-000-00C, BSC 2003 [162289]
800-IED-EBS0-00402-000-00B, BSC 2003 [161727]

NOTE: Repository outline is shown by the solid blue line and the four source regions are shown by the dashed red lines.

Figure 6-27. Source Regions for Radionuclide Release in the SZ Transport Abstraction Model

6.5.2.14 Maximum Alluvial Porosity

The value of maximum or total alluvial porosity is used to calculate the adjusted (or new) K_d value in the effective porosity conceptualization of transport in the alluvium (see Equation 6-3). The average total porosity of alluvium from corroborative data given in Table 6-10 is 0.35. The calculated value of average total porosity in alluvium from the borehole gravimeter data from well EWDP-19D1 is significantly lower, as shown in Table 6-11 The approximate average value of maximum alluvial porosity from these two sources is 0.30. Note that the uncertainty distribution in effective porosity of alluvium is truncated at a maximum value of 0.30 (Figure 6-10).

6.5.2.15 Average Fracture Porosity

The value of average fracture porosity of volcanic rocks is used to calculate the retardation factor of sorbing radionuclides in the rubblized material of fracture zones. This retardation factor in the fracture zones only applies when the flowing interval porosity exceeds the average fracture porosity. The average fracture porosity is conceptualized to be the total fracture porosity of the volcanic units, not including any matrix porosity in the rubblized material of fracture zones. The average fracture porosity is taken as the median of the uncertainty distribution assigned to the flowing interval porosity (FPVO) (see Table 6-8) which is equal to 0.001.

6.5.2.16 Average Matrix Porosity

The value of average matrix porosity of volcanic rocks is used to calculate the retardation factor of sorbing radionuclides in the SZ 1-D Transport Model and in the rubblized material of fracture zones. This retardation factor in the fracture zones only applies when the flowing interval porosity exceeds the average fracture porosity. The average matrix porosity of volcanic rocks is calculated as the average of matrix porosity in hydrogeologic units numbered 11 through 14, as given in Table 6-12. The calculated average matrix porosity is 0.22.

6.5.2.17 Average Bulk Density of Volcanic Matrix

The value of average bulk density of the matrix in volcanic rocks is used to calculate the retardation factor of sorbing radionuclides in the SZ 1-D Transport Model and in the rubblized material of fracture zones. This retardation factor in the fracture zones only applies when the flowing interval porosity exceeds the average fracture porosity. The average bulk density of volcanic matrix is calculated as the weighted average of bulk density in hydrogeologic Units numbered 13 through 15, as given in Table 6-13, with double weighting given to Unit 13. The calculated average bulk density is 1.88 g/cm^3.

6.5.2.18 Matrix Porosity of Volcanic Units (Constant)

Matrix porosity (ϕ_m) is treated as a constant parameter for eight units of the nineteen SZ model hydrogeologic units. Constant, in this sense, means that ϕ_m will vary from one unit to another, but, given a particular unit, the porosity is constant for all realizations. The porosity also remains spatially constant for each unit. The parameter values and input source(s) are shown in Section 4, Table 4-1 and discussed below.

The following discussion covers data sources used in constant porosity inputs for the affected hydrogeologic units. The volcanic Units 11 through 15 do lie in the expected flow paths per BSC 2003 [162649], Section 6.6.2. All of the remaining units are expected to lie outside of any expected SZ model transport paths and thus the values of matrix porosity assigned to the remaining units have no impact on the transport simulations. However, the model requires values for ϕ_m for all units whether they play a role in transport simulations or not. Therefore values as representative as possible were used.

For the case of Units 15-13, the matrix porosity is based on the values from SN0004T0501399.003. The matrix porosity value for Units 12 and 11 were derived from matrix porosity data from the boreholes; UE-25P#1, USW H-3, SD7, USW G-3, USW H-1, USW G-4, USW H-5, and USW H-6 (DTN: SN0004T0501399.003 [155045], MO0109HYMXPROP.001 [155989], MO0010CPORGLOG.002 [155229]). Simple averages of the wells described above were calculated from the data for Units 12 and 11, as shown in spreadsheet "bulkd_matr_eff_La.xls" (DTN: SN0306T0502103.006).

Units 10 and 8 are both volcanic confining units. The value of ϕ_m for these units was obtained from the value for Unit 14, which is a volcanic confining unit for which there are site-specific data. The ϕ_m value for Unit 9 (volcanic unit) was obtained by averaging the values for the three overlying Crater Flat group Units (11-13). These averages were used as the matrix porosity inputs to the SZ site-scale model for their respective units as shown in Table 6-12.

Table 6-12.   Values of Matrix Porosity (ϕ_m) for Several Units of the SZ Model

SZ Unit Name	SZ Unit Number	Matrix Porosity (ϕ_m)
Upper Volcanic Aquifer (Topopah)	15	0.15
Upper Volcanic Confining Unit (Calico Hills)	14	0.25
Lower Volcanic Aquifer, Prow Pass	13	0.23
Lower Volcanic Aquifer, Bullfrog	12	0.18
Lower Volcanic Aquifer, Tram	11	0.21
Lower Volcanic Confining Unit	10	0.25
Older Volcanic Aquifer	9	0.21
Older Volcanic Confining Unit	8	0.25

DTN: SN0310T0502103.010

6.5.2.19 Bulk Density of Volcanic Matrix

Bulk density (ρ_b) is defined by Freeze and Cherry (1979 [101173], p. 337) as the "oven-dried mass of the sample divided by its field volume". It is a factor in Equation 6-2, used to determine retardation of a solute due to chemical adsorption in groundwater. That equation is employed in the SZ site-scale flow and transport model as part of the FEHM code (Zyvoloski et al. 1997 [110491], p. 42).

Bulk density is treated as a constant parameter for seventeen of the nineteen units of the SZ model hydrogeologic units. Constant, in this sense, means that ρ_b varies from one unit to another, but, given a particular unit, the bulk density stays the same for all realizations. The bulk density also remains spatially constant for each unit. Bulk density in hydrogeologic Units 19 and 7 is treated as an uncertain parameter and is discussed in Section 6.5.2.7. The parameter values and input source(s) are described in Section 4. This section contains a discussion of the analyses used to develop the values. The volcanic Units 11 through 15 do lie in the expected flow paths per BSC 2003 [162649], Section 6.6.2.   All of the remaining units are expected to lie outside of any expected SZ model transport paths and thus the values of bulk density assigned to the remaining units have no impact on the transport simulations.

Estimates for bulk density were either based on the use of an analogous unit, or a calculation was required, as discussed below. For some units, including part of the volcanic units and the carbonate units, the calculation involved averaging a group of referenced bulk density values. Some of the volcanic units required the use of a referenced graph to calculate bulk density as a certain function of matrix porosity (for which values had already been determined). Finally, two units (granite and lava flows) required the use of a general equation that relates bulk density to porosity. Many of the calculations required referencing either the matrix porosities or the effective porosities that were tabulated in Table 6-12 and Table 6-14 respectively.

The estimated bulk densities are summarized in Table 6-13 and the methods used to obtain these values are summarized in the discussion below.

Table 6-13. Values of Bulk Density (ρ_b) for All Units of the SZ Site-Scale Model

SZ Unit Name	SZ Unit Number	Bulk Density (ρ_b) (g/cm^3)
Valley Fill Confining Unit	18	2.50
Cenozoic Limestone	17	2.77
Lava Flows	16	2.44
Upper Volcanic Aquifer (Topopah)	15	2.08
Upper Volcanic Confining Unit (Calico Hills)	14	1.77
Lower Volcanic Aquifer, Prow Pass	13	1.84
Lower Volcanic Aquifer, Bullfrog	12	2.19
Lower Volcanic Aquifer, Tram	11	2.11
Lower Volcanic Confining Unit	10	1.77
Older Volcanic Aquifer	9	2.05
Older Volcanic Confining Unit	8	1.77
Upper Carbonate Aquifer	6	2.77
Lower Carbonate Aquifer Thrust	5	2.77
Upper Clastic Confining Unit	4	2.55
Lower Carbonate Aquifer	3	2.77
Lower Clastic Confining Unit	2	2.55
Granites	1	2.65

NOTE: Units 19 and 7 are treated as uncertain parameters and discussed in Section 6.5.2.7.

Carbonates Units 3, 5, 6, and 17 - Bulk density for Units 3, 5, 6 and 17 is determined from an average of a series of bulk density values from the Roberts Mountain Formation and the Lone Mountain Formation of borehole UE-25p#1 (DTN: MO0010CPORGLOG.002 [155229]). A simple average was calculated using these values (see spreadsheet "bulkd_matr_eff_La.xls" (DTN: SN0306T0502103.006)).

Clastic Units 2, 4, and 18 - Bulk density values for Unit 4 are determined from an average of a series of sedimentary deposit formation bulk densities from borehole UE-25P#1 (DTN: MO0010CPORGLOG.002 [155229]). There are no bulk density data available for the Clastics hydrogeologic units. A simple average was calculated using these values (see spreadsheet "bulkd_matr_eff_La.xls" (DTN: SN0306T0502103.006)). The bulk density assigned to Unit 4 was used as an analogous value for Unit 2, because Unit 2 is also a clastic confining unit. Unit 4 is also used as an analogous unit for Unit 18 because data do not exist for this unit and the value was rounded to 2.5.

Volcanic Units 8, 10, 13, 14, and 15 - The Rock Properties Model (BSC 2002 [159530]) contains a graph (Figure 24b, on page 71) that relates point values of ρ_b to ϕ_m in volcanic tuff. The graph demonstrates a strong linear correlation between the two parameters. The equation for the straight-line fit to the scatterplot is shown below (DTN: SN0004T0501399.002 [155046])

$$\rho_b = 2.5019 - 2.8924 \cdot \phi_m \qquad \text{(Eq. 6-30)}$$

Table 6-8 lists the values of ϕ_m for the Units (13-15) that were used to calculate ρ_b. Hydrogeologic Units 8 and 10 are volcanic confining units. The value of ρ_b for these units was obtained from the value for Unit 14, which is a volcanic confining unit for which we have site-specific data.

Volcanic Units 11 and 12 - Bulk density for Units 11 and 12 is determined from values of the so-called "middle volcanic aquifer," which is equivalent to the SZ Units 11 and 12 (DTN: MO0109HYMXPROP.001 [155989] and MO0010CPORGLOG.002 [155229]). The bulk density values come from the boreholes SD7, USW H-1, UE-25b#1, J-13, UE-25a#1, USW GU-3, USW G-3, USW G-4, UE-25p#1, and USW G-1. A simple average was calculated from those values (see spreadsheet "bulkd_matr_eff_La.xls" (DTN: SN0306T0502103.006)).

Volcanic Unit 9 - Unit 9 is a "volcanic aquifer". Its value was obtained by averaging the values for the three overlying volcanic Crater Flat group Units (11-13) and Unit 15.

Lava Flows (Unit 16) and Granites (Unit 1) - Rearrangement of the terms from an equation by Hillel 1980 [101134], p. 12, Equation 2.14) yields the following general relationship between bulk density and porosity:

$$\rho_b = (1 - \phi_T) \cdot \rho_{grain} \qquad \text{(Eq, 6-31)}$$

where ρ_{grain} equals particle density [M/L^3]. The same text reference considers it appropriate that ρ_{grain} can be equal to 2.65g/cm^3 (Hillel 1980 [101134], p. 9). As both of these units are not in the transport model path, it is suitable to use the particle density value and effective porosity to calculate bulk density (Equation 6-31) (see spreadsheet "bulkd_matr_eff_La.xls" (DTN: SN0306T0502103.006)). The effective porosity values were used for Equation 6-31 because the effective porosity is very similar to the total porosity for the lava flow and granite

units. The porosity values were taken from Table 6-12. The lava flow unit has an effective porosity of 0.08 and the granite unit has a porosity of 0.0001. Therefore the bulk densities assigned for those units are 2.44 and 2.65 g/cm^3 respectively.

6.5.2.20 Effective Porosity

Effective Porosity (ϕ_e) is treated as a constant parameter for nine of the nineteen SZ model hydrogeologic units. Constant, in this sense means that ϕ_e varies from one unit to another, but, given a particular unit, the porosity is the same for all realizations. The effective porosity is also homogeneous within each unit. The input source(s) are described in Section 4, Table 4-1.

The nine hydrogeologic units discussed in this Section do not occur within the flow path from beneath the repository; therefore, these values do not impact the simulated transport of radionuclides. However, representative values are used. The Bedinger et al. 1989 [129676], Table 1, p. A18 report includes hydrogeologic data for the Basin and Range Province of the Southwestern U.S. The Bedinger et al. report covers a region that extends into eight states and includes the Yucca Mountain site. Bedinger et al. 1989 [129676] was used as the source for data on the Valley Fill Confining Unit (18), the Cenozoic Limestone Unit (17), Lava Flow Unit (16), Upper Carbonate Aquifer Unit (6), Lower Carbonate Aquifer Thrust Unit (5), Upper Clastic Confining Unit (4), Lower Carbonate Aquifer Unit (3), Lower Clastic Confining Unit (2) and the Granites Unit (1). All of the carbonate units were assigned the same value.

The effective porosity values from Bedinger et al. 1989 [129676], Table 1 page A18 (DTN: MO0105HCONEPOR.000 [155044]) are used for all of the hydrogeologic units described in this paragraph. The upper and lower carbonate aquifer, the lower carbonate thrust aquifer and the cenozoic limestone units (designated as Units 6, 3, 5 and 17) respectively, use the mean value of Carbonate Rocks. The Cenozoic Limestone Unit is assigned the same value as the carbonate units because it is a similar rock type to the carbonate rocks. The value for granites (Unit 1) is set equal to the estimate for metamorphic rock with a depth more than 300 m. Unit 16 is assigned the average of the Lava Flows, fractured and moderately dense, from the MO0105HCONEPOR.000 [155044] source. Units 4 and 2 utilize the mean value from the Clastic Sedimentary Units. Unit 18, utilizes the Basin fill mean value for fine-grained clay and silt cited in Table 1 of Bedinger et al. 1989 [129676]. This information is summarized in the spreadsheet "geonames.xls" (DTN: SN0306T0502103.006). Table 6-14 lists the constant values used for each unit, for the SZ Transport Abstraction Model for TSPA-LA.

Table 6-14. Values of Effective Porosity (ϕ_e) for Several Units of the SZ Transport Abstraction Model

SZ Unit Name	SZ Unit Number	Effective Porosity (ϕ_e)
Valley Fill Confining Unit	18	0.32
Cenozoic Limestone	17	0.01
Lava Flows	16	0.08
Upper Carbonate Aquifer	6	0.01
Lower Carbonate Aquifer Thrust	5	0.01
Upper Clastic Confining Unit	4	0.18
Lower Carbonate Aquifer	3	0.01
Lower Clastic Confining Unit	2	0.18
Granites	1	0.0001

DTN: SN0310T0502103.009

6.5.3   Summary of Computational Models

Both the SZ Transport Abstraction Model and the SZ 1-D Transport Model are intended for use in the analyses for TSPA-LA. The results of the multiple realizations of SZ transport with the SZ Transport Abstraction Model, in the form of multiple breakthrough curves, are coupled with the TSPA simulations using the convolution integral method. The SZ 1-D Transport Model is intended for direct incorporation into the TSPA model. The SZ 1-D Transport Model is developed independently of the TSPA model, but contains the elements necessary for implementation within the TSPA model.

6.5.3.1 SZ Transport Abstraction Model

The groups of radioelements for simulated transport in the SZ Transport Abstraction Model are summarized in Table 6-15. There are nine groupings of radionuclides indicated by the first column in Table 6-15.   The modes of radioelement transport are as: 1) solute, 2) colloid-facilitated transport of radionuclides reversibly attached to colloids, and 3) colloid-facilitated transport of radionuclides irreversibly attached to colloids. As indicated in Table 6-15 the non-sorbing radioelements of carbon, technetium, and iodine are grouped together because their migration is identical. Americium, thorium, and protactinium reversibly attached to colloids are grouped together because of their similar sorption characteristics. Note that plutonium and americium may be transported both reversibly and irreversibly attached to colloids.

Table 6-15. Radioelements Transported in the SZ Transport Abstraction Model

Radionuclide Number	Transport Mode	Radioelements
1	Solute	Carbon, Technetium, Iodine
2	Colloid-Facilitated (Reversible)	Americium, Thorium, Protactinium
3	Colloid-Facilitated (Reversible)	Cesium
4	Colloid-Facilitated (Reversible)	Plutonium
5	Solute	Neptunium
6	Colloid-Facilitated (Irreversible)	Plutonium, Americium
7	Solute	Radium
8	Solute	Strontium
9	Solute	Uranium
10	Colloid-Facilitated (Fast Fraction of Irreversible)	Plutonium, Americium

DTN: SN0310T0502103.010 and SN0310T0502103.012

The radioelement breakthrough curves from the SZ Transport Abstraction Model for the 200 Monte Carlo realizations of SZ flow and transport are generated in the following manner. A steady-state groundwater flow field is produced for each of the 200 realizations prior to transport simulations. Variations in the groundwater specific discharge are included by scaling all values of permeability in the base case SZ Site-Scale Flow Model (BSC 2003 [162649]) and the values of specified recharge, using the value of the GWSPD parameter. Variations in horizontal anisotropy in permeability are included by scaling the values of north-south and east-west permeability within the zone of volcanic rocks influenced by anisotropy, using the value of the HAVO parameter. Each steady-state groundwater flow solution is stored to be used as the initial conditions in the radionuclide transport simulations. The SZ_Pre v. 2.0 software code (STN: 10914-2.0-00, SNL 2003 [163281]) is a pre-processor that is used to prepare the FEHM v. 2.20 software code (STN: 10086-2.20-00, LANL 2003 [161725]) input files for each of the 200 realizations. The pre-processor reads the values of the parameters from an input file containing a table of values for all 200 realizations, performs relevant parameter transformations, and writes the appropriate values to the various FEHM v. 2.20 software code (STN: 10086-2.20-00, LANL 2003 [161725]) input files. A total of 7200 individual simulations (200 realizations × 9 radioelement groups × 4 source regions) of SZ transport are conducted and the particle tracking output files are saved. The particle tracking simulations of matrix diffusion use the type curves of the analytical solution for matrix diffusion in DTN: LA0302RP831228.001 [163557]. The SZ_Post v. 3.0 software code (STN: 10915-3.0-00, SNL 2003 [163571]) is a post-processor that is used to extract the breakthrough curves from the FEHM v. 2.20 software code (STN: 10086-2.20-00, LANL 2003 [161725]) output files and concatenate all 200 realizations into a single file

for input to the SZ_Convolute v. 3.0 software code (STN: 10207-3.0-00, SNL 2003 [164180]) for use in the TSPA-LA.

For implementation of the SZ Transport Abstraction Model in the TSPA model, the specific radionuclides and the timing of climate change events must be specified in the control file for the SZ_Convolute v. 3.0 software code (STN: 10207-3.0-00, SNL 2003 [164180]). The radionuclides for each radioelement and their corresponding values of half-life are specified in order for the SZ_Convolute v. 3.0 software code (STN: 10207-3.0-00, SNL 2003 [164180]) to calculate the decay of these radionuclides during simulated transport in the SZ. The number of climate states and the times at which climate changes occur during the TSPA model simulation are also specified in the control file for the SZ_Convolute v. 3.0 software code (STN: 10207-3.0-00, SNL 2003 [164180]). The multiplier of groundwater flow rate in the SZ (relative to present conditions) for each climate state is also specified for the TSPA simulation. The values for this factor are given in Tablel 6-5.

6.5.3.2 SZ 1-D Transport Model

Implementation of the SZ 1-D Transport Model in the TSPA Model requires that the "stand-alone" version of the model developed in this report be correctly integrated into the TSPA Model. The SZ 1-D Transport Model was developed in anticipation of integration into the TSPA Model, but the following aspects of the integration must be checked for implementation in the TSPA Model. The radionuclide flux into and out of the SZ 1-D Transport Model must be properly linked to the other components of the TSPA Model. The radionuclide decay and ingrowth chains and the corresponding half-life values of radionuclides must be consistent with the other components of the TSPA Model. The parameter values for the 200 realizations of the SZ Transport Abstraction Model are stored as a table in the TSPA Model and the SZ 1-D Transport Model must be correctly linked with this table of values to ensure consistency with the SZ Transport Abstraction Model on a realization-by-realization basis. The parameter vectors used in the SZ Transport Abstraction Model that need to be incorporated into the table values used by the SZ 1-D Transport Model are contained in Attachment I of this AMR and in DTN: SN0310T0502103.009. The variable controlling changes in climate state in the TSPA Model must be correctly linked with the SZ 1-D Transport Model.

6.6 BASE-CASE MODEL RESULTS

Base-case model results from the SZ Transport Abstraction Model consist of radionuclide mass breakthrough curves at the accessible environment of the biosphere, approximately 18 km down gradient from the repository. A suite of breakthrough curves is generated for each species or class of radionuclides based on multiple realizations of the model. Variability in the results among these multiple realizations reflects uncertainty in groundwater flow and radionuclide transport behavior in the SZ. Variations in transport behavior among the species are also represented in these results.

6.6.1 Overview

The results of the 200 SZ Transport Abstraction Model realizations are shown in Figure 6-28 to Figure 6-36. Each figure shows the relative mass arriving at the accessible environment as a function of time and a histogram of median transport times, for a given category of radionuclides from Table 6-15. Note that the breakthrough curves and transport times shown in these figures are for a continuous, steady source at the water table below the repository (source region 1), initiated at time equal to zero. Also note that the breakthrough curves shown in these figures are for present climatic conditions and do not include the effects of radioactive decay. Recall that the process of radioactive decay is implemented in the SZ_Convolute v. 3.0 software code (STN: 10207-3.0-00, SNL 2003 [164180].

Although individual breakthrough curves may be difficult to discern in some of the figures, both the timing and the shapes of the breakthrough curves vary among the realizations. Variability in the timing of the breakthrough is reflected in the histograms of median transport time, for the bulk of the radionuclide mass arrival at the accessible environment. Variability in the shapes of the breakthrough curves is a function of differences in matrix diffusion and dispersivity among the realizations.

These results differ from the results presented in BSC 2003 [164870] for neptunium, plutonium reversibly attached to colloid, cesium reversibly attached to colloids, and uranium. The simulations with the SZ Transport Abstraction Model for these radioelement classes were updated because the uncertainty distributions for sorption coefficients (DTN: LA0310AM831341.002 [165891]) had been changed somewhat. The results presented here for the breakthrough curves do not differ significantly from the results in BSC 2003 [164870] for transport times of less than 100,000 years, given the overall uncertainty among the 200 realizations.

In adition, simulated breakthrough curves for the fast fraction of plutonium and americium irreversibly attached to colloids are developed for this report, as shown in Figure 6-37. Transport of these radionuclides in the SZ is simulated to occur with no retardation of colloids in the volcanic units or alluvium and with no matrix diffusion in the volcanic units.
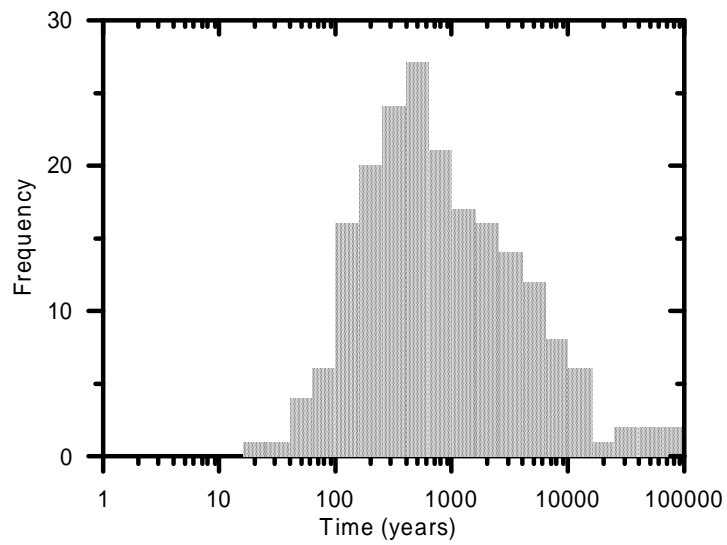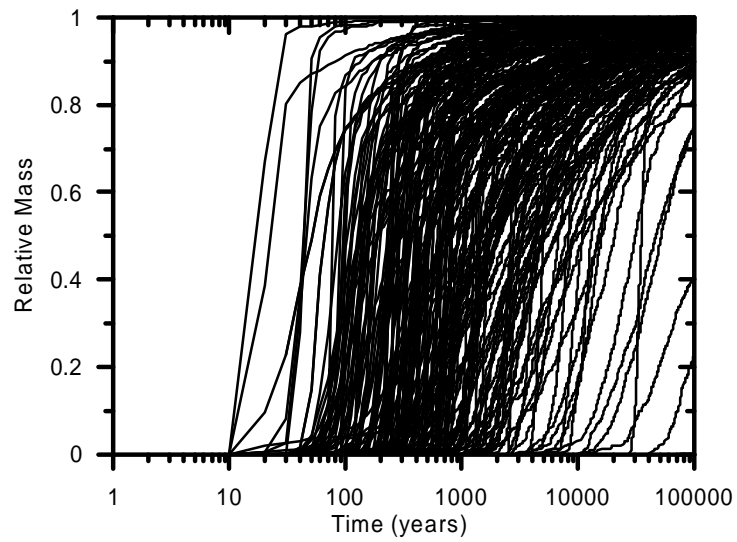
NOTE: Mass breakthrough curves and median transport times are for present climate and do not include radionuclide decay. Results shown for 200 realizations.

Figure 6-28. Mass Breakthrough Curves (Upper) and Median Transport Times (lower) for Carbon, Technetium, and Iodine at 18-km Distance
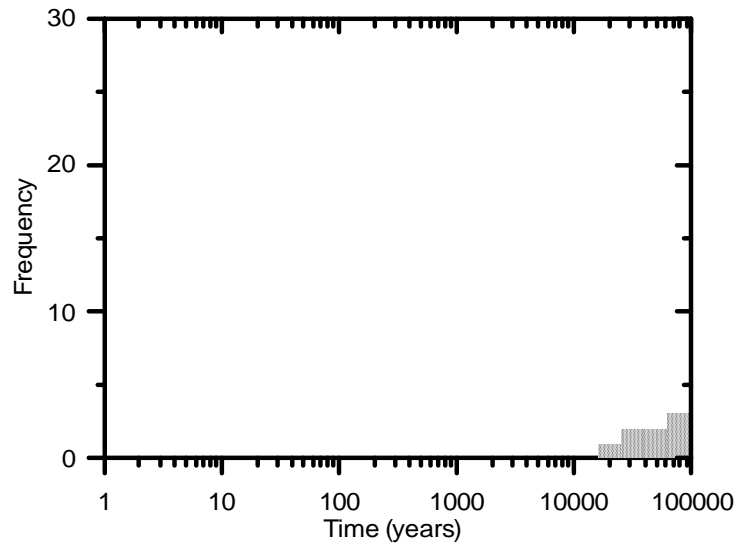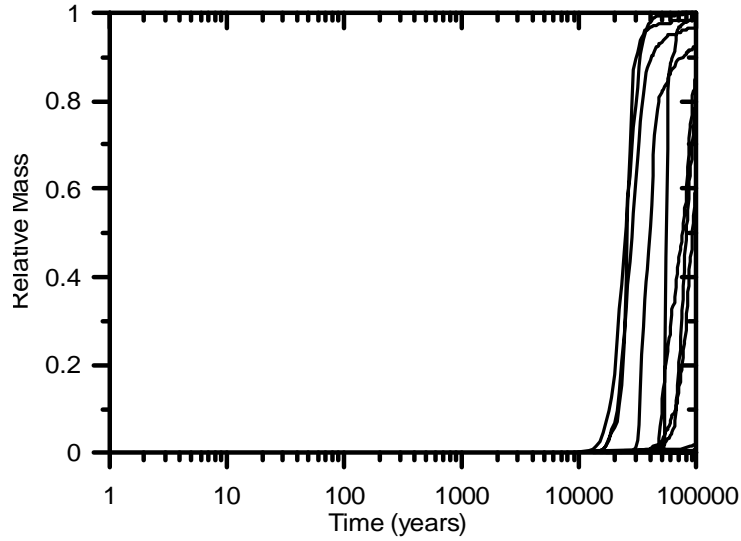
DTN: SN0310T0502103.010

NOTE: Mass breakthrough curves and median transport times are for present climate and do not include radionuclide decay. Results shown for 200 realizations.

Figure 6-29. Mass Breakthrough Curves (Upper) and Median Transport Times (lower) for Americium, Thorium, and Protactinium on Reversible Colloids at 18-km Distance
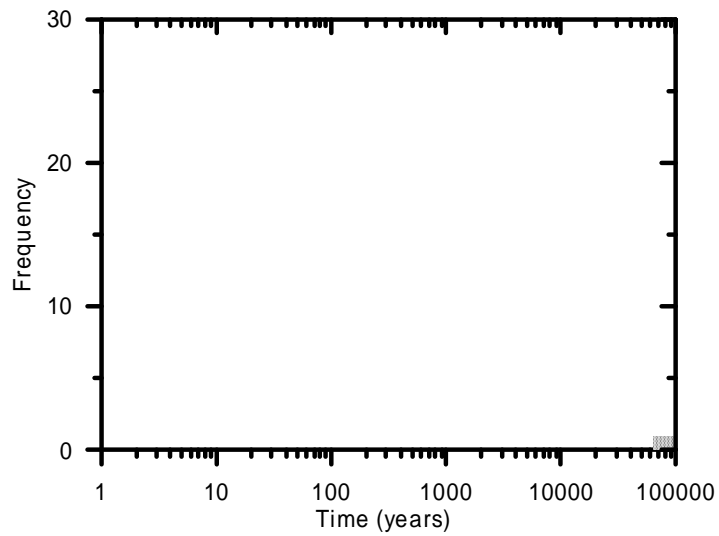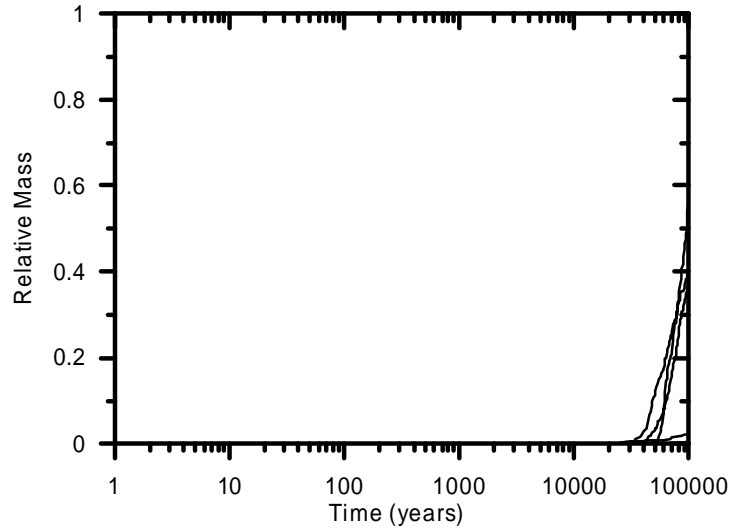
NOTE: Mass breakthrough curves and median transport times are for present climate and do not include
radionuclide decay. Results shown for 200 realizations.

Figure 6-30. Mass Breakthrough Curves (Upper) and Median Transport Times (lower) for Cesium on
Reversible Colloids at 18-km Distance
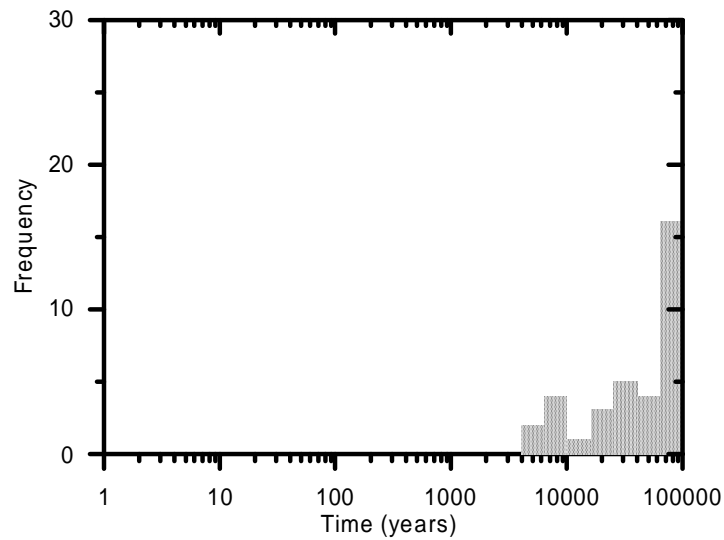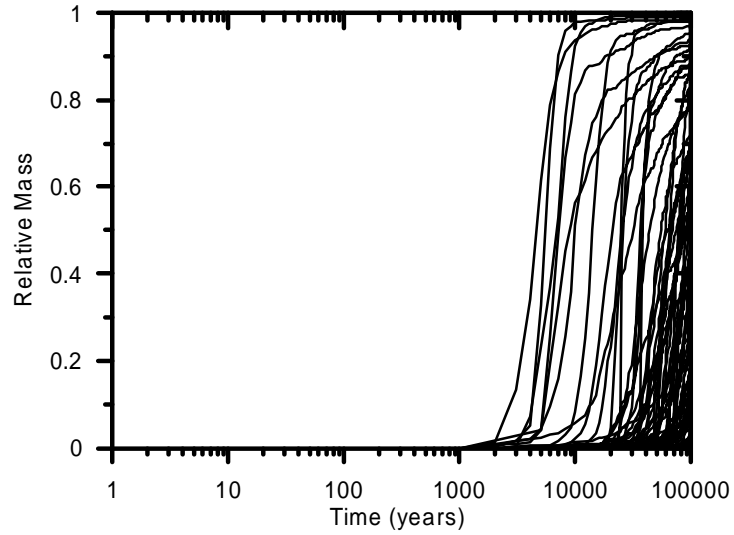
DTN: SN0310T0502103.010

NOTE: Mass breakthrough curves and median transport times are for present climate and do not include
radionuclide decay. Results shown for 200 realizations.

Figure 6-31. Mass Breakthrough Curves (Upper) and Median Transport Times (lower) for Plutonium on
Reversible Colloids at 18-km Distance
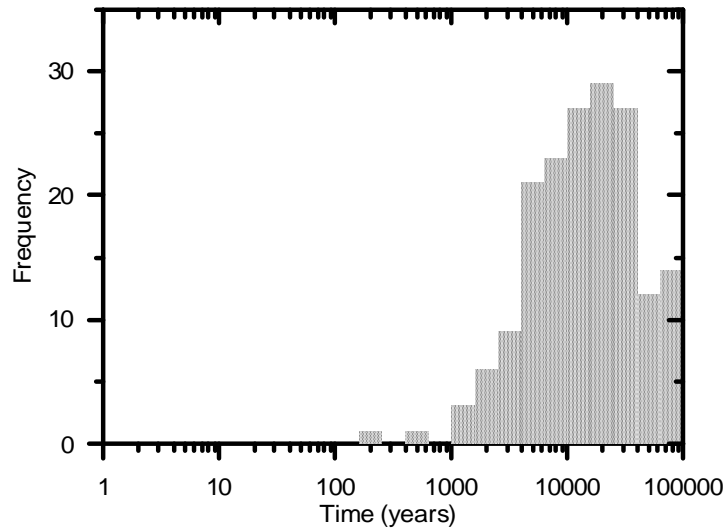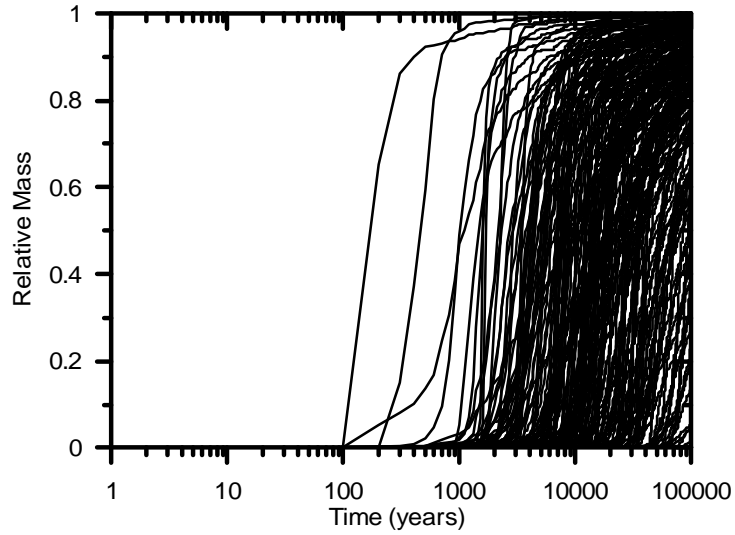
DTN: SN0310T0502103.010

NOTE: Mass breakthrough curves and median transport times are for present climate and do not include radionuclide decay. Results shown for 200 realizations.

Figure 6-32. Mass Breakthrough Curves (Upper) and Median Transport Times (lower) for Neptunium at 18-km Distance
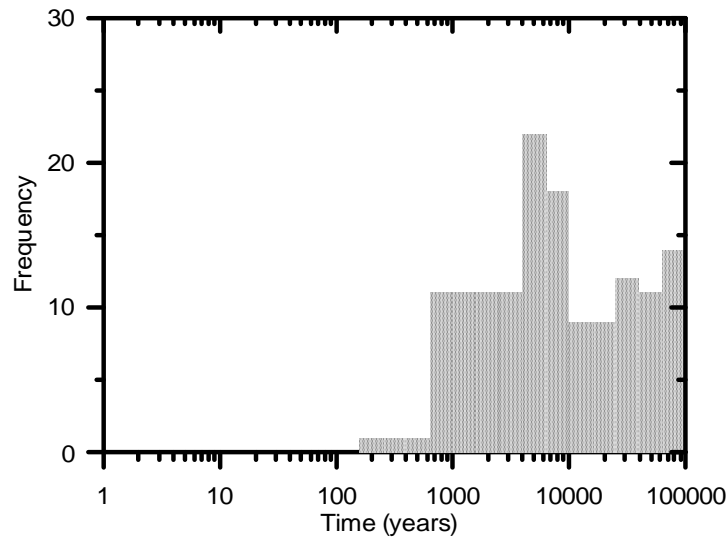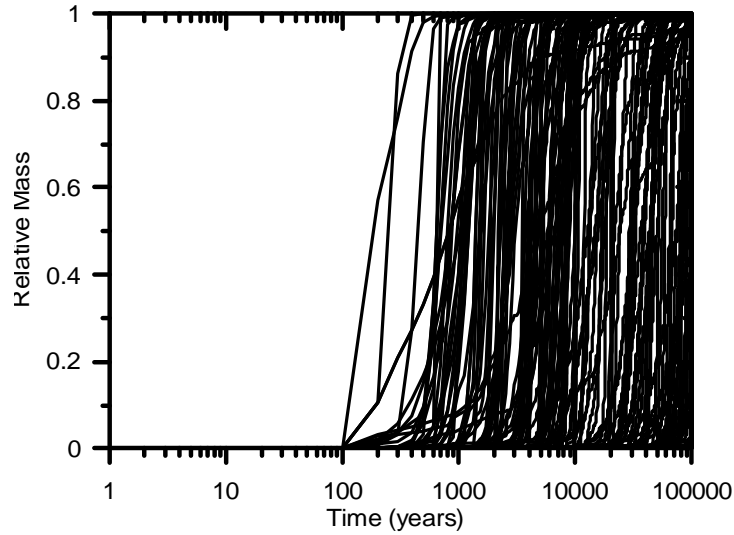
DTN: SN0310T0502103.010

NOTE: Mass breakthrough curves and median transport times are for present climate and do not include radionuclide decay. Results shown for 200 realizations.

Figure 6-33. Mass Breakthrough Curves (Upper) and Median Transport Times (lower) for Plutonium and Americium on Irreversible Colloids at 18-km Distance
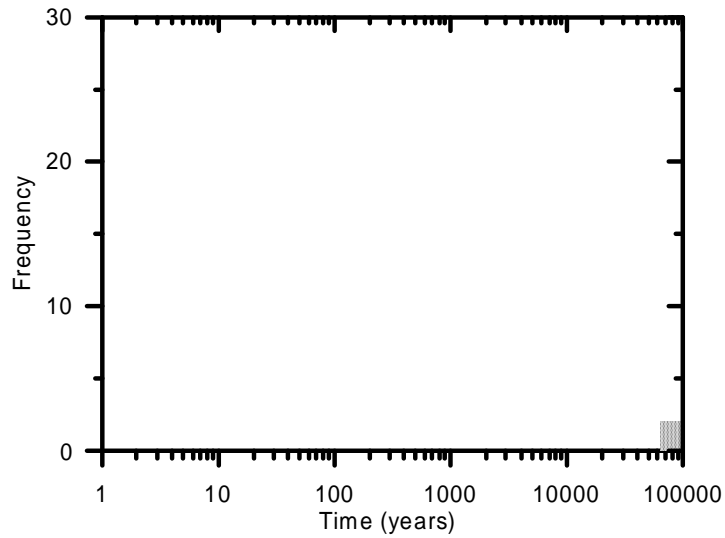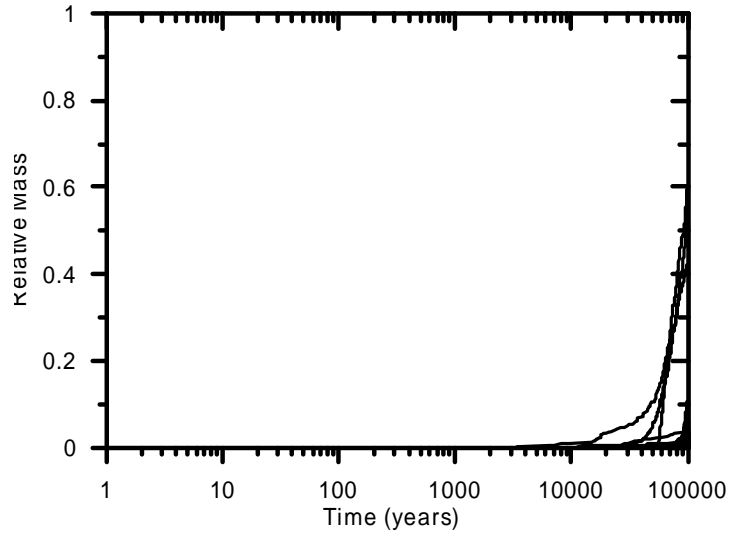
DTN: SN0310T0502103.010

NOTE: Mass breakthrough curves and median transport times are for present climate and do not include
radionuclide decay. Results shown for 200 realizations.

Figure 6-34. Mass Breakthrough Curves (Upper) and Median Transport Times (lower) for Radium at 18-
km Distance
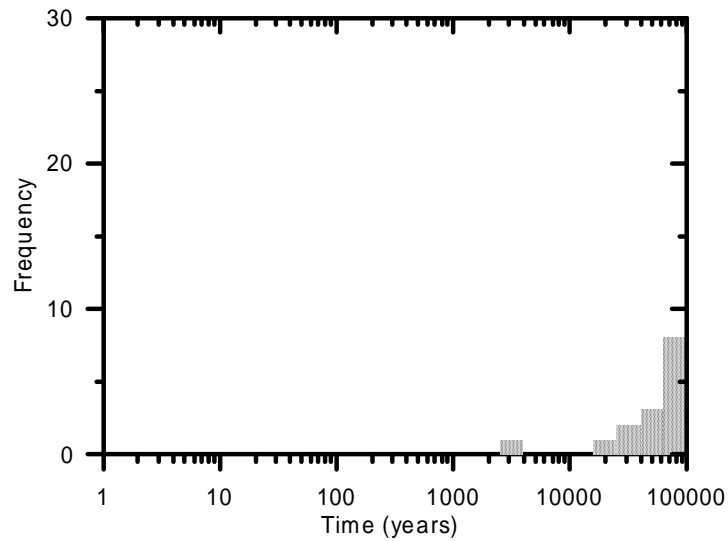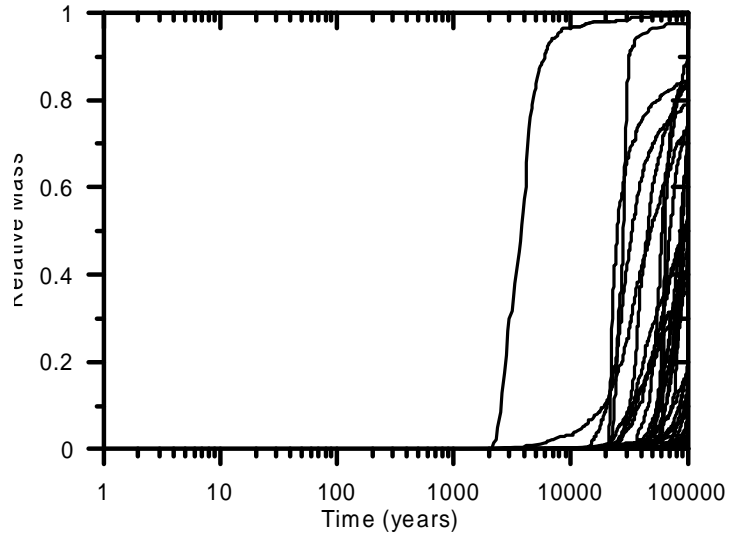
DTN: SN0310T0502103.010

NOTE: Mass breakthrough curves and median transport times are for present climate and do not include
radionuclide decay. Results shown for 200 realizations.

Figure 6-35. Mass Breakthrough Curves (Upper) and Median Transport Times (lower) for Strontium at
18-km Distance
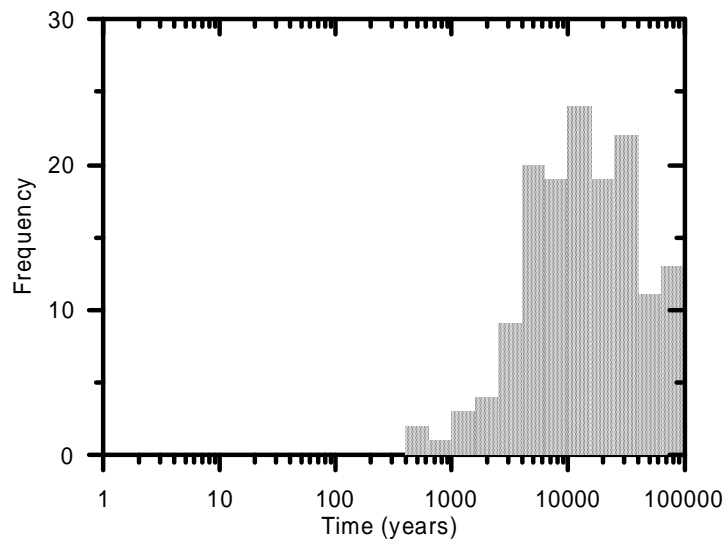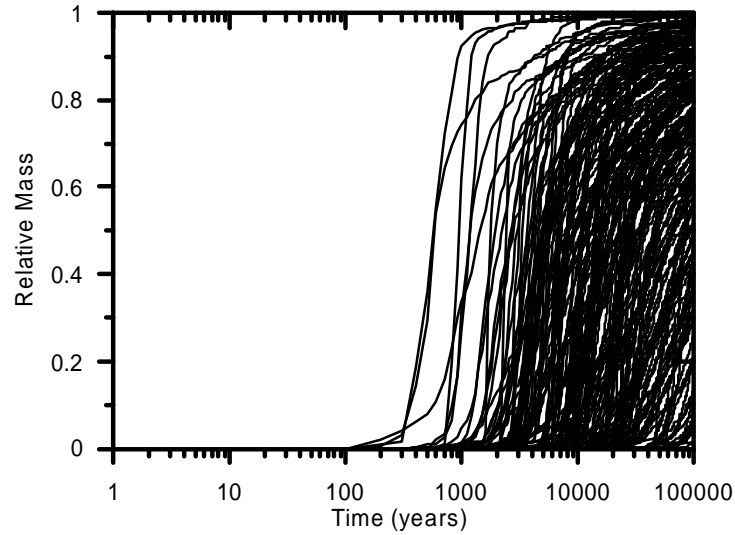
NOTE: Mass breakthrough curves and median transport times are for present climate and do not include radionuclide decay. Results shown for 200 realizations.

Figure 6-36. Mass Breakthrough Curves (Upper) and Median Transport Times (lower) for Uranium at 18-km Distance
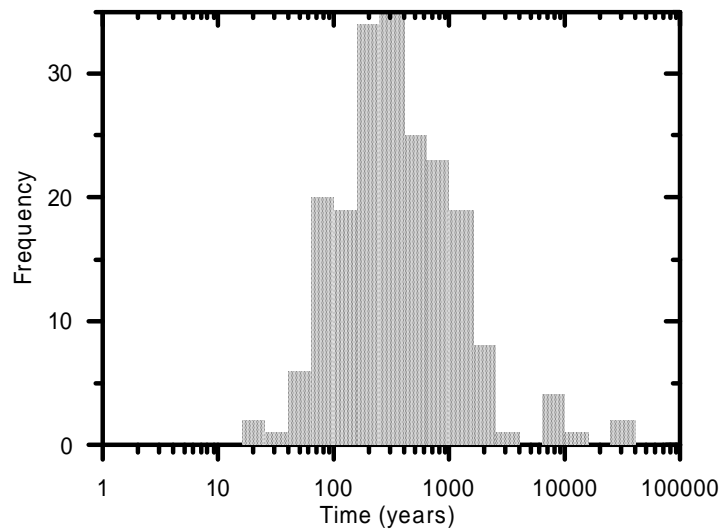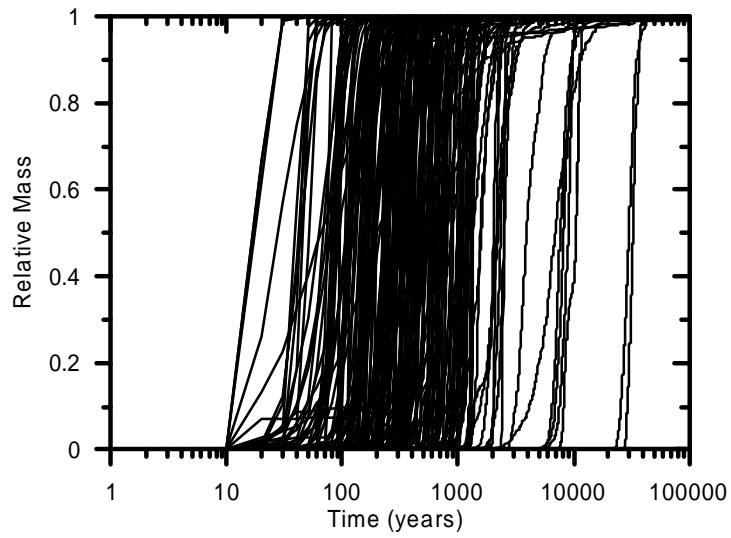
DTN: SN0310T0502103.012

NOTE: Mass breakthrough curves and median transport times are for present climate and do not include
radionuclide decay. Results shown for 200 realizations.

Figure 6-37. Mass Breakthrough Curves (Upper) and Median Transport Times (lower) for the Fast
Fraction of Plutonium and Americium on Irreversible Colloids at 18-km Distance

6.7 DESCRIPTION OF BARRIER CAPABILITY

The SZ forms a barrier to the migration of radionuclides and the exposure of the potential receptor population to these radionuclides in two ways. Delay in the release of radionuclides to the accessible environment during transport in the SZ allows radioactive decay to diminish the mass of radionuclides that are ultimately released. Dilution of radionuclide concentrations in groundwater used by the potential receptor population occurs during transport in the SZ and in the process of producing groundwater from wells. Further discussion of the SZ flow system as a barrier to radionuclide migration at Yucca Mountain is found in Eddebbarh et al. 2003 [163577].

6.7.1 Analyses of Barrier Capability

The simulated transport times of radionuclides in the SZ give a direct indication of the barrier capability of the SZ with regard to the delay in the release of radionuclides to the accessible environment. Uncertainty in the radionuclide transport times in the SZ is represented in the multiple realizations of the SZ system with the SZ Transport Abstraction Model and shown in the breakthrough curves for various radionuclides in Figure 6-28 to Figure 6-36. As shown by these figures, the effectiveness of the SZ as a barrier to transport varies significantly among the classes of radionuclides included in the analyses. The ranges of median transport times and the median transport times from all realizations for the various radionuclides are summarized in Table 6-16.

Variations in the radionuclide transport time among the realizations shown in Figure 6-28 to Figure 6-36 reflect the aggregate uncertainty in the underlying input parameters to the SZ Transport Abstraction Model. Although formal sensitivity analyses have not been applied to these results, sensitivity analyses have been performed on previous SZ transport modeling results (Arnold et al. 2003 [163857]). Those analyses indicate that uncertainties in groundwater specific discharge, sorption coefficients, and retardation of colloids are major factors in the simulated uncertainty in radionuclide transport times. Parameters related to matrix diffusion and geologic uncertainty have significant, but secondary importance with regard to the uncertainty in radionuclide transport times.

For non-sorbing species, such as carbon, technetium, and iodine, the delay afforded by the SZ may be less than 100 years to as much as 100,000 years, within the range of uncertainty indicated by the simulation results shown in Figure 6-28. The median transport time for non-sorbing species among all realizations is about 620 years. For the moderately sorbing species of neptunium, simulated median transport times range from about 200 years to greater than 100,000 years, with a median transport time among all realizations of 17,100 years (see Table 6-16). For the strongly sorbing species of radium, simulated median transport times range from 80,200 to greater than 100,000 years, with a median transport time among all realizations of greater than 100,000 years (see Table 6-16).

Analyses with the SZ Transport Abstraction Model indicate that there is considerable uncertainty in the delay to release of radionuclides to the accessible environment for all radionuclides. The upper bounds of uncertainty in the transport times are greater than 100,000 years (the upper limit of time in the transport simulations) for all radionuclides, with the exception of the fast fraction

of plutonium and americium irreversibly attached to colloids. The lower bounds of the uncertainty in transport times are indicated by the ranges given in Table 6-16.

It should be noted that the summary of simulated transport times presented in Table 6-16 is given for SZ groundwater flow under present climatic conditions. Under glacial-transition climatic conditions that are expected to occur within the next 10,000 years, the groundwater flow rate would be significantly higher. Groundwater flow rates in the SZ are estimated to be 3.9 times higher under glacial-transition climate conditions (see Section 6.5.1) corresponding to transport times of approximately 3.9 shorter than those presented in Table 6-16.

Table 6-16. Summary of Simulated Transport Times in the SZ Under Present Climatic Conditions

Species	Range of Median Transport Time (years)	Median Transport Time Among All Realizations (years)
Carbon Technetium Iodine	20 - >100,000	620
Reversible Colloids: Americium Thorium Protactinium	25,000 - >100,000	>100,000
Reversible Colloids: Cesium	80,000 - >100,000	>100,000
Reversible Colloids: Plutonium	5,000 - >100,000	>100,000
Neptunium	200 - >100,000	17,100
Irreversible Colloids: Plutonium Americium	200 - >100,000	19,400
Radium	80,200 - >100,000	>100,000
Strontium	3,300 - >100,000	>100,000
Uranium	600 - >100,000	23,300
Fast Fraction of Irreversible Colloids: Plutonium Americium	20 – 32,620	310

6.7.2 Summary of Barrier Capability

Taken as a whole, these analyses indicate that the SZ is expected to be a significant barrier to the transport of radionuclides to the accessible environment within the 10,000-year period of regulatory concern for the repository at Yucca Mountain. The expected behavior of the SZ system is to delay the transport of sorbing radionuclides and radionuclides associated with

colloids for many thousands of years, even under future wetter climatic conditions. Non-sorbing radionuclides are expected to be delayed for hundreds of years during transport in the SZ.

However, analyses of uncertainty in radionuclide transport in the SZ indicate that delays in the release of non-sorbing radionuclides could be as small as tens of years. The transport times in the SZ of neptunium, uranium, and of plutonium and americium irreversibly attached to colloids could be as small as hundreds of years, based on the analyses of uncertainty conducted with the SZ Transport Abstraction Model. It is important to note that ranges of uncertainty based on analyses with 200 Monte Carlo realizations extend to relatively low probability (approximately 0.5% probability) and thus include relatively unlikely results. Nonetheless, lower values in the ranges of transport time are possible, given the degree of uncertainty included in the model.

The radioactive decay of radionuclides during transport in the SZ enhances the barrier capability of the SZ by reducing the mass of radionuclides ultimately released to the accessible environment. The effectiveness of the decay process is attenuating releases from the SZ is related to the delay in the SZ and the half-life of the radionuclide. For radionuclides with longer transport times in the SZ and relatively short half-lives, this process renders the SZ an extremely effective barrier. Sr-90 and Cs-137 transport times would exceed several thousand half-lives, i.e., greater than 100,000 years, based on the median transport time among the realizations (Table 6-16). For comparison, the reduction in radioactivity after 20 half-lives is more than six orders of magnitude. For some radionuclides there would be a modest reduction in radionuclide mass during transport in the SZ. Pu-239 that is irreversibly attached to colloids would be expected to experience about 0.8 half-lives, based on the median transport time among all realizations (Table 6-16). Several radionuclides would experience little attenuation due to radioactive decay during transport in the SZ. Tc-99, I-129, and Np-237 would have only very small reductions in mass during the delay in release afforded by the SZ, due to their long half-lives (2.13×10^5 years for Tc-99 to 1.59×10^7 years for I-129).

The dilution of radionuclides in the SZ and during pumping from wells by the future hypothetical community in which the RMEI resides is not quantitatively assessed with the transport modeling approach used in the SZ Transport Abstraction Model. The relatively low values of transverse dispersivity in the uncertainty distribution for this parameter suggests that a large amount of dilution in radionuclide concentration during transport from beneath the repository to the accessible environment in the SZ is not expected. It is likely that the amount of dilution implicit in capturing the contaminant plume in 3000 acre-ft/year for use by the hypothetical community in which the RMEI resides would be greater than the dilution during transport in the SZ.

6.8 GROSS ALPHA CONCENTRATION

Regulations in 10 CFR 63.331 (10 CFR 63 [156605]) limit the gross alpha concentration and Ra-226 and Ra-228 concentration in groundwater. These groundwater protection standards apply to the accessible environment in the Yucca Mountain region and potential impacts of the repository must be compared to them. One aspect of the analysis is an assessment of the natural background concentrations in groundwater near the site because the standards for both gross alpha activity and combined Ra-226 and Ra-228 activity concentrations (respectively 15 pCi/L

and 5 pCi/L, 10 CFR 63 [156605], Section 63.331,Table 1)) are inclusive of natural background concentrations.

6.8.1   Gross Alpha Activity Data

A testing program to measure ambient radiation levels in groundwater was conducted in FY 1998. This work was performed under the YMP QA program. Groundwater samples were collected in June, July, and September of 1998 from each of six wells and two springs. The details and findings of this evaluation were reported in CRWMS M&O 1999 [150420]. The data of interest for this study are the reported gross alpha concentrations (picocuries per liter (pCi/L)) (CRWMS M&O 1999 [150420], Section 3.2.1, Table 3) and submitted, with gross beta measurements, to TDMS as DTN: MO9904RWSJJS98.000 [165866].

In CRWMS M&O 1999 [150420], p. 9 it was stated when gross alpha concentrations in groundwater exceed 5 pCi/L, calculation of average combined Ra-226 and Ra-228 concentration was required. However, CRWMS M&O 1999 [150420], Section 3.2.1 demonstrates the mean gross alpha concentration at each sample location was below 5 pCi/L in FY 1998, and continues by stating that in such cases, it was not necessary to calculate combined Ra-226 and Ra-228 concentration. As a consequence, data concerning Ra-226 and Ra-228 concentrations were not presented.

6.8.2   Counting Statistics and Error Prediction

Because of the random nature of radioactive decay and the relatively low concentrations of alpha emitting radionuclides in natural groundwater, it is necessary to understand the statistical fluctuations of the analytical method in relation to uncertainty.

Counting Statistics and Uncertainty

The following discussions on the statistics of radioactive decay measurements are taken from Knoll 1989 [161052], Chapter 3. When a counter is used to detect the number of radioactive decays in a given period of time, the distribution of counts from multiple trials have a Poisson distribution. If a single measurement is taken of n counts, then the estimate of the actual average number of counts ($\bar{n}$) in that period is n (Knoll 1989 [161052], p.84). Furthermore, the sample variance ($\bullet^2$) is also n, implying that the standard deviation ($\bullet$) is $n^{0.5}$ (Knoll 1989 [161052], p.85). For large values of n, the Poisson distribution can be approximated by a normal (i.e., Gaussian) distribution, thereby allowing confidence limits for the true mean ($\bar{n}$) to be established. Measurements involving radioactive decay are generally conducted for sufficient time to establish conditions for this approximation to be valid. One example given by Knoll 1989 [161052], Table 3-6 is for a measurement of $n = 100$, then there is a 90% probability that the true mean ($\bar{n}$) is in the interval $n \pm 1.64\sigma$, or 83.6 to 116.4. The symmetry of the Normal distribution indicates that in this example, that there is a 5% chance of the true mean being below 83.6 and a 5% chance of it being above 116.4.

<u>Uncertainty Propagation</u>

Measurements involving the counting of radioactive decay events are subject to spurious counts from natural background radiation.   The effect of this natural background on the desired results can be negated to a certain extent by performing the measurement twice, once with the sample to be quantified and once without the sample.   The former measurement gives a count of the desired signal plus unwanted background noise, while the latter provides an estimate of the background noise. If the counting times for both trials are equal, then the net counts from the sample to be characterized is then the difference between the two measured counts.

Following the approach presented by Knoll (1989 [161052], p.88), if there were two counts taken the first x being associated with the sample and background noise and the second y corresponding to the background noise, then the net counts attributable to the sample being assessed is the difference between x and y. The variance ($\bullet^2$) associated with the net value is the sum of the variances of the two measurements:

$$\sigma_{net}^2 = \sigma_x^2 + \sigma_y^2 \qquad \text{(Eq. 6-32)}$$

Because of the stochastic nature of both radioactive decay and background radiation, it is possible for a sample of low activity to give rise to a total count that is lower than the independently measured background count. These cases produce a negative estimate for the net sample activity. If these measurements to quantify a small level of activity were to be repeated several times, then the stochastic nature of the processes will result in a range of net activity estimates.   Some of these results would underestimate the true activity while others would overestimate the true value. Combining the data sets allows the random fluctuations observed in single measurements to be averaged over multiple measurements and thereby reduce statistical variations. This approach is adopted here.

If there are n measurements of a variable *x*, where measurement *i* is denoted by x_i having a variance of σ_i^2 then the average ($\bar{x}$)is given by:

$$\bar{x} = \frac{1}{n}\sum_1^n x_i \qquad \text{(Eq. 6-33)}$$

Knoll 1989 [161052], Equations 3-38 and 3-40 provides an estimate of the standard deviation (σ_x) in $\bar{x}$ as:

$$\sigma_{\bar{x}} = \frac{1}{n}\sqrt{\sum_1^n \sigma_i^2} \qquad \text{(Eq. 6-34)}$$

6.8.3 Applicable Sample Locations

Gross alpha concentration data in groundwater from eight locations in the vicinity of the receptor were collected in CRWMS M&O 1999 [150420]. Six of these locations were identified as being in the sub-basin (Alkali Flat-Furnace Creek Sub-basin) that contains Yucca Mountain, as shown in the first column of Table 6-17. The data from these six locations were selected to be the basis of estimating the groundwater gross alpha concentration at the receptor's location. The data from the Cherry Patch Well and Fairbanks Spring were not used as these locations are not in the groundwater sub-basin containing the proposed repository.

It was appreciated that other weighting schemes to obtain a mean activity level from these data were available. Weights could be based on some function of distance of the sampled wells from the receptor location or on the uncertainties of the individual measurements. In the interests of keeping the analysis simple without having to provide justification from any particular scheme it was elected to use simple averaging.

6.8.4 Data Analysis

The calculation of the mean activity values and the estimated standard deviation is shown in Table 6-17. It should be noted that the measurements of gross alpha concentrations on these groundwater samples are for all alpha emitters, whereas the regulations in 10 CFR 63.331 (10 CFR 63 [156605]) exclude radon and uranium from the standard for gross alpha activity. Consequently, the measurements shown in Table 6-17 overestimate the gross alpha activity exclusionary of radon and uranium.

Table 6-17. Data Table showing Calculation of Mean and Standard Deviation of Gross Alpha Concentration

Location	Date	Gross Alpha (x_i) (pCi/L)	Uncertainty[1] ± (pCi/L)	Sigma (σ_i) (pCi/L)	σ_i^2 (pCi/L)^2
NDOT[2] Well	24-Jun-98	-0.08	1.56	0.78	0.608
	29-Jul-98	0.32	1.1	0.55	0.303
	23-Sep-98	-1.40	0.79	0.40	0.156
Gilgan's South Well	24-Jun-98	-0.63	0.86	0.43	0.185
	29-Jul-98	0.64	0.86	0.43	0.185
	23-Sep-98	-0.74	0.69	0.35	0.119
UE-25 J-12	23-Jun-98	0.06	0.96	0.48	0.230
	28-Jul-98	0.27	0.72	0.36	0.130
	22-Sep-98	0.27	0.8	0.40	0.160
UE-25 J-13	23-Jun-98	0.05	0.94	0.47	0.221
	28-Jul-98	0.50	0.73	0.37	0.133
	22-Sep-98	-0.18	1.2	0.60	0.360
UE-25 c#2	23-Jun-98	1.20	1.33	0.67	0.442
	28-Jul-98	1.49	0.94	0.47	0.221
	22-Sep-98	0.73	1.67	0.84	0.697
Crystal Pool	22-Jun-98	1.04	1.27	0.64	0.403
	27-Jul-98	1.75	1.64	0.82	0.672
	25-Sep-98	-0.85	1.21	0.61	0.366
Σx_i		4.44		$\Sigma\sigma_i^2$	5.59
Mean Gross Alpha $\bar{x}$		0.25		$\sigma_{\bar{x}}$	0.13

NOTES: [1] Uncertainty is defined as being two standard deviations (sigma) (CRWMS M&O 1999 [150420], Section 3.2.1, Note to Table 3 given on page 9)

[2] Nevada Department of Transport

6.8.5   Results

From the discussion in Section 6.8.2 from Knoll 1989 [161052], p.86, there is a 90% chance that the true mean of a parameter (σ) will fall in the interval of $\bar{x} \pm 1.64\sigma_{\bar{x}}$ and that in only 5 % of the cases will the true value exceed $\bar{x} + 1.64\sigma_{\bar{x}}$. From the values presented in Table 6-17 to two decimal places, the best estimate for the mean gross alpha concentration in groundwater is 0.25 pCi/L with a 95% confidence that the concentration will not exceed 0.46 pCi/L. The overall uncertainty in the mean gross alpha concentration has a physically defined lower bound of 0.0 pCi/L. The upper bound of the uncertainty in the gross alpha concentration can be reasonably defined using a value that is 3 times the standard deviation above the expected value, which can be calculated as 0.64 pCi/L. A value that is 3 times the standard deviation above the expected value corresponds approximately to the 99.9[th] percentile in a normal distribution. The overall uncertainty distribution of the mean gross alpha concentration can thus be defined as a truncated

normal distribution with a mean of 0.25 pCi/L, a standard deviation of 0.13 pCi/L, a lower bound of 0.0 pCi/L, and an upper bound of 0.64 pCi/L.

In the absence of data on the combined concentrations of Ra-226 and Ra-228, it should be conservatively assumed for the standards involving these radionuclides that they are responsible for all gross alpha activity. For of Ra-226 and Ra-228 the mean concentration is 0.25 pCi/L with a 95% confidence that the concentration will not exceed 0.46 pCi/L. These results are summarized in Table 6-18.

Table 6-18.   Summary of Alpha Concentration Results in Amargosa Valley Groundwater

Parameter	Expected Value pCi/L	Upper (95%) Limit pCi/L
Gross Alpha Concentration	0.25	0.46
Combined Concentration of Ra-226 and Ra-228	0.25	0.46

6.8.6   Corroborative Data

Two reports were identified that provided measurements (non-QA) of gross alpha and radium concentrations in groundwater in the vicinity of the receptor that could be used to corroborate the concentrations derived to demonstrate compliance with the groundwater protection standards. These data are discussed below.

In CRWMS M&O 1998 [104963] the closest measurement site to the location of the receptor is the NDOT well near the intersection of highways US 95 and route 373. At this location, the annual average gross alpha activity concentration in groundwater during FY 1997 was reported as –0.54 ± 1.20 pCi/L (CRWMS M&O 1998 [104963], Table 5). The format is the mean value of 4 quarterly measurements ± two standard deviations. Table 4 of CRWMS M&O 1998 [104963] gives, for the same location and year, an average combined Ra-226 and Ra-228 concentrations in groundwater of 0.32 ± 0.33 pCi/L. Both these measurements of activity concentrations are consistent with the values provided in Table 6-18.

Some additional project data of gross alpha and radium activity concentrations in ground water are reported in CRWMS M&O 1997 [147759], Table 4. These data were based on samples taken during the first and second quarters of 1997. At each location of interest discussed in Section 6.8.3, gross alpha concentrations were reported to be below the detection limit; a limit that was not defined in the report. The combined Ra-226 and Ra-228 activity concentration (rounded here to two significant figures) ranged from a low value of 0.29 ± 0.27 pCi/L at the NDOT well to a high value of 0.70 ± 0.47 pCi/L at Crystal Pool. These values are consistent with those reported in Section 6.8.5.

In Townsend 2001 ([156604], p.8-1), the preamble to Section 8, Groundwater Monitoring, identifies that for the calendar year covered by the report (CY 2000), some results for radioactivity analysis were somewhat higher than historical data. It was also mentioned that the (unidentified) organization providing oversight of groundwater monitoring activities had also experienced similar difficulty in obtaining accurate analytical data. Because, there was no

indication as to whether this caveat applied to specific data sets or to all data, it must be assumed that all data based on radioactivity analysis were systematically biased to higher values.

The measurement site in Townsend 2001 ([156604], Figure 8.3) closest to the point of compliance is the Amargosa Valley RV Park, which is shown to be near the intersection of highways US 95 and route 373 (i.e., close to the NDOT well of CRWMS M&O 1998 [104963]). The samples for this site were taken on 14 November 2000 and reported concentrations were based on a single measurement.

In Townsend 2001 ([156604]) the gross alpha concentration in groundwater was reported to be 0.78 ± 0.50 pCi/L (Table 8.3), the Ra-226 concentration was 0.59 ± 0.40 pCi/L (Table 8.6), and the Ra-228 concentration was 0.43 ± 0.79 pCi/L (Table 8.7). By combining the two Ra measurements as discussed in Knoll 1989 [161052] (Equation 3-38, p. 88), the combined concentration of Ra-226 and Ra-228 is 1.02 ± 0.89 pCi/L.

Given that for a normal distribution the 95% confidence limits are at the mean value ± 2 standard deviations, the following statements can be made for the concentrations reported in Townsend 2001 ([156604]).

Gross alpha: 0.28 pCi/L < actual concentration < 1.28 pCi/L

Ra-226 and Ra-228:   0.13 pCi/L < actual concentration < 1.91 pCi/L

As the data reported in Townsend 2001 [156604] are stated to have systematically overestimated the concentrations, the above concentration ranges are not inconsistent with those in Table 6-18.

7. VALIDATION

This section of the report documents the validation of the SZ Transport Abstraction Model and the SZ 1-D Transport Model. For the SZ Transport Abstraction Model, a comparison is made between the abstraction model and the underlying process model, which is discussed in the report *Site-Scale Saturated Zone Transport* (BSC 2003 [162419]). This comparison tests the appropriateness and accuracy of the convolution integral method used in the SZ Transport Abstraction Model. Similarly, the validation of the SZ 1-D Transport Model consists of a qualitative comparison between the abstraction model and the site-scale process model mentioned above (BSC 2003 [162419]). In all cases, the validations of these models are performed for a range of behavior that is representative of the uncertainties being evaluated for the TSPA analyses.

7.1 VALIDATION PROCEDURES

As discussed above, validation of both the SZ Transport Abstraction Model and the SZ 1-D Transport Model involves comparison with the underlying process model (BSC 2003 [162419]). In making these comparisons, three cases for radionuclide transport are defined for implementation: median case, fast case, and slow case. The median case uses median values from uncertainty distributions for the relevant flow and transport parameters. The fast case uses parameter values set at the 90th percentile or the 10th percentile, depending on the parameter, that result in more rapid transport of radionuclides through the SZ. For example, the flowing interval spacing is set to its 90th percentile value, and the sorption coefficient is set to its 10th percentile value for transport of neptunium in the fast case. The slow case uses parameter values set at the 90th percentile or 10th percentile that result in less rapid transport of radionuclides through the SZ. These three cases approximately span the range of uncertainty in results of the SZ Transport Abstraction Model with regard to radionuclide transport in the SZ, as shown in Figure 6-28 and Figure 6-32. The parameter values used in the median, fast, and slow cases are summarized in Table 7-1.

The SZ Site-Scale Transport Model (BSC 2003 [162419]) was run for each of the three model validation cases by varying the input parameters to conform to the values given in Table 7-1. The steady-state groundwater flow solution for each case was first established by running the flow model (BSC 2003 [162649]) to equilibrium with the specified values of the parameters GWSPD and HAVO. The particle-tracking algorithm in the FEHM v. 2.20 software code (STN: 10086-2.20-00, LANL 2003 [161725]) was then used to obtain the simulated mass breakthrough curves with the SZ site-scale transport model at the regulatory boundary of the accessible environment.

Table 7-1. Parameter Values in the Three Cases for SZ Transport Model Validation

Parameter Name	Parameter Description	Median Case	Fast Case	Slow Case
FISVO	Flowing interval spacing in volcanic units	1.29 (19.5 m)	1.82 (66.1 m)	0.67 (4.68 m)
HAVO	Ratio of horizontal anisotropy in permeability	4.2	16.25	1.0
LDISP	Longitudinal dispersivity	2.0 (100 m)	2.96 (920 m)	1.03 (10.9 m)
FPLAW	Western boundary of the alluvial uncertainty zone	0.5	0.1	0.9
FPLAN	Northern boundary of the alluvial uncertainty zone	0.5	0.1	0.9
NVF19	Effective porosity in shallow alluvium	0.18	0.114	0.245
NVF7	Effective porosity in undifferentiated valley fill	0.18	0.114	0.245
FPVO	Fracture porosity in volcanic units	-3.0 (10^{-3})	-3.89 (1.29×10^{-4})	-1.50 (0.0316)
DCVO	Effective diffusion coefficient in volcanic units	-10.3 (5.0×10^{-11} m^2/s)	-10.68 (2.08×10^{-11} m^2/s)	-9.65 (2.22×10^{-10} m^2/s)
GWSPD	Groundwater specific discharge multiplier	0.0 (1.0)	0.477 (3.0)	-0.477 (0.333)
bulkdensity	Bulk density of alluvium	1910 kg/m^3	1810 kg/m^3	2010 kg/m^3
KDNPVO	Neptunium sorption coefficient in volcanic units	1.3 ml/g	1.04 ml/g	1.6 ml/g
KDNPAL	Neptunium sorption coefficient in alluvium	6.35 ml/g	4.26 ml/g	8.44 ml/g

NOTE: Values in parentheses are the parameter values from log-transformed uncertainty distributions.

7.1.1 SZ Transport Abstraction Model

Validation of the SZ Transport Abstraction Model is accomplished by running this model using the breakthrough curves for the three validation cases from the SZ Site-Scale Transport Model (BSC 2003 [162419]). The SZ Transport Abstraction Model uses the convolution integral method as implemented by the SZ_Convolute v. 3.0 software code (STN: 10207-3.0-00, SNL 2003 [164180]) to produce the radionuclide mass breakthrough to the accessible environment, given the time-varying input of mass at the water table below the repository for the TSPA. Note that model validation tests were performed with the SZ_Convolute v. 2.2 software code (STN: 10207-2.2-00, SNL 2003 [163344]).

For the first validation test, a constant input of 1 g/year from the UZ is applied at the upstream boundary of the SZ Transport Abstraction Model. This is essentially the same transport boundary condition used in the SZ Site-Scale Transport Model (BSC 2003 [162419]) to derive the SZ breakthrough curves for input to the abstraction model. Consequently, the output of the SZ Transport Abstraction Model should reproduce the breakthrough curve used as the input in the validation test. This validation test is conducted for both a non-sorbing species and for neptunium. The validation test is also run for the three validation cases described in the previous section. To facilitate comparison of the results, the transport simulations in both the SZ Site-Scale Transport Model and the SZ Transport Abstraction Model are performed without radioactive decay.

As a second validation test, the mass balance of radionuclides transported in the SZ Transport Abstraction Model is checked. This check is performed by setting the upstream boundary condition equal to 1 g/year for time up to 1000 years and reducing this to 0 g/year for the remainder of the simulation. Thus, the total radionuclide mass input to the SZ Transport Abstraction Model is 1000 grams. Since radioactive decay is not included in this validation test, the cumulative output of the model over a long simulation time should also be 1000 grams. This second validation test is also run for the three validation cases described in the previous section (Table 7-1).

It should be noted that several additional test cases for the SZ_Convolute v. 2.2 software code (STN: 10207-2.2-00, SNL 2003 [163344]) have been conducted for the purposes of software verification (BSC 2003, *Validation Test Report for SZ_Convolute, V 2.2*, SDN: 10207-VTR-2.2-00, MOL.20021202.0341 [163587]). These tests verify the ability of the convolution integral method, as implemented by the SZ_Convolute v. 2.2 software code (STN: 10207-2.2-00, SNL 2003 [163344]), to simulate accurately radionuclide transport with variable input boundary conditions, radioactive decay, and variations in groundwater flux with climate change. Although not directly applied to the radionuclide transport results of the SZ Transport Abstraction Model presented in this report, the numerical testing of the software code used in this model provides additional confidence in the validity of the model

7.1.2 SZ 1-D Transport Model

Validation of the SZ 1-D Transport Model is conducted by running this model and comparing the results to the output of the SZ Site-Scale Transport Model (BSC 2003 [162419] and DTN: LA0306SK831231.001 [164362]). The SZ 1-D Transport Model is implemented using the GoldSim v. 7.50.100 software code (STN: 10344-7.50.100-00, BSC 2003 [161572]). Ultimately, the SZ 1-D Transport Model is fully integrated into the TSPA model; however, for the purposes of model development and validation, a stand-alone version of this model is used.

For the validation test, a constant input of 1 g/year from the UZ is applied at the upstream boundary of the SZ 1-D Transport Model. This is the same radionuclide mass boundary condition used in the SZ Site-Scale Transport Model (BSC 2003 [162419]). The breakthrough curves from the SZ 1-D model should approximately match the output of the site-scale transport model. This validation test is conducted for both a non-sorbing species and for neptunium, and is run for the three validation cases described in the previous section. To facilitate comparison of the results, the transport simulations in both the SZ Site-Scale Transport Model and the SZ 1-D Transport Model are performed without radioactive decay.

It should be noted that several additional test cases for the GoldSim v. 7.50.100-00 software code (STN: 10344-7.50.100-00), BSC 2003 [161572] have been conducted for the purposes of software verification (BSC 2002, *Validation Test Report(VTR) for GoldSim, V* 7.50.100, SDN: 10344-VTR-7.50.100-00, MOL.20030312.0227 [163962]). These tests verify the ability of the GoldSim v. 7.50.100-00 software code (STN: 10344-7.50.100-00, BSC 2003 [161572]) to accurately simulate radioactive decay and ingrowth. Although not directly applied to the radionuclide transport results of the SZ 1-D Transport Model presented in this report, the numerical testing of the software code used in this model provides additional confidence in the validity of the model.

Groundwater flow rates and flow-path lengths derived from the SZ Site-Scale Transport Model (BSC 2003 [162419]) were used in the development of the SZ 1-D Transport Model. However, both the approximate nature of the equivalency between the two models and the reduction in dimensionality in the 1-D transport model limit the ability of the 1-D model to match the results of the site-scale transport model.

7.2 VALIDATION CRITERIA

Model validation follows the *Technical Work Plan for: Saturated Zone Flow and Transport Modeling and Testing* (BSC 2003 [166034], Section 2.5). The TWP states that Level-II validation will be achieved by satisfying the criteria listed as items a) through f) in Appendix B of the *Scientific Processes Guidelines Manual* (BSC 2002 [160313] and implementing one post-development validation method. In the cases of the SZ Transport Abstraction Model and the SZ 1-D Transport Model, the post-development method was chosen to be the corroboration of the abstraction model results to the results of the validated process model from which the abstraction was derived (BSC 2003 [166034], Section 2.5). In addition, the TWP validation plan for the SZ Flow and Transport Abstraction Model includes a check of output for mass balance.

The acceptance criterion for validation of both the SZ Transport Abstraction Model and the SZ 1-D Transport Model is a favorable qualitative comparison between the simulated SZ breakthrough curves from these two models and the breakthrough curve from the SZ Site-

Scale Transport Model (BSC 2003 [162419] and DTN: LA0306SK831231.001 [164362]). The breakthrough curves are compared at 10%, 50%, and 90% mass breakthrough in the evaluation of this criterion. Breakthrough curves are compared for a non-sorbing species and for neptunium. Breakthrough curves for the median, fast, and slow cases outlined above are compared. Qualitative comparison of breakthrough curves is conducted by visual examination of graphs made of the breakthrough curves.

An additional acceptance criterion for the validation of the SZ Transport Abstraction Model is a check of the radionuclide mass balance in the model. The mass input to the model should equal the mass output from the model over long time periods. Discrepancies of a few percent are acceptable due to both less-than-complete discharge of radionuclide mass from the model and numerical (truncation) errors in the computer software implementing the numerical integration used in the convolution integral method.

These acceptance criteria reflect the essential functions of the SZ system with regard to the transport time and radionuclide mass delivery to the accessible environment.

7.3 RESULTS OF VALIDATION ACTIVITIES

The numerical results of the model validation activities described above are presented primarily as a series of plots of simulated breakthrough curves. A quantitative comparison of models with regard to radionuclide mass balance is also presented for the SZ Transport Abstraction Model.

7.3.1 SZ Transport Abstraction Model Validation Results

Results of the SZ Transport Abstraction Model and the SZ Site-Scale Transport Model (BSC 2003 [162419]) for a non-sorbing species are shown as simulated breakthrough curves in Figure 7-1. This figure shows results for the median, fast and slow cases of SZ transport. Note that all simulations were conducted without radioactive decay. The simulated breakthrough curves from the SZ Site-Scale Transport Model are shown with the solid and dashed lines for the three cases. The results from the SZ Transport Abstraction Model are shown as the open symbols that are superimposed on the breakthrough curves from the site-scale model.

NOTE: Results from the SZ Site-scale Transport Model (BSC 2003 [162419]) are shown for the median case (solid line), fast case (short-dashed line), and slow case (long-dashed line). Results from the SZ Transport Abstraction Model are shown for the median case (open circle), fast case (open square), and slow case (open triangle). Breakthrough curves do not include radioactive decay.

Figure 7-1. Simulated Breakthrough Curves Comparing the Results of the SZ Transport Abstraction Model and the SZ Site-Scale Transport Model for a Non-Sorbing Radionuclide

Visual comparison of the open symbols and the lines in Figure 7-1 indicates very close agreement in the results from the SZ Transport Abstraction Model and the SZ Site-Scale Transport Model for all three cases of SZ transport. The one exception is the first point in the results of the SZ Transport Abstraction Model for the fast case, which is lower than the corresponding breakthrough curve from the SZ Site-Scale Transport Model. It should be noted that the time step used in the abstraction model is 20 years, which differs from the 10-year time step used in the site-scale model for the fast case. This difference in time-step size accounts for the small discrepancy between the models at the first time step.

Results of the SZ Transport Abstraction Model and the SZ Site-Scale Transport Model (BSC 2003 [162419] and DTN: LA0306SK831231.001 [164362]) for neptunium are shown as simulated breakthrough curves in Figure 7-2. This figure shows results for the median, fast, and slow cases of SZ transport. Note that all simulations were conducted without radioactive decay. The simulated breakthrough curves from the SZ Site-Scale Transport Model are shown with the solid and dashed lines for the three cases. The results from the SZ Transport Abstraction Model are shown as the open symbols that are superimposed on the breakthrough curves from the site-scale model.

Figure 7-2. Simulated Breakthrough Curves Comparing the Results of the SZ Transport Abstraction Model and the SZ Site-Scale Transport Model for Neptunium

Visual comparison of the open symbols and the lines in Figure 7-2 indicates very close agreement in the results from the SZ Transport Abstraction Model and the SZ Site-Scale Transport Model for all three cases of SZ transport of neptunium.

Figure 7-3 shows the simulated breakthrough curve from the SZ Transport Abstraction Model of a non-sorbing species for the median case. This simulation applies a radionuclide mass influx boundary condition of 1 g/year for the first 1000 years of the simulation, which results in a total mass input of 1000 grams. The mass balance in the SZ Transport Abstraction Model is checked by summing the total mass output from the simulated breakthrough curve shown in Figure 7-3 over the 100,000 years of the simulation. The output sum is 981 grams, which is 98.1% of the input mass. Examination of the simulated breakthrough curve from the SZ Site-Scale Transport Model for the median case indicates that 98 % of the mass has reached the accessible environment within 100,000 years. Consequently, the discrepancy between total input mass and total output mass can be explained as the radionuclide mass retained in the SZ system after 100,000 years. The total output mass from the SZ Transport Abstraction Model for the fast case and the slow case is 99.8% and 99.5% of the input mass, respectively. Mass breakthrough for the median case has a longer "tail" than the slow and fast cases due to matrix diffusion.

Consequently, the total mass output is somewhat lower for the median case than the slow and fast cases in this validation test.
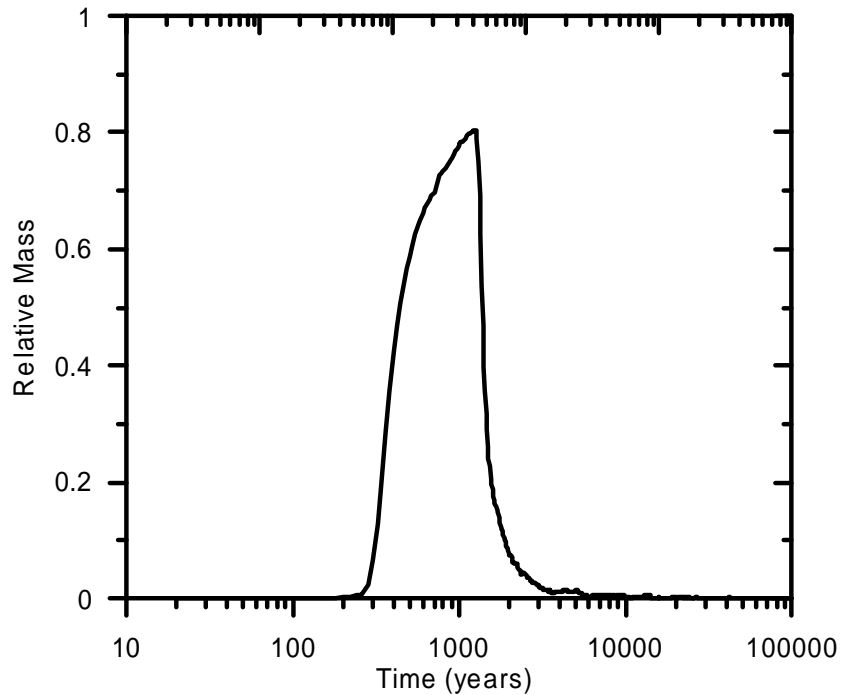
NOTE: Results from the SZ Transport Abstraction Model are shown for the median case. The breakthrough curve does not include radioactive decay.

Figure 7-3. Simulated Breakthrough Curve for a Non-Sorbing Radionuclide from a 1000-Year-Duration Source

7.3.2   SZ 1-D Transport Model Validation Results

Results of the SZ 1-D Transport Model and the SZ Site-Scale Transport Model for a non-sorbing species are shown as simulated breakthrough curves in Figure 7-4. This figure shows results for the median, fast, and slow cases of SZ transport. Note that all simulations were conducted without radioactive decay. The simulated breakthrough curves from the SZ Site-Scale Transport Model are shown with the solid and dashed lines for the three cases. The results from the SZ 1D Transport Model are shown as the open symbols superimposed on the breakthrough curves from the SZ Site-Scale Transport Model.

Visual comparison of the open symbols and the lines in Figure 7-4 indicates close agreement in the results for a non-sorbing species from the SZ 1-D Transport Model and the SZ Site-Scale Transport Model for the median case of SZ transport. There is generally close comparison in the overall shapes of the breakthrough curves from the SZ 1-D Transport Model and the SZ Site-Scale Transport Model, as indicated by the times of 10%, 50%, and 90% of mass breakthrough, with somewhat greater deviation for the upper tails of the breakthrough curves

Results of the SZ 1-D Transport Model and the SZ Site-Scale Transport Model for neptunium are shown as simulated breakthrough curves in Figure 7-5. This figure shows results for the median, fast and slow cases of SZ transport. Note that all simulations were conducted without radioactive decay. The simulated breakthrough curves from the SZ Site-Scale Transport Model are shown with the solid and dashed lines for the three cases. The results from the SZ 1-D Transport Model are shown as the open symbols superimposed on the breakthrough curves from the SZ Site-Scale Transport Model.

Visual comparison of the open symbols and the lines in Figure 7-5 indicates close agreement in the results for neptunium from the SZ 1-D Transport Model and the SZ Site-Scale Transport Model for the median case of SZ transport. The comparison is slightly less close for the fast case and slow case. There is generally close comparison in the overall shapes of the breakthrough curves from the SZ 1-D Transport Model and the SZ Site-Scale Transport Model.

NOTE: Results from the SZ Site-Scale Transport Model (BSC 2003 [162419]) are shown for the median case (solid line), fast case (short-dashed line), and slow case (long-dashed line). Results from the SZ 1-D Transport Model are shown for the median case (open circle), fast case (open square), and slow case (open triangle). Breakthrough curves do not include radioactive decay.

Figure 7-4. Simulated Breakthrough Curves Comparing the Results of the SZ 1-D Transport Model and the SZ Site-Scale Transport Model for a Non-Sorbing Radionuclide
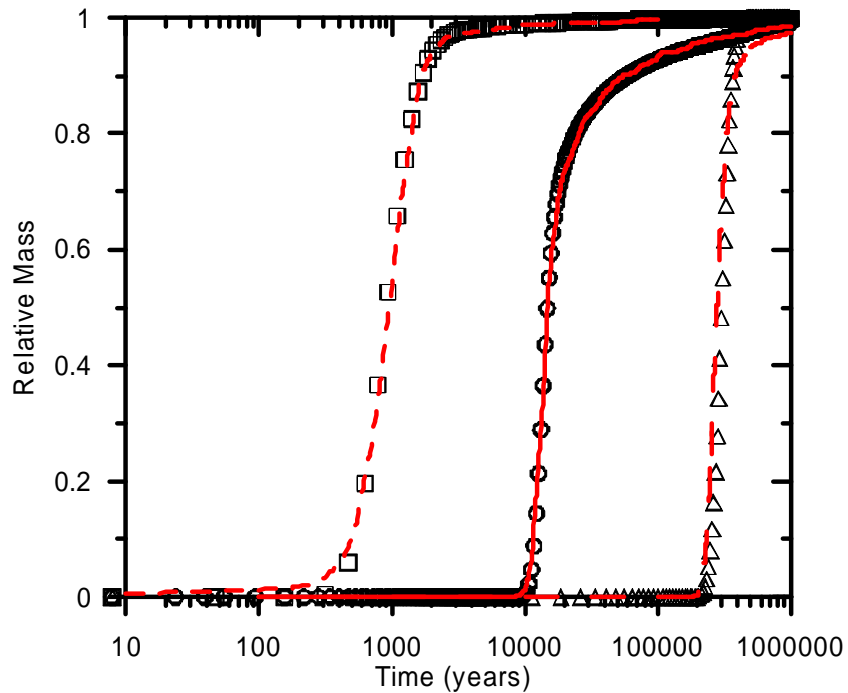
Output DTN: SN0306T0502103.005

NOTE: Results from the SZ Site-Scale Transport Model (BSC 2003 [162419]) are shown for the median case (solid line), fast case (short-dashed line), and slow case (long-dashed line). Results from the SZ 1-D Transport Model are shown for the median case (open circle), fast case (open square), and slow case (open triangle). Breakthrough curves do not include radioactive decay.

Figure 7-5. Simulated Breakthrough Curves Comparing the Results of the SZ 1-D Transport Model and the SZ Site-Scale Transport Model for Neptunium

7.4 CONCLUSIONS

7.4.1 SZ Transport Abstraction Model Validation

Validation testing of the SZ Transport Abstraction Model indicates good agreement with the SZ Site-Scale Transport Model (BSC 2003 [162419]). Acceptance criteria established for the model validation regarding the qualitative comparison of simulated breakthrough curves and the quantitative evaluation of radionuclide mass balance are met. Results of the validation testing indicate that the SZ Transport Abstraction Model is valid for the approximate range of uncertainty incorporated into the model through parameter uncertainty distributions. Results also indicate that the SZ Transport Abstraction Model is valid for both non-sorbing and sorbing radionuclide species for its intended use.

It should be noted that the SZ is more effective as a barrier for highly sorbing, short-lived radionuclides such as Sr-90 and Cs-137, relative to neptunium, as used in this validation testing. The validation testing does not demonstrate the delay afforded by the SZ in the migration of these radionuclides; nor does it demonstrate the impact of radionuclide decay. However, the importance of the SZ as a barrier to Sr-90 and Cs-137 transport, with regard to both delay and decay, is discussed in Section 6.7.

The small deviation from the SZ Site-Scale Transport Model results at early times for the fast case is a result of the time-step size used in the simulation. Such deviations in the abstraction model for realizations with very fast transport in the SZ would not be significant within the context of the TSPA analyses using this model. The discrepancy in radionuclide mass balance identified in the validation testing is a small percentage and is readily understood with regard to long-term mass retention in the SZ due to the matrix diffusion process. No future activities are needed to complete this model validation for its intended use.

7.4.2 SZ 1-D Transport Model Validation

Validation testing of the SZ 1-D Transport Model indicates acceptable agreement with the SZ Site-Scale Transport Model (BSC 2003 [162419]). Qualitative acceptance criteria regarding the comparison of the simulated breakthrough curves with the results of the SZ Site-Scale Transport Model are met. Results of the validation testing indicate that the SZ 1-D Transport Model is valid for the approximate range of uncertainty incorporated into the model through parameter uncertainty distributions. Results also indicate that the SZ 1-D Transport Model is valid for both non-sorbing and sorbing radionuclide species for its intended use.

It is relevant to consider the purpose and use of the SZ 1-D Transport Model in the evaluation of validation testing results. This model is used for the purpose of simulating radioactive decay and ingrowth for four decay chains. This simplified model is required because the SZ Transport Abstraction Model is not capable of simulating ingrowth by radioactive decay. It is not anticipated that the decay products in these decay chains would be significant contributors to total radiological dose; however, groundwater protection regulations require assessment of groundwater concentrations for some of these decay products. The results of the SZ 1-D Transport Model are used only for the decay products in these decay chains within the TSPA analyses.

It must also be considered that there are fundamental differences between the SZ 1-D Transport Model and the SZ Site-Scale Transport Model that limit the degree of consistency that can be expected between these two models. Groundwater flow and radionuclide transport simulation in the SZ Site-Scale Transport Model occur in three dimensions with a relatively complex representation of geological heterogeneity from the hydrogeologic framework model. Radionuclide transport in the SZ 1-D Transport Model is simulated in a significantly simplified representation of the SZ system consisting of three pipe segments. Each pipe segment has properties that represent the average characteristics in that area of the SZ Site-Scale Transport Model.

Considering these factors, the SZ 1-D Transport Model provides a very good approximation of simulated radionuclide transport in the three-dimensional system of the SZ. No future activities are needed to complete this model validation for its intended use.

8. CONCLUSIONS

8.1 SUMMARY OF MODELING ACTIVITY

The SZ Transport Abstraction Model and the SZ 1-D Transport Model are developed for use in the TSPA analyses. In addition, analyses of uncertainty in input parameters for these models are conducted and the results are documented as uncertainty distributions. Values of uncertain parameters are sampled for 200 realizations of the SZ flow and transport system. Simulations are conducted for these 200 realizations with the SZ Transport Abstraction Model and the results are documented.

Analyses of parameter uncertainty and multiple realizations of the SZ system using the SZ Transport Abstraction Model constitute an assessment of uncertainty in the SZ system for direct implementation in the TSPA model. The simulated radionuclide mass breakthrough curves from the SZ Transport Abstraction Model are coupled to the TSPA analyses using the convolution integral method (via the SZ_Convolute v. 3.0 software code (STN: 10207-3.0-00, SNL 2003 [164180])).

In addition, the SZ 1-D Transport Model is developed for direct implementation with the GoldSim v. 7.50.100 software code (STN: 10344-7.50.100-00, BSC 2003 [161572]) in the TSPA. The uncertain input parameters defined for the SZ Transport Abstraction Model are to be used in the SZ 1-D Transport Model for consistency between the two models when used in the probabilistic analyses of TSPA.

The SZ Transport Abstraction Model and the SZ 1-D Transport Model are validated and the results of these validation activities are documented in this report. Validation of the SZ Transport Abstraction Model indicates very close agreement with the underlying SZ Site-Scale Transport Model using the convolution integral method. Although the SZ 1-D Transport Model is significantly simplified relative to the three-dimensional SZ Transport Abstraction Model, validation of the SZ 1-D Transport Model indicates close agreement between the models for representative radionuclides over a broad range of uncertainty in SZ transport behavior.

The technical bases of FEPs included in the models are presented in this report and designed to address the parameters and components of the SZ Transport Abstraction Model and the SZ 1-D Transport Model. The role of the SZ as a natural barrier to the transport of radionuclides is assessed in relation to the results of the SZ Transport Abstraction Model. In addition, the model development and analyses presented in this AMR are related to acceptance criteria specified in the YMRP (NRC 2003 [163274]).

Information on the correlation between distribution coefficients (K_d 's) used in the sampling of uncertain parameters for the SZ Transport Abstraction Model and the SZ 1-D Transport Model is given in Table 4-3 and Table 6-8 Positive correlation between the distribution coefficient for uranium in volcanic units and alluvium is specified, based on the potentially similar hydrochemical conditions in both aquifers. Positive correlation between the distribution coefficient for neptunium in volcanic units and alluvium is specified, based on the potentially

similar hydrochemical conditions in both aquifers. Positive correlation between the distribution coefficient for plutonium in volcanic units and alluvium is specified, based on the potentially similar hydrochemical conditions in both aquifers. Positive correlation between the distribution coefficients for uranium and neptunium is specified, based on similarities in the chemical behavior of these radioelements. The technical bases for correlations between distribution coefficients (or the lack thereof) are documented in BSC 2003 [162419], Attachment I, Section I.10.

Evaluation of uncertainty in horizontal anisotropy of permeability is summarized in Section 6.5.2.10. Complete documentation of the technical basis for this evaluation of uncertainty is given in BSC 2003 [162415], Section 6.2.6. Results of this evaluation indicate that there is a greater probability of enhanced permeability in the north-south direction, but a small probability of greater permeability in the east-west direction. Implementation of uncertainty in horizontal anisotropy in the SZ Transport Abstraction Model and the SZ 1-D Transport Model is discussed in Section 6.5.3.1 and Section 6.5.1.2, respectively.

The impacts of spatial variability of parameters affecting radionuclide transport in the alluvium are incorporated in the evaluation of uncertainties in model parameters in Section 6.5.2.3, Section 6.5.2.7, Section 6.5.2.8, Section 6.5.2.9, and Section 6.5.2.11. Uncertainties in individual parameters affecting radionuclide transport, as influenced by spatial variability, are combined in the probabilistic analyses with the SZ Transport Abstraction Model. The technical bases for uncertainty in distribution coefficients are documented in BSC 2003 [162419], Attachment I.

Information on the geological uncertainty in the location of the contact between tuff and alluvium and the consequent uncertainty in the flow path lengths in the alluvium is presented in Section 6.5.2.2. This evaluation of uncertainty includes currently available information from the Nye County drilling program. Reevaluation of the uncertainty in the northern and western extent of the alluvium resulted in significant reduction in this uncertainty relative to the previous evaluation in CRWMS M&O 2000 [147972], Section 6.2.

The sensitivity analysis of matrix diffusion in the SZ Transport Abstraction Model is presented in the assessment of alternative conceptual models in Section 6.4. The results of this sensitivity analysis indicate that a minimal matrix diffusion ACM is captured within the range of uncertainty used in the SZ Transport Abstraction Model.

8.2 MODEL OUTPUTS

8.2.1   Developed Output

The technical output from this report is contained in four DTNs that are summarized in Table 8-1.

Table 8-1. Summary of Developed Output

Output DTN	Description
SN0310T0502103.009	Uncertainty distributions for parameters used in the SZ Transport Abstraction Model. Sampling output of uncertain parameters for 200 realizations is also included (see Attachment I). This DTN also includes a description of each uncertain parameter.
SN0310T0502103.010	Input and output files for the SZ Transport Abstraction Model. This DTN also contains the output breakthrough curves for use in the TSPA analyses.
SN0306T0502103.005	Input and output files for the SZ 1-D Transport Model.
SN0306T0502103.006	Data spreadsheets to support data uncertainty development.
SN0310T0502103.012	Input and output files for the SZ Transport Abstraction Model for the fast fraction of radionuclides irreversibly attached to colloids. This DTN also contains the output breakthrough curves for use in the TSPA analyses.
MO0310SPANGRAC.000	Results of the background gross alpha concentration analysis

Results of the parameter uncertainty analyses from this AMR are contained in DTN: SN0310T0502103.009. These results include the uncertainty distributions for parameters that were developed in this analysis or incorporated from other analyses and the input file for the GoldSim v. 7.50.100 software code (STN: 10344-7.50.100-00) for sampling 200 realizations from these uncertainty distributions. This DTN also contains the output file from the GoldSim v. 7.50.100 software code (STN: 10344-7.50.100-00) containing the parameter vectors to be used in the SZ Transport Abstraction Model.

Results of the SZ Transport Abstraction Model from this AMR are contained in DTN: SN0310T0502103.010. These results consist of the input and output files from the FEHM v. 2.20 software code (STN: 10086-2.20-00), the SZ_Pre v. 2.0 software code (STN: 10914-2.0-00), and the SZ_Post v. 3.0 software code (STN: 10915-3.0-00) used in the analyses. The results that form a direct input to the TSPA model are the files containing the breakthrough curves from the SZ Transport Abstraction Model for the 200 realizations of radionuclide transport. The breakthrough curves for use in the TSPA model (i.e., the breakthrough curves at the regulatory boundary of the accessible environment) are defined by the first column (time) and the third column (relative mass) in the output files.

The input and output files for the SZ 1-D Transport Model are contained in DTN: SN0306T0502103.005. The input file of the SZ 1-D Transport Model for the GoldSim v. 7.50.100 software code (STN: 10344-7.50.100-00, BSC 2003 [161572]) is intended for incorporation into the TSPA model.

The data spreadsheets contained in DTN: SN0306T0502103.006 contain the data used and support the analyses of parameter uncertainty summarized in this report and in DTN: SN0310T0502103.009. The spreadsheets mentioned by filename in this report are contained in DTN: SN0306T0502103.006.

Results of the SZ Transport Abstraction Model for the fast fraction of radionuclides irreversibly attached to colloids from this AMR are contained in DTN: SN0310T0502103.012. These results consist of the input and output files from the FEHM v. 2.20 software code (STN: 10086-2.20-00), the SZ_Pre v. 2.0 software code (STN: 10914-2.0-00), and the SZ_Post v. 3.0 software code (STN: 10915-3.0-00) used in the analyses. The results that form a direct input to the TSPA model are the files containing the breakthrough curves from the SZ Transport Abstraction Model for the 200 realizations of radionuclide transport. The breakthrough curves for use in the TSPA model (i.e., the breakthrough curves at the regulatory boundary of the accessible environment) are defined by the first column (time) and the third column (relative mass) in the output files.

The results of the background gross alpha concentration analysis (as documented in Section 6.8) are contained in DTN: MO0310SPANGRAC.000.

8.2.2 Output Uncertainties and Limitations

The assessment of uncertainty in model parameters and model outputs is an integral part of the analyses performed in this AMR. Uncertainty in model parameters is quantitatively represented with the statistical distributions developed and contained in DTN: SN0310T0502103.009. Uncertainty in radionuclide transport in the SZ Transport Abstraction Model is embodied in the breakthrough curves for the 200 realizations contained in DTN: SN0310T0502103.010. The SZ 1-D Transport Model is intended for direct incorporation into the TSPA Model, with which uncertainty will be assessed using Monte Carlo probabilistic analyses.

All relevant uncertainties in data and model parameters, as they affect groundwater flow and radionuclide transport, have been included in the SZ Transport Abstraction Model and the SZ 1-D Transport Model. Uncertainties have been propagated through the results of the SZ Transport Abstraction Model (i.e., the radionuclide breakthrough curves for multiple realizations) documented in this report. These output uncertainties meet the YMRP (NRC 2003 [163274]) acceptance criterion 3 for the propagation of data uncertainty through model abstraction for flow paths in the saturated zone and for radionuclide transport in the saturated zone.

Use of the SZ Transport Abstraction Model and the SZ 1-D Transport Model is subject to the limitations and restrictions imposed by the assumptions listed in Sections 5, 6.3, and 6.5 of this model report. Limitations in knowledge of specific parameter values are addressed in the analysis of parameter uncertainties in this report. The radionuclide breakthrough curves generated for the SZ Transport Abstraction model are limited to 100,000 years duration for present climatic conditions. This limits the time period that can be simulated with the TSPA

model using these breakthrough curves for the SZ. Because the SZ breakthrough curves are scaled for higher groundwater flow rates under future climatic conditions, the time period that can be simulated with the TSPA model would be significantly less than 100,000 years. If the glacial-transition climate state is applied for most of simulation period in the TSPA model, the SZ breakthrough curves would be scaled by a factor of approximately 4, limiting the TSPA model simulation time to about 25,000 years.

9. INPUTS AND REFERENCES

9.1 DOCUMENTS CITED

Altman, W.D.; Donnelly, J.P.; and Kennedy, J.E. 1988. *Qualification of Existing Data for High-Level Nuclear Waste Repositories: Generic Technical Position.* NUREG-1298. Washington, D.C.: U.S. Nuclear Regulatory Commission. TIC: 200652. [103750]

Altman, W.D.; Donnelly, J.P.; and Kennedy, J.E. 1988. *Peer Review for High-Level Nuclear Waste Repositories: Generic Technical Position.* NUREG-1297. Washington, D.C.: U.S. Nuclear Regulatory Commission. TIC: 200651. [103597]

Arnold, B.W.; Kuzio, S.P.; and Robinson, B.A. 2003. "Radionuclide Transport Simulation and Uncertainty Analyses with the Saturated-Zone Site-Scale Model at Yucca Mountain, Nevada." *Journal of Contaminant Hydrology, 62-63,* 401-419. New York, New York: Elsevier. TIC: 254205. [163857]

Bear, J. 1972. *Dynamics of Fluids in Porous Media.* Environmental Science Series. Biswas, A.K., ed. New York, New York: Elsevier. TIC: 217356. [156269]

Bedinger, M.S.; Sargent, K.A.; Langer, W.H.; Sherman, F.B.; Reed, J.E.; and Brady, B.T. 1989. *Studies of Geology and Hydrology in the Basin and Range Province, Southwestern United States, for Isolation of High-Level Radioactive Waste—Basis of Characterization and Evaluation.* U.S. Geological Survey Professional Paper 1370-A. Washington, D.C.: U.S. Government Printing Office. ACC: NNA.19910524.0125. [129676]

Bower, K.M.; Gable, C.W.; and Zyvoloski, G.A. 2000. *Effect of Grid Resolution on Control Volume Finite Element Groundwater Modeling of Realistic Geology.* LA-UR-001870. [Los Alamos, New Mexico: Los Alamos National Laboratory]. TIC: 248256. [149161]

BSC (Bechtel SAIC Company) 2001. *Data Qualification Report: Calculated Porosity and Porosity-Derived Values for Lithostratigraphic Units for Use on the Yucca Mountain Project.* TDR-NBS-GS-000020 REV 00. Las Vegas, Nevada: Bechtel SAIC Company. ACC: MOL.20010531.0193. [163479]

BSC (Bechtel SAIC Company) 2001. *Data Qualification Report: Matrix Hydrologic Properties and Alcove 1 Infiltration Rate Data for Use on the Yucca Mountain Project.* TDR-NBS-HS-000014 REV 00. Las Vegas, Nevada: Bechtel SAIC Company. ACC: MOL.20010924.0268. [163566]

BSC (Bechtel SAIC Company) 2001. *FY 01 Supplemental Science and Performance Analyses, Volume 1: Scientific Bases and Analyses.* TDR-MGR-MD-000007 REV 00 ICN 01. Las Vegas, Nevada: Bechtel SAIC Company. ACC: MOL.20010801.0404; MOL.20010712.0062; MOL.20010815.0001. [155950]

BSC (Bechtel SAIC Company) 2001. *Probability Distribution for Flowing Interval Spacing.* ANL-NBS-MD-000003 REV 00 ICN 02. Las Vegas, Nevada: Bechtel SAIC Company. ACC: MOL.20010625.0304. [156965]

BSC (Bechtel SAIC Company) 2002. *Guidelines for Developing and Documenting Alternative Conceptual Models, Model Abstractions, and Parameter Uncertainty in the Total System Performance Assessment for the License Application.* TDR-WIS-PA-000008 REV 00, ICN 01. Las Vegas, Nevada: Bechtel SAIC Company. ACC: MOL.20020904.0002. [158794]

BSC (Bechtel SAIC Company) 2002. *Rock Properties Model Analysis Model Report.* MDL-NBS-GS-000004 REV 00 ICN 03. Las Vegas, Nevada: Bechtel SAIC Company. ACC: MOL.20020429.0086. [159530]

BSC (Bechtel SAIC Company) 2002. *Scientific Processes Guidelines Manual.* MIS-WIS-MD-000001 REV 01. Las Vegas, Nevada: Bechtel SAIC Company. ACC: MOL.20020923.0176. [160313]

BSC (Bechtel SAIC Company) 2002. *The Enhanced Plan for Features, Events, and Processes (FEPs) at Yucca Mountain.* TDR-WIS-PA-000005 REV 00. Las Vegas, Nevada: Bechtel SAIC Company. ACC: MOL.20020417.0385. [158966]

BSC (Bechtel SAIC Company) 2002. *Validation Test Report, GoldSim Version 7.50.100.* SDN: 10344-VTR-7.50.100-00. Las Vegas, Nevada: BSC (Bechtel SAIC Company). ACC: MOL.20030312.0227. [163962]

BSC (Bechtel SAIC Company) 2003. *Analysis of Hydrologic Properties Data.* MDL-NBS-HS-000014 REV 00. Las Vegas, Nevada: Bechtel SAIC Company. ACC: DOC.20030404.0004. [161773]

BSC (Bechtel SAIC Company) 2003. *Features, Events, and Processes in SZ Flow and Transport.* ANL-NBS-MD-000002 REV 02A. Las Vegas, Nevada: Bechtel SAIC Company. ACC: MOL.20030823.0129. [163128]

BSC (Bechtel SAIC Company) 2003. *Q-List.* TDR-MGR-RL-000005 REV 00. Las Vegas, Nevada: Bechtel SAIC Company. ACC: DOC.20030930.0002. [165179]

BSC (Bechtel SAIC Company) 2003. *Repository Design, Repository/PA IED Subsurface Facilities.* 800-IED-EBS0-00401-000-00C. Las Vegas, Nevada: Bechtel SAIC Company. ACC: ENG.20030303.0002. [162289]

BSC (Bechtel SAIC Company) 2003. *Repository Design, Repository/PA IED Subsurface Facilities.* 800-IED-EBS0-00402-000-00B. Las Vegas, Nevada: Bechtel SAIC Company. ACC: MOL.20030109.0146. [161727]

BSC (Bechtel SAIC Company) 2003. *Saturated Zone Colloid Transport.* ANL-NBS-HS-000031 REV 01. Las Vegas, Nevada: Bechtel SAIC Company. ACC: DOC.20030916.0008. [162729]

BSC (Bechtel SAIC Company) 2003. *Saturated Zone In-Situ Testing.* ANL-NBS-HS-000039 REV 00A. Las Vegas, Nevada: Bechtel SAIC Company. ACC: MOL.20030602.0291. [162415]

BSC (Bechtel SAIC Company) 2003. *Site-Scale Saturated Zone Flow Model.* MDL-NBS-HS-000011 REV 01A. Las Vegas, Nevada: Bechtel SAIC Company. ACC: MOL.20030626.0296. TBV-5203 [162649]

BSC (Bechtel SAIC Company) 2003. *Site-Scale Saturated Zone Transport.* MDL-NBS-HS-000010 REV 01A. Las Vegas, Nevada: Bechtel SAIC Company. ACC: MOL.20030626.0180. [162419]

BSC (Bechtel SAIC Company) 2003. *SZ Flow and Transport Model Abstraction.* MDL-NBS-HS-000021 REV 00. Las Vegas, Nevada: Bechtel SAIC Company. ACC: DOC.20030818.0007. [164870]

BSC (Bechtel SAIC Company) 2003. *UZ Flow Models and Submodels.* MDL-NBS-HS-000006 REV 01. Las Vegas, Nevada: Bechtel SAIC Company. ACC: DOC.20030818.0002. [163045]

BSC (Bechtel SAIC Company) 2003. *Validation Test Report, SZ_Convolute Version 2.2.* SDN: 10207-VTR-2.2-00. Las Vegas, Nevada: Bechtel SAIC Company. ACC: MOL.20021202.0341. [163587]

BSC (Bechtel SAIC Company) 2003. *Waste Form and In-Drift Colloids-Associated Radionuclide Concentrations: Abstraction and Summary.* MDL-EBS-PA-000004 REV 00. Las Vegas, Nevada: Bechtel SAIC Company. ACC: DOC.20030626.0006. [161620]

BSC (Bechtel SAIC Company) 2003. *Work Plan for: Saturated Zone Flow and Transport Modeling and Testing.* TWP-NBS-MD-000002 REV 01/ICN 01. Las Vegas, Nevada: Bechtel SAIC Company. ACC: MOL. [166034]

Buchholtz ten Brink, M.; Phinney, D.L.; and Smith, D.K. 1991. "Actinide Transport in Topopah Spring Tuff: Pore Size, Particle Size and Diffusion." *Scientific Basis for Nuclear Waste Management XIV, Symposium held November 26-29, 1990, Boston, Massachusetts.* Abrajano, T.A., Jr. and Johnson, L.H., eds. *212,* 641-648. Pittsburgh, Pennsylvania: Materials Research Society. TIC: 203656. [162954]

Buesch, D.C.; Spengler, R.W.; Moyer, T.C.; and Geslin, J.K. 1996. *Proposed Stratigraphic Nomenclature and Macroscopic Identification of Lithostratigraphic Units of the Paintbrush Group Exposed at Yucca Mountain, Nevada.* Open-File Report 94-469. Denver, Colorado: U.S. Geological Survey. ACC: MOL.19970205.0061. [100106]

Burbey, T.J. and Wheatcraft, S.W. 1986. *Tritium and Chlorine-36 Migration from a Nuclear Explosion Cavity.* DOE/NV/10384-09. Reno, Nevada: University of Nevada, Desert Research Institute, Water Resources Center. TIC: 201927. [129679]

Callahan, T.J.; Reimus, P.W.; Bowman, R.S.; and Haga, M.J. 2000. "Using Multiple Experimental Methods to Determine Fracture/Matrix Interactions and Dispersion of Nonreactive Solutes in Saturated Volcanic Tuff." *Water Resources Research, 36,* (12), 3547-3558. [Washington, D.C.]: American Geophysical Union. TIC: 250760. [156648]

Canori, G.F. and Leitner, M.M. 2003. *Project Requirements Document.* TER-MGR-MD-000001 REV 01. Las Vegas, Nevada: Bechtel SAIC Company. ACC: DOC.20030404.0003. [161770]

Coen, K. 1987. "Policy Review." Memorandum from K. Coen (LANL) to D. Norton, January 26, 1987, TWS-INC7-1/87-10, with attachment. ACC: NNA.19900112.0339; MOL.19980625.0239. [162960]

Cooper, H.H., Jr. and Jacob, C.E. 1946. "A Generalized Graphical Method for Evaluating Formation Constants and Summarizing Well-Field History." *Transactions, American Geophysical Union, 27,* (IV), 526-534. Washington, D.C.: American Geophysical Union. TIC: 225279. [150245]

CRWMS M&O 1997. *Report of Results of Hydraulic and Tracer Tests at the C-Holes Complex.* Deliverable SP23APM3. Las Vegas, Nevada: CRWMS M&O. ACC: MOL.19971024.0074. [100328]

CRWMS M&O 1997. *The Site-Scale Unsaturated Zone Transport Model of Yucca Mountain.* Milestone SP25BM3, Rev. 1. Las Vegas, Nevada: CRWMS M&O. ACC: MOL.19980224.0314. [124052]

CRWMS M&O 1997. *Yucca Mountain Site Characterization Project Radiological Programs White Paper: Radioactivity in Groundwater in the Vicinity of Yucca Mountain.* Las Vegas, Nevada: CRWMS M&O. ACC: MOL.19971215.0904. [147759]

CRWMS M&O 1998. "Saturated Zone Flow and Transport." Chapter 8 of *Total System Performance Assessment-Viability Assessment (TSPA-VA) Analyses Technical Basis Document.* B00000000-01717-4301-00008 REV 01. Las Vegas, Nevada: CRWMS M&O. ACC: MOL.19981008.0008. [100365

CRWMS M&O 1998. *Saturated Zone Flow and Transport Expert Elicitation Project.* Deliverable SL5X4AM3. Las Vegas, Nevada: CRWMS M&O. ACC: MOL.19980825.0008. [100353]

CRWMS M&O 1998. *Yucca Mountain Site Characterization Project Radiological Programs, Radioactivity in FY 1997 Groundwater Samples from Wells and Springs Near Yucca Mountain.* Rev. 00. Las Vegas, Nevada: CRWMS M&O. ACC: MOL.19990218.0213. [104963]

CRWMS M&O 1999. *Radioactivity in FY 1998 Groundwater Samples from Wells and Springs Near Yucca Mountain.* BA0000000-01717-5705-00029 REV 00. Las Vegas, Nevada: CRWMS M&O. ACC: MOL.19990622.0219. [150420]

CRWMS M&O 2000. *Modeling Sub Gridblock Scale Dispersion in Three-Dimensional Heterogeneous Fractured Media (S0015).* ANL-NBS-HS-000022 REV 00 ICN 01. Las Vegas, Nevada: CRWMS M&O. ACC: MOL.20001107.0376 [152259]

CRWMS M&O 2000. *Total System Performance Assessment for the Site Recommendation.* TDR-WIS-PA-000001 REV 00 ICN 01. Las Vegas, Nevada: CRWMS M&O. ACC: MOL.20001220.0045. [153246]

CRWMS M&O 2000. *Uncertainty Distribution for Stochastic Parameters.* ANL-NBS-MD-000011 REV 00. Las Vegas, Nevada: CRWMS M&O. ACC: MOL.20000526.0328. [147972]

CRWMS M&O 2000. *Unsaturated Zone and Saturated Zone Transport Properties (U0100).* ANL-NBS-HS-000019 REV 00. Las Vegas, Nevada: CRWMS M&O. ACC: MOL.20000829.0006. [152773]

CRWMS M&O 2001. *Features, Events, and Processes in SZ Flow and Transport.* ANL-NBS-MD-000002 REV 01. Las Vegas, Nevada: CRWMS M&O. ACC: MOL.20010214.0230. [153931]

D'Agnese, F.A.; O'Brien, G.M.; Faunt, C.C.; and San Juan, C.A. 1999. *Simulated Effects of Climate Change on the Death Valley Regional Ground-Water Flow System, Nevada and California.* Water-Resources Investigations Report 98-4041. Denver, Colorado: U.S. Geological Survey. TIC: 243555. [120425]

DOE (U.S. Department of Energy) 1997. *Regional Groundwater Flow and Tritium Transport Modeling and Risk Assessment of the Underground Test Area, Nevada Test Site, Nevada.* DOE/NV-477. Las Vegas, Nevada: U.S. Department of Energy. ACC: MOL.20010731.0303. [103021]

Domenico, P.A. and Schwartz, F.W. 1990. *Physical and Chemical Hydrogeology.* New York, New York: John Wiley & Sons. TIC: 234782. [100569]

EDCON. 2000. *Report for the Borehole Gravity Survey in the NC-EWDP-19D Well in Nye County, Nevada on Behalf of TRW Corp.* EDCON Job# 00011. Denver, Colorado: EDCON. TIC: 249823. [154704]

Eddebbarh, A.A.; Zyvoloski, G.A.; Robinson, B.A.; Kwicklis, E.M.; Reimus, P.W.; Arnold, B.W.; Corbet, T.; Kuzio, S.P.; and Faunt, C. 2003. "The Saturated Zone at Yucca Mountain: An Overview of the Characterization and Assessment of the Saturated Zone as a Barrier to Potential Radionuclide Migration." *Journal of Contaminant Hydrology, 62-63,* 477-493. New York, New York: Elsevier. TIC: 254205. [163577]

Ferrill, D.A.; Winterle, J.; Wittmeyer, G.; Sims, D.; Colton, S.; Armstrong, A.; and Morris, A.P. 1999. "Stressed Rock Strains Groundwater at Yucca Mountain, Nevada." *GSA Today, 9,* (5), 1-8. Boulder, Colorado: Geological Society of America. TIC: 246229. [118941]

Flint, L.E. 1998. *Characterization of Hydrogeologic Units Using Matrix Properties, Yucca Mountain, Nevada.* Water-Resources Investigations Report 97-4243. Denver, Colorado: U.S. Geological Survey. ACC: MOL.19980429.0512. [100033]

Freeze, G.A.; Brodsky, N.S.; and Swift, P.N. 2001. *The Development of Information Catalogued in REV00 of the YMP FEP Database.* TDR-WIS-MD-000003 REV 00 ICN 01. Las Vegas, Nevada: Bechtel SAIC Company. ACC: MOL.20010301.0237. [154365]

Freeze, R.A. and Cherry, J.A. 1979. *Groundwater.* Englewood Cliffs, New Jersey: Prentice-Hall. TIC: 217571. [101173]

Gelhar, L.W. 1986. "Stochastic Subsurface Hydrology from Theory to Applications." *Water Resources Research, 22,* (9), 135S-145S. Washington, D.C.: American Geophysical Union. TIC: 240749. [101131]

Hillel, D. 1980. *Fundamentals of Soil Physics.* New York, New York: Academic Press. TIC: 215655. [101134]

Howard, N.W. 1985. *Variation in Properties of Nuclear Test Areas and Media at the Nevada Test Site.* UCRL-53721. Livermore, California: Lawrence Livermore National Laboratory. TIC: 229690. [153266]

Jury, W.A.; Sposito, G.; and White, R.E. 1986. "A Transfer Function Model of Solute Transport Through Soil. 1. Fundamental Concepts." *Water Resources Research, 22,* (2), 243-247. [Washington, D.C.]: American Geophysical Union. TIC: 254552. [164314]

Knoll, G.F. 1989. *Radiation Detection and Measurement.* 2nd Edition. New York, New York: John Wiley & Sons. TIC: 233703. [161052]

Kotra, J.P.; Lee, M.P.; Eisenberg, N.A.; and DeWispelare, A.R. 1996. *Branch Technical Position on the Use of Expert Elicitation in the High-Level Radioactive Waste Program.* NUREG-1563. Washington, D.C.: U.S. Nuclear Regulatory Commission. TIC: 226832. [100909]

Kreft, A. and Zuber, A. 1978. "On the Physical Meaning of the Dispersion Equation and Its Solutions for Different Initial and Boundary Conditions." *Chemical Engineering Science, 33,* (11), 1471-1480. New York, New York: Pergamon Press. TIC: 245365. [107306]

Li, Y-H. and Gregory, S. 1974. "Diffusion of Ions in Sea Water and Deep-Sea Sediments." *Geochimica et Cosmochimica Acta, 38,* (5), 703-714. New York, New York: Pergamon Press. TIC: 246823. [129827]

Luckey, R.R.; Tucci, P.; Faunt, C.C.; Ervin, E.M.; Steinkampf, W.C.; D'Agnese, F.A.; and Patterson, G.L. 1996. *Status of Understanding of the Saturated-Zone Ground-Water Flow System at Yucca Mountain, Nevada, as of 1995.* Water-Resources Investigations Report 96-4077. Denver, Colorado: U.S. Geological Survey. ACC: MOL.19970513.0209. [100465]

Manger, G.E. 1963. *Porosity and Bulk Density of Sedimentary Rocks.* Geological Survey Bulletin 1144-E. Washington, D.C.: U.S. Government Printing Office. TIC: 249699. [154474]

McKenna, S.A.; Walker, D.D.; and Arnold, B. 2003. "Modeling Dispersion in Three-Dimensional Heterogeneous Fractured Media at Yucca Mountain." *Journal of Contaminant Hydrology, 62-63,* 577-594. New York, New York: Elsevier. TIC: 254205. [163578]

Miller, I. and Kossik, R. 1998. *Repository Integration Program RIP Integrated Probabilistic Simulator for Environmental Systems Theory Manual and User's Guide.* Redmond, Washington: Golder Associates. ACC: MOL.19980526.0374. [100449]

Moyer, T.C. and Geslin, J.K. 1995. *Lithostratigraphy of the Calico Hills Formation and Prow Pass Tuff (Crater Flat Group) at Yucca Mountain, Nevada.* Open-File Report 94-460. Denver, Colorado: U.S. Geological Survey. ACC: MOL.19941208.0003. [101269]

Newman, J. 1973. *Electrochemical Systems.* Englewood Cliffs, New Jersey: Prentice-Hall. TIC: 210201. [148719]

NRC (U.S. Nuclear Regulatory Commission) 2003. *Yucca Mountain Review Plan, Final Report.* NUREG-1804, Rev. 2. Washington, D.C.: U.S. Nuclear Regulatory Commission, Office of Nuclear Material Safety and Safeguards. TIC: 254568. [163274]

Reimus, Paul W.; M. J. Haga; A. I. Adams; T. J. Callahan; H.J. Turin; and D. A. Counce 2003. "Testing and Parameterizing a Conceptual Solute Transport Model in Saturated Fractured Tuffs Using Sorbing and Nonsorbing Tracers in Cross-Hole Tracer Tests." *Journal of Contaminant Hydrology, 62-63,* (April - May 2003), 613-636. New York, New York: Elsevier. [162950]

Reimus, P.W.; Haga, M.J.; Humphrey, A.R.; Counce, D.A.; Callahan, T.J.; and Ware, S.D. 2002. *Diffusion Cell and Fracture Transport Experiments to Support Interpretations of the BULLION Forced-Gradient Experiment.* LA-UR-02-6884. [Los Alamos, New Mexico]: Los Alamos National Laboratory. TIC: 253859. [162956]

Reimus, P.W.; Ware, S.D.; Benedict, F.C.; Warren, R.G.; Humphrey, A.; Adams, A.; Wilson, B.; and Gonzales, D. 2002. *Diffusive and Advective Transport of {superscript 3}H, {superscript 14}C, and {superscript 99}Tc in Saturated, Fractured Volcanic Rocks from Pahute Mesa, Nevada.* LA-13891-MS. Los Alamos, New Mexico: Los Alamos National Laboratory. TIC: 253905. [163008]

Rundberg, R.S.; Partom, I.; Ott, M.A.; Mitchell, A.J.; and Birdsell, K. 1987. *Diffusion of Nonsorbing Tracers in Yucca Mountain Tuff.* Milestone R524. Los Alamos, New Mexico: Los Alamos National Laboratory. ACC: NNA.19930405.0074. [106481]

Sandia National Laboratories 2003. *SZ_Convolute.* V 3.0-00. PC. 10207-3.0-00. [164180]

Simpson, J.H and Carr, H.Y. 1958. "Diffusion and Nuclear Spin Relaxation in Water." *The Physical Review, Second Series, 111,* (5), 1201-1202. New York, New York: American Physical Society. TIC: 246907. [139449]

Skagius, K. and Neretnieks, I. 1986. "Porosities and Diffusivities of Some Nonsorbing Species in Crystalline Rocks." *Water Resources Research, 22,* (3), 389-398. [Washington, D.C.]: American Geophysical Union. TIC: 225291. [156862]

Sudicky, E.A. and Frind, E.O. 1982. "Contaminant Transport in Fractured Porous Media: Analytical Solutions for a System of Parallel Fractures." *Water Resources Research, 18,* (6), 1634-1642. Washington, D.C.: American Geophysical Union. TIC: 217475. [105043]

Townsend, Y.E. and Grossman, R.F., eds. 2001. *Nevada Test Site Annual Site Environmental Report for Calendar Year 2000.* DOE/NV/11718-605. Las Vegas, Nevada: U.S. Department of Energy, Nevada Operations Office. TIC: 251545. [156604]

Triay, I.R.; Birdsell, K.H.; Mitchell, A.J.; and Ott, M.A. 1993. "Diffusion of Sorbing and Non-Sorbing Radionuclides." *High Level Radioactive Waste Management, Proceedings of the Fourth Annual International Conference, Las Vegas, Nevada, April 26-30, 1993. 2,* 1527-1532. La Grange Park, Illinois: American Nuclear Society. TIC: 208542. [145123]

USGS (U.S. Geological Survey) 2001. *Hydrogeologic Framework Model for the Saturated-Zone Site-Scale Flow and Transport Model.* ANL-NBS-HS-000033 REV 00 ICN 02. Denver, Colorado: U.S. Geological Survey. ACC: MOL.20011112.0070. [158608]

USGS (U.S. Geological Survey) 2001. *Water-Level Data Analysis for the Saturated Zone Site-Scale Flow and Transport Model.* ANL-NBS-HS-000034 REV 01. Denver, Colorado: U.S. Geological Survey. ACC: MOL.20020209.0058. [157611]

USGS (U.S. Geological Survey) n.d. Bulk Density. [Denver, Colorado: U.S. Geological Survey]. ACC: NNA.19940406.0076. [154495]

Viswanath, D.S. and Natarajan, G. 1989. *Data Book on the Viscosity of Liquids.* 714-715. New York, New York: Hemisphere Publishing Corporation. TIC: 247513. [129867]

Wilson, M.L.; Gauthier, J.H.; Barnard, R.W.; Barr, G.E.; Dockery, H.A.; Dunn, E.; Eaton, R.R.; Guerin, D.C.; Lu, N.; Martinez, M.J.; Nilson, R.; Rautman, C.A.; Robey, T.H.; Ross, B.; Ryder, E.E.; Schenker, A.R.; Shannon, S.A.; Skinner, L.H.; Halsey, W.G.; Gansemer, J.D.; Lewis, L.C.; Lamont, A.D.; Triay, I.R.; Meijer, A.; and Morris, D.E. 1994. *Total-System Performance Assessment for Yucca Mountain – SNL Second Iteration (TSPA-1993).* SAND93-2675. Executive Summary and two volumes. Albuquerque, New Mexico: Sandia National Laboratories. ACC: NNA.19940112.0123. [100191]

Zyvoloski, G.; Kwicklis, E.; Eddebbarh, A.A.; Arnold, B.; Faunt, C.; and Robinson, B.A. 2003. "The Site-Scale Saturated Zone Flow Model for Yucca Mountain: Calibration of Different Conceptual Models and their Impact on Flow Paths." *Journal of Contaminant Hydrology, 62-63,* 731-750. [New York, New York]: Elsevier. TIC: 254340. [163341]

Zyvoloski, G.A.; Robinson, B.A.; Dash, Z.V.; and Trease, L.L. 1997. *Summary of the Models and Methods for the FEHM Application—A Finite-Element Heat- and Mass-Transfer Code.* LA-13307-MS. [Los Alamos, New Mexico]: Los Alamos National Laboratory. TIC: 235587. [110491]

9.2   CODES, STANDARDS, REGULATIONS, AND PROCEDURES

10 CFR 63. Energy: Disposal of High-Level Radioactive Wastes in a Geologic Repository at Yucca Mountain, Nevada.   Readily available. [156605]

AP-2.22Q, Rev. 1, ICN 0. *Classification Analyses and Maintenance of the Q-List.* Washington, D.C.: U.S. Department of Energy, Office of Civilian Radioactive Waste Management. ACC: DOC.20030807.0002. [164786]

AP-AC.1Q, Rev. 0, ICN 0. *Expert Elicitation.* Washington, D.C.: U.S. Department of Energy, Office of Civilian Radioactive Waste Management. ACC: MOL.19991019.0014. [138711]

AP-SI.1Q, Rev. 5, ICN 0. *Software Management.* Washington, D.C.: U.S. Department of Energy, Office of Civilian Radioactive Waste Management. ACC: DOC.20030422.0012. [163085]

AP-SIII.10Q, Rev. 2, ICN 0. *Models.* Washington, D.C.: U.S. Department of Energy, Office of Civilian Radioactive Waste Management. ACC: DOC.20030929.0003. [165553]

9.3 SOFTWARE

BSC (Bechtel SAIC Company) 2003. *Software Code: GoldSim.* 7.50.100. PC. 10344-7.50.100-00. [161572]

LANL (Los Alamos National Laboratory) 2001. *Software Code: CORPSCON.* V5.11.08. 10547-5.11.08-00. [155082]

LANL (Los Alamos National Laboratory) 2003. *Software Code: FEHM.* V2.20. SUN, PC. 10086-2.20-00. [161725]

Sandia National Laboratories (SNL) 2003. *Software Code: SZ_Convolute.* V2.2. PC, Windows 2000. 10207-2.2-00. [163344]

SNL (Sandia National Laboratories) 2003. *Software Code: SZ_Convolute.* V3.0. PC, Windows 2000. 10207-3.0-00. [164180]

Sandia National Laboratories (SNL) 2003. *Software Code: SZ_Post.* V3.0. Sun, SunO.S. 5.7. 10915-3.0-00. [163571]

Sandia National Laboratories (SNL) 2003. *Software Code: SZ_Pre.* V2.0. Sun, Solaris 7. 10914-2.0-00. [163281]

9.4   SOURCE DATA, LISTED BY DATA TRACKING NUMBER

GS010908312332.002. Borehole Data from Water-Level Data Analsis for the Saturated Zone Site-Scale Flow and Transport Model. Submittal date: 10/02/2001. [163555]

GS031008312315.002. TRANSPORT PARAMETERS FROM ANALYSIS OF CONSERVATIVE (NON-SORBING) TRACER TESTS CONDUCTED IN THE FRACTURED TUFF AT THE C-HOLE COMPLEX FROM 1996 TO 1999. Submittal date: 10/09/2003. [166261]

GS030108314211.001. Interpretation of the Lithostratigraphy in Deep Boreholes NC-EWDP-18P, NC-EWDP-22SA, NC-EWDP-10SA, NC-EWDP-23P, NC-EWDP-19IM1A, and NC EWDP-19IM2A, Nye County Early Warning Drilling Program, Phase III. Submittal date: 02/11/2003. [163483]

LA0002JC831341.001. Depth Intervals and Bulk Densities of Alluviums. Submittal date: 03/08/2000. [147081]

LA0302RP831228.001. Type Curve Data for FEHM Macro "SPTR" Based on Sudicky and Frind Solution. Submittal date: 02/11/2003. [163557]

LA0303HV831352.002. Colloid Retardation Factors for the Saturated Zone Fractured Volcanics. Submittal date: 03/31/2003. [163558]

LA0303HV831352.004. Colloid Retardation Factors for the Saturated Zone Alluvium. Submittal date: 03/31/2003. [163559]

LA0303PR831231.002. Estimation of Groundwater Drift Velocity from Tracer Responses in Single-Well Tracer Tests at Alluvium Testing Complex. Submittal date: 03/18/2003. [163561]

LA0303PR831231.005. SIMPLE CALCULATIONS FOR SZ IN-SITU TESTING AMR. Submittal date: 03/19/2003. [166259]

LA0306SK831231.001. SZ Site-Scale Transport Model, FEHM Files for Base Case. Submittal date: 06/25/2003. [164362]

LA0310AM831341.002. Saturated Zone Distribution Coefficients (KDS) for U, NP, PU, CS, AM, PA, SR, TH, RA, C, TC, AND I.. Submittal date: 10/21/03. [165891]

LB03023DSSCP9I.001. 3-D Site Scale UZ Flow Field Simulations for 9 Infiltration Scenarios. Submittal date: 02/28/2003. [163044]

MO0003SZFWTEEP.000. Data Resulting from the Saturated Zone Flow and Transport Expert Elicitation Project. Submittal date: 03/06/2000. [148744]

MO0010CPORGLOG.002. Calculated Porosity from Geophysical Logs Data from "Old 40" Boreholes. Submittal date: 10/16/2000. [155229]

MO0105GPLOG19D.000. Geophysical Log Data from Borehole NC EWDP 19D. Submittal date: 05/31/2001. [163480]

MO0105HCONEPOR.000. Hydraulic Conductivity and Effective Porosity for the Basin and Range Province, Southwestern United States. Submittal date: 05/02/2001. [155044]

MO0109HYMXPROP.001. Matrix Hydrologic Properties Data. Submittal date: 09/17/2001. [155989]

MO9904RWSJJS98.000. RADIOANALYTICAL WATER DATA FOR SAMPLES COLLECTED IN JUNE, JULY, AND SEPTEMBER 1998.. Submittal date: 04/08/1999. [165866]

SN0004T0501399.002. Correlation of RH (Relative Humidity) Porosity and Bulk Density. Submittal date: 04/13/2000. [155046]

SN0004T0501399.003. Statistical Summary of Porosity Data. Submittal date: 04/13/2000. [155045]

SN0302T0502203.001. Saturated Zone Anisotropy Distribution Near the C-Wells. Submittal date: 02/26/2003. [163563]

SN0306T0504103.005. Revised Groundwater Colloid Mass Concentration Parameters for TSPA (Total System Performance Assessment). Submittal date: 06/30/2003. [164132]

SN0306T0504103.006. Revised Sorption Partition Coefficients (KD Values) for Selected Radionuclides Modeled in the TSPA (Total System Performance Assessment). Submittal date: 06/30/2003. [164131]

SN9907T0571599.001. Probability Distribution of Flowing Interval Spacing. Submittal date: 07/15/1999. [122261]

9.5   OUTPUT DATA, LISTED BY DATA TRACKING NUMBER

MO0310SPANGRAC.000. NATURAL GROSS ALPHA CONCENTRATION IN AMARGOSA VALLEY GROUNDWATER. Submittal date: 10/23/2003.

SN0306T0502103.005. SATURATED ZONE (SZ) 1-D TRANSPORT MODEL. Submittal date: 06/05/2003.

 SN0306T0502103.006. DATA SPREADSHEETS TO SUPPORT PARAMETER UNCERTAINTY DEVELOPMENT. Submittal date: 06/05/2003.

SN0310T0502103.009. REVISED SATURATED ZONE TRANSPORT ABSTRACTION MODEL UNCERTAIN INPUTS. Submittal date: 10/09/2003.

SN0310T0502103.010. REVISED SATURATED ZONE FLOW AND TRANSPORT MODEL ABSTRACTION INPUTS AND RESULTS. Submittal date: 10/09/2003.

SN0310T0502103.012. SATURATED ZONE FLOW AND TRANSPORT MODEL ABSTRACTION INPUTS AND RESULTS FOR FAST FRACTION OF IRREVERSIBLE COLLOIDS. Submittal date: 10/24/2003.

10. ATTACHMENTS

ATTACHMENT I – Stochastic Parameter Values

ATTACHMENT I

Table I-1. Stochastic Parameter Values

DTN: SN0310T0502103.009

real. #	FPLAW	FPLAN	NVF19	NVF7	FISVO	FPVO	DCVO	KDNPVO	KDNPAL	KDSRVO	KDSRAL
1	0.70451	0.028309	0.15851	0.11373	1.3862	-3.7026	-10.092	1.7762	6.3364	268.07	259.27
2	0.61702	0.70184	0.11408	0.081329	0.84234	-3.0161	-10.116	1.2311	4.8505	258.99	113.51
3	0.35217	0.61633	0.083152	0.20585	1.0234	-3.3666	-10.146	1.09	4.2112	113.11	290.67
4	0.43734	0.35304	0.20587	0.19441	0.83422	-3.8921	-10.539	1.3057	7.6552	290.9	159.82
5	0.3726	0.4368	0.19441	0.16058	0.92304	-4.461	-10.042	1.5285	6.1118	160.14	199.68
6	0.38137	0.37493	0.16033	0.17169	1.4084	-2.3306	-10.426	1.1931	6.4302	200.28	240.98
7	0.96095	0.38323	0.17133	0.16309	0.81193	-2.6095	-10.325	1.556	5.7365	240.86	85.61
8	0.96721	0.96199	0.1631	0.16459	1.1285	-3.3333	-10.197	1.2925	7.73	86.233	122.88
9	0.063508	0.96547	0.16442	0.26596	1.3996	-3.1397	-10.612	1.1273	4.6382	122.69	82.931
10	0.39763	0.063782	0.26525	0.26907	1.2126	-3.2812	-10.518	1.2363	7.7179	83.165	99.983
11	0.12641	0.39708	0.26845	0.1011	0.63908	-3.2658	-10.619	1.2345	6.2902	100.11	249.1
12	0.83363	0.12855	0.10207	0.16643	1.5206	-1.199	-10.572	1.8288	7.5701	248.31	79.438
13	0.82638	0.83084	0.16658	0.12153	1.3272	-1.15	-10.174	1.2777	6.451	79.842	156.96
14	0.46725	0.82571	0.12117	0.22766	0.62506	-3.976	-10.626	1.22	4.9316	156.83	245.64
15	0.11482	0.46679	0.2272	0.22709	1.6764	-3.2319	-10.431	1.4189	6.8839	244.94	185.29
16	0.24233	0.11166	0.22688	0.17505	1.0682	-3.8285	-10.185	1.5742	7.3231	183.88	46.974
17	0.8055	0.24472	0.17513	0.11746	1.2021	-1.8383	-10.366	1.6247	7.8869	47.598	285.48
18	0.1329	0.80984	0.11813	0.14376	1.0712	-1.8602	-10.758	1.2913	5.1106	284.54	222.27
19	0.73058	0.13299	0.14387	0.22266	1.4018	-3.0689	-10.059	1.7072	5.8951	223.16	46.513
20	0.34072	0.73141	0.22261	0.12312	1.3451	-3.856	-10.26	1.7658	8.6697	45.328	329.38
21	0.048591	0.34315	0.12247	0.21023	1.0043	-3.5674	-10.801	1.5571	7.4175	327.85	136.96
22	0.74837	0.048613	0.21035	0.15875	1.4574	-1.9719	-9.921	1.6685	7.7301	137.24	181.17
23	0.93881	0.74785	0.15923	0.093691	1.2402	-3.8166	-10.485	1.5587	6.4626	180.92	138.35
24	0.55458	0.93563	0.09379	0.21283	1.1247	-2.2296	-10.372	1.0925	1.9633	139.62	247.14
25	0.79283	0.55378	0.21273	0.25453	1.668	-3.3458	-10.476	1.7332	6.3834	246.15	228.25
26	0.37734	0.79098	0.25543	0.18598	1.816	-4.0395	-10.185	5.906	7.6101	227.35	115.13

real. #	FPLAW	FPLAN	NVF19	NVF7	FISVO	FPVO	DCVO	KDNPVO	KDNPAL	KDSRVO	KDSRAL
27	0.67108	0.37594	0.18625	0.2203	0.94555	-2.1743	-10.24	1.5551	7.8466	116.36	264.39
28	0.65266	0.67222	0.22046	0.16351	1.6175	-1.3137	-10.538	0.83687	6.7485	264.74	194.12
29	0.62918	0.65188	0.1638	0.20193	1.5918	-2.8203	-10.13	1.6876	10.779	194.18	155.64
30	0.24883	0.62618	0.20225	0.199	1.3545	-2.032	-10.341	1.135	2.4415	156.36	325.19
31	0.71164	0.2459	0.19922	0.19577	0.76344	-3.2677	-10.437	1.3511	6.4552	325.42	362
32	0.36584	0.7122	0.1961	0.14524	2.4058	-2.4327	-9.9314	1.5141	6.5489	361.97	105.28
33	0.47113	0.36787	0.14464	0.20748	1.2638	-2.4921	-9.6565	1.5069	6.2446	103.82	313.97
34	0.58157	0.47388	0.20749	0.16199	1.8275	-2.5698	-10.565	1.0319	5.3839	313.5	308.63
35	0.17154	0.58391	0.16242	0.17587	1.381	-3.5586	-9.9702	1.1229	4.5499	307.59	232.62
36	0.27276	0.17077	0.17593	0.19016	1.7866	-2.2884	-9.9878	1.2241	6.5466	230.98	72.64
37	0.16841	0.2727	0.18985	0.13151	1.3153	-3.2946	-10.231	1.4754	5.7734	71.65	395.34
38	0.21269	0.16757	0.13141	0.14914	1.5424	-3.0598	-10.645	1.0729	4.3751	395.81	200.88
39	0.60151	0.21358	0.14881	0.13017	1.6877	-2.7243	-9.3455	1.1663	4.6523	201.21	362.94
40	0.15729	0.60256	0.13036	0.13857	1.4451	-3.7297	-10.322	1.2935	5.863	363.36	239.29
41	0.3647	0.15605	0.13923	0.19281	1.2456	-3.5069	-9.6366	1.402	7.3494	238.67	353.32
42	0.59284	0.36398	0.19225	0.12862	1.5022	-3.7412	-10.208	1.1224	6.6715	353.63	219.29
43	0.43429	0.59413	0.1289	0.16172	1.0933	-3.6399	-9.7391	1.7931	4.4304	218.86	293.52
44	0.074964	0.43453	0.1616	0.1909	1.3933	-2.6663	-10.274	1.2546	6.7603	293.54	329.87
45	0.69768	0.072714	0.19154	0.17113	1.7338	-3.7591	-10.037	1.0482	4.24	329.95	260.63
46	0.53002	0.69555	0.17083	0.10469	0.60159	-3.3102	-9.9122	5.9484	12.998	260.58	195.92
47	0.066897	0.53497	0.10634	0.20539	1.5563	-2.6836	-10.14	1.3471	6.3144	195.81	278.81
48	0.81253	0.067039	0.20548	0.18333	1.629	-3.1487	-10.338	1.7807	8.2368	279.26	147.09
49	0.307	0.81175	0.18364	0.10332	1.1917	-3.954	-10.079	1.1421	5.1387	146.39	242.3
50	0.42421	0.30885	0.10441	0.2239	1.6554	-2.3446	-10.461	5.8964	12.116	242.61	342.55
51	0.31471	0.42162	0.22428	0.15377	1.015	-2.8939	-10.193	1.7596	7.6537	342.37	42.645
52	0.59783	0.31468	0.15362	0.16942	1.0887	-3.9623	-9.8347	1.3367	6.3723	41.049	296.42
53	0.54881	0.59673	0.16958	0.15458	0.92816	-1.937	-10.881	1.826	5.3289	296.98	317.67
54	0.25186	0.54916	0.15499	0.19171	1.3722	-3.4313	-10.022	2.9922	10.605	316.68	177.7
55	0.64107	0.25325	0.19159	0.18521	0.58809	-3.1758	-9.9578	1.4494	6.9642	177.84	322.55
56	0.45988	0.64197	0.18541	0.14594	0.70644	-3.4213	-10.38	1.3908	5.5995	322.77	120.09
57	0.35868	0.45653	0.14567	0.19779	1.1816	-2.6824	-9.9416	1.8202	8.3781	119.49	144.75
58	0.80213	0.35725	0.19771	0.17377	1.8448	-2.8405	-10.526	1.4432	8.2585	144.07	102.59

real. #	FPLAW	FPLAN	NVF19	NVF7	FISVO	FPVO	DCVO	KDNPVO	KDNPAL	KDSRVO	KDSRAL
59	0.89925	0.80492	0.17397	0.16094	1.8056	-3.5446	-10.465	1.7504	8.3775	102.46	238.09
60	0.22248	0.89986	0.16077	0.22181	0.8828	-2.5185	-10.569	2.0366	7.6319	238.24	40.481
61	0.77121	0.22433	0.22181	0.24279	1.776	-3.0919	-10.209	4.6391	8.5555	39.125	60.504
62	0.75746	0.77304	0.24181	0.14055	1.4833	-3.3141	-10.914	1.3779	5.6484	61.745	174.98
63	0.55579	0.75953	0.14106	0.21688	0.29449	-1.9893	-10.676	1.5845	6.0788	175.27	368.07
64	0.13508	0.5581	0.2173	0.2146	0.97023	-1.5186	-10.388	1.6112	7.9421	368.85	358.4
65	0.9875	0.13511	0.21415	0.18662	0.67711	-3.6141	-9.5831	1.4423	7.3588	358.6	93.383
66	0.47965	0.98618	0.18644	0.12437	1.0221	-2.0912	-9.6872	1.6498	6.3947	93.089	351.55
67	0.90123	0.47822	0.12407	0.28381	1.3397	-2.146	-10.594	1.4092	4.8544	350.82	273.61
68	0.57866	0.90303	0.28224	0.17637	1.1865	-2.81	-9.7422	1.5295	7.097	272.91	29.222
69	0.87669	0.57844	0.17686	0.24362	1.3222	-3.8028	-10.099	1.7656	8.2015	29.194	109.73
70	0.52246	0.87687	0.24338	0.18948	1.4151	-1.0566	-11.127	1.689	7.9085	110.4	55.672
71	0.71788	0.52221	0.18946	0.23674	1.8942	-3.0485	-10.55	1.5342	7.2882	54.464	122.53
72	0.81847	0.71882	0.23781	0.182	1.7624	-1.4862	-10.686	1.0478	4.0931	122.07	225.24
73	0.63474	0.81922	0.18229	0.20867	0.738	-2.7404	-10.522	1.3844	5.8392	225.84	177.4
74	0.46117	0.63266	0.20818	0.22519	1.7318	-1.6079	-10.25	1.1146	5.563	177.5	220.21
75	0.68208	0.46283	0.22459	0.19667	1.533	-2.9264	-10.382	1.4729	4.6409	220.36	251.38
76	0.33346	0.68422	0.19617	0.1746	1.7237	-2.2736	-10.267	3.8397	5.4484	250.42	379.89
77	0.58661	0.33143	0.17454	0.2033	2.5288	-1.9123	-10.169	1.108	5.8758	379.91	348.05
78	0.84781	0.58957	0.20353	0.15752	0.18779	-2.5558	-9.4799	3.6575	8.1698	347.72	65.785
79	0.055061	0.84838	0.15727	0.1908	1.4319	-3.0857	-9.7859	1.7059	8.3184	65.77	340.28
80	0.72545	0.059548	0.19074	0.23065	0.65772	-2.3987	-10.66	1.0474	6.9709	340.32	288.61
81	0.78233	0.72652	0.23023	0.09896	1.0081	-3.3729	-9.8592	4.7524	7.3093	288.29	337.65
82	0.41537	0.78383	0.10033	0.21009	1.5687	-2.7055	-10.051	1.3448	4.2383	338.42	396.46
83	0.79615	0.4153	0.21009	0.21848	0.1867	-1.7701	-9.868	1.116	4.5096	396.97	24.361
84	0.26279	0.79769	0.21877	0.169	1.8692	-3.9839	-9.3285	1.3663	6.2532	24.087	256.82
85	0.32585	0.26149	0.16913	0.22126	1.0848	-2.2475	-11.197	3.2666	8.0548	257.05	51.292
86	0.21935	0.32771	0.22133	0.14731	0.43697	-2.0638	-10.149	1.2834	6.8038	50.403	118.69
87	0.57287	0.21868	0.14692	0.15714	1.0417	-3.1822	-10.698	1.1281	5.642	117.57	303.07
88	0.05408	0.5743	0.15668	0.14015	0.69929	-2.0111	-10.532	1.5478	6.9799	302.88	23.539
89	0.10576	0.054487	0.13962	0.18832	1.2717	-3.5333	-10.005	1.6866	5.067	22.372	375.01
90	0.40754	0.10529	0.18845	0.096424	1.6977	-3.3872	-11.258	2.6858	8.1054	374.3	142.05

real. #	FPLAW	FPLAN	NVF19	NVF7	FISVO	FPVO	DCVO	KDNPVO	KDNPAL	KDSRVO	KDSRAL
91	0.91603	0.40782	0.098203	0.11647	0.90599	-3.6232	-9.5364	1.2958	7.3349	143.11	32.802
92	0.89135	0.91567	0.11686	0.16758	1.7454	-2.7577	-10.47	1.7117	6.3243	33.088	128.36
93	0.19019	0.89023	0.16751	0.24842	0.46766	-3.9928	-11.072	1.5973	5.532	129.99	59.201
94	0.87315	0.19372	0.24868	0.24104	1.2729	-3.8725	-10.503	1.4454	8.2211	58.595	204.12
95	0.66517	0.87134	0.24128	0.13522	1.7668	-3.2063	-10.678	1.3136	6.3196	203.25	333.28
96	0.024123	0.66764	0.13509	0.2357	0.79926	-1.415	-10.318	1.3962	5.1403	333.2	96.423
97	0.23899	0.022985	0.23591	0.20122	0.78641	-1.5294	-9.9071	1.6784	10.47	96.617	343.73
98	0.093079	0.23563	0.20126	0.079449	0.50753	-3.6823	-10.585	1.5156	6.2799	344.24	33.838
99	0.26953	0.090888	0.078007	0.14284	1.6105	-1.6374	-9.8223	2.0086	12.343	33.832	205.03
100	0.54079	0.26698	0.14297	0.1121	0.7266	-2.4384	-11.023	1.3193	4.8847	205.87	348.78
101	0.41165	0.54048	0.11173	0.14771	1.2905	-4.5523	-10.31	1.114	5.4429	349.62	77.497
102	0.52854	0.41152	0.14803	0.18493	1.053	-3.5782	-9.7593	5.3252	7.4087	77.534	76.842
103	0.60808	0.52661	0.18474	0.16809	1.8672	-3.9083	-10.633	1.6194	5.0404	76.359	36.081
104	0.94548	0.60856	0.1683	0.18302	1.8887	-3.5167	-10.633	1.0013	4.9632	36.121	311.98
105	0.86326	0.94988	0.18294	0.19313	1.9802	-2.8632	-10.973	1.2785	5.8423	312.49	63.968
106	0.12173	0.86184	0.19307	0.25889	2.2252	-3.196	-9.9776	1.5042	8.3694	64.993	210.78
107	0.84161	0.12403	0.259	0.23369	0.81543	-2.9144	-10.666	1.0022	4.0211	210.19	132.5
108	0.70681	0.84374	0.23391	0.12085	1.0518	-2.6365	-10.296	1.6652	8.0432	133.56	371.99
109	0.83677	0.70737	0.12071	0.22943	1.0756	-1.2562	-10.492	1.404	7.1784	372.31	378.64
110	0.99128	0.83905	0.22953	0.20708	1.0619	-1.6871	-9.5526	1.8088	6.2277	377.8	384.4
111	0.010519	0.99171	0.20724	0.2288	1.1152	-3.8399	-9.5112	1.5117	8.0958	383.78	389.32
112	0.62269	0.011542	0.22836	0.28924	1.5627	-1.7758	-9.4549	0.46893	2.0554	388.62	81.669
113	0.084204	0.62223	0.29036	0.067107	1.1593	-2.3046	-9.3949	1.3874	5.0674	81.049	131.2
114	0.25597	0.083179	0.063538	0.19537	1.7925	-1.8199	-10.623	1.0262	4.8538	131.47	141.54
115	0.74132	0.25944	0.19539	0.10837	1.8399	-1.0372	-10.499	1.4555	4.3711	140.73	134.5
116	0.007434	0.74115	0.10822	0.14618	1.3104	-4.793	-10.473	1.4463	4.6318	135.74	152.57
117	0.93236	0.008269	0.14655	0.21192	1.0318	-2.5914	-10.486	1.2589	4.8102	151.56	300.09
118	0.32035	0.93043	0.21235	0.049913	0.25923	-3.925	-10.447	1.6972	8.4928	299.64	166.3
119	0.030233	0.32271	0.054478	0.25292	1.8314	-3.5417	-10.015	1.3911	6.5942	167.99	355.78
120	0.28508	0.034057	0.25215	0.15635	1.6384	-2.197	-10.408	1.0517	4.3142	355.96	366.8
121	0.10144	0.28681	0.15579	0.084439	1.4232	-4.8885	-9.7061	4.1216	8.6042	365.99	216.81
122	0.48434	0.10353	0.087276	0.15092	1.2272	-1.3375	-9.6162	1.7822	10.632	216.07	125.11

real. #	FPLAW	FPLAN	NVF19	NVF7	FISVO	FPVO	DCVO	KDNPVO	KDNPAL	KDSRVO	KDSRAL
123	0.82334	0.4826	0.15078	0.11532	1.2217	-3.394	-10.28	1.1916	6.8495	126.33	25.85
124	0.20394	0.82124	0.1155	0.17726	1.8577	-4.3628	-10.513	0.55633	5.2954	25.77	364.38
125	0.8532	0.20325	0.1773	0.2256	0.64581	-3.4685	-11.163	0.60824	5.5611	364.43	319.08
126	0.037624	0.85435	0.22552	0.13752	2.2805	-3.8812	-9.6208	1.6654	8.6597	318.59	252.72
127	0.48593	0.038573	0.1374	0.23209	1.8027	-3.0395	-9.9522	1.1375	4.852	253.06	189.7
128	0.86876	0.48711	0.2322	0.090398	1.4724	-1.8783	-10.167	1.5864	7.4125	189.11	188.25
129	0.1544	0.86639	0.087853	0.17752	0.8727	-3.6625	-10.349	1.2554	6.6315	189	371.09
130	0.14816	0.15141	0.17766	0.23528	1.4626	-1.7361	-10.354	1.7691	6.1952	371.34	48.507
131	0.043598	0.14898	0.2347	0.12704	0.8525	-4.2851	-9.5649	0.57225	6.1647	49.552	391
132	0.76846	0.043645	0.12788	0.12639	1.9175	-3.0322	-10.707	1.5393	8.5753	392.36	358.05
133	0.11602	0.76916	0.12658	0.091042	0.77682	-1.663	-9.3758	1.5539	6.1291	357.09	270.33
134	0.50019	0.11576	0.091188	0.21608	1.5858	-3.7717	-9.697	1.4248	5.1128	268.94	91.21
135	0.29848	0.50385	0.21619	0.11938	0.66707	-3.782	-10.108	1.7533	7.8604	91.012	266.13
136	0.92706	0.29908	0.11876	0.1795	0.9665	-4.1659	-10.598	1.3229	6.3067	266.24	87.774
137	0.94102	0.92914	0.17972	0.15236	1.6015	-2.1023	-10.123	1.4054	4.568	87.49	381.85
138	0.95563	0.94338	0.1525	0.25203	1.0371	-3.8468	-10.607	1.3532	6.9416	382.11	73.304
139	0.97152	0.95988	0.25117	0.25751	1.4984	-2.9884	-9.4764	1.4846	7.5599	75.05	305.76
140	0.16243	0.97467	0.25758	0.26263	1.3352	-3.4489	-10.64	1.4352	6.1782	306.58	52.742
141	0.29141	0.16433	0.26227	0.27269	1.3693	-1.3574	-9.9925	1.0025	4.2885	52.555	108.71
142	0.31613	0.29468	0.27054	0.12983	0.90791	-1.2856	-10.691	1.304	5.0186	107.51	310.21
143	0.30444	0.31977	0.12929	0.1517	1.1741	-1.2235	-10.553	1.2773	6.5328	309.31	127.74
144	0.34719	0.30198	0.15141	0.15513	2.5485	-1.1431	-9.9839	1.6238	4.665	126.78	278.2
145	0.73918	0.34993	0.15548	0.15306	1.2035	-3.7544	-10.508	1.5304	6.9865	278.09	224.01
146	0.38633	0.73982	0.15327	0.15945	0.94859	-3.4626	-10.086	1.7279	6.2592	223.97	234.71
147	0.88281	0.38841	0.15936	0.21123	1.7483	-3.4067	-10.258	1.4001	7.0045	235.6	98.655
148	0.91034	0.88286	0.21103	0.16498	1.5123	-3.4429	-10.217	0.9905	2.7287	98.884	173.85
149	0.51841	0.91188	0.16505	0.2382	0.12866	-3.3353	-10.578	0.96945	3.0842	172.58	398.45
150	0.27749	0.51972	0.23803	0.24697	1.4763	-2.2129	-10.391	1.8137	7.36	399.04	182.7
151	0.018691	0.27629	0.2464	0.18134	1.6242	-3.245	-9.3007	1.6874	6.8565	182.75	106.24
152	0.90977	0.017058	0.18162	0.14925	0.88989	-1.5786	-10.367	1.6278	7.3442	106.39	346.76
153	0.78691	0.90918	0.14972	0.071036	1.1644	-1.444	-10.56	1.7089	8.5463	345.34	282.36
154	0.61273	0.78833	0.073847	0.24478	1.5462	-2.9437	-9.806	1.532	4.5883	283.74	20.174

real. #	FPLAW	FPLAN	NVF19	NVF7	FISVO	FPVO	DCVO	KDNPVO	KDNPAL	KDSRVO	KDSRAL
155	0.44835	0.61154	0.24491	0.21959	1.509	-3.4983	-10.066	1.644	6.1311	20.054	272.36
156	0.44417	0.44562	0.21926	0.19385	2.3672	-4.6266	-11.292	1.578	7.6511	270.96	316.33
157	0.92465	0.44049	0.19402	0.17247	1.2376	-1.4517	-10.102	1.5821	7.0916	315.47	94.793
158	0.076609	0.92395	0.17275	0.17226	1.297	-2.0342	-9.9661	1.036	4.1036	95.841	169.24
159	0.97647	0.077995	0.17184	0.25011	1.2888	-2.622	-10.589	1.8158	6.7876	169.73	294.38
160	0.88672	0.97946	0.24939	0.10731	1.3071	-3.1179	-10.4	1.4875	6.203	294.14	280.49
161	0.65647	0.88508	0.10708	0.27559	1.3647	-3.1224	-10.027	1.4853	7.3059	281.47	392.49
162	0.18665	0.65755	0.2747	0.2403	1.4503	-1.3913	-10.072	1.3696	4.7212	392.92	192.19
163	0.64606	0.18543	0.23956	0.19953	0.86176	-3.9385	-9.369	5.6796	11.544	192.4	212.7
164	0.17568	0.6463	0.19972	0.13401	1.2833	-1.1169	-10.347	1.0218	5.7699	212.65	209.44
165	0.95061	0.17555	0.13472	0.19829	1.1026	-1.5522	-10.29	3.2702	12.928	209.18	215.42
166	0.14335	0.95267	0.19855	0.13239	0.68419	-2.4821	-10.302	1.1476	4.9715	215.41	233.45
167	0.75389	0.14211	0.13248	0.26065	0.35455	-3.6937	-10.285	1.4987	6.0234	233.3	262.83
168	0.088815	0.75375	0.26063	0.12567	1.5235	-2.5044	-10.222	1.7817	7.7213	262.21	88.429
169	0.23232	0.08869	0.12491	0.21379	1.4276	-3.7156	-10.133	1.1922	5.8916	89.341	207.49
170	0.76434	0.23274	0.21353	0.11061	1.1196	-1.2367	-10.602	1.0342	6.3693	207.28	148.16
171	0.28202	0.7616	0.11071	0.14232	1.2168	-3.7935	-10.308	1.3828	7.5455	147.76	56.742
172	0.67838	0.28377	0.1421	0.21493	1.1411	-2.1576	-10.453	1.0248	4.8431	56.111	30.192
173	0.53511	0.67815	0.2155	0.15048	1.1566	-3.9196	-10.686	1.3506	7.8087	30.992	286.7
174	0.56885	0.53997	0.15046	0.20288	2.0937	-3.5938	-11.111	5.5651	10.593	286.98	254.82
175	0.20533	0.5681	0.20264	0.18426	2.1634	-2.1331	-10.054	5.0921	12.993	254.19	153.59
176	0.40471	0.20916	0.18434	0.18769	0.61684	-3.4847	-10.156	1.0081	2.0458	153.92	185.52
177	0.9995	0.40055	0.18774	0.13838	1.1696	-2.4075	-10.442	1.5078	6.559	186.74	162.09
178	0.42544	0.99674	0.13813	0.1669	0.74682	-2.8729	-10.359	1.76	6.093	160.92	166.26
179	0.22637	0.42607	0.16701	0.29202	1.7114	-2.7766	-10.421	1.8183	8.4675	165.99	386.06
180	0.85993	0.22959	0.29861	0.17001	1.7077	-3.649	-10.414	0.37838	4.25	385.73	387.44
181	0.69081	0.85616	0.17039	0.14118	1.2552	-3.218	-9.4402	1.5396	6.3219	388.13	42.922
182	0.000316	0.69391	0.14143	0.23223	0.71843	-1.0082	-9.4219	1.6811	7.6176	44.051	170.83
183	0.66425	0.000898	0.23224	0.20456	0.98249	-3.165	-10.84	0.82101	1.8184	170.21	68.282
184	0.77963	0.6644	0.20481	0.02251	1.6687	-3.6051	-10.4	1.2373	4.7156	67.757	336.51
185	0.19856	0.77701	0.026558	0.20066	0.75819	-1.714	-10.656	1.4965	5.9137	336.43	333.76
186	0.39325	0.19937	0.2007	0.21764	1.5619	-2.3599	-9.8929	1.3319	6.6568	334.86	197.72

real. #	FPLAW	FPLAN	NVF19	NVF7	FISVO	FPVO	DCVO	KDNPVO	KDNPAL	KDSRVO	KDSRAL
187	0.72376	0.39066	0.21781	0.13599	1.1067	-4.9164	-9.9021	4.4429	10.666	197.9	62.435
188	0.68892	0.7222	0.13594	0.16567	0.55484	-2.4516	-10.331	1.063	4.4061	61.878	112.56
189	0.98274	0.6877	0.1656	0.2091	1.5759	-2.0718	-10.67	4.0276	8.2587	112.62	326.39
190	0.45275	0.98273	0.20896	0.20396	1.8807	-3.6752	-10.546	1.699	8.1244	326.54	71.187
191	0.50526	0.45272	0.20412	0.28052	1.3502	-3.2414	-9.9247	1.3218	7.4539	70.071	298.21
192	0.49598	0.50781	0.27675	0.17357	1.6501	-2.2593	-10.652	1.4167	6.163	298.79	151.05
193	0.51183	0.49782	0.17314	0.18015	1.1476	-2.3726	-10.017	1.5236	4.1231	150.2	38.786
194	0.56134	0.51179	0.18047	0.17902	1.4929	-1.0761	-10.45	0.036671	6.0078	38.545	304.18
195	0.63937	0.56322	0.17911	0.18073	1.469	-3.1087	-10.948	1.5217	5.8151	303.54	376.34
196	0.18288	0.63794	0.18074	0.18708	1.4386	-2.9756	-9.9997	1.0782	4.5618	376.21	230.27
197	0.49279	0.18439	0.18748	0.19706	0.99788	-3.0038	-9.5125	1.2419	5.6844	229.91	321.71
198	0.33957	0.49261	0.19742	0.13392	1.5377	-2.9649	-10.239	1.2661	7.7128	321.32	162.65
199	0.097933	0.33587	0.13394	0.17855	1.1373	-2.7936	-9.9428	1.1672	5.5324	163.61	275.46
200	0.02951	0.098121	0.17837	0.15841	1.2559	-2.5445	-10.415	0.37655	1.9883	274.65	268.56

real. #	KDUVO	KDUAL	GWSPD	BULKDEN SITY	CORAL	CORVO	SRC4Y	SRC4X	SRC3X	SRC2Y	SRC2X
1	6.3929	4.0476	0.8181	1791.7	1.0875	1.0042	0.39801	0.12912	0.82832	0.11435	0.46636
2	5.4235	4.3547	-0.85495	1889.7	3.5582	1.6714	0.12714	0.83286	0.46792	0.2438	0.11184
3	6.091	4.121	-0.1215	1820.9	3.5695	1.1986	0.83439	0.82826	0.11009	0.80568	0.24456
4	6.0964	4.1487	-0.44224	1984.5	0.90319	1.3675	0.82819	0.4672	0.24114	0.13093	0.80542
5	7.4704	6.9729	0.39432	1983.7	1.1434	1.5138	0.46584	0.11053	0.80879	0.73468	0.13052
6	7.5767	7.1394	0.3885	1904.1	0.90338	0.83369	0.11165	0.24447	0.13119	0.34017	0.73259
7	6.7357	2.9464	-0.03684	1815.2	2.9725	1.0459	0.24061	0.80742	0.73112	0.046301	0.34463
8	6.9733	4.2057	-0.46085	1855.7	2.9604	0.81838	0.80897	0.13118	0.34463	0.7483	0.04631
9	5.4813	3.1882	-0.30786	1978.3	1.4071	0.91882	0.13468	0.73388	0.04603	0.93663	0.74671
10	6.1144	5.8512	0.36448	1823.5	0.90334	1.5367	0.73421	0.34146	0.74618	0.55383	0.93928
11	8.0149	5.8404	-0.43612	1957.8	0.90373	0.79926	0.34235	0.045831	0.93877	0.79495	0.55274
12	7.3052	4.4718	0.27522	1878.4	2.8768	1.1894	0.049235	0.74967	0.55011	0.37712	0.79438
13	5.7365	3.13	-0.19072	1777.8	0.9034	1.5267	0.74852	0.93563	0.79164	0.67425	0.37882
14	6.3898	3.6295	-0.97733	1961.7	2.5538	1.3075	0.93625	0.55419	0.37553	0.65406	0.67351
15	8.0955	5.7631	0.29233	2028.3	0.94105	0.77849	0.55335	0.79368	0.67241	0.62614	0.65251
16	5.418	3.2064	0.66404	1920	0.90314	1.6522	0.79004	0.37616	0.65068	0.24578	0.62768
17	7.2363	5.4719	0.059967	1973.9	2.6065	1.4544	0.37912	0.67379	0.62866	0.7112	0.24627
18	6.297	3.9963	0.3514	1885.7	3.4344	0.77844	0.67485	0.65038	0.24892	0.3687	0.71087
19	6.1532	2.8633	-0.14488	1944.9	1.7505	1.8446	0.65415	0.62701	0.711	0.47078	0.36665
20	6.3443	5.5418	0.20717	1940.3	2.8112	1.0993	0.62895	0.24539	0.36569	0.58084	0.47477
21	7.247	6.249	0.18479	1935.4	1.0695	1.288	0.24752	0.71071	0.47397	0.17007	0.5826
22	6.6527	4.799	0.15118	1856.8	2.2828	1.1135	0.71398	0.36774	0.58472	0.27474	0.1718
23	7.1839	5.711	-0.30353	1953.7	2.2025	1.5333	0.36813	0.47456	0.17021	0.1663	0.27316
24	6.3895	4.1293	0.25181	1883.7	2.0793	1.4721	0.47446	0.58489	0.27248	0.21154	0.16614
25	6.9776	5.251	-0.15875	1904.5	0.90375	1.0179	0.58135	0.17051	0.16512	0.60233	0.21337
26	14.466	5.1801	-0.03341	1925.9	2.4697	1.5852	0.17104	0.27259	0.21288	0.15556	0.60328
27	5.7245	5.0737	0.099475	1836.3	1.04	1.3493	0.27161	0.1696	0.60274	0.36263	0.15521
28	5.4412	3.6421	-0.38882	1862.7	1.4328	1.1809	0.16813	0.2111	0.15655	0.59017	0.36338
29	7.345	5.3989	-0.27169	1834.9	1.8884	1.7837	0.21312	0.60029	0.36028	0.43416	0.59491
30	6.6146	4.1024	-0.39819	1847.3	0.90353	2.3132	0.60039	0.15621	0.59053	0.070562	0.43237

real. #	KDUVO	KDUAL	GWSPD	BULKDEN SITY	CORAL	CORVO	SRC4Y	SRC4X	SRC3X	SRC2Y	SRC2X
31	6.4572	4.4969	-0.34483	1930.7	0.90382	0.94597	0.15578	0.36256	0.43289	0.69568	0.072704
32	6.7446	4.9141	0.11944	1831.2	0.90351	1.7452	0.36078	0.59297	0.074871	0.53396	0.69861
33	6.5102	3.3664	-0.41112	1882.9	0.90364	1.7258	0.59401	0.43237	0.69566	0.066305	0.53255
34	6.3393	3.7497	-0.16609	1928.7	1.9686	1.4833	0.43426	0.073074	0.53246	0.81035	0.069985
35	5.9997	3.344	0.10967	1896.5	0.90348	0.77891	0.073323	0.6975	0.067696	0.30531	0.81321
36	5.9559	3.508	-0.07847	1796.8	1.0186	2.8271	0.6963	0.53488	0.81113	0.42313	0.30702
37	7.7597	4.9963	-0.76296	1950.8	1.9415	1.3809	0.53406	0.06581	0.30994	0.3125	0.42397
38	5.4215	3.3073	0.23755	1916.7	1.2853	2.3632	0.065321	0.81078	0.4221	0.59713	0.31337
39	7.5782	4.0865	0.037959	1792.3	0.90322	1.5062	0.81429	0.30812	0.31475	0.54755	0.59695
40	6.8481	4.9427	-0.81314	1978.7	2.3987	2.2149	0.30883	0.42455	0.59518	0.25434	0.54791
41	6.4336	4.348	0.37313	1870.6	1.6641	1.4434	0.42078	0.31241	0.54998	0.64335	0.25415
42	5.9679	2.9858	-0.23107	1894.9	0.9032	1.6805	0.31042	0.59809	0.25497	0.45955	0.64074
43	7.6914	5.3518	-0.08994	1872.4	2.8904	1.8892	0.59966	0.549	0.64079	0.35531	0.45927
44	6.5365	4.7282	-0.2259	1929.2	0.90393	1.5782	0.54701	0.25493	0.45549	0.80303	0.35881
45	3.8988	2.9717	0.11488	1919	1.2471	1.3553	0.25287	0.64012	0.35869	0.89767	0.8011
46	7.76	5.7864	0.054703	1857.7	0.90394	1.634	0.64341	0.45504	0.80265	0.22022	0.89575
47	6.9593	3.8645	-0.29576	1938.4	1.9461	1.1435	0.45681	0.35554	0.89736	0.77279	0.22201
48	6.3023	4.2993	0.16765	1902	1.729	1.5204	0.35767	0.8033	0.22106	0.75653	0.7745
49	7.1005	3.8948	-0.05232	1881.8	0.90376	2.0395	0.80219	0.8976	0.77391	0.55844	0.75595
50	7.2944	4.9688	-0.17085	1976.9	2.1536	0.77839	0.89527	0.22021	0.75624	0.13669	0.55693
51	6.9967	4.7739	0.35802	2009.1	1.3766	1.6906	0.22262	0.77394	0.55501	0.98761	0.13778
52	6.1107	3.6678	0.4722	1850.2	1.0029	1.7566	0.77311	0.75559	0.136	0.47673	0.98982
53	5.5058	5.1336	-0.32842	1968.2	2.8598	1.2814	0.75897	0.55733	0.98911	0.90165	0.47795
54	8.0283	4.4488	0.3249	1965	3.2589	1.7758	0.55928	0.13643	0.47798	0.57992	0.9017
55	7.1634	4.0579	0.30516	1921.4	0.90367	1.0305	0.13924	0.9852	0.90361	0.87597	0.57623
56	7.7182	5.7363	0.069194	1824.4	2.7248	1.1388	0.98859	0.47716	0.57516	0.52119	0.8799
57	16.934	6.1005	-0.43183	2082	2.6468	0.93337	0.47781	0.9021	0.87838	0.71927	0.52202
58	6.3677	3.5446	0.92526	1905.5	1.7898	1.5033	0.90019	0.57664	0.52429	0.81645	0.71732
59	8.0137	5.6306	-0.02427	2011	0.90342	0.77833	0.57734	0.87993	0.7155	0.63189	0.8157
60	7.5803	5.5676	0.47755	1925.5	3.6555	0.77871	0.87726	0.52225	0.81696	0.46085	0.63455
61	7.8045	4.8121	0.093825	2000.3	1.4533	1.2651	0.52405	0.71818	0.63403	0.6836	0.4645
62	6.8065	3.2399	0.44786	1914.8	3.2957	2.4448	0.71743	0.81913	0.46208	0.33488	0.68352

real. #	KDUVO	KDUAL	GWSPD	BULKDEN SITY	CORAL	CORVO	SRC4Y	SRC4X	SRC3X	SRC2Y	SRC2X
63	7.8024	8.2148	0.027231	1955.4	1.8794	2.2914	0.81684	0.63478	0.68113	0.58819	0.33071
64	6.3658	4.5135	0.26113	1979.9	3.1858	0.87284	0.63336	0.46033	0.33102	0.84547	0.58869
65	6.6401	6.1286	0.38063	1936	1.6237	2.1973	0.46483	0.68187	0.58955	0.056247	0.84656
66	8.0802	4.8948	0.15618	1902.7	2.4911	1.6189	0.68036	0.33279	0.84721	0.72827	0.058062
67	7.5176	6.0288	-0.04535	1947.4	2.9073	0.77816	0.33359	0.58683	0.055556	0.78499	0.72763
68	6.292	4.6899	0.21756	1876.5	2.1063	0.98331	0.5888	0.84941	0.72882	0.41564	0.78044
69	7.9056	5.4261	-0.19898	1927.3	1.3901	0.77861	0.84696	0.057968	0.78458	0.79874	0.41834
70	7.6321	5.7935	0.10325	1990.4	2.3218	1.0352	0.059202	0.72741	0.41612	0.26343	0.79713
71	7.3797	5.1016	0.41512	1786.2	0.91759	1.4684	0.72908	0.783	0.79694	0.32595	0.26112
72	6.5261	4.4622	-0.90291	1957.5	1.9062	1.2751	0.78309	0.41711	0.26183	0.21814	0.32885
73	7.6682	5.2846	0.2696	1971.2	3.0586	1.4506	0.41849	0.79753	0.3285	0.57109	0.21954
74	5.9958	3.9643	0.33449	1893.6	0.90317	1.5424	0.79539	0.26215	0.21556	0.051789	0.57407
75	6.3393	4.9391	-0.0988	1974.5	2.5336	2.6217	0.26288	0.32672	0.57298	0.10611	0.052027
76	7.6319	5.9195	0.3558	1860.1	2.769	2.1371	0.32568	0.21746	0.053163	0.40591	0.10719
77	5.7279	2.9262	-0.2854	1874.8	1.2181	0.7788	0.21624	0.57483	0.10741	0.91972	0.40777
78	7.3452	5.4588	-0.20391	1849.7	2.8383	2.0286	0.57311	0.052277	0.40829	0.8908	0.91655
79	7.8172	5.6723	-0.33597	1924.3	0.90379	1.6683	0.05449	0.10898	0.91926	0.19459	0.89262
80	7.2748	4.293	0.088795	1785.3	0.90398	1.9847	0.10825	0.4085	0.89123	0.87371	0.19373
81	13.835	5.7162	-0.95629	1813.8	0.90365	2.8559	0.40932	0.91507	0.19271	0.66865	0.87036
82	6.9084	3.6944	-0.46886	1891.7	1.847	0.77807	0.91592	0.89045	0.87402	0.022481	0.66851
83	6.2653	3.9482	-0.11054	2018.2	0.90316	1.5616	0.89293	0.19045	0.66901	0.23693	0.024774
84	5.4962	3.5414	0.57263	2006.8	0.90333	0.77854	0.19004	0.87062	0.023309	0.091047	0.2352
85	7.7176	4.87	0.47059	1842.7	1.1819	1.0206	0.87302	0.66938	0.2368	0.26906	0.091802
86	5.916	2.9113	-0.3659	1998.4	3.3469	1.7082	0.6656	0.024152	0.090667	0.54398	0.26823
87	5.885	3.1148	0.44164	1944.2	3.2399	0.77803	0.023333	0.23528	0.26661	0.41455	0.54303
88	6.5153	4.2502	0.19729	1751.8	0.90358	2.5253	0.23803	0.090919	0.54429	0.52672	0.41381
89	18.883	6.1699	-1.2709	1853.8	3.1498	1.1287	0.093541	0.26709	0.4112	0.6066	0.52874
90	7.4636	6.0913	-0.31499	1806.3	2.2535	0.77822	0.26696	0.54419	0.52817	0.94606	0.60614
91	5.5562	3.4321	-0.57236	1861.2	0.90307	1.0671	0.54172	0.41108	0.60997	0.86265	0.94816
92	15.126	6.0081	-0.27432	1917.9	0.90372	0.77868	0.41491	0.52686	0.94891	0.12263	0.86301
93	7.5253	5.2247	0.050354	1892.7	0.90328	1.3907	0.52942	0.60533	0.86005	0.84008	0.12295
94	6.0635	2.2972	-0.10337	1915.2	0.9038	1.9143	0.60947	0.9471	0.12418	0.70779	0.84136

real. #	KDUVO	KDUAL	GWSPD	BULKDEN SITY	CORAL	CORVO	SRC4Y	SRC4X	SRC3X	SRC2Y	SRC2X
95	6.1259	3.6118	0.032758	1931.1	1.7069	0.90439	0.94625	0.86346	0.84482	0.83642	0.70974
96	6.019	3.0688	0.13087	2035.9	1.2067	2.0823	0.86403	0.12324	0.70673	0.9929	0.83838
97	6.7596	3.7298	0.73013	1995.7	1.6498	0.77824	0.12021	0.84037	0.83719	0.014448	0.9937
98	6.65	4.7642	0.43066	1819	1.9956	1.3968	0.84499	0.70858	0.99258	0.62177	0.010011
99	7.1823	4.2707	-0.45167	1988.1	3.4882	2.1656	0.70993	0.83907	0.011816	0.080484	0.62177
100	6.451	4.6949	0.40649	1952.6	3.1045	0.7812	0.83656	0.99291	0.62029	0.25668	0.084052
101	7.4039	4.9982	0.24501	1986.7	0.90337	0.77897	0.99369	0.011109	0.084139	0.74363	0.25783
102	7.4767	6.296	0.40263	2096.8	3.03	0.77829	0.012139	0.6206	0.25558	0.008536	0.74421
103	7.0457	5.9683	0.9646	1736.1	2.4303	1.7389	0.62312	0.083331	0.74082	0.93232	0.008844
104	5.7161	3.1765	-1.3741	1934.3	2.9977	0.77877	0.082851	0.25726	0.005755	0.32377	0.93333
105	5.9557	5.8845	0.14663	1800.5	3.6849	1.4182	0.25651	0.74433	0.93264	0.031595	0.32274
106	6.9747	5.3933	-0.65556	1859.7	0.90304	1.0833	0.74383	0.008921	0.32254	0.28928	0.032629
107	8.938	5.8838	-0.29014	1960.3	2.0719	2.503	0.007082	0.93162	0.032139	0.10235	0.28732
108	11.561	8.4623	0.28677	1711.5	0.90325	2.5914	0.9343	0.32226	0.28774	0.48315	0.10135
109	6.12	1.9755	-1.4049	2027.8	0.90377	2.6724	0.32398	0.033875	0.10227	0.82137	0.48128
110	6.9574	5.0698	0.65206	1874.1	2.5889	2.7358	0.034804	0.28617	0.48419	0.20142	0.82385
111	5.7228	3.0312	-0.2145	1765.8	0.90302	0.8074	0.28713	0.10452	0.82206	0.85408	0.20133
112	5.5625	3.6783	-1.1351	1866.8	3.4201	1.0809	0.10321	0.48255	0.20087	0.03713	0.85191
113	7.3147	5.5068	-0.25443	1811.7	0.90397	1.1169	0.48009	0.82013	0.85325	0.48798	0.038156
114	6.3164	1.9046	-0.47282	1906.2	0.9031	1.0955	0.82478	0.20143	0.036873	0.86745	0.48608
115	7.5921	6.2268	-0.02221	1981.5	0.90386	1.1662	0.20399	0.85208	0.48667	0.15011	0.86707
116	5.6012	3.9339	0.38733	1845.1	0.90331	1.7033	0.85464	0.036304	0.86896	0.14649	0.15383
117	1.2364	2.4753	-0.35313	1991.5	1.4715	1.2305	0.038431	0.48549	0.15269	0.041893	0.14705
118	6.6036	3.7894	0.42255	1773.4	2.934	2.2435	0.4888	0.86597	0.1496	0.76799	0.042585
119	5.6675	3.1009	-1.0969	1907.4	0.90361	2.4104	0.86947	0.1505	0.041331	0.11687	0.76983
120	8.0168	4.5391	-0.01547	1997.7	3.0755	1.434	0.15471	0.14696	0.76917	0.50225	0.11804
121	7.805	5.8264	0.4368	1830.6	0.90311	1.0568	0.1482	0.041927	0.11919	0.29972	0.50172
122	7.3702	3.4667	-0.41438	1827.8	1.4778	0.77813	0.043749	0.76965	0.50249	0.92993	0.29938
123	6.7213	5.929	-0.41778	1776.7	3.1256	2.3797	0.76795	0.11768	0.29931	0.94398	0.92995
124	4.3306	2.6339	-1.0303	1966.5	0.90346	1.7621	0.11763	0.50186	0.92988	0.9591	0.94279
125	6.2064	4.5436	0.31744	1818.1	0.90345	1.5484	0.50125	0.29969	0.9417	0.9723	0.95904
126	7.6523	5.9877	-0.45746	1910.2	0.90312	1.3264	0.29829	0.92712	0.95959	0.16336	0.9735

real. #	KDUVO	KDUAL	GWSPD	BULKDEN SITY	CORAL	CORVO	SRC4Y	SRC4X	SRC3X	SRC2Y	SRC2X
127	5.563	3.2852	0.001514	1868.8	2.6949	1.3193	0.92626	0.94495	0.97011	0.29355	0.16075
128	6.1336	3.2702	-0.24028	2024.4	0.90336	2.4598	0.94317	0.95688	0.16089	0.31924	0.29198
129	6.3297	2.6876	0.63084	2032.1	1.5522	0.77853	0.95718	0.97024	0.29356	0.30068	0.31688
130	8.0247	5.6069	0.70954	2044.3	0.9039	2.7802	0.97338	0.16089	0.31924	0.34894	0.30226
131	5.8546	3.1558	0.77432	2060.7	3.4028	2.2586	0.16471	0.29112	0.30169	0.73742	0.34723
132	6.8369	4.6179	0.8669	1834	3.4585	1.6053	0.2919	0.31659	0.34685	0.38542	0.73879
133	7.0371	3.8323	-0.40523	1867.7	3.5324	0.86487	0.31639	0.30034	0.7382	0.8844	0.38707
134	8.0813	6.22	-0.24736	1873.1	3.5873	1.5948	0.30114	0.34737	0.38911	0.91417	0.88103
135	7.7775	6.2657	-0.21795	1869.7	0.9035	0.84208	0.34709	0.7389	0.8827	0.51527	0.91491
136	8.0432	6.5706	-0.23599	1879.7	0.90388	2.6439	0.73959	0.38723	0.91191	0.27739	0.51637
137	7.1933	7.4878	-0.18222	1959.9	0.90395	0.77896	0.3856	0.88123	0.51821	0.01555	0.27512
138	5.4294	3.3293	0.28472	1888.1	0.90392	1.721	0.8846	0.91276	0.27884	0.90859	0.015142
139	7.4959	3.8249	-0.13344	2003.3	0.96295	0.77857	0.91058	0.51807	0.019829	0.78559	0.9075
140	7.0592	3.9127	0.45875	2015.8	2.5618	0.96496	0.51863	0.27877	0.90669	0.61248	0.78753
141	5.8007	3.847	0.55231	1913.2	1.1215	1.7325	0.27928	0.018004	0.78506	0.44553	0.6123
142	6.8881	4.0184	0.022971	1864.3	3.212	1.0603	0.017035	0.90513	0.61484	0.44206	0.44827
143	7.4777	5.5041	-0.26788	1747.7	3.339	1.6273	0.90617	0.7874	0.44935	0.92037	0.44137
144	7.7513	4.1826	-1.319	2012.9	1.6067	1.4599	0.78778	0.61244	0.44289	0.077399	0.92211
145	7.312	6.0396	0.51974	1971.7	0.90383	1.4942	0.61002	0.44738	0.92177	0.9795	0.075209
146	14.261	6.1585	0.34072	1931.8	0.90305	0.9128	0.44868	0.44026	0.078919	0.88632	0.9771
147	6.8555	4.6736	0.13291	1900.1	3.3213	1.2546	0.44447	0.92422	0.97874	0.65608	0.88741
148	6.0243	3.7619	-0.06401	1898.7	2.7905	2.8905	0.92373	0.077673	0.88803	0.18793	0.65881
149	5.5135	2.0896	-0.07036	2019.6	2.0286	1.2974	0.076063	0.97623	0.65712	0.646	0.1872
150	10.004	6.1315	0.60144	1800.4	1.3319	0.95621	0.977	0.88897	0.18621	0.17963	0.6468
151	7.2786	5.6864	-0.70644	2065.3	1.3096	2.1114	0.88659	0.65894	0.64638	0.9533	0.17576
152	7.0625	5.0306	0.88838	2004.3	3.3771	1.6455	0.65842	0.18734	0.17977	0.14185	0.9527
153	7.3807	4.394	0.46244	1941.7	0.90323	0.77801	0.18664	0.64891	0.95287	0.75049	0.14379
154	5.5048	4.3793	0.1871	1840.8	3.6119	1.6096	0.64507	0.17691	0.14233	0.086316	0.75248
155	7.5409	6.1992	-0.37093	1939.2	3.2128	1.7536	0.17711	0.95118	0.75482	0.23203	0.087912
156	6.3404	2.9992	0.17419	1838.4	2.2216	0.88998	0.95059	0.14242	0.086579	0.7641	0.23087
157	6.1266	7.8565	-0.38192	2039.2	0.90356	1.2436	0.14252	0.75409	0.23232	0.28118	0.76162
158	6.9607	6.0621	0.75051	1826.1	2.1818	1.6866	0.75153	0.088803	0.76344	0.67984	0.28492

real. #	KDUVO	KDUAL	GWSPD	BULKDEN SITY	CORAL	CORVO	SRC4Y	SRC4X	SRC3X	SRC2Y	SRC2X
159	8.1312	5.1999	-0.42699	1963.6	0.90353	1.6433	0.08683	0.2337	0.28051	0.53945	0.67884
160	5.6327	3.4208	0.29815	1803.9	3.5015	2.797	0.23407	0.76141	0.67786	0.56739	0.53767
161	7.5186	5.1585	-0.61352	1852.5	0.90344	1.3361	0.76128	0.2824	0.53504	0.20679	0.5676
162	7.238	3.3742	-0.3168	1966.2	2.6324	1.4226	0.28348	0.67679	0.56754	0.4036	0.20555
163	8.0541	6.3283	0.31264	1864.5	0.90326	1.4115	0.6774	0.5359	0.20907	0.99995	0.40382
164	1.2445	3.2461	-0.26077	1945.8	0.9037	1.4326	0.53853	0.56976	0.40303	0.42927	0.99514
165	7.6782	5.5608	0.21202	1917.8	2.6793	1.4902	0.56716	0.20581	0.99747	0.22505	0.42972
166	4.29	3.0393	0.042953	1923.5	0.90386	1.5815	0.20914	0.40267	0.42578	0.85881	0.22675
167	7.0772	3.5934	0.082558	1846.9	2.304	0.85035	0.40148	0.99633	0.22882	0.69465	0.85692
168	8.1091	5.5989	-0.3463	1890.8	1.6854	1.4043	0.99946	0.429	0.85968	0.002816	0.69442
169	6.5584	3.7778	-0.11436	2150	1.8197	1.1554	0.42931	0.22809	0.69398	0.66467	0.004499
170	7.6312	5.2625	0.9848	1896.2	0.90363	0.77864	0.22617	0.85547	0.000323	0.77513	0.66304
171	6.7437	4.737	-0.08534	1851.6	1.1755	0.77818	0.85851	0.69354	0.66257	0.19757	0.77725
172	5.6544	4.8472	-0.32558	1992.9	3.6966	1.6616	0.69111	0.003257	0.77945	0.39292	0.19571
173	6.0848	3.487	0.42615	1949.6	1.2557	1.5596	0.003656	0.66345	0.19765	0.72304	0.3905
174	10.67	4.2364	0.23043	1675.6	0.90369	1.1742	0.66204	0.77506	0.39062	0.68608	0.72139
175	19.991	8.772	-1.4274	1942.6	3.1009	1.3104	0.77547	0.19838	0.72232	0.98368	0.68895
176	5.7069	4.3221	0.1918	1969.8	2.3748	1.2113	0.19977	0.39453	0.68752	0.45485	0.98231
177	5.8428	3.5686	0.32826	1844.1	0.903	1.2221	0.39164	0.72283	0.98031	0.50929	0.45473
178	14.033	5.9529	-0.36243	1888.8	2.2491	2.6986	0.72173	0.68745	0.45427	0.49792	0.50512
179	6.969	5.3194	-0.1308	1955.7	2.7377	2.7263	0.68811	0.98268	0.5089	0.51067	0.49559
180	4.8706	1.7248	0.26453	1948.5	0.90359	0.77843	0.98291	0.45113	0.49716	0.56127	0.51465
181	7.2743	5.2177	0.22384	2076	1.14	1.249	0.45143	0.50761	0.51411	0.63635	0.56495
182	14.003	5.6477	0.90461	1900.3	2.4991	0.77886	0.50641	0.4978	0.56414	0.18298	0.63987
183	5.5135	3.4549	-0.05683	1911.2	2.3608	1.9716	0.49998	0.51184	0.63908	0.49347	0.18035
184	7.4711	4.1951	0.010673	1909.7	3.6328	1.9303	0.51124	0.56314	0.18468	0.33757	0.49318
185	6.7534	5.4358	-0.00257	1912.2	1.3576	1.3653	0.56096	0.63868	0.49378	0.095147	0.339
186	7.6828	5.3098	0.015309	1922.2	1.5741	0.77876	0.63832	0.18425	0.33664	0.02893	0.098947
187	8.1434	7.9127	0.072474	1937	1.5171	0.98742	0.18035	0.4943	0.0968	0.70491	0.029299
188	6.7702	4.4289	0.16452	1839.5	1.5859	1.8086	0.49056	0.33741	0.026781	0.61604	0.70419
189	7.4674	4.637	-0.37947	1909	1.7945	0.77888	0.33874	0.096534	0.70431	0.35289	0.61966
190	6.9612	4.5943	-0.00717	1877.3	2.1272	1.6963	0.096831	0.029759	0.61591	0.43939	0.35146

real. #	KDUVO	KDUAL	GWSPD	BULKDEN SITY	CORAL	CORVO	SRC4Y	SRC4X	SRC3X	SRC2Y	SRC2X
191	6.5706	4.6492	-0.19088	1809	0.90355	1.1569	0.028917	0.70069	0.35311	0.37338	0.43794
192	6.4819	4.8274	-0.50508	1763.2	1.5065	0.77832	0.70456	0.6185	0.43943	0.38091	0.37255
193	6.2727	5.1259	-1.2166	1951.2	0.921	1.7169	0.61513	0.35035	0.37237	0.96251	0.38203
194	2.3318	3.4099	0.23869	1933.3	0.9033	2.5605	0.35362	0.43951	0.38267	0.96816	0.96337
195	6.6827	4.5729	0.13794	1880	0.90309	1.4774	0.43658	0.37213	0.96475	0.063027	0.96716
196	6.4829	3.9869	-0.176	1897.5	2.4068	1.766	0.37128	0.38098	0.96775	0.39953	0.061097
197	5.7686	3.0866	-0.07449	1884.9	2.0457	1.2188	0.38369	0.964	0.061914	0.1285	0.3971
198	6.1081	2.3548	-0.15273	1887.1	0.98501	1.6249	0.96476	0.96823	0.39947	0.83442	0.12711
199	6.5657	5.3679	-0.14182	2047.7	1.3082	1.601	0.96697	0.061409	0.12965	0.82773	0.83158
200	6.7453	5.0355	0.79534	2055	1.0649	1.5667	0.061482	0.39772	0.83314	0.46639	0.82855

real. #	SRC3Y	SRC1Y	SRC1X	HAVO	LDISP	KDRAVO	KDRAAL	KD_PU_VO	KD_PU_AL	KD_PU_C0L
1	0.83233	0.24005	0.80624	17.732	1.9903	812.85	440.3	109.47	108.87	4.8775
2	0.82718	0.80526	0.13308	4.6087	1.6863	438.05	704.33	129.6	92.939	5.0531
3	0.46566	0.13442	0.73247	12.27	1.0289	707.27	688.4	38.71	77.02	4.2620
4	0.11361	0.73275	0.34383	3.2112	0.54985	688.19	663.39	79.503	109.71	4.5371
5	0.24003	0.34009	0.049709	7.6813	2.4022	663.62	323.7	93.181	124.51	4.2375
6	0.80576	0.046205	0.7459	6.9906	2.2194	321.01	742.97	102.03	100.9	4.3941
7	0.13452	0.74864	0.93901	6.0614	1.7185	741.48	430.16	101.08	112.08	5.1399
8	0.73186	0.93694	0.55457	2.18	1.8825	429.34	525.79	96.651	94.367	4.2041
9	0.34145	0.55106	0.79371	9.1734	1.7536	526.19	626.36	116.43	106.1	4.6918
10	0.047266	0.79274	0.37606	3.1527	1.7716	626.1	256.08	94.687	105.03	5.1004
11	0.74875	0.37598	0.67186	3.965	3.3158	255.36	346.45	94.86	104.08	4.8134
12	0.9384	0.67431	0.65349	4.8648	3.4105	344.48	252.75	107.78	89.193	3.8495
13	0.55426	0.65427	0.62915	1.5987	0.85794	250.6	293.32	122.12	107.76	5.3892
14	0.79285	0.62833	0.24857	2.3803	1.8079	289.57	644.32	104.11	93.974	4.9578
15	0.37977	0.24591	0.71151	1.5328	1.1538	644.32	240.83	58.263	97.825	3.8205
16	0.67304	0.71226	0.36864	1.9111	2.7247	241.27	425.57	112.1	102.21	5.5740
17	0.65016	0.36852	0.47149	5.1696	2.7109	426.26	632.99	96.424	85.471	4.6028
18	0.62547	0.47303	0.58007	1.4755	1.9399	631.8	489.65	114.56	90.109	4.8036
19	0.24894	0.58477	0.17326	3.117	1.099	489.47	166.43	98.307	85.408	4.6142
20	0.71268	0.17148	0.2719	4.9406	1.4758	166.72	727.65	109.97	87.421	5.1106
21	0.36671	0.27358	0.16723	3.6422	2.6485	726.02	580.16	67.302	102.9	4.9749
22	0.47389	0.16561	0.2131	0.74358	1.1613	578.39	161.12	123.13	84.683	4.4990
23	0.58452	0.21367	0.60303	8.6622	2.4699	159.62	829.77	91.467	93.664	5.2601
24	0.17185	0.60264	0.15762	4.4577	1.6923	830.57	376.18	96.067	102.68	4.8586
25	0.27162	0.15986	0.36181	0.70371	0.73272	375.4	481.98	91.381	96.375	4.6846
26	0.16981	0.36202	0.59096	13.014	2.4972	479.18	381.72	96.797	79.051	5.5658
27	0.21102	0.59494	0.43437	2.6796	3.1595	381.7	638.55	129.53	107.22	5.6739
28	0.60015	0.43132	0.070798	3.5794	2.1024	638.67	590.61	90.95	100.17	4.4166
29	0.15677	0.070876	0.69583	2.6814	2.615	593.85	328.84	112.58	78.996	5.5237
30	0.36158	0.69708	0.53266	4.9996	1.7618	326.95	678.7	108.37	113.21	5.4983

real. #	SRC3Y	SRC1Y	SRC1X	HAVO	LDISP	KDRAVO	KDRAAL	KD_PU_VO	KD_PU_AL	KD_PU_C0L
31	0.59138	0.53117	0.065333	4.5813	2.3314	677.42	509.58	94.841	91.582	4.9849
32	0.43049	0.068262	0.81193	2.2104	2.2912	511.98	422.18	90.197	96.013	4.1083
33	0.074454	0.81122	0.30876	6.6744	2.2459	422.1	820.66	58.974	91.679	5.9685
34	0.6978	0.3088	0.42281	3.8414	1.4862	822.12	909.44	110.04	102.71	4.8878
35	0.53021	0.42103	0.3129	3.0765	2.4162	909.46	300.12	126.65	100.7	5.6821
36	0.068291	0.31034	0.59624	12.605	1.7497	298.61	796.55	93.625	89.246	5.0253
37	0.81435	0.59788	0.5451	16.073	1.9504	794.22	779.79	103.89	104.64	5.6522
38	0.30796	0.54611	0.25403	1.9833	2.1609	779.57	599.93	120.88	97.323	4.9442
39	0.42208	0.25262	0.64219	11.416	1.2938	599.68	224.14	73.613	93.554	5.4314
40	0.31087	0.64499	0.45689	10.91	1.5451	222.51	987.6	191.27	112.55	5.5843
41	0.59771	0.45948	0.35958	4.6453	1.2728	987.07	529.6	124.49	119.63	5.2355
42	0.54692	0.35889	0.80226	1.2839	1.4037	530.28	914.05	93.929	87.977	4.8650
43	0.2541	0.80481	0.89657	19.479	2.1923	910.33	620.16	179.01	110.89	5.3636
44	0.64387	0.89955	0.2211	4.0008	1.2504	620.04	891.15	124.42	110	4.6416
45	0.45648	0.22056	0.77458	16.385	1.7351	891.41	571.89	54.883	101.28	5.0719
46	0.35594	0.77106	0.75751	4.8125	2.1801	571.12	746.07	106.71	83.562	5.6180
47	0.8044	0.75705	0.55876	15.444	1.8744	747.9	837.75	111.76	135.96	3.7922
48	0.89716	0.55861	0.13615	4.3716	0.91376	835.64	667.68	91.97	98.093	5.4487
49	0.22083	0.1361	0.98634	9.4864	2.3907	670.09	514.51	98.776	120.19	5.5328
50	0.7728	0.98683	0.4783	13.063	2.0576	514.64	715.01	126.99	102.03	4.7887
51	0.75745	0.47635	0.90182	6.2683	0.88603	712.87	399.44	83.962	118.01	5.5539
52	0.5575	0.90124	0.57823	3.9013	2.6678	399.58	628.62	112.43	99.752	4.5138
53	0.13948	0.57826	0.87579	8.0909	1.6269	627.55	864.64	126.74	107.99	4.6338
54	0.9886	0.87902	0.52465	2.8593	1.849	864.15	150.75	258.23	113.65	4.4139
55	0.47636	0.52426	0.71777	4.9025	1.6384	151.12	756.56	118.39	104.29	5.0128
56	0.90226	0.71853	0.81891	14.232	2.1894	754.26	803.41	127.89	97.509	3.7624
57	0.57565	0.81586	0.63343	0.60484	2.0898	806.44	474.02	128.39	106.51	3.9613
58	0.87726	0.63481	0.46333	9.816	1.5057	476.79	818.8	83.831	92.659	4.7692
59	0.52271	0.46349	0.68074	11.868	2.2752	818.62	336.85	88.254	102.42	5.6955
60	0.71539	0.68244	0.33489	3.5262	1.9216	336.49	394.56	122.77	115.57	5.6712
61	0.81858	0.33278	0.58895	12.424	1.7264	394.68	294.57	81.37	78.053	4.3374
62	0.63424	0.58517	0.84543	2.2896	2.6399	296.99	615.74	100.52	108.66	5.6464

real. #	SRC3Y	SRC1Y	SRC1X	HAVO	LDISP	KDRAVO	KDRAAL	KD_PU_VO	KD_PU_AL	KD_PU_C0L
63	0.46136	0.84982	0.056311	2.8305	2.956	613.08	148.46	121.59	111.49	5.3243
64	0.68066	0.057841	0.72978	1.9279	1.426	145.92	195.85	75.673	95.797	3.5267
65	0.33153	0.72969	0.78261	4.7985	2.5599	198.3	467.99	108.21	112.44	4.4555
66	0.58726	0.78325	0.4167	0.53612	2.5179	465.66	924.72	96.256	89.718	3.9177
67	0.84941	0.41653	0.79797	1.0404	2.1075	926.22	903.86	105.75	92.376	4.5297
68	0.058578	0.79803	0.26066	3.4568	1.1735	903.5	273.95	102.44	87.717	4.9694
69	0.728	0.26347	0.32972	16.911	3.6979	272.15	883.85	45.587	101.83	4.7835
70	0.78038	0.32548	0.21687	16.014	1.9618	885.32	702.03	43.519	77.264	4.9502
71	0.41596	0.21798	0.57346	1.7511	2.9809	700.89	121.54	105.41	81.802	5.1614
72	0.79808	0.57228	0.054074	15.225	2.1481	119.34	314.87	94.86	95.495	5.8209
73	0.26002	0.052024	0.10657	7.5336	2.8736	311.66	183.97	108.3	121.95	5.6385
74	0.32626	0.10795	0.40776	0.24534	2.039	183.08	339.8	114.71	119.24	4.0269
75	0.21674	0.40841	0.91631	2.0967	2.4268	339.18	589.62	63.997	86.459	5.6138
76	0.57425	0.91592	0.89188	0.92987	2.6786	588.04	473.21	128.28	117.71	5.4099
77	0.053163	0.89356	0.19002	2.3237	2.2583	471.84	575.22	84.112	105.81	5.6053
78	0.10825	0.19055	0.87486	4.5209	1.933	572.68	648.88	112.64	73.738	5.9754
79	0.40749	0.87385	0.66564	3.5023	2.361	646.51	950.64	76.018	88.667	3.3825
80	0.91533	0.66936	0.024592	4.4069	1.6742	952.86	877.79	15.936	80.824	5.1987
81	0.89182	0.024802	0.238	5.2885	2.1683	877.91	212.04	90.958	89.887	3.8823
82	0.19247	0.23768	0.092733	18.024	2.7659	208.9	860.23	125.16	100.63	4.5064
83	0.8716	0.093798	0.2697	14.834	0.82441	860.11	736.5	93.682	95.705	5.4698
84	0.66663	0.26782	0.54484	1.1753	2.4578	738.68	855.93	123.3	100.03	3.2578
85	0.022039	0.54487	0.41286	14.054	2.5864	854.64	993.11	113.89	103.17	5.7672
86	0.23834	0.41297	0.5255	9.0438	1.8464	994.47	110.54	118.18	126.14	4.6235
87	0.09303	0.52693	0.60617	13.953	2.6304	110.62	659.13	299.8	116.81	3.6374
88	0.26994	0.6098	0.94768	19.747	1.5209	658.39	174.16	120.3	82.794	4.5614
89	0.54397	0.94692	0.8623	0.17871	1.6666	172.55	331.74	120.44	115.37	3.9564
90	0.41441	0.86116	0.12201	5.8295	1.4188	329.82	767.45	106.38	107.69	4.8941
91	0.52656	0.12189	0.84487	0.84378	2.1415	766.83	108.83	104.64	115.02	5.5922
92	0.60929	0.84095	0.70556	2.267	0.76916	108.02	939.97	177.71	139.22	4.3696
93	0.94947	0.70568	0.83988	10.333	1.062	937.88	389.58	100.55	71.507	5.6284
94	0.8607	0.83864	0.99131	0.11614	1.8277	388.79	129.98	92.897	103.93	3.6732

real. #	SRC3Y	SRC1Y	SRC1X	HAVO	LDISP	KDRAVO	KDRAAL	KD_PU_VO	KD_PU_AL	KD_PU_C0L
95	0.12496	0.99254	0.012151	17.474	3.0474	127.83	358.17	113.61	80.093	4.8986
96	0.84424	0.014322	0.6206	2.7787	2.9291	359.12	191.36	125.2	89.546	5.6454
97	0.70863	0.62212	0.081579	0.34647	1.3502	192.1	534.33	123.97	109.3	4.1823
98	0.83814	0.081611	0.25537	2.5184	2.8488	534.89	840.2	69.572	68.715	4.1468
99	0.99153	0.25963	0.74219	1.0399	2.3268	841.52	281.38	118.18	124.07	3.7073
100	0.01084	0.74266	0.00638	4.0701	0.4986	282.1	868.25	94.204	92.211	5.5092
101	0.6226	0.008537	0.9333	13.369	1.4611	866.27	135.17	33.92	74.655	3.9941
102	0.082755	0.93024	0.32214	1.8159	1.0042	131.91	540.77	81.289	90.751	4.9205
103	0.25772	0.32134	0.031583	14.474	1.5392	539	882.9	17.356	81.538	4.5873
104	0.74379	0.031874	0.28828	0.39787	2.0766	880.48	236.85	95.217	98.315	5.7497
105	0.0066	0.28693	0.10244	4.0921	1.833	238.35	232.4	121.57	113.88	5.8007
106	0.9304	0.10181	0.48385	14.975	2.0524	232.95	136.31	34.896	86.943	5.8716
107	0.32214	0.48365	0.82219	1.4235	2.2089	139.73	790.5	109.12	116.02	5.9238
108	0.034931	0.82127	0.20133	1.3614	3.2142	789.56	205.25	16.508	75.807	4.2303
109	0.28848	0.20343	0.85064	0.47523	2.8115	204.97	554.05	83.719	98.454	4.5744
110	0.10153	0.85494	0.037852	11.212	1.131	552.51	367.97	106.86	117.35	4.6150
111	0.48488	0.039425	0.48927	1.1337	2.7541	369.82	936.25	54.043	84.514	4.5945
112	0.82181	0.48703	0.86816	4.2122	2.4064	935.32	947.4	101.16	84.306	4.6692
113	0.20309	0.86964	0.15423	2.581	2.735	949.48	963.04	98.817	76.071	5.4624
114	0.85318	0.15153	0.14775	17.239	3.9162	960.13	975.53	126.69	110.59	4.7348
115	0.037029	0.14723	0.043615	17.784	0.28545	973.13	244.95	80.878	82.558	5.6580
116	0.48919	0.044629	0.76977	18.48	2.2311	247.87	362.6	120.8	98.991	5.6920
117	0.86816	0.76877	0.11639	19.016	0.96482	361.16	385.18	93.073	91.229	4.9390
118	0.15324	0.11722	0.50208	1.5062	1.5153	386.4	373.33	121.41	123.17	4.5446
119	0.14901	0.50107	0.29533	2.5563	2.4838	370.58	412.47	115.09	124.87	3.4129
120	0.042737	0.29727	0.92996	2.7567	0.24038	414.2	765.76	96.594	127.87	5.6875
121	0.76893	0.92623	0.94325	2.6167	3.1079	763.07	449.47	204.67	130.96	5.5441
122	0.11682	0.94167	0.9558	2.9723	1.6573	450.84	893.8	98.19	85.118	5.1761
123	0.50185	0.95667	0.97337	10.141	0.63252	896.39	919.94	90.724	90.898	4.8374
124	0.29877	0.97469	0.16451	3.2972	1.5766	920.24	564.89	81.361	92.057	4.8294
125	0.9262	0.16335	0.29046	15.653	1.0562	566.15	347.78	105.17	91.285	5.7118
126	0.94249	0.29347	0.31994	16.673	1.963	349.81	116.51	94.688	93.119	3.8728

real. #	SRC3Y	SRC1Y	SRC1X	HAVO	LDISP	KDRAVO	KDRAAL	KD_PU_VO	KD_PU_AL	KD_PU_C0L
127	0.95651	0.31629	0.30057	4.3587	2.6953	115.03	915.08	98.763	109.14	5.9370
128	0.97227	0.30062	0.34665	2.4069	1.3783	917.36	808.56	120.32	94.609	5.6665
129	0.16375	0.34816	0.73806	0.20749	2.7931	807.17	653.26	56.345	118.5	5.3010
130	0.2908	0.73514	0.38982	16.487	0.64424	650.78	504.69	122.96	121.56	4.3202
131	0.31825	0.38902	0.88375	12.122	1.9739	502.29	497.53	96.43	99.609	5.2718
132	0.30346	0.8811	0.91445	5.5165	2.8316	497.26	928.08	109.77	90.397	4.2901
133	0.34536	0.91351	0.51775	3.7934	1.2279	932.09	167.74	96.177	71.682	5.8432
134	0.73979	0.51891	0.27618	3.7533	1.2149	170.49	978.15	63.713	120.69	4.1248
135	0.38918	0.27944	0.017364	17.149	0.71527	981.81	900.52	33.543	111.8	5.4871
136	0.88142	0.018064	0.90692	0.80096	2.5438	899.31	692.85	106.49	103.46	3.9044
137	0.91369	0.90812	0.78832	19.129	1.1016	691.49	268.16	89.996	96.932	4.4487
138	0.51854	0.78574	0.61055	15.729	2.0081	266.74	684.08	122.92	96.697	5.5024
139	0.27967	0.61066	0.44885	7.1148	1.6021	682.82	261.21	108.67	122.43	4.5558
140	0.018437	0.44944	0.44473	1.6814	3.1047	259.8	957.8	62.316	79.558	5.3464
141	0.90992	0.44492	0.92486	6.8321	3.1925	959.02	228.62	117.29	132.79	4.9658
142	0.78977	0.92496	0.077725	1.6259	3.2736	228.36	778.38	115.04	118.79	4.9995
143	0.61162	0.077621	0.97922	18.18	3.4137	776.75	180.78	105.11	105.23	4.3784
144	0.44672	0.97709	0.88689	1.3552	1.2599	177.45	308.05	97.168	86.269	4.7661
145	0.44483	0.88694	0.65537	10.812	1.5851	307.83	787.18	29.899	104.91	5.9886
146	0.92381	0.65965	0.18644	0.89423	1.6389	788.47	355.4	94.639	85.829	4.8111
147	0.077437	0.18566	0.64725	2.0794	1.6102	354.67	709.36	126.18	127.33	4.4372
148	0.97688	0.64518	0.17796	11.024	1.7018	710.03	584.97	112.95	83.89	5.6345
149	0.88764	0.17513	0.95462	2.4793	2.4779	585.05	611.31	110.25	109.74	5.3747
150	0.65902	0.95013	0.14251	7.9905	1.7862	610.1	285.37	52.359	80.593	3.1110
151	0.18671	0.14065	0.75367	4.4803	2.8909	285.78	461.67	21.46	88.309	5.3096
152	0.64903	0.75082	0.085452	4.7229	3.0224	462.78	999.51	114.38	110.43	5.5276
153	0.17695	0.087076	0.23365	1.8713	2.0351	999.67	483.77	93.823	90.563	4.3465
154	0.9512	0.23467	0.76487	3.4203	1.5586	484.97	306.89	113.63	106.18	4.7466
155	0.14091	0.76127	0.2801	19.848	0.38107	306.1	872.4	127.4	100.45	5.4393
156	0.75336	0.28179	0.67652	3.6112	3.0035	871.12	725.39	116.87	101.58	5.3692
157	0.08953	0.67582	0.53817	2.0206	2.5998	721.14	103.99	72.216	87.341	5.9484
158	0.23059	0.53548	0.56945	14.703	2.2116	101.08	695.4	40.23	95.224	4.8526

real. #	SRC3Y	SRC1Y	SRC1X	HAVO	LDISP	KDRAVO	KDRAAL	KD_PU_VO	KD_PU_AL	KD_PU_C0L
159	0.7646	0.56552	0.20822	8.3977	1.8999	698.34	798.89	108.46	148.17	4.9279
160	0.28497	0.20529	0.40255	0.08363	1.8931	798.55	277.25	197.34	96.195	4.9132
161	0.67504	0.40101	0.99992	7.3602	3.0661	275.58	455.23	102.95	88.301	4.9346
162	0.53552	0.99938	0.42575	11.705	0.9365	455.05	748.2	111.1	116.45	4.9929
163	0.56653	0.42685	0.22858	1.7744	3.5397	751.7	720.14	63.445	106.92	5.2455
164	0.20863	0.22935	0.85861	3.3344	2.9012	718.67	983.76	123.47	63.959	4.3054
165	0.40195	0.85843	0.69288	9.6034	2.3059	984.15	509.34	118.65	105.54	4.9098
166	0.99884	0.69375	0.001538	8.2444	1.3307	505.59	556.96	116.61	111.26	4.6501
167	0.4295	0.00151	0.66146	19.375	2.2877	556.95	548.66	68.395	86.894	3.9386
168	0.22599	0.66498	0.77751	3.8245	1.3026	547.43	562.63	110.89	94.915	3.5547
169	0.8586	0.77867	0.19755	4.2764	3.2398	561.48	608.45	100.01	108.24	5.4048
170	0.69437	0.1954	0.39244	4.1922	1.1982	608.46	671.99	99.386	106.64	5.1931
171	0.001231	0.39299	0.72459	4.3053	2.514	671.82	265.99	231.89	134.49	4.6748
172	0.6606	0.72016	0.68846	4.6899	0.97624	262.5	541.5	120.61	97.076	4.8286
173	0.77628	0.68789	0.98023	6.4311	1.4467	545.05	402.29	113.14	99.164	4.7081
174	0.19637	0.98146	0.45478	1.6777	2.5403	403.25	185.89	54.005	98.867	4.7295
175	0.39311	0.45483	0.50829	4.1271	1.5639	189.74	125.45	122.69	99.409	5.8882
176	0.72453	0.50536	0.49776	2.8941	2.3457	124.24	734.44	100.24	101.46	5.9004
177	0.68917	0.49845	0.51009	0.98473	2.0682	731.22	654.92	95.999	104.55	3.8036
178	0.98396	0.51107	0.56335	0.29817	2.1292	653.57	416.24	116.28	86.075	4.7517
179	0.45418	0.56394	0.63905	8.9345	1.394	416.08	492.31	103.99	98.647	4.0583
180	0.50686	0.6384	0.18176	5.6614	1.8196	493.18	435.53	118.77	92.833	5.6042
181	0.49959	0.18351	0.49236	3.0019	4.0513	437.08	445.56	34.207	81.084	5.5955
182	0.51036	0.49117	0.33981	3.713	1.862	446.28	964.34	104.91	74.407	4.8724
183	0.56418	0.33823	0.098419	3.1858	1.4389	965.64	970.23	124.85	107.46	3.9848
184	0.63522	0.098359	0.029148	3.28	2.8066	970.12	157.45	94.654	103.63	4.4748
185	0.18001	0.028657	0.7049	18.674	2.3825	155.45	458.25	63.226	93.339	5.5682
186	0.49328	0.70242	0.61821	18.723	-0.00165	458.27	216.04	106.68	96.562	4.0889
187	0.33932	0.6174	0.35471	0.66095	2.3105	213.33	848.03	116.92	94.132	5.4564
188	0.095855	0.35206	0.43994	3.3711	2.5777	848.42	845.9	129.27	94.576	4.6564
189	0.025006	0.43563	0.37403	1.2357	1.3627	843.72	521.17	120.76	129.18	3.7290
190	0.70291	0.37478	0.38384	13.799	1.7917	519.67	200.06	120.91	130.24	5.4786

real. #	SRC3Y	SRC1Y	SRC1X	HAVO	LDISP	KDRAVO	KDRAAL	KD_PU_VO	KD_PU_AL	KD_PU_C0L
191	0.61896	0.38398	0.96484	13.577	2.4475	199.43	316.94	103.58	78.41	5.7810
192	0.35329	0.96202	0.96738	3.9583	2.3695	320.09	827.3	114.03	95.042	4.9796
193	0.43628	0.9654	0.062055	1.0922	3.5458	826.09	219	85.037	83.247	5.5478
194	0.37169	0.061335	0.39868	2.1208	1.9109	218.91	760.81	93.183	114.66	4.7098
195	0.38195	0.39667	0.12538	12.783	2.0123	761.17	408.2	93.174	114.11	5.3385
196	0.96264	0.12797	0.83326	1.2474	1.9917	406.69	142.25	106.22	97.678	5.2878
197	0.96574	0.8321	0.82688	9.9052	2.0208	144.67	773.83	28.908	82.048	5.2122
198	0.063634	0.82798	0.46962	2.9301	2.1217	772.31	943.72	93.594	88.773	4.4856
199	0.39766	0.46669	0.11218	0.49962	2.2674	943.38	595.47	114.98	113.09	5.4216
200	0.12612	0.1129	0.24114	10.512	1.3256	596.34	813.08	109.78	83.544	4.6979

real. #	KD_AM_VO	KD_AM_AL	KD_AM_COL	KD_CS_VO	KD_CS_AL	KD_CS_COL	CONC_COL
1	6488.6	5700.9	5.6503	4168	178.08	3.4892	-4.4407
2	7769.2	6721	5.8331	2766.9	799.65	2.9211	-4.4107
3	5702.4	5037	5.9814	5772.4	945	3.0682	-8.7573
4	6712.4	6161.5	5.0086	6542.1	653.54	3.3114	-7.4077
5	5039.6	6078.9	5.4456	5006.4	833.8	2.6497	-8.4926
6	6166.2	5984.6	4.9920	5951.3	521.65	2.8072	-5.4465
7	6096	4478.6	5.2380	4312.3	744.24	2.6360	-5.476
8	5984.4	6343.7	6.0000	5475.1	729.51	2.7197	-7.1382
9	4483.4	4998.1	4.9762	5389.5	710.35	3.3486	-8.5426
10	6347.6	5398.5	5.6375	5296.6	405.6	2.6160	-8.0268
11	5003.5	5816.1	5.9903	3786	773.96	2.9143	-5.6308
12	5395.8	4080.1	5.7619	5640.9	512.41	3.3299	-8.4685
13	5804	4586.6	4.7149	4258.3	596.07	2.9856	-6.0663
14	4084.8	4056	6.3464	4687.9	676.07	2.3959	-7.6293
15	4591.2	4298.1	5.9175	5127.8	330.43	3.4717	-8.8063
16	4071.1	5882.9	4.6899	3493.9	431.82	3.2197	-6.018
17	4312.5	3986.6	6.5623	3882.3	328.73	2.3635	-4.6686
18	5887.7	4981.3	5.5315	3471	371.58	3.5901	-6.7922
19	3997.5	5842.8	5.7451	3656.9	692.74	2.8522	-5.715
20	4964.8	5254.5	5.5465	5206.8	318.51	2.9747	-7.4927
21	5841.3	3352.8	5.9978	3424.7	509.22	2.8589	-6.3092
22	5249.8	6267.7	5.9360	4246.1	684.76	3.3399	-6.3854
23	3350.7	5629.4	5.3838	5164.9	563.37	3.2550	-6.4937
24	6266.9	3265	6.1931	4532.5	211.99	2.7812	-8.015
25	5614	6838	5.8089	3093.9	761.1	3.4056	-6.1406
26	3268.8	4754.3	5.6274	5569	639.2	3.0266	-7.5392
27	6830	5203.4	6.5441	4917.6	203.9	2.9089	-7.1142
28	4752.1	4769.3	6.6739	3067.4	847.86	3.5824	-6.6703
29	5208.6	5863.3	5.2765	6042	461.44	3.6609	-8.3015
30	4760.6	5676.8	6.5011	4035.3	556.39	2.7344	-7.9093

real. #	KD_AM_VO	KD_AM_AL	KD_AM_COL	KD_CS_VO	KD_CS_AL	KD_CS_COL	CONC_COL
31	5868	4504.5	6.4728	4490.8	466.35	3.5520	-8.3327
32	5686.4	6049.8	5.9494	4039.5	688.99	3.5412	-8.1408
33	4496.5	5340.1	4.9233	5173.5	651.93	3.2668	-6.5819
34	6054.1	4946	6.9605	4978.7	411.96	2.5760	-8.3777
35	5335.9	6784.5	5.8382	3800	720.52	3.9447	-7.556
36	4954.1	7395.9	6.6776	5350.2	582.95	3.0918	-6.6373
37	6768.2	4367.7	5.9759	4628	502.03	3.6629	-7.2777
38	7399.6	6606.1	6.6522	4233	839.43	3.3045	-8.7023
39	4349	6544.1	5.9085	5999.7	916.61	3.6457	-6.2199
40	6613.4	5717.4	6.3962	6377.4	383.48	3.2028	-6.8793
41	6556	3873.3	6.5717	3691.6	818.98	3.4953	-8.7381
42	5719.5	8732.1	6.1461	5871.8	808.27	3.5966	-5.5862
43	3858.1	5413.4	5.8195	5824.7	660.06	3.3930	-7.7721
44	8721.8	7419.7	6.3075	5026.1	294.01	3.0345	-7.3063
45	5413.9	5800.7	5.5809	3349.8	991.22	3.4557	-7.745
46	7437.8	7226.2	5.9859	6739.4	598.1	2.8849	-6.6174
47	5796.5	5589.3	6.6128	4704.9	919.06	3.3241	-6.8126
48	7243.6	6357.7	4.6388	6398.1	672.8	3.6195	-7.9985
49	5589.2	6861.8	6.4183	5104.8	899.64	2.3345	-6.4285
50	6364.8	6003.9	6.5159	6302.1	634.71	3.5066	-7.1708
51	6866	5353.2	5.7348	4883.7	777.9	3.5638	-7.5752
52	6008.3	6205.2	6.5366	5656.5	852.87	2.9709	-5.6643
53	5358	4858.7	5.4150	6057.5	712.71	3.5795	-5.0276
54	6218.9	5834.7	5.5775	5310.3	586.49	2.7970	-8.1064
55	4843	7046.9	5.2695	4642.6	750.31	2.8776	-5.8657
56	5831.9	3132.8	5.9717	5519.3	484.63	2.7310	-5.9515
57	7035.9	6410	4.6104	4131	681.99	3.2964	-6.7658
58	3173.9	6675	4.8343	5133.9	873.87	2.3122	-8.4411
59	6397.3	5193.9	5.7110	6175.2	194.82	2.4968	-4.1002
60	6670.5	6733.1	6.6972	3036.4	784.86	2.9609	-7.0941
61	5191.2	4558.9	6.6712	5688.1	825.8	3.6766	-4.9691
62	6755	4836.8	5.1367	5911.1	550.47	3.6582	-6.6998

real. #	KD_AM_VO	KD_AM_AL	KD_AM_COL	KD_CS_VO	KD_CS_AL	KD_CS_COL	CONC_COL
63	4559.2	4322.6	6.6454	4468.5	836.11	2.6876	-5.161
64	4826	5767.5	6.2577	5976.8	421.28	3.6429	-6.9188
65	4342.6	3093.2	4.3501	3837.3	477.44	3.4355	-6.1259
66	5774	3650.4	5.3404	4101.5	378.03	2.1519	-5.5367
67	3112.8	5143.1	4.7901	3677.3	668.9	2.7602	-6.4733
68	3652.9	7554.3	5.4249	5088.1	186.91	2.4561	-7.1524
69	5141.2	7336	5.9355	3018.3	260.88	2.8035	-6.2729
70	7565.7	4199.1	5.7202	3230.6	545.33	3.2382	-7.6777
71	7361.4	7210.9	5.9101	4422.1	931.75	2.9685	-6.6509
72	4211.5	6137.8	6.0374	6460.7	911.36	3.2124	-5.3511
73	7212.3	2536.1	6.8306	6348.8	351.33	3.3517	-8.7724
74	6144.2	4428.3	6.6335	3560.8	896.71	3.6989	-6.0952
75	2583	3502.6	4.8833	6283.9	739.45	3.6343	-5.7992
76	4435.6	4576.3	6.6053	5466.5	142.3	2.5393	-7.3313
77	3519.2	5666.3	6.3674	1332.8	399.64	3.6162	-5.6828
78	4580.1	5162	6.5966	3743.7	241.47	3.4880	-7.9519
79	5656.1	5596.2	6.9741	3163.1	426.23	3.6116	-7.6875
80	5172.4	5914	4.2386	3858.5	647.46	3.9614	-8.1309
81	5609.8	7944.5	6.1038	4957.3	550.07	2.0951	-6.7135
82	5912.4	7132.6	4.7531	4448.8	634.96	3.3796	-8.7844
83	7914.7	3773.6	5.4065	4893.1	697.02	2.4256	-8.5657
84	7132.3	7012.5	6.4456	5219	955.7	2.7860	-7.3649
85	3753.5	6324.4	4.1847	6566.3	885.57	3.5229	-4.8334
86	6986.5	6980.9	6.7505	6234.4	276.95	2.0594	-5.0489
87	6306.8	8979.8	5.5658	3296	872.71	3.6879	-8.2303
88	6979.8	2198.1	4.4545	6153.4	769.22	2.8735	-5.1937
89	9020.7	5962.9	5.4814	5609.9	868.01	2.2234	-6.3262
90	2223.7	3419.5	4.8231	6129.4	995.38	2.8308	-8.9159
91	5959.5	4534.1	5.8457	6760.5	122.28	2.4814	-8.049
92	3435.1	6465.6	6.5752	698.84	707.86	3.1066	-8.6293
93	4518.4	1938.8	5.1959	5287.2	226.24	3.6012	-7.9308
94	6479.5	7749.4	6.6201	3126.2	418.09	2.7010	-6.8351

real. #	KD_AM_VO	KD_AM_AL	KD_AM_COL	KD_CS_VO	KD_CS_AL	KD_CS_COL	CONC_COL
95	1944.9	4815.2	4.4834	3829.2	794.98	3.6242	-7.3558
96	7738.3	2757.9	5.8567	5762.7	116.33	2.2479	-6.8801
97	4813.7	4650.8	6.6405	669.12	943.93	3.1094	-6.5674
98	2752.3	3626	4.9596	6518.4	474.28	3.6371	-4.579
99	4668.5	5430.8	4.9532	4078.5	156.07	2.6025	-5.2514
100	3590.2	6886.2	4.5261	2047.5	445.26	2.5987	-8.5003
101	5437.2	4246.3	6.4871	3955.1	253.85	2.2623	-5.3798
102	6878.3	7050	4.8636	3207.5	602.23	3.5479	-6.1694
103	4242.2	2836.9	5.8808	4724.6	855.89	2.5293	-5.4229
104	7071.8	5458.1	5.5038	6071.5	365.43	3.1555	-3.9017
105	2849	7165.5	6.7372	3615.2	879.29	2.8449	-8.9485
106	5452	3968.1	6.8082	6203.8	161.11	3.6822	-6.5045
107	7180.6	3947.5	6.8733	2313.5	607.45	3.6947	-8.6754
108	3975.9	2963	6.9243	4750.4	889.84	3.7506	-7.9714
109	3949.9	6585	4.9802	6255.2	310.82	3.8465	-6.0296
110	2961.6	3722.4	5.4942	3405.5	306.56	2.6266	-8.9706
111	6583.9	5508.2	5.5563	3396.5	167.18	2.8365	-4.7113
112	3744.8	4713.2	5.5211	2566.2	815.33	2.8642	-7.7037
113	5502.7	7651.4	5.6117	5859.1	271.76	2.8499	-8.8791
114	4707.5	7827.8	6.4298	3276	619.25	2.9020	-7.8504
115	7668.2	8061.2	5.6812	4801.1	451.04	3.5209	-8.5921
116	7875.1	8371.1	6.6551	3985.2	937.03	2.9405	-7.0702
117	8054.6	4033.3	6.6920	6498.8	952.66	3.6481	-5.5235
118	8382.8	4674.7	5.9025	6550.2	965.4	3.6725	-8.1812
119	4032.2	4794.8	5.4548	6613.1	975.16	3.1876	-5.3301
120	4682.7	4727.1	4.3159	6665.6	320.43	2.8162	-8.8483
121	4789.7	4923.1	6.6857	3448.6	446.62	2.1361	-7.0482
122	4733.6	6446.1	6.5263	3960.9	470.86	3.6683	-5.226
123	4918.3	5066.3	6.0719	4064.5	456.71	3.5702	-8.3913
124	6457.4	7265.2	5.7917	4014.1	493.65	3.3600	-8.4006
125	5073.8	7501.7	5.7853	4190.3	792.72	2.9976	-8.8265
126	7269	5566.2	6.7024	5728.5	527.66	2.9937	-5.8902

real. #	KD_AM_VO	KD_AM_AL	KD_AM_COL	KD_CS_VO	KD_CS_AL	KD_CS_COL	CONC_COL
127	7503.6	4620.7	4.7329	4350.1	902.78	3.6804	-8.5362
128	5573.1	2382.2	6.9325	6325	928.67	2.4095	-6.9813
129	4622.1	7497.1	6.6599	6426.1	629.98	3.8979	-7.8073
130	2420.4	6694.9	6.2405	4867.7	435.71	3.6530	-4.7451
131	7457.5	5934.5	5.1173	3908.3	127.29	3.4250	-4.6212
132	6679.9	5310	6.1987	995.09	924.13	2.6807	-4.4973
133	5936.4	5289	5.0374	6414.2	830.59	3.4087	-4.3664
134	5304.7	7600.3	6.8506	5940.5	698.01	2.6538	-8.3547
135	5285.5	3394.1	4.9341	5233.1	575.88	3.7269	-7.8364
136	7609.5	8528.2	6.4669	4588	572.62	2.5810	-7.7319
137	3398.2	7310.8	4.7676	4566.4	934.01	3.5342	-7.7884
138	8495.8	6104.3	5.3160	6480.9	220.56	2.4374	-7.6139
139	7329.9	4160.2	6.4786	3100.4	981.25	2.7538	-6.0479
140	6102.7	6062.9	5.4698	6693	907.73	3.5430	-7.4548
141	4166.5	4117.4	6.2900	6337.7	733.62	2.8222	-5.1313
142	6062	7991.4	5.9253	5422.8	349.23	3.4512	-4.9116
143	4131.1	3906.2	5.9633	3546.9	726.94	3.2263	-6.9204
144	8021.9	6524.3	5.2175	5384.1	336.27	3.2910	-7.891
145	3903.4	3468.8	5.7076	3509.5	960.78	2.7132	-8.9265
146	6511.8	4418.7	6.9969	6586.2	300.53	2.9582	-4.9539
147	3457.3	6579.8	5.7505	3359.8	803.03	3.9972	-5.7348
148	4404.6	4630.4	5.2945	5803.8	232.94	2.9797	-6.5489
149	6571.7	6183.3	6.6243	3147.6	394.75	2.7420	-7.2133
150	4650.1	5637.9	6.3304	3734.3	809.21	3.6309	-7.225
151	6185.5	5757.9	4.0403	5840.2	439.43	3.4709	-4.7824
152	5645.3	4276.8	6.2553	3929.5	747.16	2.0382	-8.6861
153	5748.4	5137.6	6.5065	5492.1	644.24	3.4298	-4.3303
154	4277.4	9300.6	5.1614	4944.8	668.14	3.5591	-5.0869
155	5131	5222.6	5.6857	5055.9	369.36	2.6922	-6.3617
156	9534.9	4376.2	6.3997	3628.1	540.59	2.9465	-8.2544
157	5223.8	7111.8	6.3160	4397.9	998.61	3.5045	-6.4036
158	4371.9	6245.4	6.9528	6778.5	559.62	3.4647	-8.2975

real. #	KD_AM_VO	KD_AM_AL	KD_AM_COL	KD_CS_VO	KD_CS_AL	KD_CS_COL	CONC_COL
159	7107.4	1511.6	5.8035	4506.4	387.34	3.9291	-4.5372
160	6262.1	6123.3	5.8876	3710.1	884.11	3.0123	-8.4216
161	1345	6652.3	5.8745	6222	759.54	3.1609	-5.9679
162	6117.2	4216	5.8954	5553.8	106.16	3.1339	-8.6561
163	6648.8	5090.8	5.9552	133.63	737.64	3.1759	-8.0717
164	4235.5	6390.9	6.1584	5437.7	821.88	3.2811	-5.909
165	5089.3	6227.3	5.0969	5895.3	357.82	3.3966	-7.878
166	6385.7	8608	5.8603	3585.5	532.58	2.6703	-6.2949
167	6223.2	5321.4	5.5933	4356.9	781.14	3.1305	-6.8452
168	8546.8	5534.4	4.8125	5669.7	755.11	2.8881	-6.7339
169	5319.2	5483.1	4.4143	5538.5	983.03	2.4729	-8.1665
170	5521.6	5542.5	6.3617	6717.7	580.56	2.1921	-7.3829
171	5495.8	5731.1	6.0755	4608.6	622.03	3.4794	-3.6765
172	5549.6	6033.4	5.6232	4816.2	613.79	3.3727	-7.2856
173	5727.9	4140	5.7782	4782.9	623.75	2.9066	-8.0952
174	6023.7	5477.9	5.6590	4843.3	664.5	2.9908	-5.2724
175	4148.4	4872.6	5.6693	5042	719.54	2.9265	-6.2288
176	5479.6	3549.9	6.8814	5344	343.37	2.9380	-8.9859
177	4879.1	2624.6	6.9058	3534	608.71	3.8063	-6.3475
178	3562.2	6292.3	4.6491	4764.2	488.67	3.8289	-5.8284
179	2691.1	5944.7	5.6981	4144.2	248.32	2.3548	-8.2179
180	6293.7	4927.5	4.8968	3190.7	150.62	2.9539	-7.4396
181	5941.6	5265.2	6.5944	1697.7	766.1	2.5494	-6.1073
182	4940.1	5004.8	6.5843	5606.2	701.74	3.6094	-6.2584
183	5261.6	5043.6	5.8215	5251.5	497.44	3.6051	-4.1654
184	5020.3	8191.8	4.8495	4209.5	568.89	3.0603	-7.1812
185	5060.4	8242.6	5.3579	4551.7	517.51	2.5082	-6.9617
186	8136.4	3206.1	6.5563	4293.2	522.73	2.7668	-7.0139
187	8289.8	5112.5	4.9119	4326.7	967.88	3.5857	-6.9487
188	3212.5	3783.9	6.4232	6625	972.79	2.5597	-6.7548
189	5101.7	6943.9	5.6010	6654.5	199	3.5129	-6.4514
190	3797.2	6920.3	4.5707	3041.1	535.96	2.8922	-8.267

real. #	KD_AM_VO	KD_AM_AL	KD_AM_COL	KD_CS_VO	KD_CS_AL	KD_CS_COL	CONC_COL
191	6929.3	5377.6	6.4533	4377.2	283.4	2.2913	-7.0285
192	6916.6	3672.1	6.7846	3319.1	863.42	3.5281	-7.651
193	5384	4451.3	5.9450	6111.5	861.69	3.6906	-8.615
194	3694.1	6790.8	6.5366	6096.6	590.15	3.2638	-8.8951
195	4459	3827.5	5.6646	4668.2	262.72	3.5723	-6.1974
196	6789.6	6419	6.2765	3248.5	403.04	2.9325	-6.5318
197	3839.3	4891.3	6.2175	3762.3	844.46	3.4436	-7.5985
198	6419.4	3017.7	6.1335	6014.8	285.99	3.4185	-7.2599
199	4889	6501.1	5.3766	3329.5	788.24	3.3858	-7.5095
200	3037	7780.9	6.3784	5721.1	489.71	2.7745	-7.4663